

ADVERTIMENT. L'accés als continguts d'aquesta tesi queda condicionat a l'acceptació de les condicions d'ús establertes per la següent llicència Creative Commons:  <https://creativecommons.org/licenses/?lang=ca>

ADVERTENCIA. El acceso a los contenidos de esta tesis queda condicionado a la aceptación de las condiciones de uso establecidas por la siguiente licencia Creative Commons:  <https://creativecommons.org/licenses/?lang=es>

WARNING. The access to the contents of this doctoral thesis it is limited to the acceptance of the use conditions set by the following Creative Commons license:  <https://creativecommons.org/licenses/?lang=en>

SIMULTANEOUS ACTIVATION OF TWO
COMPLEMENTARY TARGETS, KV7.2/3 AND
TSPO: A NOVEL TREATMENT FOR
AMYOTROPHIC LATERAL SCLEROSIS

Presented by
Vera Martín Masegosa

ACADEMIC DISSERTATION

To obtain the degree of PhD in Neuroscience from the
Universitat Autònoma de Barcelona

September 2023

Thesis supervisors
Dr. Xavier Navarro Acebes
Dra. Mireia Herrando Grabulosa

This study was funded by:

- The project 20-DDC-497 “Synergistic dual target approach to ALS therapy: simultaneous activation of two complementary targets, neuronal Kv7.2/3 channels and glial TSPO” from The Amyotrophic Lateral Sclerosis Association of the U.S.A. to Xavier Navarro Acebes.
- The project CF616892 “Simultaneous activation of two complementary targets, Kv7.2/3 and TSPO: a promising and novel treatment of Amyotrophic lateral sclerosis from Fight MND Foundation of Australia to Xavier Navarro Acebes.
- Additional support was received from CIBERNED (Grant No. CB06/05/1105), and TERA-V RICORS (Grant No. RD21/0017/008) funds from the Instituto de Salud Carlos III of Spain.

A mis padres

Index

I. Summary.....	9
II. Abbreviations	13
III. Introduction	17
1. Motor neuron diseases.....	19
2. Amyotrophic lateral sclerosis.....	19
2.1 Pathophysiology of MN degeneration in ALS	23
3. Models of ALS.....	38
3.1 <i>In vitro</i> models.....	38
3.2 <i>In vivo</i> models	40
4. GRT-X.....	43
4.1 TSPO	43
4.2 Kv7.2/3.....	48
IV. Hypothesis and objectives	53
V. Study design and methodology	57
VI. Results.....	67
Chapter I.....	69
Chapter II	91
Chapter III.....	119
Chapter IV.....	145
VII. Discussion	157
VIII. Conclusions.....	167
IX. References.....	171
X. Acknowledgements	213

I. Summary

Amyotrophic lateral sclerosis (ALS), the most frequent motor neuron disease (MND) in adults, is a fatal neurodegenerative disease characterized by the progressive degeneration of motoneurons (MNs) in the motor cortex and spinal cord, leading to muscle weakness and paralysis, and death within 2-5 years after the disease onset. The exact mechanisms triggering MN degeneration in ALS remain elusive; however, it is suggested that the neurodegenerative process results from the combination of several pathogenic mechanisms. Most assays are focused on treating a single pathogenic pathway involved, leading to limited effectiveness in improving ALS. Therefore, novel and combinatorial therapeutic approaches are currently being pursued.

The aim of this thesis was to assess the therapeutic potential of the simultaneous activation of two different targets, the voltage-gated potassium channels 7.2/3 (Kv7.2/3) and the mitochondrial translocator protein (TSPO), as a promising approach to improve the course of ALS. For this purpose, we tested the novel and dual-mechanism GRT-X drug in an *in vitro* model of spinal organotypic culture (SCOC), and then, in the murine ALS model the transgenic SOD1^{G93A} mice.

Considering that the neuroprotective effects of TSPO activation in the SOD1^{G93A} mice had been already demonstrated, we first tested the activation of Kv7.2/3 mediated by the selective compound ICA-27243 as a potential therapy. Our findings revealed that ICA-27243 prevents MN degeneration in SCOCs exposed to excitotoxicity. Additionally, intraperitoneal administration of ICA-27243 to the transgenic SOD1^{G93A} mice enhanced neuromuscular function, maintained locomotion and coordination, reduced spinal MN death and attenuated glial reactivity, suggesting it is an effective treatment to prevent the progression of ALS.

We then demonstrated that GRT-X increases MN survival in both SCOCs and isolated MN cultures exposed to toxicity induced by astrocyte-conditioned medium (ACM) derived from primary mouse astrocytes expressing mutant human SOD1 (SOD1^{G93A}-ACM) or from ALS astrocytes generated from induced pluripotent stem cells of patients carrying disease-causing mutations of SOD1 (SOD1^{D90A}-ACM) or TDP43 (TDP43^{A90V}-ACM) genes. Furthermore, we found that one of the mechanisms involved in enhancement of MN survival by GRT-X is reduction in ROS levels.

In vivo, daily oral administration of the GRT-X compound to SOD1^{G93A} mice preserved neuromuscular function, and motor activity determined by electrophysiology, rotarod and

Summary

treadmill tests. Histological studies proved that GRT-X enhanced MN survival and neuromuscular junction innervation in treated SOD1^{G93A} mice. However, the effects of GRT-X showed some differences between sexes, being more marked in female than in male-treated mice. These data proved the effectiveness of GRT-X for the eventual treatment of MN degenerative diseases.

Finally, we explored the synergistic potential of the two molecular targets assessed in this thesis. Thus, we simultaneously used the unimodal agonists of each target, ICA-27243 for Kv7.2/3 and Olesoxime for TSPO. *In vitro* studies in spinal cord slices demonstrated a synergistic effect of both pathways since MN survival was higher with the dual than with single treatments. However, the synergistic effects observed *in vitro* were not translated to *in vivo* conditions, despite this combination also improved the evolution of neuromuscular function and enhanced MN survival in the SOD1^{G93A} mice.

Collectively, the results of this thesis provided evidence that TSPO and Kv7.2/3 are promising targets for ALS and proved that GRT-X, and also ICA-27243, exert neuroprotective actions for ALS.

II. Abbreviations

ACM: Astrocyte-conditioned medium	GSH: glutathione synthase
ALS: Amyotrophic lateral sclerosis	hSOD1: Human SOD1
ALSFRS-R: ALS functional rating scale	IMM: Inner mitochondrial membrane
AMPA: α -amino-3-hydroxy-5-methyl-4-isoxazole-propionic acid	iPSC: Induced pluripotent stem cell
Arg-1: Arginase-1	KIF: Kinesin
CaM: Calmodulin	KO: Knock-out
ChAT: Choline acetyltransferase	MEP: Motor evoked potential
CMAP: Compound muscle action potential	MMP-9: Matrix metalloproteinase 9
CNS: Central nervous system	MN: Motoneuron
CRAC: Cholesterol recognition amino acid consensus	MND: Motoneuron disease
CSF: Cerebrospinal fluid	mSOD1: Mice SOD1
DIV: Days <i>in vitro</i>	mtFUS: mutant FUS
EAAT2: Excitatory amino acid transporter 2	mtSOD1: mutant SOD1
ER: Endoplasmic reticulum	mtTDP43: mutant TDP43
fALS: Familiar ALS	NMDA: N-methyl-D-aspartate
FDA: Food and Drug Administration	NMJ: neuromuscular junction
FTD: Frontotemporal dementia	OMM: outer mitochondrial membrane
FUS: Fused in sarcoma	PFA: Paraformaldehyde
GABA: γ -Aminobutyric acid	RBP: RNA-binding protein
	ROS: Reactive oxygen species
	sALS: Sporadic ALS
	SCOC: Spinal cord organotypic culture

Abbreviations

SICI: short-interval intracortical inhibition

SMA: Spinal muscular atrophy

SOD1: Superoxide dismutase

StAR: Steroidogenic acute regulatory protein

SVC: Slow vital capacity

TA: Tibialis anterior

TBOA: DL-threo- β -benzyloxyaspartate

TDP43: TAR DNA-binding protein 43

UPS: Ubiquitin-proteasome pathway

VDAC1: Voltage-dependent anion channel

VSCN: Ventral spinal cord neuronal cultures

WT: Wild type

III. Introduction

1. Motor neuron diseases

Motor neuron diseases (MND) are a set of heterogeneous neurological disorders that result in the degeneration of upper motoneurons (MNs) and/or lower MNs. Upper MNs are located in the motor cortex and are responsible for the emergence of the corticospinal and corticobulbar tracts, while the lower MNs are located in the spinal cord anterior horn and motor nuclei of cranial nerves in the brainstem and send their axons within peripheral nerves to innervate the skeletal muscles (Tiryaki & Horak, 2014). MNDs exist on a spectrum, where the extent of upper and lower MN involvement varies, resulting in different degrees of severity. There are four primary phenotypes of MND in adults, categorized by the location of origin and the extent of neurological impairment: amyotrophic lateral sclerosis (ALS), progressive bulbar palsy, progressive muscular atrophy, and primary lateral sclerosis (Statland et al., 2015). The two most commonly observed forms of MND are ALS, which predominantly affects adults, and spinal muscular atrophy (SMA), a monogenic disorder that affects children.

2. Amyotrophic lateral sclerosis

ALS, initially known as Charcot's sclerosis and also known as Lou Gehrig's disease in the USA, was first described by Jean-Martin Charcot in 1869. ALS is a heterogeneous disease characterized by the selective degeneration of both upper and lower MNs resulting in progressive paralysis of voluntary muscle that ultimately leads to death. ALS incidence changes depending on geographic localization, being higher in Europe and North America (2.1- 3.8/100.000 per year) than in Asia (0.8- 1.2/100.000 per year). ALS incidence is higher in males than in females being the global sex ratio of 1.2–1.5 (Longinetti & Fang, 2019).

The main clinical features of ALS include progressive muscle weakness, muscle atrophy, fasciculations, muscle cramps, muscle stiffness, spasticity, dysphagia (difficulty swallowing) and dysarthria (difficulty speaking) (Masrori & Van Damme, 2020). Although the main symptoms are related to motor dysfunction, non-motor manifestations are increasingly recognized. Up to 50% of patients experience cognitive and/or behavioral impairments during the course of the disease, such as impaired language, impeded working memory, apathy and irritability (Goutman et al., 2022). Additionally, approximately 13% of patients present the concomitant variant frontotemporal dementia (FTD) (Phukan et al., 2012).

Introduction

ALS classification is challenging due to the significant variability among patients. Some potential classification criteria include age at onset, disease burden, survival rate, disease progression, extramotor involvement or the extent of family history (Al-Chalabi et al., 2016). A frequently employed classification is based on the origin of MN impairment, distinguishing between spinal onset (affecting spinal MNs) and bulbar onset (affecting brainstem MNs first). Spinal onset disease accounts for 60% of cases and initially presents with muscle weakness and fasciculations in an asymmetric pattern in the upper or lower limbs. Bulbar onset disease affects approximately one-third of ALS patients and is characterized by the initial involvement of muscles controlling speech, chewing and swallowing. Bulbar onset patients generally have a shorter lifespan compared to those with spinal onset (Ragagnin et al., 2019). Moreover, in Europe, the majority of men experience spinal onset disease, while women show a greater tendency toward bulbar-onset disease (Logroscino et al., 2010).

ALS diagnosis is difficult due to the heterogeneity in clinical presentation and overlapping with other neurodegenerative diseases, which delays diagnosis between 10–16 months (Richards et al., 2020). No definitive test exists for diagnosing ALS; however, the well-established approach involves clinical history, examination and electromyography. Diagnosis is typically based on the El Escorial or Awaji criteria (Goutman et al., 2022). However, new criteria are being developed to facilitate easier and faster ALS diagnosis. For example, the novel Gold Coast criteria make diagnosis simpler and may enhance sensitivity and specificity (Hannaford et al., 2021). Emerging ALS diagnostic and prognostic biomarkers include levels of phosphorylation of the neurofilament heavy chain, as an indicator of more aggressive disease and shorter survival, elevated levels of IL-6 in ALS patients associated with disease progression, or increased ferritin levels linked to poorer survival. Furthermore, the use of magnetic resonance imaging (MRI) and positron emission tomography (PET), electroencephalogram and transcranial magnetic stimulation (TMS) techniques to analyze cortical neuronal excitability is on the rise (Goutman et al., 2022; Verber & Shaw, 2020).

Currently, the exact etiology of ALS remains unknown. Around 90–95% of the cases are sporadic (sporadic ALS, sALS) without apparent genetic link, while the remaining 5–10% of the cases are related to several genetic mutations (familial ALS, fALS). Nevertheless, patterns of selective MN degeneration and vulnerability are similar between both forms of ALS. Since the identification of the first gene involved in fALS, Cu/Zn

superoxide dismutase 1 (SOD1) (Rosen et al., 1993), over 200 genetic variants of this gene have been identified (<https://alsod.ac.uk/output/variant.php/35>), accounting for 12–24% of fALS cases. Technological advancements in next-generation sequencing have greatly influenced ALS research by enabling the identification of numerous genes associated with the disease. The most frequently mutated gene, *C9orf72*, was found in 30–50% of fALS and 10% of sALS. The non-coding GGGGCC hexanucleotide sequence located in the intronic region of human chromosome 9 open reading frame 72 undergoes an abnormal repeat expansion resulting in the formation of nuclear RNA foci (DeJesus–Hernandez et al., 2011). Mutations in the *TARDBP* gene, encoding for TDP43, are related to autosomal dominant ALS and FTD and account for 1–2% of ALS cases (Neumann et al., 2006). TDP43 is of interest in ALS pathology because it is the most predominant protein at the cytosolic aggregates in MNs of sALS and fALS patients, with or without *TARDBP* alterations (Brettschneider et al., 2013). In addition to the aforementioned genes, at least 50 other genes have been found to be involved in ALS, including *fused in sarcoma (FUS)*, *Ataxin2 (ATXN2)*, *Alsin2 (ALS2)*, *Sentaxin (SETX)*, *Profilin (PFN1)*, *Sigma non-opioid intracellular receptor (SIGMAR1)* or *Vesicle-associated membrane protein-associated protein B (VAPB)*, among others (Chia et al., 2018; Mejzini et al., 2019; Ragagnin et al., 2019).

Currently, there is no cure for ALS and patients die within 2–5 years after disease onset in the classical course. Riluzole was the first drug approved by the Food and Drug Administration (FDA) in 1995. Riluzole, categorized as an anti-excitotoxicity drug, slows ALS progression by reducing neuronal firing, lowering the persistent Na⁺ current, enhancing Ca²⁺-dependent K⁺ channels and decreasing presynaptic neurotransmitter release (Bellingham, 2011). Clinically, it only increases patients' lifespan by two to three months (Miller et al., 2012). Despite being the current standard treatment provided to ALS patients, it was reported that Riluzole has no beneficial effects on motor performance and survival in SOD1^{G93A}, TDP43^{A315T} and FUS (1–359) ALS mice models (Hogg et al., 2018).

It was not until 2017 that another drug, Edaravone, was approved by the FDA for the specific treatment of ALS. Edaravone is a free radical scavenger that eliminates lipid peroxides, hydroxyl and peroxy free radicals (Yoshino, 2019). Two long-term studies showed that Edaravone declined the score in the ALS functional rating scale (ALSFRS–R) (Okada et al., 2018; Park et al., 2022) and improved long-term survival in ALS patients (Okada et al., 2018). Nevertheless, the use of Edaravone is controversial since the beneficial outcomes observed in the Asian population were not replicated in studies with Caucasian

Introduction

ALS patients, in whom Edaravone failed in ameliorating ALS symptomatology or extending the lifespan (Fortuna et al., 2019; Witzel et al., 2022).

Recently, two more drugs were approved for the treatment of ALS: Tofersen and Relyvrio. Tofersen is an antisense oligonucleotide designed to decrease the synthesis of the SOD1 protein through ribonuclease H-dependent degradation of SOD1 mRNA. The first phase 3 trial demonstrated a decline in ALSFRS-R score but without significant difference compared to placebo. However, they observed lower levels of SOD1 protein in cerebrospinal fluid (CSF) and reduced levels of neurofilament light chains in plasma in participants who received Tofersen (T. M. Miller et al., 2022). Currently, a separate phase 3 study (ATLAS study: NCT04856982) is recruiting patients to assess the effectiveness of Tofersen in delaying onset symptoms or slowing decline in motor function in presymptomatic adult individuals who carry a SOD1 mutation and have elevated levels of neurofilament (Benatar et al., 2022).

Relyvrio, or AMX0035, is a combination of sodium phenylbutyrate and taurursodiol that mitigates endoplasmic reticulum (ER) stress and mitochondrial dysfunction. Sodium phenylbutyrate, an inhibitor of histone deacetylase, enhanced the expression of heat shock proteins that act as small molecular chaperones ameliorating toxicity from ER stress. Taurursodiol restores mitochondrial bioenergetic by reducing mitochondrial permeability and preventing apoptotic cell death (Paganoni et al., 2020), Relyvrio slowed functional decline assessed by the ALSFRS-R score compared to the placebo over a 24-week period (Paganoni et al., 2020) and increased survival by 6.5 months compared to placebo (Paganoni et al., 2021).

Masitinib, an oral tyrosine kinase inhibitor, is close to being approved as an ALS treatment. Studies conducted on the SOD1^{G93A} rat treated with Masitinib showed reduced neuroinflammation, decreased MN loss and improved survival outcomes (Trias et al., 2016). Slowed decline in ALSFRS-R together with lower deterioration in the forced vital capacity (FVC) was demonstrated in Masitinib-treated ALS patients (Mora et al., 2020). In addition, Masitinib treatment prolongs survival by over 2 years and reduces the risk of death by at least 44% as compared with placebo (Mora et al., 2021).

Although several treatments have been developed in recent years, they have limited beneficial effects on patients' lifespan; therefore, further research to improve the progression and finally offer a cure for ALS is still essential.

2.1 Pathophysiology of MN degeneration in ALS

The most characteristic hallmark of ALS is MN degeneration, which leads to loss of muscle strength. The growing interest in the disease and the imperative to find effective therapeutic approaches have unveiled several pathophysiological mechanisms that contribute to MN degeneration including excitotoxicity, oxidative stress, mitochondrial dysfunction, protein misfolding, ER stress or neuroinflammation, among others (Hardiman et al., 2017; Mancuso & Navarro, 2015; Van Damme et al., 2017). Several authors have proposed a cascade of cellular events that results in MN degeneration in ALS by summarizing different pathological mechanisms that are known to contribute to the progression of the disease (Ragagnin et al., 2019). The exact mechanism underlying MN degeneration in ALS is not yet fully understood, but it is likely a combination of multiple pathological mechanisms, that are not mutually exclusive, and culminate in a significant disruption within the network. Hence, ALS is a multifactorial disease like other neurodegenerative disorders.

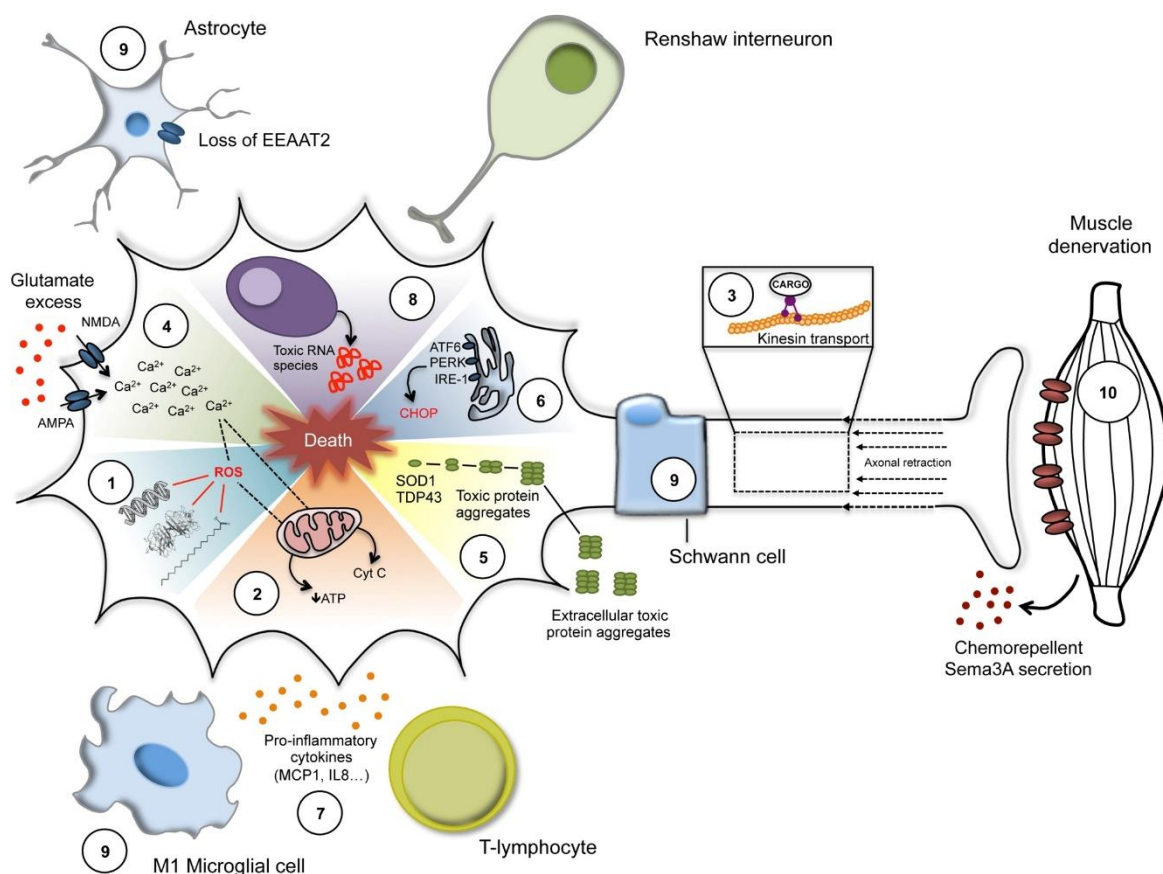


Figure 1. Main pathophysiological mechanisms contributing to MN degeneration in ALS. (1) Oxidative stress, (2) mitochondrial dysfunction, (3) impaired axonal transport, (4) excitotoxicity, (5) protein aggregation, (6) endoplasmic reticulum stress, (7) neuroinflammation, (8) abnormal RNA processing, (9) non-neuronal cells, and (10) target muscle contribution. Extracted from Mancuso & Navarro, 2015.

Mitochondrial dysfunction

Mitochondria are the main producers of energy in cells through oxidative phosphorylation. Additionally, they play important roles in phospholipids biogenesis, Ca^{2+} homeostasis and buffering and apoptosis. Mitochondrial dysfunction has been associated with numerous neurodegenerative diseases, including ALS. In fact, many ALS-related genes have a role in mitochondrial-associated function, highlighting mitochondrial dysfunction as one of the main pathological mechanisms contributing to MN degeneration in ALS. However, some authors suggest that mitochondrial dysfunction alone may not be the primary cause of ALS but rather a secondary consequence of other disease-related factors, such as protein aggregation and excitotoxicity (Smith et al., 2019).

Mitochondrial abnormalities, including structural alterations or aggregated mitochondria, are found throughout the course of the disease. Swollen and vacuolated mitochondria were identified in ALS patients (Sasaki & Iwata, 2007). Aggregated, fragmented, vacuolated, less elongated or swollen mitochondria can be found in *in vitro* and *in vivo* models carrying ALS-related mutations, such as TDP43^{Q331K} and TDP43^{M337V} (W. Wang et al., 2013), SOD1^{G93A} (Magrané et al., 2014), SOD^{G37R} and SOD1^{G85R} (Vande Velde et al., 2011), FUS^{P525L} (Sharma et al., 2016), C9orf72 (Dafinca et al., 2016) or Alsin KO (Gautam et al., 2015). Moreover, some mutations not only impact the morphology of mitochondria but also disrupt their normal functions. It was reported that fALS-mtSOD1 aggregates in the mitochondria impaired the electron transport chain and modified the redox state (Ferri et al., 2006). MtSOD1 also inhibits the conductance of the voltage-dependent anion channel (VDAC1), an integral protein located in the outer mitochondrial membrane (OMM). This inhibition diminishes adenosine triphosphate (ATP) synthesis and reduces membrane potential. Ultimately, these effects contribute to accelerated disease onset and decreased survival in mtSOD1 mice (Israelson et al., 2010). Although not being mitochondrial proteins, mutations in other ALS-related genes also impact mitochondrial function. For example, mtTDP43 binds to mRNAs from mitochondrial DNA, reducing complex I expression and impairing oxidative phosphorylation causing mitochondrial dysfunction (Wang et al., 2016). Similarly, poly(GR) protein, dipeptide repeat protein generated from mtC9orf72, preferentially binds to ribosomal proteins needed for the translation of subunits of mitochondrial complexes and, therefore, impairs mitochondrial function (Lopez-Gonzalez et al., 2016). Furthermore, the reduction in the activity of the four components of the

electron transport chain and impaired ATP synthesis was reported in both ALS patients (Wiedemann et al., 2002) and in the SOD1^{G93A} mice (Mattiuzzi et al., 2002).

Mitochondrial Ca²⁺ homeostasis is crucial for cell survival. A substantial decline in the capacity of mitochondrial Ca²⁺ buffering was observed in the very early stages of the disease within the central nervous system (CNS) in SOD1^{G93A} mice (Damiano et al., 2006). Moreover, spinal MNs display lower endogenous Ca²⁺ capacity compared to oculomotor MNs, making them highly vulnerable to Ca²⁺ dysregulation (Alexianu et al., 1994). ER-mitochondria contact sites facilitate Ca²⁺ exchange between the two organelles, and disruption of ER-mitochondria communication has been identified as a key factor contributing to the alteration of Ca²⁺ homeostasis in ALS. ER-mitochondria disruption was identified in different models with mutations in ALS-related genes such as SOD1 (Watanabe et al., 2016), *TDP43* (Stoica et al., 2014), *C9orf72* (Gomez-Suaga et al., 2022) and *SigmaR1* (Watanabe et al., 2016).

Mitochondria play a vital role in apoptosis, which is the cellular mechanism activated as a last resort when cells experience irreparable damage. Apoptosis enables the controlled removal of damaged cells from the tissue, preventing widespread degeneration. In SOD1^{G93A} mice it was detected increased levels of the pro-apoptotic proteins Bax and Bad simultaneously with diminished expression of anti-apoptotic protein Bcl-2 (Vukosavic et al., 2002). Moreover, it has been observed that the downregulation of specific miRNAs, such as miR-335-5p, contributes to an upregulation in the activity of pro-apoptotic caspases 3 and 7, along with elevated levels of reactive oxygen species (ROS) and abnormal mitochondrial morphology (De Luna et al., 2020).

Oxidative stress

Oxidative stress results from an imbalance between the production of ROS and the biological system capacity to eliminate ROS or repair ROS-induced damage. Mitochondria are the primary source of ROS due to oxidative phosphorylation, whose reactions generate free radicals such as hydrogen peroxide (H₂O₂), superoxide anions (O₂⁻), and hydroxyl radicals (HO⁻) (Sbodio et al., 2019). While oxidative stress may not be inherently harmful, the accumulation of ROS can significantly impair the capacity of the cells to confront an underlying pathological condition. In addition, the accumulation of ROS progressively damages proteins (Shaw et al., 1995), lipids (Simpson et al., 2004), DNA (Bogdanov et al., 2002) and RNA species (Chang et al., 2008) resulting in impaired cellular processes, neuroinflammation and MN degeneration. Furthermore, levels of 8-hydroxy-20-

Introduction

deoxyguanosine, a marker of oxidative DNA damage, are elevated in both sALS patients (Fitzmaurice et al., 1996) and SOD1^{G93A} mice (Aguirre et al., 2005).

Mutations in the *SOD1* gene, which encodes the enzyme responsible for catalyzing the conversion of superoxide to H₂O₂, have been implicated as contributors to MN degeneration in ALS. This highlighted the significant role of oxidative stress in the progression of the disease. Initially, it was hypothesized that mutations in the *SOD1* gene resulted in a loss of function, leading to an inability to eliminate ROS and, ultimately, causing MN loss. However, further studies demonstrated that mtSOD1- protein misfold and aggregate, resulting in a toxic gain of function rather than a loss of function (Bruijn et al., 1998). The mechanism underlying this toxic gain of function is currently unknown. Several hypotheses have been proposed to explain this toxic property, but none of them have been conclusively proven thus far (*reviewed in* Cunha-Oliveira et al., 2020). Moreover, it was demonstrated that *SOD1* knockout (KO) mice develop normally without motor deficits (Reaume et al., 1996) but display a distinctive motor axonopathy (Reaume et al., 1996; Shefner et al., 1999).

Although mutations in the *SOD1* gene have traditionally been associated with oxidative stress, it is not the only ALS-related mutation that can be linked to this pathological mechanism. *TARDBP* mutations were related to impaired levels of glutathione synthetase (GSH), increased levels of intracellular lipid peroxidation or compromised nuclear factor erythroid 2, an antioxidant response element (Moujalled et al., 2017; Tian et al., 2017). Additionally, mutations in *C9orf72* have been also associated with increased levels of ROS and down-regulation of antioxidant proteins such as *SOD1*, *SOD2* and GSH (Birger et al., 2017). In addition, it was reported that several ALS-related proteins including *SOD1*, *TDP43* (W. Wang et al., 2016) and *C9orf72* (Lopez-Gonzalez et al., 2016) can enter the mitochondria and interfere with their regular functioning, leading to higher ROS production. This establishes a cross-link between oxidative stress and other pathological mechanisms.

Excitotoxicity

Excitotoxicity is a pathological process characterized by neuronal cell death resulting from excessive or prolonged activation of excitatory neurotransmitters, primarily glutamate. It occurs due to an imbalance between the release and clearance of excitatory neurotransmitters, leading to an excessive influx of Ca²⁺ into neurons. This dysregulated

Ca^{2+} influx triggers a cascade of detrimental molecular events, including activation of Ca^{2+} -dependent proteases, lipases and nucleases which damage the neuron, oxidative stress, mitochondrial dysfunction, and activation of apoptotic signaling pathways, highlighting the interaction between the different pathological mechanisms involved in ALS.

Excitotoxicity emerged as one of the first pathological mechanisms described as a contributor to MN degeneration. Early observations revealed elevated levels of glutamate in the CSF of ALS patients compared to healthy subjects (Rothstein et al., 1990). Subsequently, it was reported a specific loss of the astroglial glutamate transporter, excitatory amino acid transporter 2 (EAAT2), the main astroglial synaptic glutamate reuptake transport protein in ALS patients (Rothstein et al., 1995). This loss of EAAT2/GLT1 results in the inability of astrocytes to efficiently clear synaptic glutamate, leading to increased glutamate levels and the consequent development of excitotoxicity, leading to MN damage.

Despite the presence of this non-cell autonomous effect, there are also certain intrinsic properties of MNs that make them more vulnerable to excitotoxicity. MNs have a high number of Ca^{2+} -permeable α -amino-3-hydroxy-5-methyl-4-isoxazole-propionic acid (AMPA) receptors, ionotropic glutamate receptors responsible for the fast synaptic transmission in the CNS. Indeed, MN death by excitotoxicity is related to Ca^{2+} influx through AMPA receptors (Van Den Bosch et al., 2000). The Ca^{2+} conductance of AMPA receptors exhibits significant variations based on the presence of the GluR2 subunit. AMPA receptors containing at least one GluR2 subunit exhibit low Ca^{2+} conductance, while those lacking a GluR2 subunit demonstrate high Ca^{2+} permeability. In addition, edited mRNA displays low Ca^{2+} permeability. *In vivo*, GluR2 mRNA undergoes editing; however, in ALS, there is a deficiency in GluR2 editing, resulting in a pathological condition characterized by increased Ca^{2+} permeability (Kwak & Kawahara, 2005). Concordantly, GluR2-KO accelerated MN degeneration and shortened the lifespan of the SOD1^{G93A} mice (Van Damme et al., 2005). Altogether, GluR2 has a crucial role in MN vulnerability to excitotoxicity.

Moreover, MNs have low Ca^{2+} buffering capacity due to the low expression of Ca^{2+} -buffering proteins. Spinal MNs do not express parvalbumin and calbindin D28K (Ince et al., 1993). Overexpression of parvalbumin in MNs exhibits a lower rise of intracellular Ca^{2+} and prevents MN loss when cultures are treated with kainic acid (Van Den Bosch et al., 2002). Concurrently, overexpression of parvalbumin in the SOD1^{G93A} mice decreased

Introduction

intracellular Ca^{2+} elevation, prevented MN loss, delayed disease onset and prolonged survival (Beers et al., 2008).

Impaired protein homeostasis

Protein homeostasis, also known as proteostasis, is the correct equilibrium between the production and the degradation of proteins. This dynamic process involves the coordinated control of protein synthesis, folding, assembly, trafficking and clearance. The imbalance of this process can lead to protein misfolding and protein aggregation, which is a pathological hallmark of several neurodegenerative disorders, including ALS.

Ubiquitin-positive inclusions are the most common inclusions in ALS histopathology and are found in both upper and lower MNs (Neumann et al., 2006). However, it is currently uncertain whether the formation of inclusions is directly responsible for cellular toxicity in ALS pathogenesis, whether these aggregates are harmless neurodegeneration-derived products, or if they actually represent a protective response by the cell to decrease levels of toxic proteins within the intracellular environment (Mancuso & Navarro, 2015).

Mutations in several ALS-related genes result in the production of abnormally folded proteins that tend to aggregate and form inclusion bodies impairing proteostasis. These are particularly *SOD1*, *TDP43*, *FUS* and *C9orf72* genes (Ruegsegger & Saxena, 2016). In addition, it was reported that mutations in ALS-related genes directly target components of the protein homeostasis network such as autophagy, ER homeostasis, and the ubiquitin-proteasome pathway (UPS) (Medinas et al., 2018; Ruegsegger & Saxena, 2016).

Misfolded forms of SOD1 had been consistently reported in sALS and fALS patients' tissue (Shibata et al., 1994), as well as in the SOD1^{G85R} (Bruijn et al., 1998) and SOD1^{G93A} mice (Bendotti et al., 2012). Misfolded SOD1 proteins evade the regular degradation process through ubiquitination, impairing both UPS and autophagy. SOD1 proteins directly interact with UPS-related proteins such as E3 ubiquitin ligases, CHIP or GP78, among others (*reviewed in* Bendotti et al., 2012). MtSOD1 aggregates also bind directly to autophagy proteins such as optineurin reducing mitophagy flux (Tak et al., 2020). Nonetheless, there are other mechanisms also associated with the misfolding and aggregation of SOD1 protein. Activation markers of ER stress have been identified in the spinal cord of ALS patients (Atkin et al., 2008) and ALS models (Kikuchi et al., 2006). In fact, it was found that in the SOD1^{G93A} mice, the SOD1 protein accumulates in the lumen of the ER and interacts with

Grp78/BiP, thereby affecting its function and ultimately impacting protein degradation by the proteasome (Kikuchi et al., 2006). However, this process may not be unidirectional, as ER stress increases the susceptibility of SOD1^{WT} protein to aggregate (Medinas et al., 2018). In addition, the presence of SOD1 protein aggregates leads to the formation of vacuoles that contain components from both the mitochondria and the ER (Salvany et al., 2022). Besides the physiological complications linked to SOD1 protein aggregation, it has been observed that it functions as a prion-like protein, resembling the behavior seen in other neurodegenerative disorders like Alzheimer's disease. Studies demonstrated that mutant and misfolded SOD1 can induce misfolding of natively structured SOD1^{WT} protein in a prion-like manner (Grad et al., 2011; Münch et al., 2011).

TDP43 is the main aggregated protein in ALS, and it is found in 97% of ALS patients (Neumann et al., 2006). Under normal physiological conditions, the TDP43 protein is predominantly found within the nucleus. However, in pathological circumstances, it undergoes ubiquitination and hyperphosphorylation, leading to the formation of cytoplasmic aggregates in neurons and glial cells (Mackenzie et al., 2010). It was also reported that phosphorylated TDP43 aggregates can be in peripheral motor nerves of ALS patients (Riva et al., 2022). It is now established that the neurodegeneration caused by TDP43 aggregates is due to a gain (White et al., 2018) or loss of function (C. Yang et al., 2014) since both situations have been observed, and they do not necessarily are mutually exclusive (Kabashi et al., 2009). Moreover, it was demonstrated that the TDP43 protein also displays prion-protein characteristics (Keating et al., 2023; Nonaka et al., 2013).

Cytoplasmic aggregates of FUS, another RNA-binding protein, are found in neurons and glial cells in ALS patients (Groen et al., 2010; Hewitt et al., 2010). MtFUS generates cytoplasmic aggregates sequestering FUS^{WT} (Takanashi & Yamaguchi, 2014). These aggregates impaired RNA granule formation (Takanashi & Yamaguchi, 2014), caused RNA splicing perturbations (Rezvykh et al., 2023) and compromised protein degradation (Marrone et al., 2019). Mutations in genes encoding RNA-binding proteins (TDP43 and FUS) entail a direct interplay between two pathological mechanisms of ALS, disrupted protein homeostasis and abnormal RNA metabolism (Medinas et al., 2017).

The intronic expansion of hexanucleotide repeat (G4C2) in the *C9orf72* gene is the most frequent mutation in ALS. The mechanism through which this expansion contributes to ALS is not fully understood. However, three distinct and potentially overlapping mechanisms have been proposed: haploinsufficiency of the *C9orf72* gene, sequestration of

Introduction

RNA-binding proteins and production of dipeptide repeat proteins (Beckers et al., 2021). Five distinct dipeptide repeat proteins have been identified and all of them exhibit toxicity. Among them, Poly(GA) is highly toxic and can sequester other dipeptides, promoting their aggregation (Lee et al., 2017). Additionally, Poly(GA) can sequester nuclear pore proteins such as HR23, disrupting the transport of proteins into and out of the cell nucleus and leading to impaired nucleocytoplasmic transport (Zhang et al., 2016). Poly(GA) also triggers neuronal death by inducing ER stress (Zhang et al., 2014) and impairing autophagy (Pu et al., 2022).

Axonal transport

MNs typically possess remarkably long axons between the soma and distant synaptic sites. The synthesis of cellular components primarily occurs within the cell body. Consequently, efficient axonal transport becomes essential to effectively deliver the newly synthesized materials to the axon. Histological analyses of post-mortem ALS patients have demonstrated disorganization of the axonal cytoskeleton and accumulation of neurofilament in MN cell bodies. These findings imply a disruption of axonal transport within MNs (Hirano et al., 1984; Julien & Mushynski, 1998). The mtSOD1 mouse also exhibits cytoskeletal defects, similar to humans, affecting neurofilaments, actin and tubulin (Collard et al., 1995). Furthermore, it was demonstrated that impaired axonal transport precedes ALS symptomatology (Bilsland et al., 2010).

Mutations in genes encoding proteins that are part of the cytoskeleton or axonal transport machinery, such as kinesins, dyneins, neurofilament heavy chain, peripherin, tubulin- β 4a, cofilin or profilin, have been associated with ALS (Burk & Pasterkamp, 2019). Mutations in the C-terminal region of the *KIF5A* gene, which encodes for kinesin (KIF)-5A protein essential for anterograde axonal transport, have been identified as a cause of ALS (Nicolas et al., 2018). Moreover, KIF5A-KO mice develop neurodegeneration and paralysis (Xia et al., 2003). ALS-related mutations, such as those in the *FUS* gene, disrupt the KIF-5C, KIF-1B, and KIF-3A mRNA expression (Hoell et al., 2011). Studies also demonstrated that mutations in the gene encoding for dynein cause α -MN loss (Hafezparast et al., 1994). In addition, mutations in the genes encoding dynein have also been observed in both fALS and sALS patients (Munch et al., 2004) and in SOD1^{G93A} mice (Bilsland et al., 2010).

Mutations in typical ALS-related genes can also be associated with defects in axonal transport. MtSOD1 interacts with the dynein-dynactin complex, disrupting its normal functioning and forming aggregates prior to the onset of symptoms, which worsens

throughout the disease (Zhang et al., 2007). Likewise, the loss of TDP43 negatively impacts axonal growth and generates changes in cytoskeletal transcriptions. Furthermore, it decreases protein synthesis and impairs mitochondrial function in the axons (Briese et al., 2020).

RNA metabolism

The discovery of TDP43, an RNA-DNA binding protein, as a major component of ubiquitinated protein inclusions in ALS patients (Neumann et al., 2006) highlighted RNA metabolism alterations as potential pathophysiological mechanisms that contribute to MN degeneration in ALS. TDP43 plays a critical role in several steps of RNA processing, including splicing, RNA stability and mRNA transport. It has been observed that TDP43 normally binds to long intronic UG-rich sequences, non-coding regions of RNA or untranslated mRNA regions. In fact, when TDP43 expression was blocked, it resulted in the alteration of 601 mRNA levels and changes in the splicing pattern of 965 mRNA transcripts, including some that are relevant to neurodegeneration (Polymenidou et al., 2011). Another study demonstrated that the removal of TDP43 leads to the inclusion of cryptic exons in an mRNA transcript called UNC13A, and interestingly, this cryptic exon was found in samples from ALS patients with TDP43 mutations (Brown et al., 2022; Ma et al., 2022). Additionally, a link has been found between RNA metabolism and axonal outgrowth. The loss of stathmin 2 (STMN2), an essential protein for axonal elongation and regeneration, occurs due to altered splicing in TDP43-KO models (Klim et al., 2019).

FUS, an RNA-binding protein, plays a crucial role in different RNA metabolism processes including transcription, alternative splicing, and nuclear-cytoplasmic mRNA transport. Under physiological conditions, it is localized in the nucleus, but in pathological conditions like ALS, FUS tends to aggregate and form cytoplasmic inclusions. These aggregates hinder FUS from carrying out its normal functions. Mutations in FUS have been identified as causes of abnormal splicing in ALS (Rezvykh et al., 2023). Indeed, FUS has been linked to more than 650 alternative splicing events, as well as alternative splicing of genes involved in neurogenesis and gene expression regulation, such as GLI family zinc finger 2 (GLI2), signal transducer and activator of transcription 3 (STAT3) and splicing factor proline- and glutamine-rich (SFPQ) (Zhou et al., 2014). MtFUS models exhibited a decrease in overall protein production and protein translation. Furthermore, upon studying the protein aggregates, it was observed that the majority of aggregated proteins were associated with translation factor activity, tRNA binding, and RNA cap binding.

Introduction

Additionally, it was also noted that fibroblasts from mtFUS-ALS patients displayed an overactivation of the nonsense-mediated decay, an mRNA surveillance system, that may have deleterious effects on stress response pathways (Kamelgarn et al., 2018). Recently, mutations in FUS have been associated with the downregulation of circRNA, a non-coding RNA involved in transcriptional regulation, protein interaction or translation enhancement (Colantoni et al., 2023).

Although C9orf72 protein does not encode an RNA-binding protein, C9orf72 is involved in RNA toxicity. One of the three proposed mechanisms to explain how mutations in C9orf72 can lead to ALS is RNA-mediated gain-of-function by sequestering essential RNA-binding proteins (RBPs) into intranuclear RNA foci. These RNA foci are aggregates of RNA and RBPs, which ultimately lead to defects in RNA processing and gene expression (Kumar et al., 2017). Actually, a distinct transcriptome profile was observed when comparing C9orf72-associated ALS and sporadic ALS to control subjects (Prudencio et al., 2015). Another proposed mechanism involves the production of dipeptide repeat protein, as commented above.

Neuroinflammation

Neuroinflammation is a common hallmark in multiple neurodegenerative diseases, including ALS, and its modulation could offer a therapeutic perspective for slowing disease progression. MN degeneration triggers the activation of microglia, astrocytes, and the complement system, which collectively contribute to the progression of the pathology. Analyses of post-mortem spinal cord tissue from sALS patients revealed the presence of inflammatory markers, including increased microglial activation, T-cell infiltration (Kawamata et al., 1992) and enhanced astroglial activation (Schiffer et al., 1996). Additionally, studies have reported elevated concentrations of certain proinflammatory mediators such as monocyte chemoattractant protein 1 (MCP-1) and IL-8 (Kuhle et al., 2009).

Microglia are the primary innate immune cells within the CNS, comprising approximately 5-12% of CNS cells (Vilhardt et al., 2017). Under physiological conditions, microglia exist in a resting state, whose primary function is to maintain homeostasis, while also participating in synaptic pruning, adult neurogenesis and modulation of neuronal networks. This highly dynamic population constantly interacts with the surrounding environment through its long ramifications. In response to stimuli, microglia undergo polarization into two distinct phenotypes: the M1 phenotype, associated with toxicity,

which releases pro-inflammatory cytokines such as NOX2, TNF- α or IL-1 β , and the M2 phenotype, known for its neuroprotective properties and it releases anti-inflammatory cytokines like IGF-1 or IL-10. However, microglial state categorization is an oversimplification since microglia show graded and context-specific responses upon activation (Geloso et al., 2017).

In the SOD1^{G93A} mice, an increased number of microglial cells have been reported as the disease progresses (Beers et al., 2011; Lewis et al., 2014; Ohgomori et al., 2016). It has been hypothesized that during the initial phases of the diseases, microglia undergo a polarization toward a neuroprotective state, but rapidly shift toward a toxic state. Nevertheless, this transition does not occur simultaneously since temporal and regional differences have been observed. In the cervical spinal cord, M2 microglia and infiltrating lymphocytes can be found for a longer period compared to the lumbar region of the spinal cord (Beers et al., 2011). Although this represents the general dynamic of microglia throughout ALS progression, a complex interplay between the two classical phenotypes is usually considered. Indeed, alongside the increase in microglial cells, it was reported an upregulation of inducible nitric oxide synthase, indicative of M1 polarization, but also an elevation in arginase-1 (Arg-1) levels, used for assessing M2 phenotype (Lewis et al., 2014). Through the examination of the released cytokines, it was found that both pro-inflammatory and anti-inflammatory cytokines were significantly upregulated during the final stages of ALS. Nevertheless, the rise in pro-inflammatory cytokines significantly outweighs the increase in anti-inflammatory cytokines (Jeyachandran et al., 2015). Additionally, there is a decrease in the microglial M1 marker CD68 and increased levels in the anti-inflammatory markers Arg-1 and TNF- α (Komiya et al., 2021). Interestingly, replacing macrophages along peripheral axons of MNs reduces proinflammatory microglial responses and upregulated genes associated with the deletion of symptoms and increase in mice survival (Chiot et al., 2020).

Although the majority of studies involving microglia have focused on SOD1 transgenic animals, models using other ALS-associated proteins also exhibit microglia changes. In the rNLS8 mice, which exhibit cytoplasmic inclusions of hTDP43 and recapitulate many features of ALS, no significant changes in microgliosis were observed despite MN loss. However, when the exposure to the hTDP43 protein was eliminated, a remarkable increase in microglia was observed which further halted MN death, suggesting a neuroprotective role of microglia (Spiller et al., 2018). Further studies using this mouse

Introduction

model revealed distinct microglial transcriptomes, with upregulated genes associated with phagocytosis or the production of neuroprotective factors (Hunter et al., 2021). In mice lacking *C9orf72*, there is an increased immune response in macrophages and microglial cells, leading to a significant upregulation of inflammatory cytokines. Interestingly, despite this enhanced immune response, there is no evidence of neurodegeneration or MN loss in these mice (O'Rourke et al., 2016).

Astrocytes are the largest cell population in the CNS and their main functions are metabolic support, ionic homeostasis, blood-brain barrier maintenance and immune modulation (Barres, 2008). In detrimental situations such as neurodegeneration, astrocytes polarize into two states, A1 and A2, similar to M1/M2 polarization of microglia. However, more than a binary choice, it should be better perceived as a spectrum. Nonetheless, it has been observed that A1 astrocytes release neurotoxic substances harmful to MNs, while A2 astrocytes have a protective effect by upregulating neurotrophic factors and anti-inflammatory cytokines (Fan & Huo, 2021).

It has been long recognized that astrocytes are closely associated with the degeneration of MNs, both in ALS patients (Schiffer et al., 1996) and in the *SOD1^{G93A}* mouse model (Levine et al., 1999). Nevertheless, astrocytes are involved in the progression, as the elimination of mSOD1 from astrocytes delays the onset of the disease (Wang et al., 2011). In addition, the deletion of astrocyte-activating factors IL-1 α , TNF α , and C1q in the *SOD1^{G93A}* mouse results in a significant decrease in astrogliosis and an increase of lifespan (Guttenplan et al., 2020). Despite the growing emphasis on the non-cell autonomous effects of astrocytes in ALS progression, it has been observed that ALS patients hiPSC-astrocytes undergo a cell-autonomous reactive transformation (Taha et al., 2022). Given the involvement of glial cells in MN degeneration, novel therapies regulating glial activation could hold promise as potential treatments (Filipi et al., 2020; Izrael et al., 2020).

Contribution of non-neuronal cells

While ALS primarily affects MNs, several studies demonstrated the impact from neighboring cells, such as astrocytes, microglia, oligodendrocytes and Schwann cells. The initial evidence of non-autonomous cell effects came from studies showing that the expression of *SOD1^{G37R}* (Pramatarova et al., 2001), *SOD1^{G93A}* or *SOD1^{G85R}* (Lino et al., 2002) exclusively in MNs did not result in motor impairment or MN degeneration in mice. Nevertheless, in chimeric animals with microglia expressing either WT or mtSOD1, it was observed that WT MNs developed ALS signs when surrounded by mtSOD1-expressing glia.

Consistently, MNs carrying mtSOD1 survived for a longer time when surrounded by a wild-type cell environment (Clement et al., 2003). This evidence highlights the significant role of non-autonomous cell effects in ALS development and progression.

To investigate whether the non-neuronal effect of microglia was involved in the onset or the progression of the disease, transgenic animals were developed to selectively suppress the expression of mtSOD1 either in MNs or in microglia. Depletion of mtSOD1 in MNs delayed the onset of the disease but had no impact on its progression. In contrast, when SOD1 was eliminated in CD11b⁺ cells, the disease progression was delayed and the mice lifespan was increased (Boillée et al., 2006), indicating that microglia accelerate ALS progression. Nonetheless, the development of a double transgenic model with 50% reduced glial reactivity in the lumbar spinal cord had no effect on MN degeneration (Gowing et al., 2008). This study raised the possibility that different states of microglia could be involved in neuroprotection or neurodegeneration. Subsequently, it was observed that early-activated microglia expressing mSOD1 display a neuroprotective profile, whereas end-stage derived mSOD1 microglia exhibit toxic properties (Liao et al., 2012).

In contrast to microglia, the generation of transgenic animals expressing mtSOD1 in astrocytes did not induce MN death (Gong et al., 2000). However, transplantation of mtSOD1-expressing astrocytes into WT rats did result in MN degeneration and increased astrogliosis, leading to impaired locomotion (Papadeas et al., 2011). Moreover, the development of transgenic rats that exclusively express human mtTDP43 in astrocytes caused progressive MN degeneration and muscle denervation, resulting in progressive paralysis (Tong et al., 2013). This highlights the non-cell autonomous effect of astrocytes in ALS. The co-culture of MNs and astrocytes obtained from mtSOD1 models (Di Giorgio et al., 2007; Nagai et al., 2007), as well as MN cultures exposed to astrocyte-conditioned medium derived from primary mouse ALS astrocytes expressing pathogenic mutant human SOD1, TARDBP or C9orf72 has been shown to reduce the viability of healthy WT MNs (Arredondo et al., 2022; Fritz et al., 2013; Mishra et al., 2020; Rojas et al., 2014). Similar results were obtained when co-culturing MNs with human (i-) astrocytes (or derived ACM), carrying mutations in SOD1 (Almad et al., 2022; Gomes et al., 2022; Meyer et al., 2014), C9orf72 (Birger et al., 2019; Meyer et al., 2014; Varcianna et al., 2019) or TARDBP (Arredondo et al., 2022) genes. The secretion of toxic factors by astrocytes, such as prostaglandins, cytokines and chemokines (Di Giorgio et al., 2008), lipids, metabolites, microRNAs and extracellular matrix proteins (Ng & Ng, 2022), has been implicated in the

Introduction

degeneration of MNs. Another factor that has been identified is poly-phosphate (polyP). Increased levels of polyP have been observed in ACM derived from ALS-astrocytes, as well as in the tissue and CSF of both sALS and fALS patients (Arredondo et al., 2022). Additionally, the astrocytic non-cell autonomous effect has been associated with ALS-related MN degeneration including hyperexcitability (Fritz et al., 2013) or oxidative stress (Rojas et al., 2014) and involvement of specific signaling pathways such as c-Abl signaling (Rojas et al., 2015), apoptosis regulator BAX (Nagai et al., 2007), apoptosis inducer TNF receptor superfamily member 21 (TNFRSF21) (Mishra et al., 2020) or necroptosis effectors RIP1 or MLKL (Re et al., 2014). Given the significant release of toxic factors by astrocytes, some authors propose investigating the diseased astrocyte secretome through proteomics, transcriptomics, metabolomics, and lipidomics approaches to reshape the astrocyte secretome with the aim of identifying novel therapeutic strategies (Ng & Ng, 2022).

Oligodendrocytes, the myelinating cells in the CNS, play a crucial role in providing metabolic support to neurons. Emerging evidence suggests the involvement of oligodendrocytes in MN degeneration. Deficits in myelin structures have been observed in the spinal cord of SOD1^{G93A} mice (Kang et al., 2013) as well as in ALS patients (Philips et al., 2013). Co-cultures of human oligodendrocytes from ALS patients carrying SOD1, TDP43, FIG4 and C9orf72 mutation with MNs have shown a significant decrease in MN survival (Ferraiuolo et al., 2016). Furthermore, the selective depletion of mtSOD1 from oligodendrocytes significantly delayed disease onset and increased survival in ALS mice (Kang et al., 2013). Notably, myelin deficits precede the symptomatic phase in SOD1^{G93A} mice, indicating that oligodendrocyte alterations may occur prior to MN degeneration and directly contribute to disease exacerbation (Bonfanti et al., 2020). Dysfunction of oligodendrocytes in ALS pathology has been associated with several pathological processes, including the presence of aggregates, potential dysfunction in myelin-related mRNA processing or reduced metabolic and trophic support from oligodendrocytes to neurons (*reviewed in Raffaele et al., 2021*).

Schwann cells have been implicated in the pathogenesis of ALS, although the precise mechanisms remain poorly understood. Studies have shown contrasting effects when examining specific mutations in Schwann cells. The expression of SOD1^{G93A} exclusively in Schwann cells did not significantly impact motor function or mouse survival (Turner et al., 2010). Conversely, another group reported that reducing active SOD1^{G37R} levels by 70% in

Schwann cells accelerated disease (Lobsiger et al., 2009). A third group reported that knockdown of SOD1^{G85R} in Schwann cells delayed disease onset and extended survival (L. Wang et al., 2012). Although the precise role of Schwann cells in ALS remains unclear, presymptomatic muscular denervation is accompanied by Schwann cell disorganization and morphological changes in the SOD1^{G93A} mouse (Carrasco et al., 2016). Furthermore, through high-density oligonucleotide microarray analyses in the same model, it has been demonstrated that genes associated with cell death, oxidative stress and mitochondrial function are deregulated in the sciatic nerve (Alves et al., 2015). Indeed, studies have revealed that inflammation of peripheral nerves in ALS patients and SOD1^{G93A} rats is driven by Schwann cells through the expression of colony-stimulating factor-1 (CSF1) and IL-34 (Trias et al., 2020).

MN vulnerability

It is well established that different populations of MNs exhibit varying vulnerability in ALS. Among the brainstem lower MNs, the hypoglossal MNs are the first to degenerate, leading to difficulties in speech, swallowing and breathing, which are typical symptoms of ALS of bulbar onset. Conversely, oculomotor MNs withstand the disease progression until the late stages, allowing for the maintenance of eye movements. As for the spinal lower MNs, α -MNs are primarily affected, with the specific type determining the speed of degeneration. The MNs in Onuf's nucleus are resistant to degeneration, thereby preserving sexual and bladder function (Rochat et al., 2016; Ragagnin et al., 2019).

There is a gradient of degeneration within the α -MNs. The fast-twitch fatigable MNs are the first to degenerate prior to the symptomatic phase in the SOD1^{G93A} mice. In a subsequent wave of degeneration, the fast-twitch fatigue-resistant MNs are affected, followed by the slow-twitch fatigue-resistant MNs, which remain relatively preserved until the later stages of the disease (Hegedus et al., 2007; Hegedus et al., 2008). The reason for this differential vulnerability is not clear, although several mechanisms and pathways could be involved in the process. One possible explanation for this differential vulnerability could be the role of interneurons. Under physiological conditions, interneurons can inhibit both fast-twitch fatigable MNs and slow-twitch fatigue-resistant MNs through glycine inhibition. However, in the SOD1^{G93A} mouse, it has been observed that this inhibition is lost during the progression of the disease, occurring first in the fast-twitch MNs and subsequently affecting the slow-twitch MNs (Allodi et al., 2021). Another possible mechanism, which is not necessarily exclusive, is the presence of neuronal matrix

metalloproteinase-9 (MMP-9). This protein is upregulated in fast MNs but not found in slow MNs, oculomotor MNs and the Onuf's nucleus, suggesting that its absence may provide some form of resistance in ALS. Furthermore, studies have shown that offspring from crossing SOD1^{G93A} mice with MMP-9 null mice maintain the neuromuscular junctions of muscles innervated by fibers dependent on fast MNs, leading to increased survival (Kaplan et al., 2014). In line with this, knocking-down MMP-9 in rNLS8 mice promotes MN survival and preserves functional neuromuscular junctions (Spiller et al., 2019). Nevertheless, MMP-9 is not the only protein that is differentially expressed, GABA_AR- α 1, parvalbumin, and soluble guanylate cyclase subunit alpha-3 are predominantly expressed in oculomotor MNs. On the other hand, dynein, peripherin, and GABA_AR- α 2 are expressed in spinal and hypoglossal MNs. Therefore, a distinct pattern of protein expression is observed between vulnerable and resistant MNs, which could partially explain the resistance of some MNs to degeneration in ALS (Comley et al., 2015). These findings are consistent with previous results where differential transcriptional profiles were observed between the oculomotor nucleus and the spinal cord using microarray analysis. Among the genes of interest, the upregulation of the Glu2 subunit of AMPA receptors was noted, which renders these oculomotor MNs less permeable to Ca²⁺ ions. Additionally, there was an upregulation of GABA_A receptor subunits, leading to a significant increase in inward Cl⁻ currents. These molecular changes contribute to the increased resistance of oculomotor MNs to excitotoxicity (Brockington et al., 2013). Despite the identification of these differential mechanisms as potential contributors to the different vulnerability of MNs in ALS, there are other factors that remain to be explored such as excitatory-inhibitory synaptic imbalance, MN excitability properties, aspects related to metabolic specialization and motor unit size (Mancuso & Navarro, 2015).

3. Models of ALS

Considering the fatality of ALS, the use of experimental models is necessary to elucidate the pathogenic mechanisms associated with MN degeneration as well as potential therapies. Over the years, *in vitro* and *in vivo* models mimicking ALS symptoms have been generated, and although each model has its advantages and limitation, they are valuable tools for ALS research.

3.1 *In vitro* models

The simplest model is cell lines, which enable the understanding of specific cellular mechanisms of neurotoxicity. The most commonly used cell line in ALS research is NSC-34,

a hybrid cell line resulting from fusing neuroblastoma cells N18TG2 with MN-enriched spinal cord cell preparations. NSC-34 expresses morphological and physiological properties of primary MNs, such as the generation of action potential, cytoskeletal organization and axonal transports. Additionally, upon differentiation, they can express specific MN markers including ChAT, GAP-43 or chromogranin B (Cashman et al., 1992). They also express glutamate receptor subunits, but interestingly, these cells are not susceptible to glutamate-induced excitotoxicity, as no detrimental effects on NSC-34 survival are observed even at concentrations of glutamate that are 1000 times higher than those considered toxic for other cell types (Hounoum et al., 2016). While these cells are not suitable for studying glutamate-dependent excitotoxicity, they do provide a valuable model for investigating pathological mechanisms associated with ALS. For instance, they have been utilized to examine the prion-like effect of SOD1^{G93A} mutation (Bartlett et al., 2022), as well as the toxicity and functional changes associated with the overexpression of ALS-related proteins like SOD1^{G93A} (Gomes et al., 2010) or C9orf72 (Jiménez-Villegas et al., 2022). This enables the association of specific mutations with pathological processes implicated in the pathophysiology of ALS, such as redox mechanisms, mitochondrial dysfunction and protein aggregation.

Another commonly used *in vitro* model for ALS research is the primary culture of MNs isolated from mouse or rat embryos. The primary limitation of this culture is its relatively short maintenance period, usually lasting only a few weeks. Additionally, these MNs are in an immature state, and several authors have raised concerns about their suitability for studying ALS since it affects fully mature MNs. However, this issue is often addressed by supplemented medium and trophic support (Bucchia et al., 2018). Nonetheless, these primary MN cultures offer significant advantages in research as they allow for the analysis of specific mechanisms occurring in MNs and provide a reliable platform for screening potential therapeutic interventions (Bucchia et al., 2018). Primary co-culture of MNs and glial cells provided information on the interactions between these two cell types (Phatnani et al., 2013). This approach has been a useful tool for studying the non-autonomous cell effects of glial cells on MNs in ALS (see above in Contribution of non-neuronal cells).

A more complex and physiological model is the spinal cord organotypic culture (SCOC), which accurately preserves the anatomical organization of the neuronal circuitry enabling the investigation of electrophysiological changes. This model also maintains the

neuronal/non-neuronal stoichiometry, thereby allowing for the study of glial cell interactions with MNs. SCOCs have proven to be highly suitable for studying glutamate-induced excitotoxicity. Well-established SCOC models have been developed using either direct exposure to glutamate (Guzmán-Lenis et al., 2009) or the selective inhibitor of glutamate transport, DL-threo- β -hydroxyaspartic acid (THA) (Rothstein et al., 1993). This model allows for evaluating MN degeneration and assessing the neuroprotective capabilities of new therapies (Gaja-Capdevila et al., 2021; Herrando-Grabulosa et al., 2016).

Although these previous models allow us to study the pathophysiology of the disease, none of them exhibit a high translational capacity. Therefore, in recent years, the use of induced pluripotent stem cells (iPSC) is booming. Using the 4 Yamanaka transcription factors (Oct4, Sox2, c-Myc, and Klf4), fibroblasts from patients can be derived in iPSC, which have then the ability to differentiate into several neural cell subtypes, such as MNs, astrocytes, oligodendrocytes or Schwann cells (Richard & Maragakis, 2015). The majority of iPSCs involved in ALS research have been derived from patients with well-known mutations associated with ALS, such as SOD1, TDP-43 or C9orf72. However, it is important to note that these mutations are only present in a small percentage, approximately 10%, of ALS patients. Therefore, in order to establish models that encompass a broader proportion of patients, iPSCs derived from sALS patients were also developed (Fujimori et al., 2018).

3.2 *In vivo* models

The discovery of mutations in genes causing ALS has facilitated the development of transgenic animals that recapitulate human disease symptoms. The identification of the first mutation in the gene encoding the SOD1 protein (Rosen et al., 1993) has positioned animal models based on this protein mutation as the most commonly employed in ALS research. A transgenic animal was generated through the induction of genetic expression, specifically by constitutively substituting a glycine with an alanine at position 93 in the protein SOD1 (SOD1^{G93A}). These animals displayed hind limb weakness starting from the third month of life, progressing to complete muscular paralysis, and ultimately resulting in death at 5-6 months of age. These manifestations correlate with loss of MNs in the spinal cord (Gurney et al., 1994). Moreover, SOD1^{G93A} mice showed dysfunction of both spinal and cortical MNs before the locomotion deficits (Mancuso et al., 2011). Although the SOD1^{G93A} model is the most commonly used, it is not the only mouse generated from mutations in the SOD1 protein. Other examples include SOD1^{G37R}, SOD1^{D90A} and SOD1^{G85R} (Gois et al., 2020). All

these models exhibit MN degeneration accompanied by motor deficits, although the onset and progression of symptoms may vary. These variations depend on factors such as the specific mutation, the number of copies of the mutation, the genetic background and sex (Mancuso et al., 2012b).

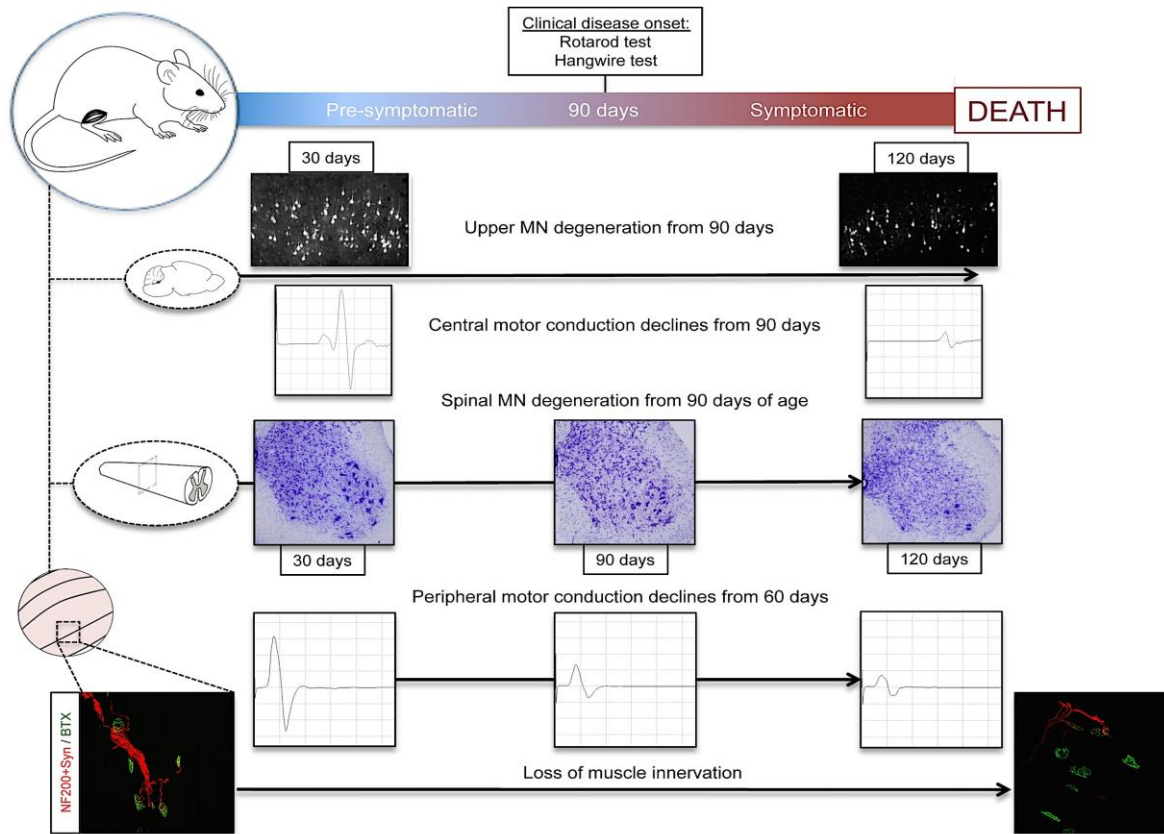


Figure 2. Main clinical and histopathological hallmarks of ALS progression in the *SOD1^{G93A}* transgenic mice. Progressive degeneration of upper and lower MN is accompanied by a decline in both central and peripheral motor conduction. Furthermore, a loss of muscular innervation can be observed. Extracted from Mancuso & Navarro (2015).

Different models based on mtTDP43 have also been developed, exhibiting variable phenotypes and MN degeneration. One of the early models involved the constitutive introduction of a mutated human TDP43 protein, with an alanine replaced by threonine at position 315 (TDP43^{A315T}). These animals exhibit ubiquitinated protein aggregates in spinal MNs along with severe motor deficits. Interestingly, they do not show cytoplasmic TDP43 aggregates (Wegorzewska et al., 2009). In contrast, TDP43^{N390D} mice exhibit cytoplasmic aggregates of TDP-43 together with alteration in autophagy and proteasome activity, MN degeneration and motor dysfunction (Huang et al., 2020). Surprisingly, mice overexpressing the TDP43^{WT} protein also exhibit ubiquitinated and phosphorylated TDP43 aggregates that coincide with the extremely rapid progression of the disease, manifested by decreased

Introduction

cortical and spinal MNs, increased astrogliosis, motor deficits and reduced survival (Wils et al., 2010).

The high prevalence of ALS forms caused by C9orf72 mutations has generated significant interest in investigating the pathogenic mechanisms associated with the G4C2-repeat expansion, hence the need to generate C9orf72 models. The first G4C2-repeat expansion mouse model was generated using AVV2/9 and these animals exhibited coordination impairment but no MN degeneration (Chew et al., 2015). Subsequently, the bacterial artificial chromosome (BAC) DNA clone containing different regions of the human C9orf72 was employed. Different outcomes were observed depending on the introduced exons and G4C2 copies (Batra & Lee, 2017). In some studies, authors reported RNA foci presence without MN degeneration or motor function abnormalities (O'Rourke et al., 2015; Peters et al., 2015). Other models displayed mild neurodegeneration (Jiang et al., 2016). Finally, a model incorporating all 11 exons of the C9orf72 gene and over 850 G4C2 copies was generated, exhibiting slight loss of force, muscle denervation, MN loss, reduced lifespan and TDP43 aggregates (Y. Liu et al., 2016).

The Wobbler mouse was proposed as an alternative experimental model of ALS due to its ability to recapitulate many of the symptoms observed in the disease. These mice display locomotion deficits, MN degeneration, astroglial and microglial reactivity and muscular denervation. At molecular levels, they exhibit elevated expression of the TDP43 protein, which forms cytoplasmatic aggregates, impaired axonal transport, ER stress and alterations in mitochondrial structure and function (Moser et al., 2013).

Using mice generated based on mutations in ALS-related genes represent only a small fraction of ALS cases. Therefore, developing novel animal models that can encompass a broader spectrum of cases would present a more optimal avenue. A novel model approach involves the use of humanized mice. Initially, it was demonstrated that the transplantation of derived-glial-rich neuronal progenitors for human iPSC in the lumbar cord of SOD1^{G93A} improved motor function and survival (Kondo et al., 2014). Recently, chimeric models have been established in which human iPSC-derived microglia is transplanted into the brain to study its effects (Fattorelli et al., 2021; Hasselmann et al., 2019). Considering the role of microglia in the progression of the disease, the transplantation of iPSC-derived microglia from ALS patients into WT mice would be a chimeric model that would provide valuable information about the disease, as well as options for developing therapies with high translational potential.

4. GRT-X

The GRT-X compound (N-[(3-fluorophenyl)-methyl]-1-(2-methoxyethyl)-4-methyl-2-oxo-(7-trifluoromethyl)-1H-quinoline-3-carboxylic acid amide) is a small molecule whose main characteristic is the ability to activate the neuronal potassium channel Kv7.2/3 and the glial protein TSPO. Unpublished preliminary data obtained by Grünenthal, the pharmaceutical company that developed the compound, show that GRT-X is capable of activating the neuronal Kv7.2/3 channels with high efficiency ($EC_{50} = 0.37 \mu\text{M}$) generating a potent hyperpolarization. Additionally, the GRT-X compound exhibits a high affinity for the glial protein TSPO in rats ($K_i 66 \text{ nM}$) and in humans (4600 nM).

GRT-X was originally discovered as a novel analgesic in a model of neuropathic pain and its anti-hyperalgesic effect was attributed, in part, to the activation of TSPO and, in part, to the activation of Kv7.2/3 (unpublished data). Furthermore, this analgesic effect was also demonstrated in a diabetic neuropathy model (Bloms-Funke et al., 2022a). Additionally, in a crush lesion of cervical spinal nerves in rats, GRT-X acted as a neuroprotectant and promoted neuroregeneration by enhancing neuronal survival, accelerating the growth of MNs and sensory neurons, as well as expediting the recovery of normal behavior and sensory responses to cold, heat and mechanical stimuli (Bloms-Funke et al., 2022a). Moreover, in an epilepsy model (6-Hz), GRT-X demonstrated remarkable efficacy in reducing seizures. The authors attributed this effect to the activation of Kv7.2/3 channels, which generates hyperpolarization, effectively preventing hyperexcitability. Additionally, the increased production of allopregnanolone contributes to enhanced GABAergic inhibition at both synaptic and extrasynaptic receptor sites, further increasing the anti-seizure effect (Bloms-Funke et al., 2022b). Therefore, due to its unique pharmacological profile, which includes the ability to reduce hyperexcitability and generate neurosteroids that are neuroprotective, GRT-X was repurposed as a novel therapy for ALS.

4.1 TSPO

Translocator protein TSPO, formerly known as peripheral benzodiazepine receptor (PBR) is an 18 kDa protein located in the OMM, specifically concentrated at outer/inner mitochondrial membrane contact sites (Scarf et al., 2009) in association with VDAC and the adenine nucleotide carrier (ANT) (Mcenery et al., 1992). TSPO is composed of 169 highly conserved amino acid residues. It is structured into 5 transmembrane α -helical domains, where the amino terminus is located in the mitochondrial periplasm and the carboxyl-terminal in the cytoplasm (Joseph-Liauzun et al., 1998). Initially, it was thought

Introduction

that TSPO forms complexes of four to six molecules creating a single pore (Boujrad et al., 1996), but it seems that the TSPO functional form is a dimer (Caballero et al., 2013). TSPO is found in nearly all tissues, although its expression levels vary, being the highest levels found in steroidogenic regions such as adrenal and gonadal tissues. In the CNS, TSPO expression is relatively low and primarily limited to glial cells, although it is also expressed in tanycytes and certain neuronal populations (Lee et al., 2020c; Rupprecht et al., 2010).

Functions of the TSPO

TSPO function has been widely associated with steroidogenesis due to its high presence in steroid-synthesizing tissues, the presence of a cholesterol recognition/interaction amino acid consensus (CRAC) sequence (Li & Papadopoulos, 1998), changes in steroidogenesis when TSPO agonists or antagonists are added (Mukhin et al., 1989; Papadopoulos et al., 1990) or steroidogenesis alterations caused in conditional TSPO-KO mice (Fan et al., 2015; Farhan et al., 2021).

TSPO is believed to play a crucial role in the initial step of cholesterol transport, which involves transferring cytoplasmic cholesterol into the mitochondria for steroid generation. The exact mechanism by which cholesterol is transported across the OMM is not yet fully understood. One possible hypothesis suggests that cytosolic proteins such as steroidogenic acute regulatory protein (StAR) StARD4 and StARD5 bind to free cholesterol in the cytoplasm and transport it to the OMM. Once there, it may bind to the CRAC motif of TSPO, which acts as a pore to facilitate the transfer of cholesterol from the OMM to the inner mitochondrial membrane (IMM) (Papadopoulos et al., 1997). The IMM is where the P450_{scc} or CYP11A1 protein is located, responsible for catalyzing the initial conversion of this pathway, transforming cholesterol into pregnenolone (Liang & Rasmuson, 2018). However, there are alternative hypotheses suggesting that TSPO might not be directly involved in this process and that the StAR protein itself may be responsible for transporting cholesterol to the mitochondria and introducing it into the IMM (Miller & Auchus, 2011). Interestingly, StAR-KO mice exhibited reduced levels of steroids indicating the essential role of this protein in cholesterol transport (Hasegawa et al., 2000).

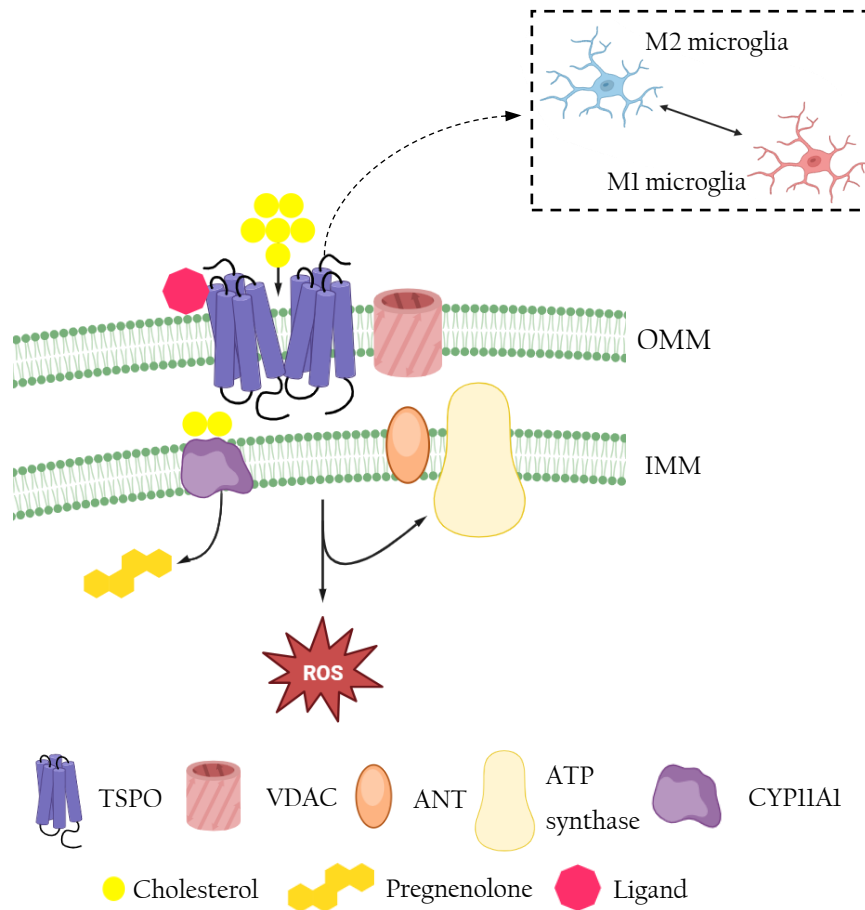


Figure 3. Functions TSPO has been associated to. TSPO, which is localized at the OMM, has been associated with different cellular functions. TSPO is thought to have a role in the first step of steroidogenesis allowing the entrance of cholesterol into the mitochondria. Furthermore, ligands of TSPO modulate differentially ROS levels. TSPO ligands can also modify ATP production as well as metabolism. Additionally, TSPO is usually used as a neuroinflammation marker, and it can influence both M1 and M2 polarization.

Controversially, conditional TSPO-KO models were generated in Leydig cells (Morohaku et al., 2014), as well as global TSPO-KO models (Banati et al., 2014; Tu et al., 2014) where TSPO expression was completely eliminated and no alterations were observed in steroid levels such as testosterone (Morohaku et al., 2014; Tu et al., 2014), estradiol (Tu et al., 2014) or progesterone (Banati et al., 2014; Tu et al., 2014). During these studies, the question arose whether the TSPO homolog, TSPO2, could have a compensatory effect. TSPO2 exhibits variations compared to TSPO, as it is expressed in the ER and nuclear membrane. It was demonstrated that TSPO2 expression did not change when TSPO is deleted, indicating no such compensatory effect (Banati et al., 2014). Indeed, it was shown that TSPO2 plays a role in distributing cholesterol during erythropoiesis in the bone marrow (Fan et al., 2009) and coordinates maturation and proliferation of erythroblasts (Kiatpakdee et al., 2020). Therefore, these studies demonstrated that TSPO was not

Introduction

essential for steroidogenesis, although there are other authors who indicate the opposite, suggesting that TSPO is crucial in this process. Thus, while it is evident that TSPO plays a role in steroidogenesis, the extent of its essentiality remains uncertain.

However, steroidogenesis is not the only function associated with TSPO. One of the most commonly associated functions of TSPO is neuroinflammation. While TSPO is typically poorly expressed under normal conditions (Chen & Guilarte, 2008; Veenman et al., 2008) in pathological conditions such as stroke, encephalitis, gliomas and neurodegenerative diseases (ALS, Parkinson's disease, Huntington, Alzheimer's disease and multiple sclerosis) enhanced TSPO levels have been reported mainly in glial cells but also in neurons (Papadopoulos et al., 2006; Chen and Guilarte, 2008; Veenman et al., 2008). In fact, TSPO has become a widely used marker for neuroinflammation and microglia activation (Guilarte et al., 2022) and it has been employed to detect *in vivo* glial activation in ALS patients (Zürcher et al., 2015). Interestingly, it has been demonstrated that the enhanced expression of TSPO could be an adaptive response mechanism. Studies have shown that the overexpression of TSPO reduces the production of pro-inflammatory cytokines and increases the expression of genes associated with the alternatively activated M2 stage. On the other hand, the knockdown of TSPO has the opposite effect, leading to increased pro-inflammatory responses (Bae et al., 2014). However, it was demonstrated that TSPO KO inhibits microglia M1 polarization and microglia M2 state activation (Yao et al., 2020).

Another function that has long been associated with TSPO is mitochondrial bioenergetics (Hirsch et al., 1998). In mouse microglial cells, it has been observed that the TSPO KO decreases mitochondrial membrane potential (Bader et al., 2019), as well as reduces oxygen consumption, and ATP production (Banati et al., 2014; Yao et al., 2020). The authors of this last study suggest a possible link between TSPO and the F_0 subunit of ATP synthase, mediated by the exchange of ions between VDAC and ANT, proteins that interact with TSPO (Banati et al., 2014). In glioma cells, it has been observed that TSPO- KO inhibits mitochondrial function, leading to a decrease in oxidative phosphorylation. This is accompanied by an increase in glycolytic metabolism, enhanced glucose uptake and its conversion to lactic acid (Fu et al., 2020). However, a study culturing microglia from TSPO- KO mice demonstrated that glycolytic metabolism is reduced, along with oxidative phosphorylation (Yao et al., 2020). Interestingly, when TSPO was transfected into Jurkat cells, a cell type that does not express TSPO, it was observed that these cells increased

mitochondrial ATP production and upregulated genes involved in mitochondrial respiration (Liu et al., 2017).

Considering the localization of TSPO, it is not surprising that it may also be involved in the production of ROS. Different TSPO ligands lead to an increase in ROS production in astrocyte, microglia and neuron cultures (Jayakumar et al., 2002). Furthermore, it has been demonstrated that overexpression of TSPO disrupts the TSPO:VDAC ratio, resulting in elevated ROS levels that hinder the relocation of sequestosome 1 (SQSTM1/p62), inhibiting the ubiquitination of proteins and leading to mitochondrial dysfunction (Gatliff et al., 2014). In glioma cells, TSPO-KO also leads to increased ROS production (Fu et al., 2020). Interestingly, there may be a bidirectional effect, as it has been observed that elevated ROS levels can induce an increase in TSPO expression. This effect is likely due to TSPO's ability to interact with the subunits of the NADPH oxidase 2 (NOX2) protein, which is responsible for generating ROS (Loth et al., 2020).

TSPO activation as potential ALS therapy

Olesoxime, also known as TRO19622, is a cholesterol-like compound and a ligand of TSPO. In primary cultures of MNs in the absence of neurotrophic factors, concentrations ranging from 0.1 to 10 μ M demonstrated a dose-dependent rescue of MNs (Bordet et al., 2007). Additionally, Olesoxime increased the survival of human MN derived from ALS-patient-iPSC (Yang et al., 2013). The researchers also assessed the effect of Olesoxime in the SOD1^{G93A} mice and observed a delay in disease onset as determined by a slower decline in body weight loss and better performance in the grid test. Furthermore, treatment with Olesoxime significantly increased the lifespan of the mice, resulting in a 10% extension compared to vehicle-treated mice. Based on these results, the authors concluded that the effect of Olesoxime primarily impacted disease onset rather than its progression (Bordet et al., 2007).

Subsequently, a more exhaustive study of Olesoxime in the SOD1^{G93A} mouse model was conducted. In contrast to the previous study, the drug was administered via pellets and not through subcutaneous administration. This study revealed that Olesoxime preserved the integrity of neuromuscular junctions and reduced microglial and astroglial activation. Furthermore, it attenuated MN loss by more than 20%. However, it only prevented the death of those undergoing FasL-induced death, showing no efficacy against death triggered by sLIGHT, two distinct death signaling pathways involved in ALS that affect different types of MNs (Sunyach et al., 2012).

Based on the promising results obtained in previous studies, where Olesoxime demonstrated a reduction in MN degeneration, maintained the integrity of neuromuscular junctions and decreased glial reactivity and, most importantly, extended survival, it was evaluated in a phase II-III clinical trial. The trial involved 512 patients aged 18-80 with El Escorial criteria of defined or probable ALS who were already receiving Riluzole treatment. The study lasted 18 months, with the primary efficacy outcome being survival. Secondary measures included ALSFRS-R and slow vital capacity (SVC). Unfortunately, no significant differences in survival were observed between the Olesoxime group and the placebo group. Additionally, there were no significant differences between the groups in terms of ALSFRS-R and SVC (Lenglet et al., 2014).

4.2 Kv7.2/3

Potassium channels play a pivotal role in a multitude of functions, including frequency and duration of the action potential, modulation of membrane potential, muscle contraction, neurotransmitter release and hormonal secretion. Over 80 different potassium channel variants have been identified and categorized into five families: 1) Voltage-gated potassium channels, 2) Inwardly rectifying potassium channels (Kir), 3) Tandem pore domain potassium channels (K2P), 4) Slo family, and 5) Ca^{2+} -activated SK family (SKCa) (González et al., 2012; Kuang et al., 2015). The voltage-gated potassium channels comprise a family that is divided into two groups based on their structure and functionality. On one hand, there are channels involved in conductivity (Kv1-4, Kv7, Kv10-12, EAG, and ERG), participating in the generation and propagation of action potentials in excitable cells. On the other hand, there is the nonconducting group of gating modulators (Kv5-6, Kv8-9), which are not directly involved in generating ion currents but play a significant role in regulating and modulating the activity of other potassium channels (González et al., 2012). The Kv7 family is a five-member K^+ channel encoded by KCNQ genes. While Kv7.1 is mainly expressed in the heart, Kv7.2-Kv7.5 channels are expressed in the nervous system. For the channel to be functional, four KCNQ subunits need to assemble. All KCNQ subunits can form homomeric channels, or heteromeric channels formed by specific combinations, such as Kv7.2/3 or Kv7.2/5 (Jentsch, 2000).

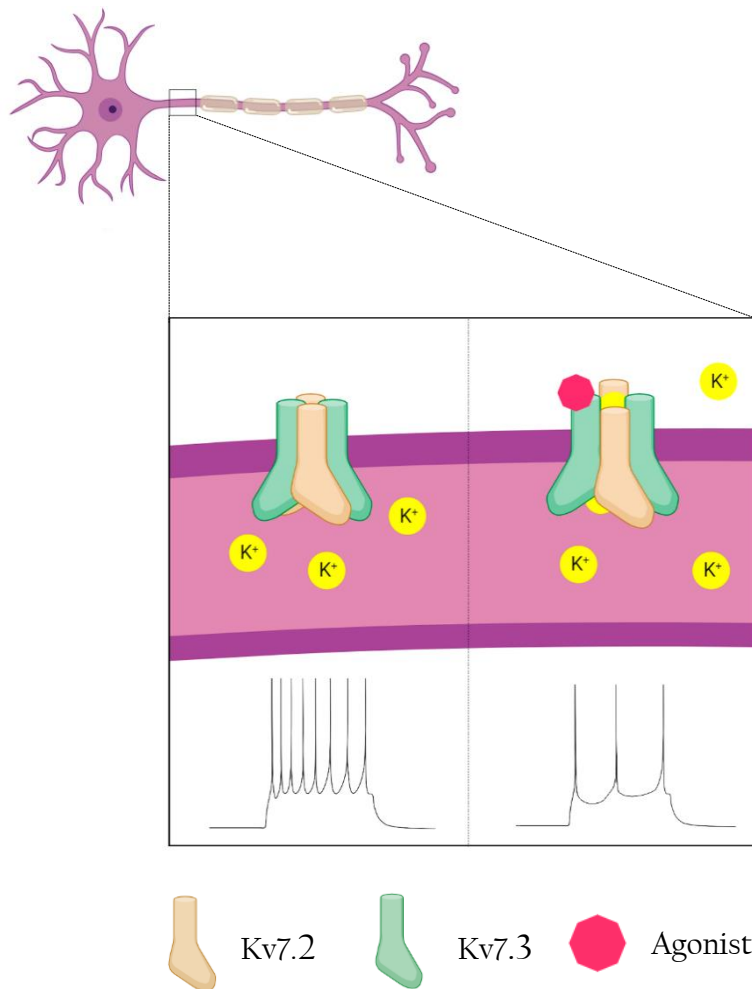


Figure 4. Kv.2/3 agonist reduces hyperexcitability. In situations of hyperexcitability, as found in ALS, there is a repetitive firing of action potentials. When Kv7.2/3 agonists bind to the channel, they allow the efflux of K^+ , triggering the M-current, a strong hyperpolarizing current that reduces neuronal firing frequency, thereby regulating neuronal excitability.

Kv proteins consist of approximately 659–940 amino acids and feature six transmembrane domains. The C-terminal and N-terminal regions are located in the intracellular space. They have a remarkably long C-terminal domain, which is organized into four helices and contains the necessary domains for tetramerization. Additionally, the intracellular long C-terminal domain has binding sites for several regulatory proteins, including phosphatidylinositol 4,5-bisphosphate (PIP2), calmodulin (CaM), syntaxin 1, protein kinase A and C, and ankyrin-G (Barrese et al., 2018). Indeed, CaM binds to the B-domain of the C-terminal domain of Kv7.3 in a Ca^{2+} -dependent manner, facilitating the assembly with Kv7.2, resulting in the heteromeric functional Kv7.2/3 protein. Furthermore, in this heteromeric channel, ankyrin-G allows for the accumulation of these channels at the

Introduction

axon initial segment, a specialized region involved in the generation and propagation of action potentials in neurons (Liu & Devaux, 2014).

Mutations identified in Kv7.2 or Kv7.3 are primarily linked to epilepsy (Devaux et al., 2016; Maghera et al., 2020; Urrutia et al., 2021). Additionally, mutations in the genes encoding for these channels have been associated with long-term neurodevelopmental outcomes (Lee et al., 2020a) and pain resilience (Yuan et al., 2021).

Kv7.2 and Kv7.3 channels are clearly implicated in controlling neuronal excitability. Since neuronal excitability is one of the pathological mechanisms that can lead to the degeneration of MNs in ALS, the activation of these channels represents promising targets for reducing excitability due to several reasons: i) They function as outward channels that can be activated even at subthreshold potentials (-80 mV); ii) They play a critical role in stabilizing the membrane potential in the presence of depolarizing currents; iii) They have the ability to suppress spiking activity and reduce repetitive or burst-firing patterns; iv) They are predominantly found at the axon initial segment, making them essential regulators of action potential threshold (Brown and Passmore, 2009; Shah and Aizenman, 2014; Deardorff et al., 2021). Furthermore, the heteromeric form of Kv7.2/3 channels generates the M-current, a slowly activating and non-inactivating potassium current that effectively regulates neuronal excitability. By hyperpolarizing the membrane potential and reducing the firing rate of action potentials, the M-current exerts significant control over neuronal activity.

Kv7.2/3 activation as potential ALS therapy

Retigabine (or ezogabine) is a medication that acts as an opener of Kv7.2/3 channels and has previously been approved as an antiepileptic drug (Porter et al., 2007). Its primary effect is to reduce hyperexcitability by increasing the M-current generated by an efflux of K^+ .

In studies using rat hypoglossal MN cultures exposed to DL-threo- β -benzyloxyaspartate (TBOA), which induces strong hyperexcitability, Retigabine prevented TBOA-induced cell death. Moreover, this neuroprotective effect is accompanied by a decrease in TBOA-induced ROS production, a reduction of MN bursting and alleviation of hyperexcitability by enhancement of the M-Current (Ghezzi et al., 2018). In another study, MNs were generated from iPSC derived from fibroblasts of ALS patients harboring mutations in SOD1 (SOD1^{D90A} and SOD1^{G85R}), C9orf72, or FUS (FUS^{M511FS} and

FUS^{H517Q}). It was observed that these cells exhibited increased hyperexcitability compared to control cells. Remarkably, Retigabine effectively suppressed spontaneous action potential firing in these cells, demonstrating its potential to reduce neuronal excitability (Wainger et al., 2014). In agreement, Retigabine decreased the mean firing rates of MN-iPSC and primary mouse MN (Moakley et al., 2019).

In a cross-over trial, patients taking only Riluzole were compared to those taking Riluzole in combination with a daily dose of 300 mg of Retigabine. In this study, it was observed that Retigabine reduced the strength duration time constant while increasing the rheobase, which was attributed to a pronounced hyperpolarization of the membrane potential. Additionally, a decrease in refractoriness and refractory period was observed, consistent with membrane hyperpolarization. Despite observing changes in excitability, no significant changes were seen in the ALSFRS-R score (Kovalchuk et al., 2018).

A phase II randomized clinical trial was subsequently conducted, involving 65 patients aged 18-80 with a diagnosis of ALS based on El Escorial criteria. Patients could be either taking or not a fixed dose of Riluzole and were divided into three groups: placebo and two different doses of Retigabine, 600 mg/day or 900 mg/day. The primary outcome of the study was the measurement of short-interval intracortical inhibition (SICI), which reflects the dynamics of inhibitory cortical motor circuits. A dose-dependent increase in SICI was observed, suggesting a reduction in hyperexcitability. Furthermore, the patients in these groups showed preserved motor evoked potentials (MEP) and compound muscle action potentials (CMAP). In fact, there was a positive correlation between the increase in SICI and the increase or maintenance of CMAP amplitude. These results further support the notion of reduced hyperexcitability. Unfortunately, Retigabine did not affect disease progression, as no differences were observed between the groups in terms of ALSFRS-R or SVC. The authors attribute this lack of effect to the relatively short duration of the study, which lasted only four weeks (Wainger et al., 2021). Nevertheless, it is important to note that the FDA has issued a warning regarding the risk of retinal damage and potential vision loss associated with the use of Retigabine (*Reference ID: 3369445; accessdata.fda.gov*).

Another compound known as ICA-27243 (N-(6-chloro-pyridin-3-yl)-3,4-difluoro-benzamide) acts as a selective opener of Kv7.2/3 channels. This compound enhances the M-current and reduces excitability. However, it exhibits a lower affinity for homomeric Kv7.4 channels (Blom et al., 2010), Kv7.3 channels (Padilla et al., 2009) and heteromeric Kv7.5/3 channels (Padilla et al., 2009; Blom et al., 2010) compared to Retigabine.

Introduction

So far, there have been no published studies specifically investigating the use of ICA-27243 for treating ALS or other neurodegenerative diseases. However, there is evidence suggesting its potential effectiveness in human neuroblastoma cell line SH-SY5Y, in which ICA-27243 was found to activate the M-current, resulting in hyperpolarization. Additionally, the effects of ICA-27243 were examined in both *in vitro* and *in vivo* epilepsy models, and in both cases, the compound was found to suppress seizure-like activity (Wickenden et al., 2008). Other studies treating rodent convulsant models with ICA-27243 also demonstrated antiseizure efficacy (Roeloffs et al., 2008). Therefore, these studies provide clear evidence that ICA-27243 has the ability to hyperpolarize neurons, suggesting its potential efficacy in modulating excitability. Consequently, ICA-27243 emerges as a promising candidate for regulating excitability in ALS.

IV. Hypothesis and objectives

Currently, there is no effective treatment for ALS and the approved treatments primarily target a single pathogenic pathway involved in MN degeneration, resulting in low effectiveness in improving ALS. Consequently, novel and combinatorial therapeutic strategies are currently being pursued.

The hypothesis of this work is that the simultaneous activation of two complementary targets, the neuronal voltage-gated potassium channels 7.2/3 and the glial mitochondrial translocator protein TSPO, by the novel synthesized GRT-X chemical compound could be a novel potential therapeutic strategy for treating ALS.

The thesis's general objective is to assess if the novel dual-action compound GRT-X can significantly increase the survival and function of spinal MNs in ALS models.

To address this general aim, the thesis has been divided into four chapters with the following specific objectives:

Chapter I: ICA- 27243 improves neuromuscular function and preserves MNs in the transgenic SOD1^{G93A} mice.

- To evaluate the neuroprotective effect of the compound ICA- 27243 on spinal cord organotypic cultures (SCOCs) exposed to acute excitotoxic glutamate treatment.
- To study the effect of ICA- 27243 in the SOD1^{G93A} mice by assessing functional outcomes by means of electrophysiology and locomotion tests, histological results for MN counting, analysis of glial reactivity and preservation of muscle innervation.

Chapter II: GRT- X prevents degeneration of MN exposed to mouse and human ALS astrocyte- conditioned medium.

- To assess the effects of GRT- X on MN survival in primary ventral spinal cord neuronal cultures (VSCNs) and SCOCs exposed to:
 - Astrocyte- conditioned medium (ACM) derived from primary mouse ALS astrocytes expressing mutant human SOD1 (SOD1^{G93A}- ACM).
 - Astrocyte- conditioned medium (ACM) derived from ALS patient astrocytes generated from iPSC carrying disease-causing mutations of SOD1 (SOD1^{D90A}- ACM) or TDP43 (TDP43^{A90V}- ACM).

Chapter III: The compound GRT-X promotes neuroprotection in the SOD1^{G93A} mice.

- To determine the maximum tolerated dose of GRT-X for B6JSL mice.
- To confirm that GRT-X crosses the blood-brain barrier in mice.
- To test the potential therapeutic effect of GRT-X in the SOD1^{G93A} mice, by analyzing electrophysiology, motor function, MN survival and preservation of muscular innervation.

Chapter IV: Synergistic effect between the unimodal compounds Olesoxime and ICA-27243

- To investigate the potential synergy between Kv7.2/3 and TSPO for protecting MNs in SCOCs using the unimodal agonists, Olesoxime and ICA-27243.
- To analyze the potential synergistic effect of the two targets in the SOD1^{G93A} mice.

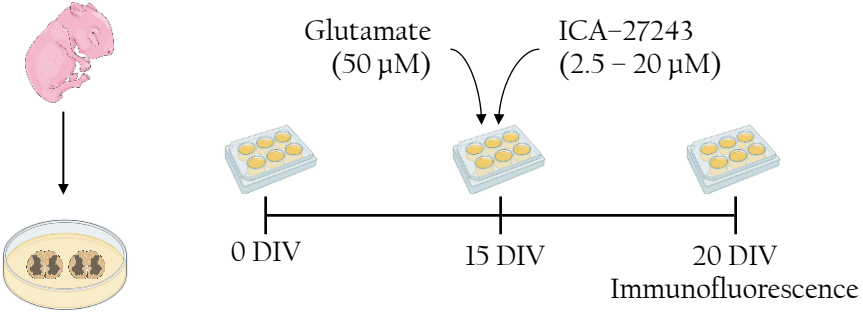
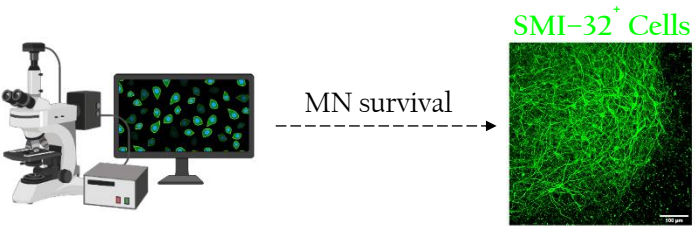
V. Study design and methodology

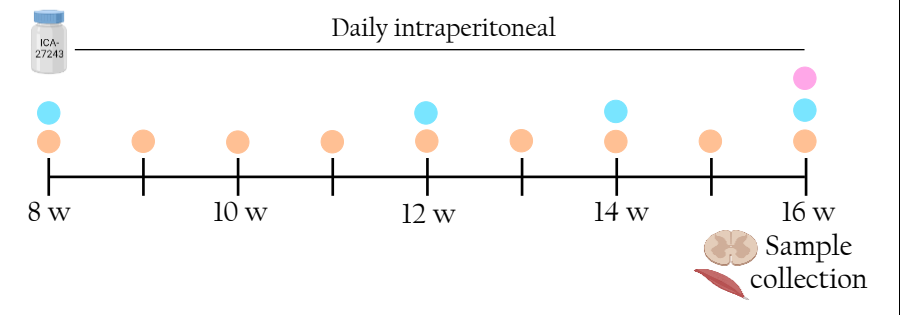



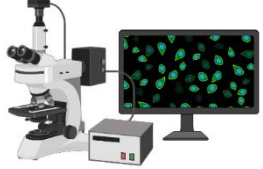
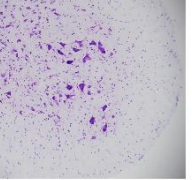
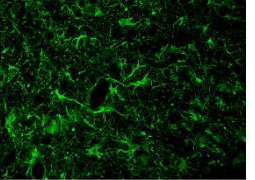
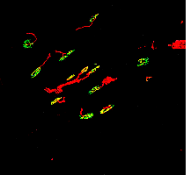
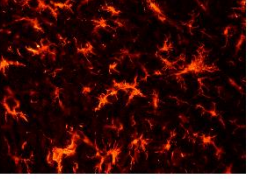
Chapter I. ICA-27243 improves neuromuscular function and preserves MNs in the transgenic SOD1^{G93A} mice

In this first chapter, the neuroprotective effects of ICA-27243 and its potential as a therapy for ALS are assessed.

Firstly, we have investigated the neuroprotective effects of ICA-27243 on MN survival in an *in vitro* MN degeneration model, using spinal cord organotypic cultures (SCOCs) exposed to acute glutamate addition to induce excitotoxic cell death.

Secondly, we treated daily female SOD1^{G93A} mice from the 8th until the 16th week of age. Throughout this period, we conducted electrophysiology and locomotion tests. After euthanasia, we evaluated MN survival, glial reactivity and preservation of neuromuscular junctions.

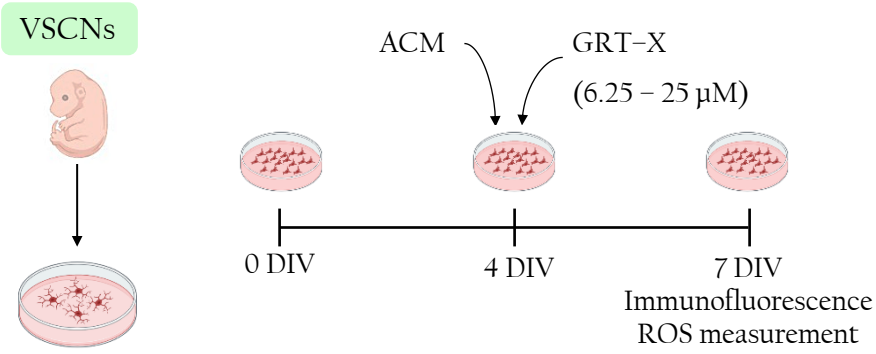
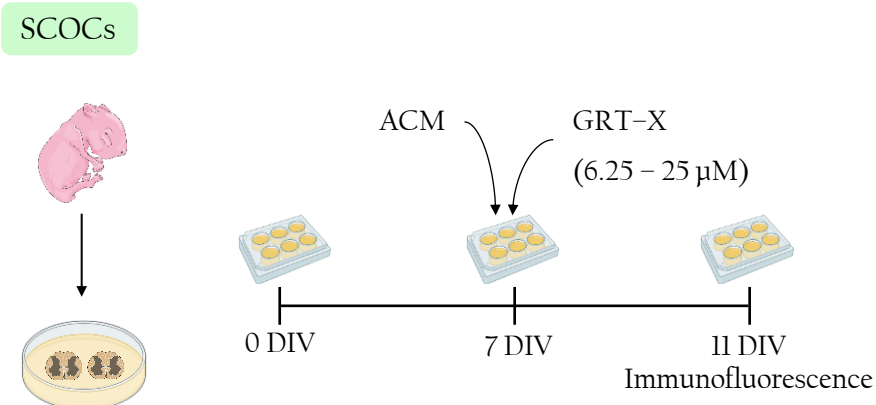
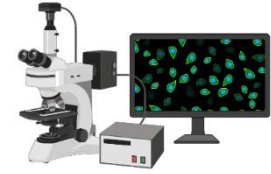
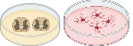
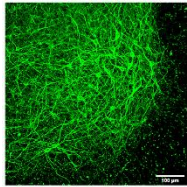

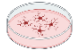
In vitro	
Animal	Sprague–Dawley rats
Age	P7–P8
Sex	♀ / ♂
Experimental design	
Histological analyses	

In vivo	
Animal	B6SJL-Tg [SOD1-G93A] 1Gur / B6SJL wild type
Age	8–16 weeks
Sex	♀
Experimental design	
Functional evaluation	<div>Electrophysiology</div>  <div>Rotarod test</div>  <div>Treadmill test</div> 
Histological analyses	<div><div>MN survival</div><div>Cresyl Violet</div><div>Glial reactivity</div><div>GFAP</div><div>NF-200 Synaptophysin α-bungarotoxin</div><div>Muscular innervation</div><div>Iba-1</div></div>

Chapter II. GRT-X prevents degeneration of MN exposed to mouse and human ALS astrocyte-conditioned medium

The main objective of this second chapter is to demonstrate the neuroprotective potential of the dual-mechanism novel drug GRT-X in two *in vitro* models.

Primary ventral spinal cord neuronal cultures (VSCNs) were prepared from rat E14 pups and spinal cord organotypic cultures (SCOCs) from rat P8 pups. Both cultures were exposed to astrocyte-conditioned medium (ACM) derived from primary mouse ALS astrocyte expressing human SOD1^{G93A} (SOD1^{G93A}-ACM) or from ALS patients astrocytes generated from induced pluripotent stem cells (iPSC) carrying ALS-causing mutations of SOD1 (SOD1^{D90A}-ACM) or TDP43 (TDP43^{A90V}-ACM). All cultures were cotreated with GRT-X. Then we evaluated MN survival by assessing SMI-32⁺ cells in VSCNs and SCOCs. Additionally, intracellular ROS/RNS levels were assessed in VSCNs.

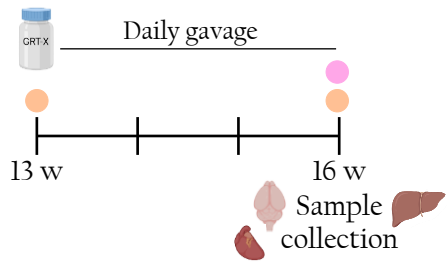
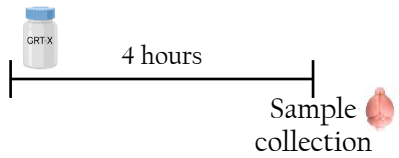

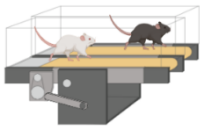
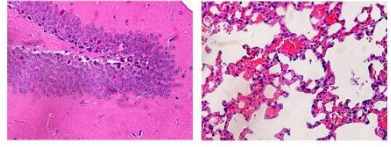

In vitro	
Animal	Sprague–Dawley rats
Age	E14 / P7–P8
Sex	♀ / ♂
Experimental design	<div><div><div>VSCNs</div></div><div><div>SCOCs</div></div></div>
Histological analyses	<div><div>MN survival</div><div><div>SMI-32⁺ Cells</div></div></div>
Molecular analyses	<div><div>ROS levels measurement</div><div>CM-H₂DCF-DA solution</div></div>

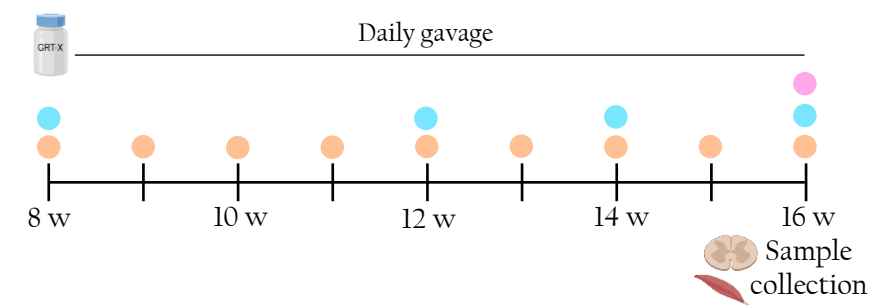


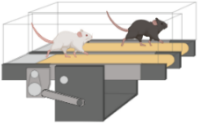
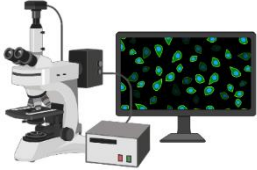
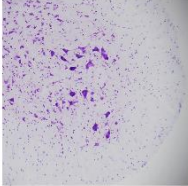
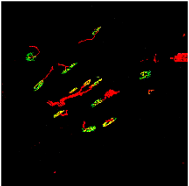
Chapter III. The compound GRT-X promotes neuroprotection in the SOD1^{G93A} mice

The third chapter of the thesis is focused on the preclinical evaluation of the therapeutic potential of GRT-X for ALS.

First, we analyzed the potential toxicity of the compound in the B6SJL mice and corroborated if it can cross the blood-brain barrier (BBB) reaching the CNS.

Second, we treated SOD1^{G93A} mice daily with GRT-X by gavage from the 8th until the 16th week of age. During this period, we performed electrophysiology and locomotion tests. Following euthanasia, we assessed MN survival and preservation of neuromuscular junctions.

<i>In vivo</i>		
Animal	B6SJL-Tg [SOD1-G93A] 1Gur / B6SJL wild type	
Age	13–16 weeks	16 weeks
Sex	♀ / ♂	♀ / ♂
Experimental design		
Functional evaluation	<div>Rotarod test</div>  <div>Treadmill test</div> 	
Histological and molecular analyses	<div>H & E staining</div> 	 <div>HPLC to analyze [GRT-X] in the brain.</div>

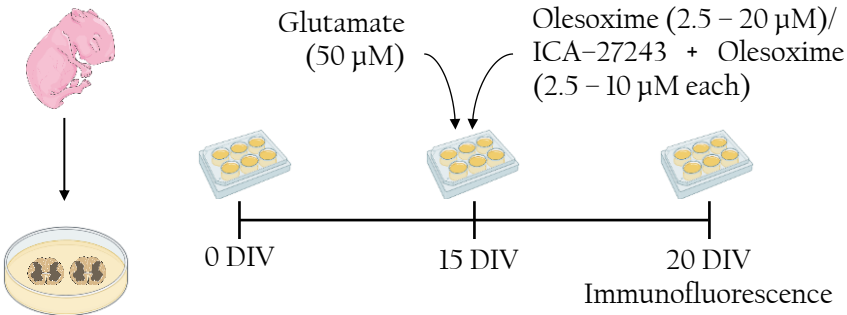
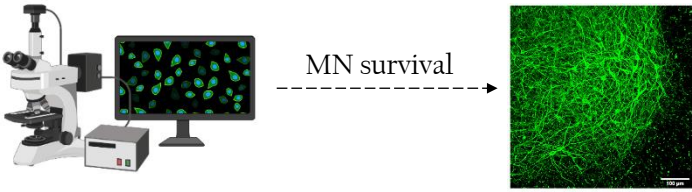
In vivo	
Animal	B6SJL-Tg [SOD1-G93A] 1Gur / B6SJL wild type
Age	8–16 weeks
Sex	♀ / ♂
Experimental design	 <p>The diagram illustrates the experimental timeline. A horizontal timeline starts at 8 weeks and ends at 16 weeks. Above the timeline, a blue bottle labeled 'GRT-X' is shown with a line indicating 'Daily gavage' from 8 weeks to 16 weeks. Below the timeline, orange dots represent weekly sample collection points at 8, 9, 10, 11, 12, 13, 14, 15, and 16 weeks. Blue dots are placed at 8, 12, and 14 weeks. A pink dot is placed at 16 weeks. At the 16-week mark, a brain icon and a red arrow labeled 'Sample collection' are shown.</p>
Functional evaluation	<div>Electrophysiology</div>  <div>Rotarod test</div>  <div>Treadmill test</div> 
Histological analyses	<div></div> <div>MN survival</div> <div>Cresyl Violet</div>  <div>Muscular innervation</div> <div>NF-200 Synaptophysin α-bungarotoxin</div> 

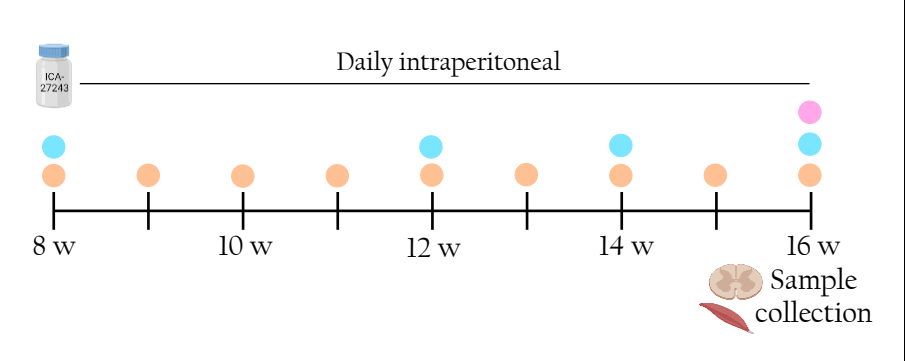



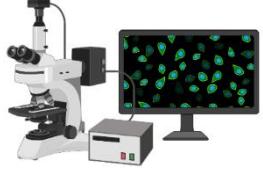
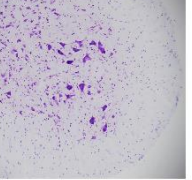
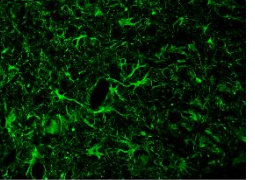
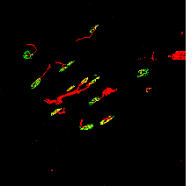
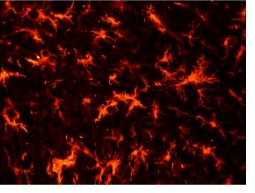
Chapter IV. Synergistic effect between the unimodal compounds Olesoxime and ICA-27243

The aim of this annex is to assess the possible synergy between the two targets used in this thesis, the glial protein TSPO and the neuronal Kv7.2/3 channel, using the unimodals agonist ICA-27243 and Olesoxime.

Initially, we determined the therapeutic potential of Olesoxime individually in SCOCs exposed to acute glutamate. Subsequently, we treated simultaneously SCOCs exposed to acute glutamate with a combination of Olesoxime and ICA-27243 to investigate the possible synergy between the targets.

Secondly, we administered daily female SOD1^{G93A} with a combination of ICA-27243 and Olesoxime from the 8th until the 16th week of age. During this period, we conducted electrophysiology and locomotion test. After euthanasia, we assessed MN survival, glial reactivity and preservation of neuromuscular junctions.

<i>In vitro</i>	
Animal	Sprague–Dawley rats
Age	P7–P8
Sex	♀ / ♂
Experimental design	 <p>The diagram illustrates the experimental timeline. It starts with a Sprague–Dawley rat at P7–P8, which is then cultured in a petri dish. At 0 DIV, cells are seeded into a 96-well plate. At 15 DIV, the cells are treated with Glutamate (50 µM) and a combination of Olesoxime (2.5 – 20 µM) and ICA-27243 + Olesoxime (2.5 – 10 µM each). At 20 DIV, immunofluorescence is performed. The timeline is marked with 0 DIV, 15 DIV, and 20 DIV.</p>
Histological analyses	 <p>The diagram shows the workflow for histological analyses. It starts with a microscope and a computer monitor displaying a field of green cells. An arrow labeled 'MN survival' points to a fluorescence micrograph showing green cells, labeled 'SMI-32⁺ Cells'.</p>

In vivo	
Animal	B6SJL-Tg [SOD1-G93A] 1Gur / B6SJL wild type
Age	8–16 weeks
Sex	♀
Experimental design	
Functional evaluation	<div>Electrophysiology</div>  <div>Rotarod test</div>  <div>Treadmill test</div> 
Histological analyses	<div><div>MN survival</div><div>Cresyl Violet</div><div>Glial reactivity</div><div>GFAP</div><div>NF-200 Synaptophysin α-bungarotoxin</div><div>Muscular innervation</div><div>Iba-1</div></div>

VI. Results

Chapter I

ICA-27243 improves neuromuscular function and preserves motoneurons in the transgenic SOD1^{G93A} mice

ICA-27243 improves neuromuscular function and preserves motoneurons in the transgenic SOD1^{G93A} mice

Vera M. Masegosa^{*,†}, Xavier Navarro^{*,†}, Mireia Herrando-Grabulosa^{*,†,‡}

* Department of Cell Biology, Physiology and Immunology, Institute of Neuroscience, Universitat Autònoma de Barcelona, Bellaterra, Spain

† Centro de Investigación Biomédica en Red de Enfermedades Degenerativas (CIBERNED), Instituto de Salud Carlos III, Madrid, Spain

Submitted to Neurotherapeutics.

ABSTRACT

Amyotrophic lateral sclerosis (ALS) is a progressive neurodegenerative disease characterized by the death of upper and lower motor neurons (MNs). Excessive neuronal excitability has been implicated in MN degeneration; thus, modulation of hyperexcitability appears as a promising therapeutic strategy. Potassium channels are attractive targets since they can be activated at subthreshold voltages and can regulate neuronal excitability. In this study, we assayed the effects of N-(6-Chloro-pyridin-3-yl)-3,4-difluorobenzamide compound, known as ICA-27243, as a potential treatment for ALS. ICA-27243 is a highly selective Kv7.2/7.3 opener used mainly in epilepsy models. In the *in vitro* model of spinal cord organotypic culture (SCOCs) exposed to acute excitotoxicity, ICA-27243 prevented MN degeneration in a dose-dependent manner. Administration of ICA-27243 to transgenic SOD1^{G93A} ALS mice improved the decline of neuromuscular function, maintained locomotion and coordination in the rotarod, decreased spinal MN death and attenuated glial reactivity. In conclusion, we report here for the first time that ICA-27243 is an effective treatment for ALS, emphasizing the potential of targeting Kv channels to reduce neuronal hyperexcitability.

Keywords: ICA-27243, amyotrophic lateral sclerosis, SOD1^{G93A} transgenic mice, motoneuron degeneration, hyperexcitability.

INTRODUCTION

Amyotrophic lateral sclerosis (ALS), the most common motor neuron disease (MND), is a fatal neurodegenerative disorder characterized by the selective death of upper and lower motor neurons (MNs). The progressive loss of spinal and cortical MNs results in muscle weakness, paralysis, and ultimately death within 2-5 years after diagnosis. Most cases of ALS are sporadic with no apparent cause (sporadic ALS, sALS), while approximately 5-10% of cases exhibit inheritance (familial ALS, fALS) with mutations in some genes such as Cu/Zn superoxide dismutase 1 (*SOD1*), hexanucleotide repeat expansions in chromosome 9 open reading frame 72 (*C9ORF72*), TAR DNA-binding protein 43 (*TARDBP*), among others (Mejzini et al., 2019).

Several physiopathological mechanisms have been identified as contributors to MN degeneration in ALS pathology, including mitochondrial dysfunction, oxidative stress, ER stress, excitotoxicity, protein misfolding, and others (Hardiman et al., 2017; Mancuso & Navarro, 2015). One of the most relevant mechanisms is neuronal hyperexcitability, a state where the neuron displays an abnormally high level of excitability, leading to a decreased threshold for firing action potentials when the neuron is stimulated (Starr & Sattler, 2018). Hyperexcitability induces massive Ca^{2+} inflow through voltage-dependent Ca^{2+} channels, damaging the cells by triggering calcium-dependent proteases, lipases and nucleases (Van Den Bosch et al., 2006). Different causes have been proposed for this hyperexcitability, including an increase in Na^+ conductance and decreased K^+ conductance (Kanai et al., 2006; Kuo et al., 2005), loss of inhibitory function in GABAergic and glycinergic interneurons (Allodi et al., 2021) and disruptions in K^+ homeostasis due to perisynaptic astrocyte dysfunction (Do-Ha et al., 2018). Hyperexcitability has been found in both ALS patients and ALS animal models (J. S. Bae et al., 2013). Moreover, studies have demonstrated hyperexcitability occurs in the early stages of the disease, prior to MN loss (Devlin et al., 2015; Iwai et al., 2016). As the disease progresses, a shift from hyperexcitability to a hypoexcitability state takes place (Devlin et al., 2015; Naujock et al., 2016). However, other studies suggest hypoexcitability at early stages, occurring before the motor axons withdraw from the neuromuscular junction (NMJ) (Martínez-Silva et al., 2018). Nonetheless, both cortical and axonal hyperexcitability have been observed before MN degeneration. Cortical hyperexcitability is attributed to a persistent increase in Na^+ current density and a hypothesized reduction in K^+ conductance (Pieri et al., 2009). Therefore, we propose that

activating Kv7.2/7.3 channels in order to enhance K⁺ conductance, and thereby reduce membrane excitability, could be an effective therapy for ALS.

The Kv7 family is a five-member K⁺ channel encoded by KCNQ genes. While Kv7.1 is mainly expressed in the heart, Kv7.2- Kv7.5 are expressed in the nervous system. The KCNQ proteins, which have six transmembrane domains, form tetrameric channels that can be assembled as either homomers or heteromers (Jentsch, 2000). S1 and S4 transmembrane segments form the voltage-sensing domain (VSD) and channel gating depends on the S4 segment. The pore domain (PD) is formed by the S5 and S6 segments along with the interconnecting loop. Kv7 channels are characterized by a lengthy intracellular C-terminus organized in four helices that contain domains necessary for tetramerization. In addition, it contains most of the binding sites for regulatory proteins such as phosphatidylinositol 4,5-bisphosphate (PIP2), calmodulin (CaM), syntaxin 1, protein kinase A and C, and ankyrin-G (Barrese et al., 2018).

KCNQ channels are attractive targets to reduce excitability because: i) they are outwards channels that can be activated at subthreshold potential (−80 mV); ii) they stabilize the membrane potential in the presence of depolarizing currents; iii) they can suppress spiking activity and reduce repetitive or burst-firing; iv) they are present at the axon initial segment, meaning they are crucial in regulating action potential threshold (Brown & Passmore, 2009; Deardorff et al., 2021; Shah et al., 2013). Additionally, the heteromeric form of Kv7.2/7.3 underlies the M-current, a slowly activating and non-inactivating potassium current that regulates neuronal excitability by hyperpolarizing the membrane potential and reducing the firing rate of action potentials.

Based on its intrinsic characteristics, the Kv7.2/7.3 channel activation has been used for the treatment of conditions associated with neuronal hyperexcitability, such as epilepsy, migraine, anxiety and addiction to psychostimulants (Brown & Passmore, 2009). In spinal cord organotypic cultures (SCOCs) of mouse pups, enhanced activity of Kv7 channels was found to be involved in the decrease of excitability of spinal MNs (Lombardo et al., 2018). Pharmacological treatment has also been used in order to evaluate the effects of Kv7.2/7.3 channel activation. Retigabine, a specific activator of Kv7.2/7.3, reduces hyperexcitability, ROS production and MN bursting and prevents MN loss in rat hypoglossal MN cultures exposed to DL-threo-β-benzyloxyaspartate (TBOA), which blocks glutamate elimination generating excitotoxicity (Ghezzi et al., 2018). Moreover, Retigabine blocked hyperexcitability and dose-dependently increased the survival of SOD1^{A4V/+} ALS

hiPSC-derived MNs (Wainger et al., 2014). Retigabine treatment also decreased the firing rate of hPSC-derived and mouse MNs (Moakley et al., 2019). Retigabine was shown to reduce both cortical and spinal excitability in ALS patients (Kovalchuk et al., 2018; Wainger et al., 2021). However, the FDA issued a warning regarding the risk of retinal damage and potential vision loss associated with the use of Retigabine (Reference ID: 3369445; accessdata.fda.gov).

Another selective ligand of Kv7.2/7.3 channels is the N-(6-Chloro-pyridin-3-yl)-3,4-difluorobenzamide compound, also known as ICA-27243. In an SH-SY5Y cell culture, it was reported that ICA-27243 shifted the voltage-dependence of Kv7.2/7.3 activation to hyperpolarized potential and suppressed seizure-like activity (Wickenden et al., 2008). Its anti-seizure efficacy was demonstrated in different rodent seizure models (Roeloffs et al., 2008). ICA-27243 and retigabine could also attenuate chronic inflammatory pain (Hayashi et al., 2014). However, ICA-27243 has not been tested in any MND model. In this study, we assayed for the first time the effectiveness of the therapy with the Kv7.2/7.3 channel activator ICA-27243 in *in vitro* and *in vivo* models of MN degeneration.

METHODS

Spinal cord organotypic cultures

Spinal cord organotypic cultures (SCOCs) were prepared as previously described (Rothstein et al., 1993; Mòdol-Caballero et al., 2018). Shortly, spinal cords from P7–P8 Sprague–Dawley rats were aseptically collected and placed in ice–cold Gey’s Balanced Salt Solution (Cat. #G9779, Sigma–Aldrich) containing glucose (6.4 mg/mL). After removing the meninges, the spinal cords were sliced transversely into 350 µm thick sections using a McIlwain Tissue Chopper (The Mickle Laboratory Engineering Co.). The L4–L5 lumbar sections were then transferred onto Millicell–CM porous membranes (0.4 µm; Millipore, Burlington, MA, USA) and placed in a six–well plate containing 1 mL of incubation medium, consisting of 50% MEM (Cat. #M5775, Sigma), 25 mM Hepes (Cat. #H4034–25G, Sigma), 25% heat–inactivated Horse Serum (Cat. #2605088, Gibco), 2 mM glutamine (Cat. #101806, INC Biomedical Inc.), and 25% Hank’s Balanced Salt Solution (HBSS) supplemented with 25.6 mg/ml glucose (Cat. #14175–095, Gibco; pH 7.2). After 7 days *in vitro* (DIV) at 37°C and 5% CO₂ for culture stabilization, the medium was changed twice a week until 15 DIV.

At 15 DIV, excitotoxicity was induced in SCOCs by exposing slices to Locke solution (137 mM NaCl, 2.5 mM CaCl₂, 5 mM KCl, 5.6 mM D–glucose, 0.3 mM KH₂PO₄, 4 mM NaHCO₃, 0.3 mM Na₂HPO₄, 0.01 mM glycine and 10mM HEPES; pH 7.2) containing L–glutamic acid (Cat. # G8415, Sigma–Aldrich,) at a final concentration of 50 µM for 30 minutes. Immediately after, ICA-27243 (N–(6–chloro–pyridin–3–yl)–3,4–difluoro–benzamide, synthesized by Grünenthal GmbH, was added at 2.5 µM, 5 µM, 10 µM and 20 µM in DMSO. Locke solution without glutamate was added to the control. Slices were maintained until 20 DIV at 37°C and 5% CO₂. Next, slices were fixed with 4% paraformaldehyde (PFA), and immunostained to assess MN survival, as described below.

MN viability assessment

As previously described (Herrando–Grabulosa et al., 2020), slices were blocked with 5% normal horse serum (Cat. #S0910500, Biowest) and 0.3% Triton–X–100 in PBS (PBS–TX) and incubated for 48 hours with primary anti–neurofilament H non–phosphorylated antibody (SMI–32; 1:250, Cat. #801701, Biolegend). Subsequently, slices were incubated with secondary antibody Alexa Fluor 488 donkey anti–mouse IgG (1:500, Cat. # A21202, Invitrogen), washed and mounted on glass slides. Z–stack fluorescence images were acquired with a Zeiss LSM 510 Meta confocal microscope. MNs

were identified by SMI-32 positive immunostaining, localization in the ventral horn and morphological features. Blind counting of all MNs meeting these criteria was performed in each spinal cord hemisection using the Cell Counter tool from ImageJ software. Each condition was replicated in 3-4 independent cultures.

Animals and treatment

Female transgenic SOD1^{G93A} mice (B6SJL-Tg [SOD1-G93A] 1Gur) and their non-transgenic wild-type (WT) littermates were utilized in the study. Transgenic offspring were identified by PCR amplification of DNA extracted from the tail using the next primer sequences: 1) hSOD1-forward CATCAG CCCTAATCCATCTGA, 2) hSOD1-reverse CGCGACTAACAA TCAAAGTGA, 3) miL2-forward CTAGGCCACAGAATTGAA AGATCT and 4) miL2-reverse GTAGGTGGAAATTCTAGC ATCATCC. All animals were maintained under standard conditions and handled in accordance with the guidelines set by the European Union Council (Directive 2010/63/EU). The experimental protocols were approved by the Ethics Committee of the Universitat Autònoma de Barcelona.

To assess the neuroprotective effect of ICA-27243 female mice were distributed in the following experimental groups: WT untreated (n=7), WT + ICA-27243 10mg/kg (n=6), SOD1^{G93A} + vehicle (n=5), and SOD1^{G93A} + ICA-27243 10mg/kg (n=6). ICA-27243 was administered daily intraperitoneally (i.p.) throughout the experiment at 10 mg/kg/day. ICA-27243 was dissolved in 5% dimethyl sulfoxide (DMSO) + 95% hydroxypropyl methylcellulose 0.5% (HPMC) (Cat. #H9262, Sigma), adding 2% Tween 80 (Cat. #1754, Sigma).

Electrophysiological tests

Baseline motor nerve conduction tests were performed at 7 weeks of age (prior to drug administration) to balance the groups. Then, tests were carried out at 8, 12, 14 and 16 weeks of age. The sciatic nerve was stimulated using single pulses of 20 μ s duration delivered from a Grass S88 stimulator via needle electrodes placed at the sciatic notch. The compound muscle action potential (CMAP) was recorded from the tibialis anterior (TA) and plantar interossei (PL) muscles with microneedle electrodes, with the active electrode placed on the muscle and the reference at the fourth toe (Mancuso et al., 2011). Muscle evoked potentials (MEP) were recorded from TA muscle to assess the central descending pathways by stimulating the motor cortex with subcutaneous needle electrodes.

Locomotion tests

Motor coordination and locomotion were assessed using the rotarod test and treadmill test. The rotarod test was conducted by placing mice on a rotating rod at 14 rpm and measuring the longest latency before falling, with an arbitrary cut-off time of 180 s. This test was carried out weekly from 8 to 16 weeks of age and the first week in which mice were unable to walk for the full 180 s was determined as the onset of disease. The treadmill test was carried out at the end of the follow-up. It consists of gradually increasing the speed from 6 rpm to 30 rpm, and recording the maximum velocity at which mice could maintain the treadmill pace.

Histological and immunofluorescence analyses

At 16 weeks of age, mice were euthanized by administering an overdose of sodium pentobarbital and transcardially perfused with 4% paraformaldehyde in PBS. The lumbar segment of the spinal cord and the TA muscle were harvested and cryopreserved in 30% sucrose solution in PBS. To assess MN survival, the L4-L5 segment of the spinal cord was serially cut into 20 μ m thick transverse sections using a cryostat (Leica) and collected sequentially on 10 slides. Cresyl violet 3.1 mM stain was applied to the slices for 3 hours. Then, slides were washed, dehydrated, and mounted with DPX. MNs were identified based on their location in the lateral ventral horn and strict morphological and size criteria, including polygonal shape, prominent nucleoli, and diameter larger than 20 μ m.

To assess microglial and astroglial reactivity, other series of lumbar sections were blocked with 10% normal donkey serum (Cat. #S30, Millipore) with 0.2 mM glycine (Cat. #G8898, Sigma) in PBS-Tx 0.3%. Then, sections were incubated overnight at 4°C with primary antibody rabbit anti-ionized calcium-binding adapter molecule 1 (Iba-1; 1:500, Cat. #019-19741, Wako) and rat anti-glial fibrillary acidic protein (GFAP; 1:500, Cat. #13-0300, Invitrogen). Following several washes, the sections were incubated with the appropriate secondary antibody: Cy3 donkey anti-rabbit (1:500; Cat. #AP182C, Millipore) and Alexa Fluor 488 donkey anti-rat (1:500; Cat. #A-21208, Invitrogen). Sections were dehydrated and mounted with DPX (Thermofisher). To assess glial cell reactivity, images of the ventral horn of slices were captured at 40x with a fluorescence microscope (Olympus BX51) under identical conditions. The integrated density was measured using Image J software.

In order to evaluate the innervation of neuromuscular junctions (NMJ), the TA muscle was longitudinally cut into 50 μm thick sections. Sections were blocked with 10% normal donkey serum in PBS-Tx 0.3% for 1 hour, and then incubated for 48 hours at 4°C with primary antibodies including anti-neurofilament 200 (NF200) (1:1000; Cat. #AB5539, Millipore) and anti-synaptophysin (1:500; Cat. #AB32127, Abcam). Sections were washed and incubated overnight at 4°C with Alexa Fluor 594 conjugated secondary antibody (1:200; Cat. #A11042 and #A21207, Invitrogen) and Alexa Fluor 488 conjugated alfa-bungarotoxin (1:200; Cat. #B13422, Life Technologies). The sections were mounted in Fluoromount-G medium (SouthernBiotech, USA) and Z-stack fluorescence images were obtained using a Zeiss LSM 510 Meta confocal microscope. The proportion of innervated NMJs was determined by categorizing each endplate as occupied (innervated or partially innervated) or vacant (denervated), with at least 60 endplates analyzed per animal.

Statistical analysis

Data analyses were conducted using GraphPad Prism 9 software. All data are expressed as mean \pm SEM. The electrophysiological and functional measurements were subjected to repeated-measures two-way ANOVA, while histological data were analyzed using one-way ANOVA. Multiple comparisons were performed using the post-hoc Bonferroni test. Differences were considered significant at $*p < 0.05$.

RESULTS

ICA- 27243 dose- dependently prevents MN degeneration in SCOCs under excitotoxic conditions

In SCOCs, the number of MNs preserved, assessed as the number of SMI-32⁺ cells in the ventral horn, was significantly reduced with the addition of 50 μ M glutamate for 30 minutes (61 ± 2 % MN preserved) compared to control slices (100 ± 3 % MN preserved) (Fig. 1). We found that the application of 10 μ M ICA- 27243 significantly prevented MN death, with MN survival rate of 82% (82 ± 5 %), while doses of 2.5, 5 and 20 μ M were ineffective (65 ± 2 ; 68 ± 2 ; 67 ± 9 % MN preserved, respectively).

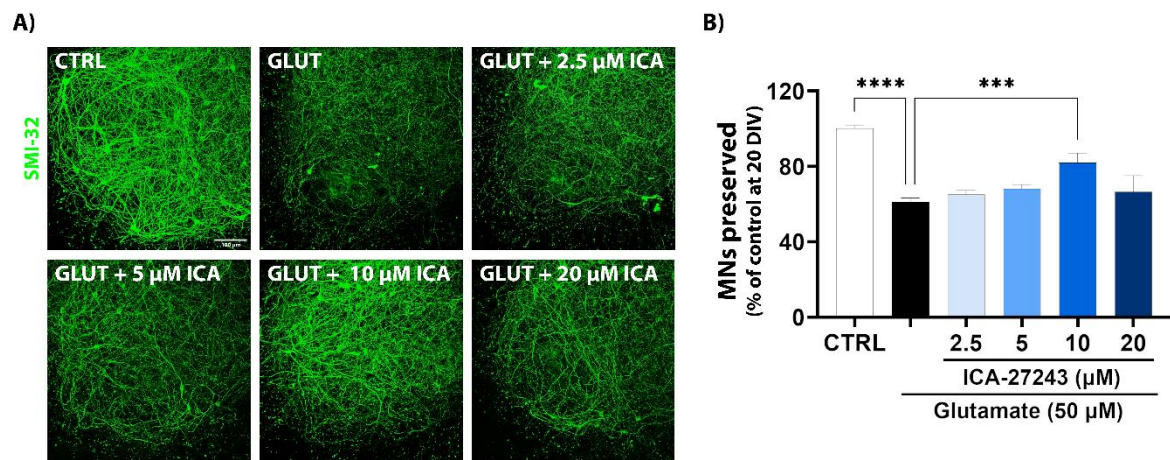


Figure 1 | ICA- 27243 prevents MN death in SCOCs exposed to glutamate. (A) Representative confocal images of the ventral horn of spinal cord hemislices labeled for SMI- 32, at 20 DIV of tested conditions. Scale bar 100 μ m. (B) Bar graph showing neuroprotective effect of 10 μ M ICA- 27243 in SCOCs exposed to glutamate. Data are shown as mean \pm SEM (n= 12- 35 hemisections per treatment). One-way ANOVA followed by Bonferroni's post hoc test: ****p<0.0001 and ***p<0.001 versus Glutamate condition.

ICA- 27243 treatment preserves neuromuscular function and slows disease progression in SODI^{G93A} mice

The neuroprotective effect of ICA- 27243 was assessed in female transgenic SODI^{G93A} mice administered daily at 10 mg/kg/day, compared with SODI^{G93A} mice receiving vehicle. All the mouse groups maintained a substantial gain in body weight throughout the study. WT and SODI^{G93A} mice treated with ICA- 27243 did not show significant differences in body weight compared to their respective controls, although weight differences are observed between SODI^{G93A} and WT mice, as expected (Fig. 2A). Additionally, no secondary

effects were observed in the treated mice, indicating that ICA-27243 at the dosage used did not induce any toxicity.

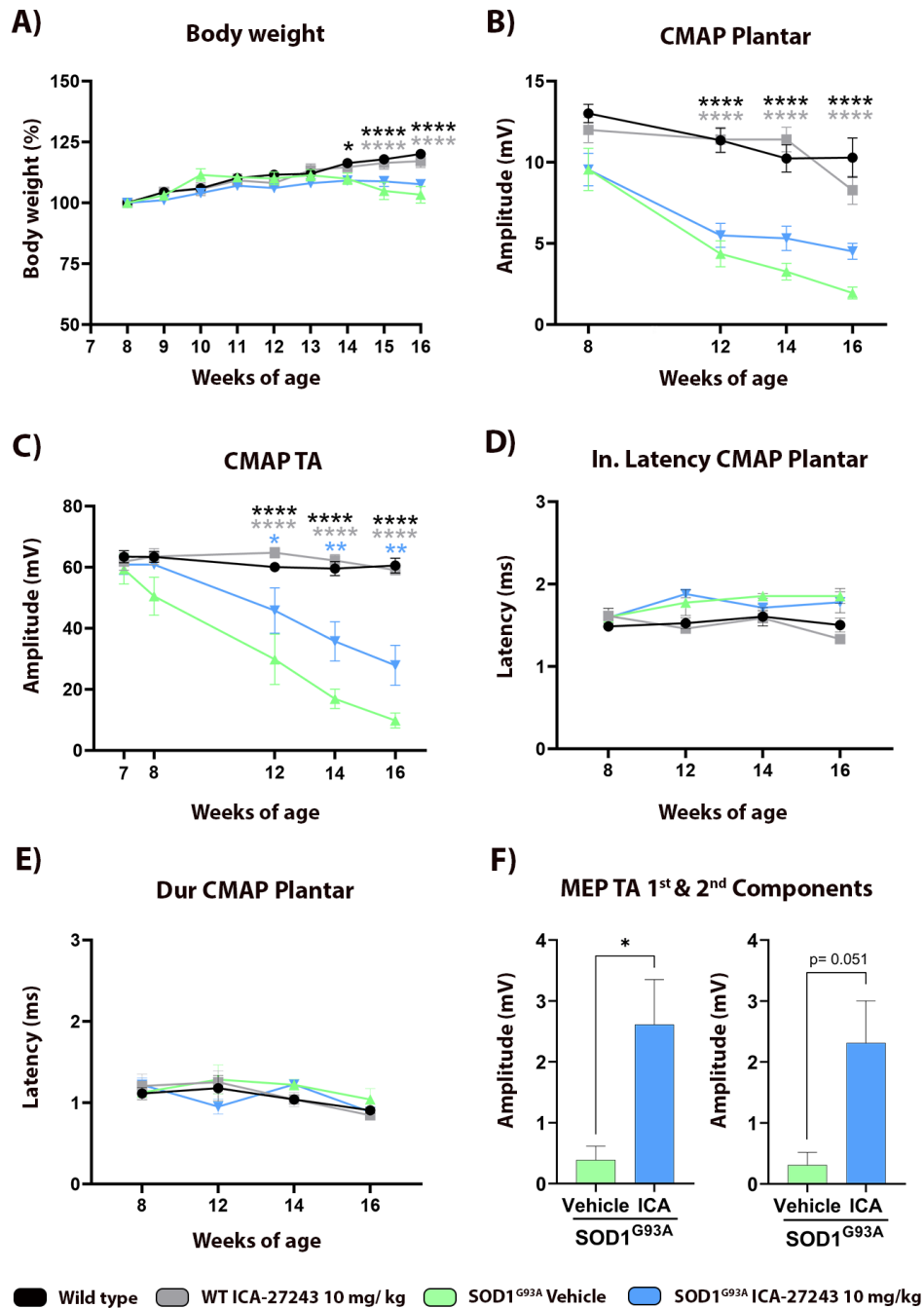


Figure 2 | ICA-27243 treatment enhances neuromuscular function in SOD1^{G93A} mice. (A) Plot showing body weight (expressed as percentage of baseline) throughout the experiment. (B-C) Plots of the CMAP amplitude of plantar interossei (Plantar) and tibialis anterior (TA) muscles along follow-up. (D) Plot of the initial latency of the CMAP of the Plantar muscle along follow-up. (E) Plot of the duration of the M wave of the Plantar CMAP during follow-up. (F) Plots of the amplitude of the first and of the second component of the MEP recorded in the TA muscle. Data are mean \pm SEM, analyzed by One-way (F) and Two-way (A-E) ANOVA followed by Bonferroni's post hoc test. **** $p < 0.0001$; ** $p < 0.01$; * $p < 0.05$ vs SOD1^{G93A} vehicle group. Animals per group: WT, $n=7$; WT + ICA-27243, $n=6$; SOD1^{G93A} + vehicle, $n=5$; SOD1^{G93A} + ICA-27243, $n=6$.

Electrophysiological tests were conducted to record CMAPs and MEPs of the TA and PL muscles, at the asymptomatic stage (8 weeks), early symptomatic stage (12 weeks), mid-symptomatic stage (14 weeks) and at the end of the follow-up (16 weeks). Motor nerve conduction test indicated that ICA-27243 significantly preserved the amplitude of the CMAP of the TA muscle of treated SODI^{G93A} mice at 12, 14 and 16 weeks of age (Fig 2C), whereas it had a low effect preventing the CMAP decline in the PL muscle at late stages of the disease (Fig. 2B), compared to vehicle SODI^{G93A} mice. Electrophysiological results showed a slower latency to the onset of the M wave of the PL muscle in the SODI^{G93A} vehicle group and SODI^{G93A} mice treated with ICA-27243, compared to WT groups (Fig. 2D), as previously demonstrated (Mancuso et al., 2011). However, no differences were found between treated and untreated groups. Similarly, no differences were observed in the M wave duration between all groups (Fig. 2E). Regarding the MEPs recorded in the TA muscles, SODI^{G93A} mice treated with ICA-27243 had significantly higher amplitude in the first component and a tendency in the second component compared to vehicle SODI^{G93A} mice (Fig. 2F).

The results of the rotarod test indicated that ICA-27243 treatment significantly improved the functional outcome at both 15 and 16 weeks (Fig. 3A). Thus, the onset of motor impairment in SODI^{G93A} mice treated with ICA-27243 was delayed by at least two weeks, since vehicle mice exhibited decline in the rotarod from 14 weeks whereas treated mice maintained on the rod for the 180 sec until the end of the follow-up (Fig. 3B). In the treadmill test, the performance of SODI^{G93A} mice was also notably enhanced with administration of ICA-27243 (Fig. 3C). In summary, ICA-27243 treatment showed significant improvement in all tests of motor activity in the SODI^{G93A} mice.

The assessment of NMJ innervation of the TA muscles at the end of the study showed that ICA-27243 treatment significantly increased the proportion of occupied endplates (75 ± 6 % occupied endplates) compared to untreated SODI^{G93A} mice (31 ± 8 % occupied endplates). This finding supports the preservation of CMAP amplitudes observed in nerve conduction tests and the improvement in locomotion tests.

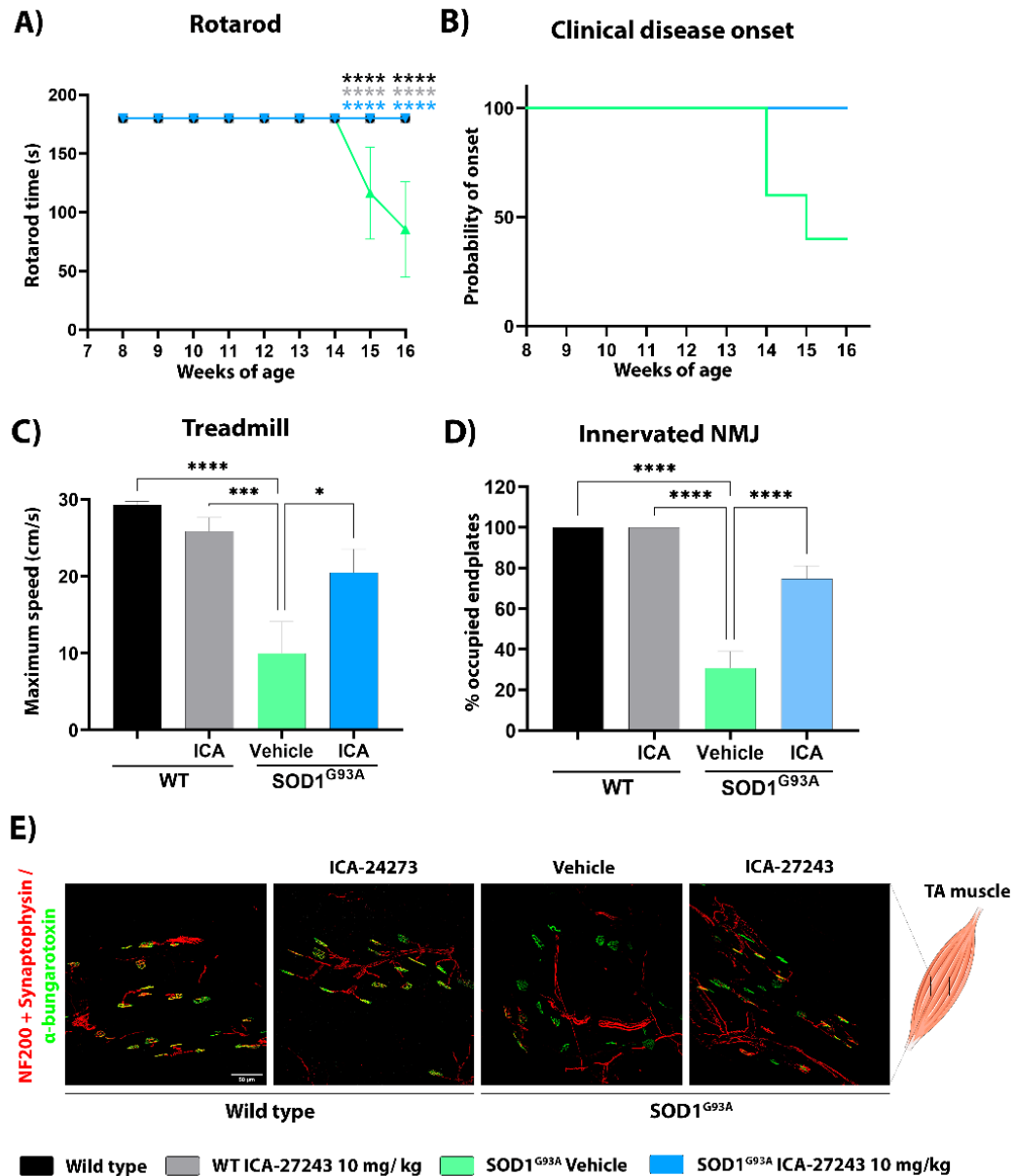


Figure 3 | ICA- 27243 administration maintains motor activity in SOD1^{G93A} mice. (A) Graph showing the impact of ICA- 27243 treatment on motor function, evaluated by the rotarod test. (B) Clinical disease onset determined as the first day when a decline in performance was observed in the rotarod test. (C) Graph showing the effect of ICA- 27243 on locomotion measured as the maximum speed supported on the treadmill test. (D) Plot graph showing histological analyses of NMJ of the TA muscle, represented as the proportion of occupied endplates at 16 weeks of age. (E) Representative confocal images of NMJ in the TA muscle of WT and SOD1^{G93A} mice with or without ICA- 27243 treatment at 16 weeks of age. Scale bar: 50 μm. Data are mean ± SEM. One- way (C- D) and Two- way (A) ANOVA followed by Bonferroni's post hoc test: ****p < 0.0001; ***p < 0.001; *p < 0.05 vs SOD1^{G93A} vehicle group.

ICA- 27243 promotes MN survival in the lumbar spinal cord and reduces glial activation in the SOD1^{G93A} mice

The quantification of MNs in the ventral horn of L4-L5 spinal cord slices demonstrated that untreated SOD1^{G93A} mice had only 33% of surviving MNs (7.4 ± 1 MNs) at 16 weeks of age, compared to untreated WT mice (22.3 ± 0.4 MNs) and WT ICA- 27243 treated mice (22.2 ± 0.5 MNs) (Fig. 4A- B). In contrast, SOD1^{G93A} mice treated with ICA- 27243 had a significantly higher number of spinal MNs (13.0 ± 0.3 surviving MNs) than untreated SOD1^{G93A} mice, reaching up to 58% of MN found in WT mice.

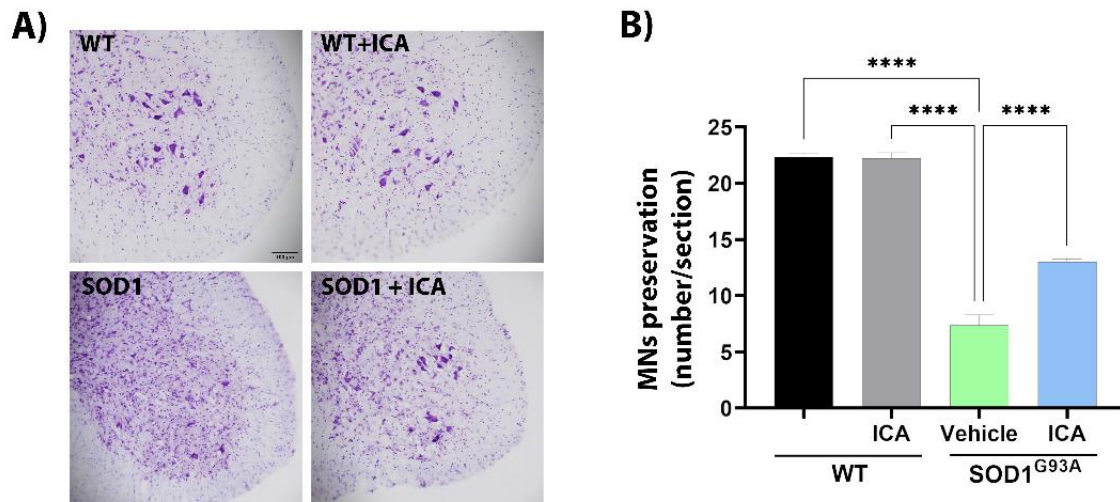


Figure 4 | Neuroprotective effects of ICA- 27243 administration on MNs in SOD1^{G93A} mice at 16 weeks. (A) Representative images of the ventral horn of L4-L5 spinal cord stained with Cresyl violet of WT and SOD1^{G93A} mice with or without ICA- 27243 treatment at 16 weeks of age. Scale bar 100 μ m. (B) Bar graph showing the neuroprotective effect of 10 mg/kg of ICA- 27243, with significantly more MNs per section of the spinal cord than in vehicle SOD1^{G93A} mice. Data are mean \pm SEM. One- way ANOVA followed by Bonferroni's post hoc test: **** $p < 0.0001$ vs SOD1^{G93A} vehicle group.

Both astroglial and microglial reactivity were markedly increased in SOD1^{G93A} mice compared to both groups of WT mice. Treatment with ICA- 27243 attenuated glial reactivity, even though it did not reach a significant difference compared to SOD1^{G93A} mice (Fig. 5A- C).

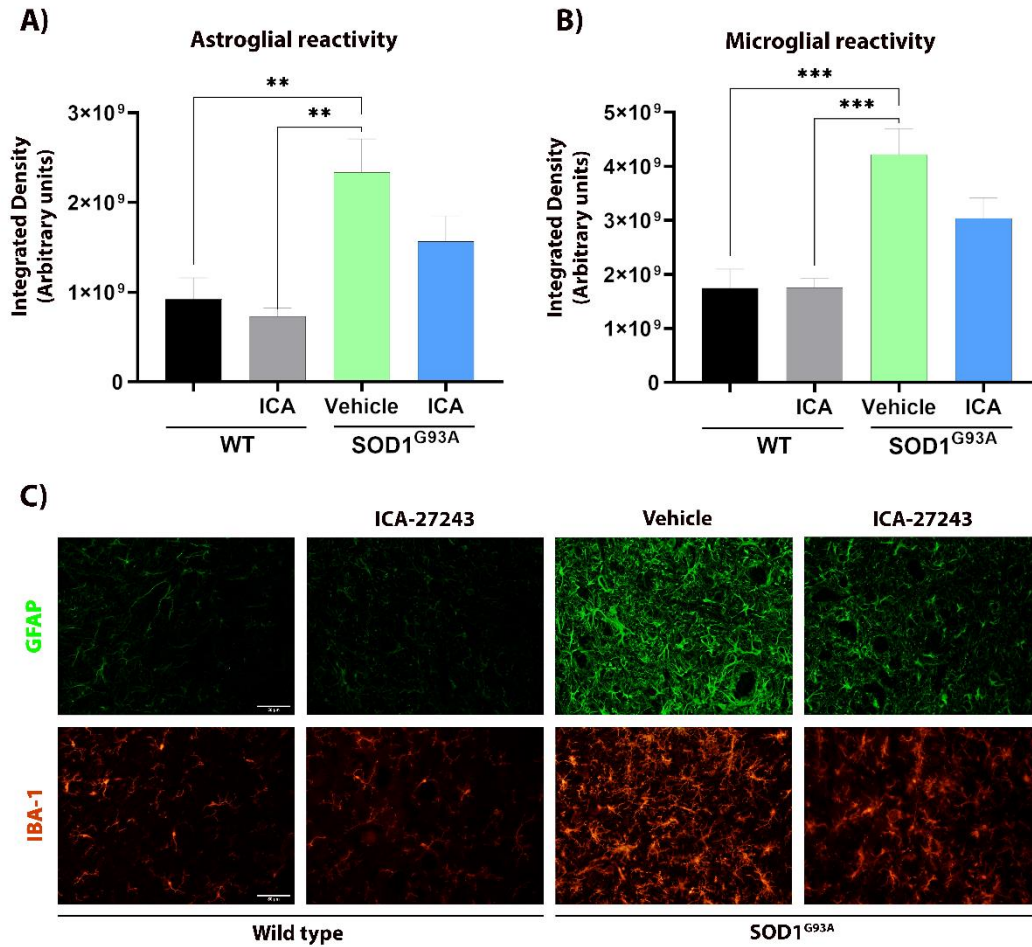


Figure 5 | Administration of ICA-27243 attenuates glial reactivity in SOD1^{G93A} mice at 16 weeks. Bar graphs showing astroglial (A) and microglial (B) reactivity represented as the integrated density in the ventral horn of the spinal cord. (C) Representative images of glia immunoreactivity assessed by GFAP and IBA-1 labeling in the ventral horn of L4-L5 spinal cord slices of WT and SOD1^{G93A} mice with or without ICA-27243 treatment at 16 weeks of age. Scale bar: 50 μ m. Data are mean \pm SEM. One-way (A-B) ANOVA followed by Bonferroni's post hoc test: *** $p < 0.001$; ** $p < 0.01$ vs SOD1^{G93A} vehicle group.

DISCUSSION

The present study demonstrates for the first time that ICA-27243 exhibits neuroprotective effects on spinal cord MNs. *In vitro*, ICA-27243 prevented MN loss in SCOCs treated with glutamate to generate excitotoxicity. *In vivo*, ICA-27243 maintained neuromuscular function, enhanced motor activity, reduced the loss of MNs and attenuated glial activation in the spinal cord of the ALS transgenic SOD1^{G93A} female mice. These findings highlight the interest of compounds modulating neuronal excitability as suitable therapeutic agents.

ICA-27243 was first tested in a SCOC excitotoxic model. The SCOC provides a reliable *in vitro* system for assessing the neuroprotective impact on MNs. It maintains the synaptic connectivity, anatomical organization of the neural circuitry and cellular stoichiometry of both neuronal and non-neuronal elements within the spinal cord slice. This integrated perspective renders SCOC a valuable tool for testing novel drugs for MND therapy before *in vivo* testing (Rothstein et al., 1993; Guzmán-Lenis et al., 2009; Mòdol-Caballero et al., 2018). After the excitotoxic insult, cultures treated with 10 μ M of ICA-27243 presented a higher number of α -MNs, indicating a neuroprotective effect. Since ICA-27243 has not direct action on glutamate excitotoxic effects, the beneficial results can be interpreted as an enhancement in other protective mechanisms in response to the insult. ICA-27243 is a M-current activator with high selectivity for Kv7.2/7.3, and it can induce a hyperpolarizing shift in the voltage-dependent activation of its target (Wickenden et al., 2008). Furthermore, the addition of KCl, which increases extracellular K⁺, to mouse SCOCs reduces the intrinsic excitability due to the increase of the M-current (Lombardo et al., 2018). Hence, the primary impact of ICA-27243 would be to enhance the M-current, thereby diminishing hyperexcitability and providing an explanation for the neuroprotective effects observed in our model.

To assess the neuroprotective effects in the context of ALS, we tested ICA-27243 in the SOD1^{G93A} transgenic mice, the most widely used ALS preclinical model, since they reproduce most of the clinical and histopathological characteristics of ALS disease (Ripps et al., 1995). We have found that a daily dose of 10 mg/kg of ICA-27243 attenuates the progressive decrease in the CMAP amplitude of hindlimb muscles and, importantly, of the MEPs in the treated compared with the vehicle SOD1^{G93A} mice, indicating effective preservation of the peripheral and the central motor pathways. There were not differences

in the latency to the onset and the duration of the M wave, indicating no changes in the conduction velocity of remaining motor fibers (Mancuso et al., 2011). In contrast, treatment of SOD1^{G93A} mice with Riluzole, commonly used in the clinic, was not able to improve the decline of the CMAP amplitude, that was similar to vehicle SOD1^{G93A} mice (Li et al., 2013). Furthermore, our findings revealed that the administration of ICA-27243 resulted in improved outcomes in locomotion tests compared to vehicle SOD1^{G93A} mice. Previous studies have demonstrated the positive effects of ICA-27243 on locomotion in female Sprague–Dawley rats, where a dosage of 10 mg/kg reduced abnormal involuntary movements in L-Dopa-induced dyskinesias (Sander et al., 2012). ICA-27243 likely contributes to maintaining the NMJ integrity, probably due to a reduction of the persistent depolarization observed in the motor axon in the SOD1 model (Boërio et al., 2010; Moldovan et al., 2012). This reduction in depolarization is likely achieved through an increase of K⁺ outflow currents. Collectively, ICA-27243 effectively preserves motor function and behavior in the SOD1^{G93A} ALS transgenic mice.

Treatment with ICA-27243 significantly prevented MN degeneration in the SOD1^{G93A} mice. As previously discussed, ICA-27243 enhances the M-current reducing excitability. Therefore, we may expect a reduced influx of Ca²⁺ and a downregulation of the Ca²⁺-dependent cascade of cytotoxic events, such as mitochondrial dysfunction or increased ROS levels (Lewinski & Keller, 2005; Van Den Bosch et al., 2006). In fact, a decrease in the production of ROS was observed in cultured hypoglossal MNs treated with Retigabine and DL-threo-β-benzyloxyaspartate, concomitant with increased MN survival rate, enhancement of the M-current and reduction of hyperexcitability (Ghezzi et al., 2018). In a different study, MN survival in ALS-patients iPSC treated with Retigabine was related to ER-stress downregulation (Wainger et al., 2014). Numerous studies have shown that hyperexcitability, excitotoxicity, oxidative stress and mitochondrial dysfunction are interacting molecular pathways being altered throughout the progression of ALS pathology (Hardiman et al., 2017). In this way, we hypothesize that since Retigabine and ICA-27243 have a common target, the Kv7.2/3 channel, the neuroprotective effect seen in our study with ICA-27243 could be due to modifications in membrane excitability that positively impact on one or more of the molecular pathways mentioned. Although both Retigabine and ICA-27243 increase K⁺ efflux enhancing M-current, their binding sites are different (Padilla et al., 2009), thus, the derived effects may vary between the two compounds. ICA-27243 specifically enhances the activation Kv7.2/7.3 channels, having little impact on Kv7.5/3 or Kv7.3 channels, whereas Retigabine indiscriminately increases all Kv7 channel

currents (Padilla et al., 2009). Hence, further studies are needed to better understand the neuroprotective properties of ICA-27243 in ALS models.

In addition, we observed that ICA-27243 can attenuate astroglial and microglial reactivity. This action cannot be directly attributable to ICA-27243 effects, since Kv7.2/7.3 channels are predominantly located in the axon initial segment and Ranvier nodes of neurons (Deardorff et al., 2021), and may be secondary to the reduced neuronal death. However, when Retigabine was administered in an experimental autoimmune encephalomyelitis mouse model, the infiltration of Iba-1⁺ cells was decreased (Kapell et al., 2023).

In conclusion, we have demonstrated for the first time that ICA-27243 is an effective treatment that can preserve neuromuscular function, enhance motor activity and prevent MN degeneration in the spinal cord of SOD1^{G93A} mice and in SCOCs. These data highlight that Kv channels, specially Kv7.2/3, represent a potential target for mitigating hyperexcitability in a range of diseases including ALS.

Chapter II

GRT-X prevents degeneration of motoneurons exposed to mouse and human ALS astrocyte-conditioned medium

GRT-X prevents degeneration of motoneurons exposed to mouse and human ALS astrocyte-conditioned medium

Vera M. Masegosa^{1,2&}, Elsa Fritz^{3&}, Daniela Corvalan³, Fabiola Rojas³, Xavier Navarro^{1,2},
Brigitte van Zundert^{3,4}, Mireia Herrando-Grabulosa^{1,2}

¹Department of Cell Biology, Physiology and Immunology, Institute of Neurosciences, Universitat Autònoma de Barcelona, Bellaterra, Spain

²Centro de Investigación Biomédica en Red (CIBER), Instituto de Salud Carlos III, Madrid, Spain

³Institute of Biomedical Sciences (ICB), Faculty of Medicine & Faculty of Life Sciences, Universidad Andres Bello, Santiago, Chile

⁴Department of Neurology, University of Massachusetts Chan Medical School (UMMS), Worcester, MA, USA

& first co-authors

ABSTRACT

Amyotrophic lateral sclerosis (ALS) is a fatal neurodegenerative disease, affecting motoneurons (MNs). Non-cell autonomous mechanisms contribute to ALS, wherein astrocytes release toxic factor(s) detrimental to MNs. Despite the multifactorial nature of ALS, single-pathway-focused therapies have limited effectiveness in improving ALS. Therefore, novel combinatorial therapies are currently being pursued. Here, we evaluate whether the simultaneous activation of two complementary targets, the voltage-gated potassium channels 7.2/3 (Kv7.2/3) and the mitochondrial translocator protein (TSPO), by a novel synthesized GRT-X compound is an effective neuroprotective treatment in ALS *in vitro* models. We exposed primary ventral spinal cord neuronal cultures and spinal cord organotypic cultures to astrocyte-conditioned medium (ACM) derived from primary mouse ALS astrocytes expressing mutant human SOD1 (SOD1^{G93A}-ACM) or from ALS patient astrocytes generated from induced pluripotent stem cells carrying disease-causing mutations of SOD1 (SOD1^{D90A}-ACM) or TDP43 (TDP43^{A90V}-ACM). We report that the diverse human and mouse ALS-ACM compromise MN viability that is protected by GRT-X. Moreover, ALS-ACM increases oxidative stress levels that are diminished with GRT-X treatment. Together, we show that the complementary activation of TSPO and Kv7.2/3 by GRT-X could be a potential treatment for ALS due to its capacity to protect MNs from non-cell-autonomous toxicity induced by diseased astrocytes.

Keywords: GRT-X, astrocyte conditioned medium, amyotrophic lateral sclerosis, motoneuron death, ROS

INTRODUCTION

Motoneuron diseases are a heterogeneous group of diseases that cause the progressive degeneration of the motoneurons (MNs). The most common is amyotrophic lateral sclerosis (ALS), a devastating neurodegenerative disease characterized by the selective degeneration of both upper and lower MNs, resulting in death, in most cases, by respiratory failure within 2-5 years after diagnosis. Around 90-95% of the cases are sporadic with no apparent genetic link (sporadic ALS, sALS), while the remaining 5-10% of the cases are related to several genetic mutations (familial ALS, fALS) (Hardiman et al., 2017). Since the first gene was discovered in fALS, superoxide dismutase 1 (*SOD1*) more than 200 genetic variants of this gene have been reported (<https://alsod.ac.uk/output/variant.php/35>). *SOD1*^{G93A} variant led to the development of the first mouse model for ALS where mutant human *SOD1*^{G93A} is ubiquitously overexpressed (Gurney et al., 1994). Among other ALS-causing genes, mutations in the *TARDBP* gene (encoding for 43 kDa TAR DNA-binding protein (TDP43) are related to autosomal dominant ALS and account for 1-2% of ALS cases (Neumann et al., 2006). At least 50 other genes have been identified to be involved in ALS such as *C9orf72* or fused in sarcoma (*FUS*), among others (Mejzini et al., 2019).

Many pathogenic mechanisms contribute to MN degeneration in ALS such as oxidative stress, glutamate excitotoxicity, endoplasmic reticulum stress, protein misfolding, hyperexcitability, and others (Mancuso & Navarro, 2015; Hardiman et al., 2017). Moreover, the contribution of non-neuronal cells to ALS progression was demonstrated since wild-type MNs developed ALS signs when surrounded by ALS mutant genes-expressing non-neuronal cells such as astrocytes (Clement et al., 1996). Cultures of wild-type MNs with mouse or human astrocytes harboring ALS/FTD mutant genes also evidenced the astrocytic non-cell autonomous effect in MN degeneration (Van Harten et al., 2021; Stoklund Dittlau et al., 2023). Thus, primary ALS and ALS/FTD astrocytes derived from transgenic mouse models harboring pathogenic gene mutations in *SOD1*, *TARDBP* and *C9orf72* reduce healthy wild-type MNs in co-cultures or after application of astrocyte-conditioned medium (ACM) (Di Giorgio et al., 2007; Nagai et al., 2007; Fritz et al., 2013; Rojas et al., 2014; Mishra et al., 2020; Arredondo et al., 2022). Chronic infusion of ACM obtained from astrocyte harboring *SOD1*^{G93A} mutation triggers spinal MN death and neuromuscular dysfunction in healthy rats (Ramírez-Jarquín et al., 2017). Decreased MN survival was also found in studies with human (i-) astrocytes (or derived ACM), carrying

mutations in *SOD1* (Meyer et al., 2014; Almad et al., 2022), *C9orf72* (Meyer et al., 2014; Birger et al., 2019), or *TARDBP* (Arredondo et al., 2022) genes.

Currently, there is no effective therapy for ALS; therefore, finding novel and combinational therapeutic strategies is currently being pursued. Here, we used the GRT-X compound (N- [(3-fluorophenyl) -methyl] -1- (2-methoxyethyl) -4-methyl-2-oxo-(7-trifluoromethyl) -1H-quinoline-3-carboxylic acid amide), a small molecule whose main characteristic is the capacity of targeting the mitochondrial translocator protein (TSPO) and the voltage-gated potassium channels 7.2/3 (Kv7.2/3) simultaneously. It has been recently demonstrated that GRT-X has a neuroprotective and neuroregenerative effect after a lesion of cervical spinal nerves in rats (Bloms-Funke et al., 2022a). Furthermore, GRT-X was effective as an anti-seizure drug in rodent models of epilepsy (Bloms-Funke et al., 2022b).

TSPO is expressed in glial cells, neurons and endothelial and ependymal cells and localized in the outer mitochondrial membrane in enriched steroidogenic regions (Papadopoulos et al., 1990). Its function has been widely associated with steroidogenesis (Fan et al., 2015), but also linked to other functions such as mitochondrial bioenergetics (Liu et al., 2017; Fu et al., 2020), redox mechanisms (Jayakumar et al., 2002; Gatliff et al., 2014) and neuroinflammation (Chen & Guilarte, 2008). Enhanced TSPO levels in glial cells and neurons were reported in pathological conditions, including ALS, although under physiological conditions TSPO is poorly expressed (Veenman & Gavish, 2000). Thus, TSPO has been considered an interesting target for ALS.

Olesoxime, a ligand of TSPO, increased dose-dependently MN survival, reduced oxidative stress levels and promoted neurite outgrowth in *in vitro* studies (Bordet et al., 2007). In the *SOD1*^{G93A} mice, Olesoxime improved the decline of performance on the grid test and rotarod and increased survival (Bordet et al., 2007). Reduced microglial and astroglial activation and attenuated MN loss and muscle denervation were observed in Olesoxime-treated ALS mice (Sunyach et al., 2012). Unfortunately, in a phase II–III clinical trial, Olesoxime did not produce significant beneficial effects on ALS patients (Lenglet et al., 2014).

Heteromeric Kv7.2/3 channels underly the M-current, which stabilizes the resting membrane potential and reduces neuronal excitability (Soldovieri et al., 2011). Since hyperexcitability is a common feature of ALS (van Zundert et al., 2008), potassium channels

are an attractive target for ameliorating the disease. Retigabine was shown to reduce hyperexcitability, ROS production, MN bursting and prevent MN loss in rat hypoglossal MN cultures (Ghezzi et al., 2018). Retigabine also blocked hyperexcitability and increased *in vitro* survival of $SOD1^{A4V/+}$ ALS hiPSC-derived MNs (Wainger et al., 2014), and a phase II randomized clinical trial demonstrated its effectiveness in reducing MN excitability in ALS patients (Wainger et al., 2021).

In this study, we assayed if the simultaneous activation of these two complementary targets, TSPO and Kv7.2/3, by the GRT-X compound, may prevent MN loss and ROS production in primary spinal cord MN cultures (VSCNs) and spinal cord organotypic cultures (SCOC) treated with ACM collected from human and mouse astrocytes with ALS/FTD-linked mutations in *SOD1* and *TARDBP* genes.

MATERIALS AND METHODS

Animals for primary spinal cord neural cultures (VSCNs)

All protocols involving rodents (including rat spinal cord cultures; see below) were carried out according to the NIH and ARRIVE guidelines and were approved by the Ethical and Bio-security Committees of Universidad Andres Bello. Sprague–Dawley rats, to obtain embryonic ventral spinal cord cultures (E14) were maintained and bred at the animal facility of Universidad Andres Bello.

The animal experimental procedure was approved by the Ethics Committee of Universitat Autònoma de Barcelona and followed the European Communities Council Directive 2010/63/EU and ARRIVE guidelines.

Astrocyte-conditioned medium preparation from primary mouse astrocyte cultures

Primary mouse astrocyte cultures and astrocyte-conditioned medium (ACM) were prepared as described previously (Fritz et al., 2013; Rojas et al., 2014; Arredondo et al., 2022). Briefly, cultures of astrocytes were prepared from P1–P2 transgenic mice expressing human SOD1^{WT} and SOD1^{G93A}. Cultures were maintained in DMEM (Hyclone, Cat. #SH30081.02) containing 10% FBS (Gibco, Cat. #16000–044), 1% L-glutamine (Gibco, Cat. #25030–081) and 1% penicillin–streptomycin (Gibco, Cat. #15140–122) at 37°C and 5% CO₂. After 3 weeks, cultures reached confluence and contained >95% GFAP+ astrocytes. Using an orbital shaker (200 rpm in the incubator), residual microglia was removed overnight (7h), leaving cultures enriched for S100β and Aldh1L1. Medium was replaced with neuronal growth medium: 70% MEM (Gibco, Cat. #11090–073), 25% Neurobasal Medium (Gibco, Cat. #21103–049), 1% N2 supplement (Gibco, Cat. #17502–048), 1% L-glutamine (Gibco, Cat. #2503–081), 1% penicillin–streptomycin (Gibco, Cat. #15140–122), 2% horse serum (Gibco, Cat. #15060–114) and 1% sodium pyruvate (Gibco, Cat. #11360–070). ACM was collected after 7 days, supplemented with 4.5 mg/ml D-glucose (final concentration) and stored at –80°C. The SOD1^{WT}-ACM and SOD1^{G93A}-ACM used to evaluate MN survival were diluted 8-fold in primary MN spinal cord cultures [Minimal essential medium (MEM) supplemented with Neurobasal medium, N2 supplement, L-glutamine, penicillin–streptomycin, horse serum and sodium pyruvate] and 9-fold in SCOCs medium [MEM medium supplemented with HEPES, heat-inactivated horse serum, glutamine and HBSS supplemented with glucose].

Astrocyte-conditioned medium preparation from human iPSC-induced astrocytes cultures

Human mutant SOD1 (Chen et al., 2014) and mutant TDP43 (Zhang et al., 2013) astrocytes were generated from fully reprogrammed iPSC lines that were previously induced from skin fibroblasts biopsies by retroviral transduction using the four Yamanaka factors (OCT4, SOX2, KLF4, and cMYC). The SOD1^{D90A} iPSC line (commercially available from WiCell, WC034i) was generated from a 50-year-old female ALS patient and the control iPSC line was generated from an age-matched (50-year-old) healthy female (WiCell, STANI40i-243C1). The TDP43^{A90V} iPSC line was generated from an ALS/FTD 75-year-old male patient carrying an A90V mutation in TARDBP (TDP43^{A90V}) and from a healthy subject (56-year-old female, termed control), a family member without mutations (Zhang et al., 2013). Differentiation to NPCs (Zhang et al., 2013; Arredondo et al., 2022) and mature astrocytes were performed as described previously for mutant TDP43 and control subject iPSCs (Arredondo et al., 2022). Same protocol was used here for mutant SOD1 and control subject iPSCs. Briefly, iPSCs were maintained in feeder-free conditions using mTeSR1 medium (STEMCELL Technologies, Cat. # 85850). EBs were generated in EB Differentiation Medium [KnockOut DMEM/F12 media (Gibco, Cat. #12660-012) supplemented with 10% KnockOut serum replacement (Gibco, Cat. #10828-028), 1x GlutaMax (Gibco, Cat. #35050-061), 1x NEAA (Gibco, Cat. #11140-050), and 2-mercaptoethanol (Sigma-Aldrich, Cat. #M3148)] and maintained in suspension for one week. Rosette-shaped neuroepithelial cells were obtained after plating the EBs in plates coated with poly-L-ornithine (Sigma-Aldrich, Cat. #P4957) and laminin (Sigma-Aldrich, Cat. #L2020) and grown for one week in Neural Induction Medium [KnockOut DMEM/F12 supplemented with N2 (Gibco, Cat. #17502-048), NEAA, 2 mg/mL heparin (Sigma-Aldrich, Cat. #H3149), and 10 ng/mL β FGF (Gibco, Cat. #PHG0021)]. Rosettes were manually isolated under the microscope, re-plated in plates pre-treated with Matrigel (Corning, Cat. #354277) and grown for one more week in Neural Expansion Medium [Neurobasal supplemented with Glutamax, NEAA, B-27 (Gibco, Cat. #17504-044), and β FGF]. Rosettes were disaggregated using Accutase Cell Detachment Solution (EMD Millipore, Cat. # SCR005) to generate a monolayer culture of Neural Progenitor Cells (NPCs). NPCs were differentiated to astrocyte precursor cells by culturing for 2 weeks in astrocyte precursor medium [KO DMEM/F12, 1x StemPro NSCs Supplement (Gibco, Cat. #A10508-01), 10 ng/mL Activin A (Gibco, Cat. #PHC9564), 10 ng/mL Heregulin (R&D

Systems, Cat. #377-HB-050), 200 ng/mL IGF1 (R&D System, Cat. #P291-G1-200), 20 ng/mL β FGF, 20 ng/mL EGF (Gibco, Cat. #PHG0311), 1x GlutaMAX] (Shaltouki et al., 2013). Then, precursor cells were incubated for 2 additional weeks in astrocyte maturation and maintenance medium [DMEM/F12, B27, 10 ng/mL Heregulin, 5 ng/mL BMP2 (BioVision, Cat. #4577-50) and 2 ng/mL CNTF (R&D Systems, Cat. #257-NT-010)] (Malik et al., 2014). Immunofluorescence assays were performed to confirm the development from NPCs (Nestin⁺) to APCs (CD44⁺) and to a mature astrocytic phenotype (Cx43⁺ and S100 β ⁺) of these cultures (as in (Arredondo et al., 2022)). In parallel, medium of d28 human iPSC-induced astrocyte cultures was replaced with Neuronal Growth Medium [MEM (Gibco, Cat. #11090-073) supplemented with 25% Neurobasal media (Gibco, Cat. #21103-049), 1% N2 supplement (Gibco, Cat. #17502-048), 1% L-glutamine (Gibco, Cat. #25030-081), 1% penicillin-streptomycin (Gibco, Cat. #15140-122), 2% horse serum (Gibco, Cat. #15060-114; lot 1517711) and 1% sodium pyruvate (Gibco, Cat. #11360-070)]. ACM was collected after 7 days, supplemented with 4.5 mg/ml D-glucose (final concentration) and stored at -80°C. TDP43^{WT}-ACM, TDP43^{A90V}-ACM, SOD1^{WT}-ACM and SOD1^{D90A}-ACM used to evaluate MN survival were diluted 6-fold.

Primary MN spinal cord cultures

Pregnant Sprague-Dawley rats were anesthetized with CO₂, and primary ventral spinal cultures (VSCNs) were prepared from E14 pups (Fritz et al., 2013; Rojas et al., 2014; Arredondo et al., 2022). Briefly, spinal cords were removed and placed into ice-cold HBSS (Gibco, Cat. #14185-052) with 50 μ g/ml penicillin/streptomycin (Gibco, Cat. #15070-063). Using a small razor blade, the spinal cord's dorsal part was removed from the ventral part. The ventral cord was grinded and enzymatically treated by incubating for 20 min at 37°C in pre-warmed HBSS containing 0.25% trypsin (Gibco, Cat. #15090-046). Cells were maintained in neuronal growth medium (see above) for 7–9 DIV at 37°C under 5% CO₂, and supplemented with 45 μ g/ml E18 chick leg extract; medium was refreshed every 3 days. After 7 DIV cells were fixed for MN survival analysis.

Spinal cord organotypic cultures

Spinal cord organotypic cultures (SCOCs) were prepared as previously described (Rothstein et al., 1993; Herrando-Grabulosa et al., 2016). Briefly, spinal cords from P7–P8 Sprague-Dawley rats were aseptically harvested and placed in ice-cold Gey's Balanced Salt Solution (Sigma-Aldrich) containing glucose (6,4 mg/mL). Once meninges were removed,

spinal cords were transversally cut into 350 μm thick slices using a McIlwain Tissue Chopper (The Mickle Laboratory Engineering Co.). L4-L5 lumbar sections were transferred on Millicell-CM porous membranes (0.4 μm ; Millipore, Burlington, MA, USA) into a six-well plate containing 1 mL of incubation medium: 50% MEM (Sigma, Cat. #M5775), 25 mM Hepes (Sigma, Cat. #H4034-25G), 25% heat-inactivated Horse Serum (Gibco, Cat. #2605088), 2 mM glutamine (INC Biomedical Inc, Cat. #101806) and 25% Hank's Balanced Salt Solution (HBSS) supplemented with 25.6 mg/ml glucose (Gibco, Cat. #14175-095). Cultures were left to stabilize for 7 DIV at 37°C and 5% CO₂, and thereafter the medium was changed twice a week until stress induction.

GRT-X dose-response curve

Dose-response curve of GRT-X was performed in VSCNs. After 4 DIV, the MN cultures were treated at 0.1 μM , 0.5 μM , 1 μM , 2.5 μM , 5 μM , 7.5 μM and 10 μM of GRT-X and DMSO as vehicle (at the highest concentration used for GRT-X treatment) for 3 days. At 7 DIV, cultures were fixed, and survival analysis was performed as detailed below in the immunofluorescence section.

GRT-X treatment under excitotoxic stress

Excitotoxicity was induced at 15 DIV in SCOCs by transferring slices to Locke solution (137 mM NaCl, 2.5 mM CaCl₂, 5 mM KCl, 5.6 mM D-glucose, 0.3 mM KH₂PO₄, 4 mM NaHCO₃, 0.3 mM Na₂HPO₄, 0.01 mM glycine and 10 mM Hepes; pH 7.2) containing L-glutamic acid (Sigma-Aldrich, Cat. #G8415) at a final concentration of 50 μM for 30 min. GRT-X at 6.25 μM , 12.5 μM and 25 μM was added simultaneously. DMSO at the highest concentration used for GRT-X treatment was added as vehicle condition. Locke solution was also added to control and vehicle conditions without glutamate. After treatments, slices under the different conditions were maintained for 5 DIV, then, fixed with 4% paraformaldehyde (PFA) and immunostained to determine MN survival as detailed below.

GRT-X treatment under ACM

VSCNs were exposed at 4 DIV to the mouse SOD1^{WT}-ACM and SOD1^{G93A}-ACM (both diluted 1:8) or to the human SOD1^{WT}-ACM, SOD1^{D90A}-ACM, TDP43^{WT}-ACM and TDP43^{A90V}-ACM (all diluted 1:6). For studies performed with mouse ACMs, GRT-X was used at 0.5 μM , for the ones with human ACMs, pharmacological treatment with GRT-X was applied at concentrations of 1 μM and 2.5 μM . Culture medium without ACM was used

as control (CTRL medium). At 7 DIV, cultures were fixed and immunostaining analysis was performed to determine MN survival.

The SCOCs were exposed at 7 DIV to the same mouse ACM (1:9) or human ACM (1:6) used in VSCNs. GRT-X was applied at 6.25 μ M, 12.5 μ M and 25 μ M in SCOCs until 11 DIV. Culture medium without ACM was added as control (CTRL medium). Finally, immunofluorescence was performed for MN counting.

MN viability analysis by immunofluorescence

In VSCNs, MNs and interneurons were immunolabeled and counted as previously described (Fritz et al., 2013; Arredondo et al., 2022). Briefly, cultures were fixed with 4% PFA at 7 DIV and incubated with primary antibody against microtubule-associated protein 2 (MAP2, 1:200; Invitrogen; Cat. #OSM00030W) to label interneurons and MN and with anti-neurofilament H non-phosphorylated (SMI-32, 1:1,000, Biolegend; Cat. #8071701), specifically expressed in MNs in culture (Arredondo et al., 2022). After incubation of the appropriate fluorescent secondary antibodies, MNs were visualized with epifluorescent illumination on an Olympus IX81 microscope (equipped with a Q-Imaging Micropublisher 3.3 Real-Time Viewing camera) using a 20x objective. MAP2- and SMI32-positive neurons were counted off-line using Fuji ImageJ. At least 12 randomly chosen fields were analyzed to calculate the percentage of SMI-32-positive MNs within the total number of MAP2-positive cells per condition. Each condition was replicated in 3–4 independent cultures.

In SCOCs, MNs were immunolabeled as previously described (Herrando-Grabulosa et al., 2016). Shortly, slices were fixed with 4% PFA, blocked with 5% normal horse serum (Biowest; Cat. # S0910500) and 0.3% Triton-X-100 in PBS (PBS-TX) and incubated with primary antibody against SMI-32 (1:250, Biolegend; Cat. #801701) for 48h. After incubation of secondary antibody Alexa Fluor488 donkey anti-mouse IgG (1:500, Invitrogen; Cat. #A21202) and DAPI (1:2000, Sigma; Cat. #D9564-10MG) Z-stack fluorescence images were captured using a Zeiss LSM 510 Meta confocal microscope. MNs in the slices were identified by SMI-32 immunostaining and their localization in the ventral horn and morphology. All identified MNs were counted in each hemispinal cord by the Cell Counter tool of ImageJ software. Each condition was replicated in 3–4 independent cultures.

Intracellular ROS/RNS measurement with CM-H2DCF-DA

Intracellular levels of reactive oxygen species (ROS) and reactive nitrogen species (RNS) were measured with CM-H2DCF-DA (Invitrogen, Cat. #C6827). CM-H2DCF-DA solution (5 mM) was prepared in DMSO and diluted in culture medium to a final concentration of 1 μ M. To facilitate CM-H2DCF-DA membrane penetration, avoid hydrolysis and maintain cell integrity, 0.004% Pluronic acid F-127 (Invitrogen, Cat. No. P-3000MP) was added to the culture medium (Appaix et al., 2012).

After the application of ACM in VSCNs, cells were washed to remove ACMs and exposed to CM-H2DCF-DA 37°C in the dark, labeling both MNs and interneurons. CM-H2DCF-DA-containing culture medium was removed and cultures were suspended in fresh culture medium (500 μ l final volume). Next, cells were immediately imaged using an inverted Nikon Eclipse Ti-U microscope equipped with a SPOT Pursuit™ USB CameraCCD (14-bit), Epi-fl Illuminator, mercury lamp, and Sutter SmartShutter with a lambda SC controller. Exposure time was kept below 4s with excitation and emission wavelengths 492-495nm and 517-527nm, respectively. At least three independent fields were used for each condition (all fields were exposed for the exact same amount of time) and at least 10 cells per field were used for the quantification of the fluorescence signal. Fluorescence intensity was calculated for each region of interest of the cell body using the image analysis module in ImageJ software. Cells with a relative intensity unit (RIU) of ≥ 1.5 were counted as positive.

Data analyses

All data are expressed as mean \pm SEM. One-way ANOVA, followed by Bonferroni's post-hoc test was used to detect significant changes. Differences were considered significant at * $p < 0.05$, ** $p < 0.01$, *** $p < 0.001$, **** $p < 0.0001$. At least 3-4 independent cultures/conditions.

RESULTS

GRT-X up to 2.5 μ M does not generate toxicity in primary VSCNs

A dose-response curve of GRT-X was performed to determine the maximum concentration of GRT-X tolerated by MNs in VSCNs when treated from 4 to 7 DIV. At 7 DIV, spinal cord cultures were fixed and neuronal survival was assayed by double immunostaining for MAP2 to identify all neurons and SMI32 to selectively identify MNs. The data show that concentrations up to 2.5 μ M of GRT-X did not significantly reduce MN survival (Fig. 1A-B). Therefore, concentrations of 0.5 μ M, 1 μ M and 2.5 μ M of GRT-X were chosen for further studies performed in VSCNs.

GRT-X prevents MN degeneration in SCOCs exposed to glutamate

Due to the different cellular and culture medium composition of the SCOCs compared with primary MN cultures, we investigated the effectiveness of different GRT-X concentrations to exert neuroprotection in SCOCs exposed to glutamate. Acute excitotoxic damage induced by adding glutamate at 50 μ M for 30 minutes reduced the number of SMI-32⁺ MNs in the ventral horn by 45% (55 \pm 2 % MN preserved), compared to untreated slices (control, 100 \pm 2 % MN preserved; Fig. 1C-E). The addition of GRT-X at 6.25, 12.5 and 25 μ M showed a significant dose-dependent reduction in MN death (45 \pm 4; 76 \pm 3; 85 \pm 3 % MN preserved, respectively) reaching a maximum protective effect at 25 μ M. No MN loss was detected in SCOCs under vehicle (DMSO), when exposed to Locke solution without glutamate.

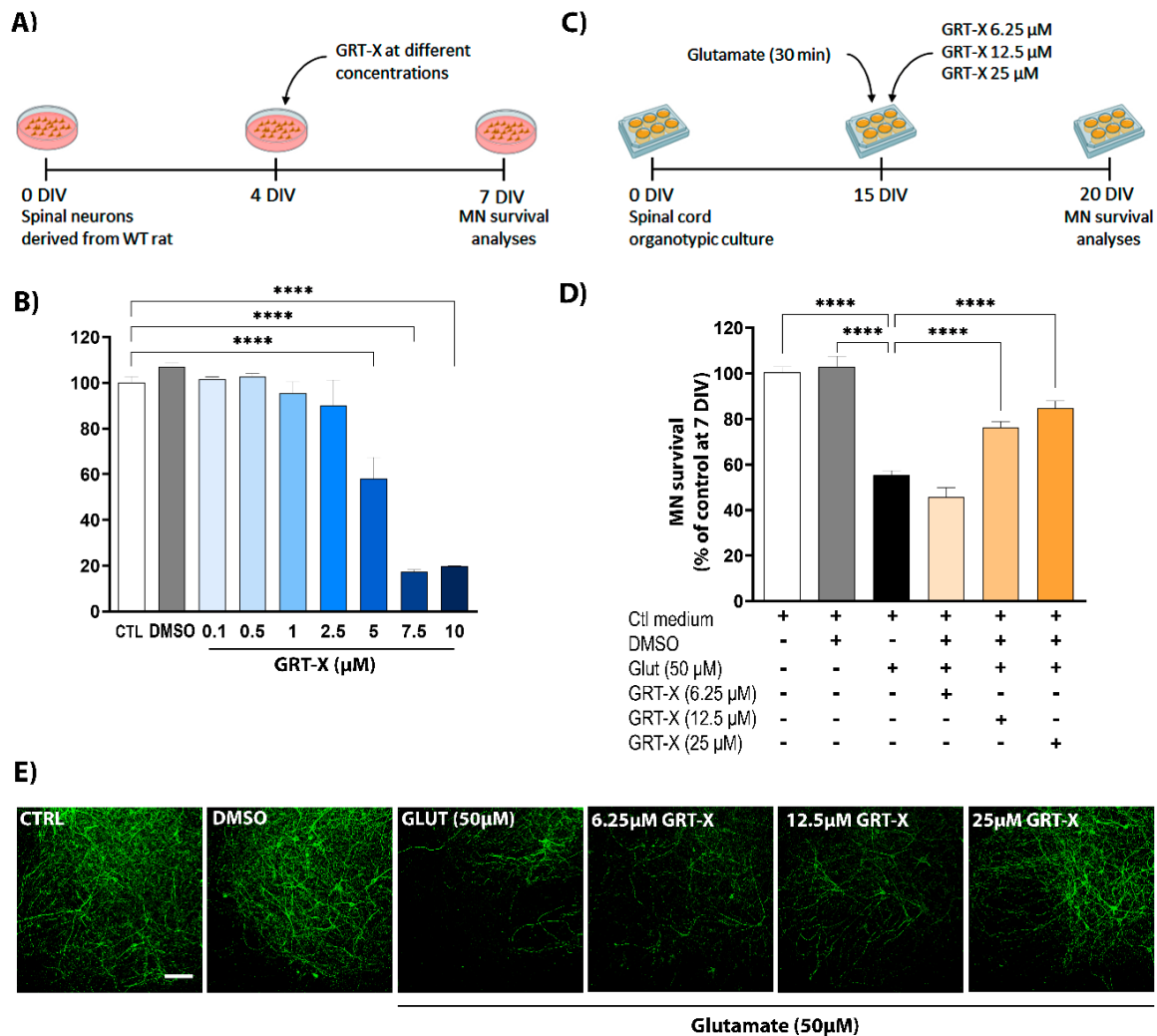


Figure 1. Dose-response effect of GRT-X in spinal cord cultures and spinal cord slices (A) Experimental design of GRT-X toxicity assessment in spinal MN cultures derived from WT rats. (B) Graph showing the percentage of MN survival (SMI32⁺/MAP2⁺ cells) in VSCNs exposed to increasing concentrations of GRT-X from 0.1 to 10 μ M. Untreated (CTRL) and vehicle (DMSO) were used as controls. (C) Experimental design of the evaluation of GRT-X neuroprotective capacity in SCOCs under excitotoxicity conditions (50 μ M glutamate exposure for 30 min). (D) Plot showing the percentage of SMI-32⁺ surviving MNs in the ventral horn of spinal cord hemislices after glutamate exposure with or without GRT-X treatment. Untreated slices (CTRL medium) and vehicle (DMSO) were used as controls. (E) Representative images of 20 DIV spinal cord ventral horns exposed to glutamate (GLUT 50 μ M) in the presence and absence of GRT-X at three concentrations (6.25, 12.5 and 25 μ M). MNs were visualized in fixed slices with immunofluorescence staining for SMI32⁺ (green). Scale bar 100 μ m. Data are shown as mean \pm SEM. One-way ANOVA with Bonferroni's post hoc test: **** $p < 0.0001$ versus Glutamate condition or Control condition).

GRT-X rescues MNs from death in VSCNs and SCOCs when exposed to mouse $SOD1^{G93A}$ -ACM

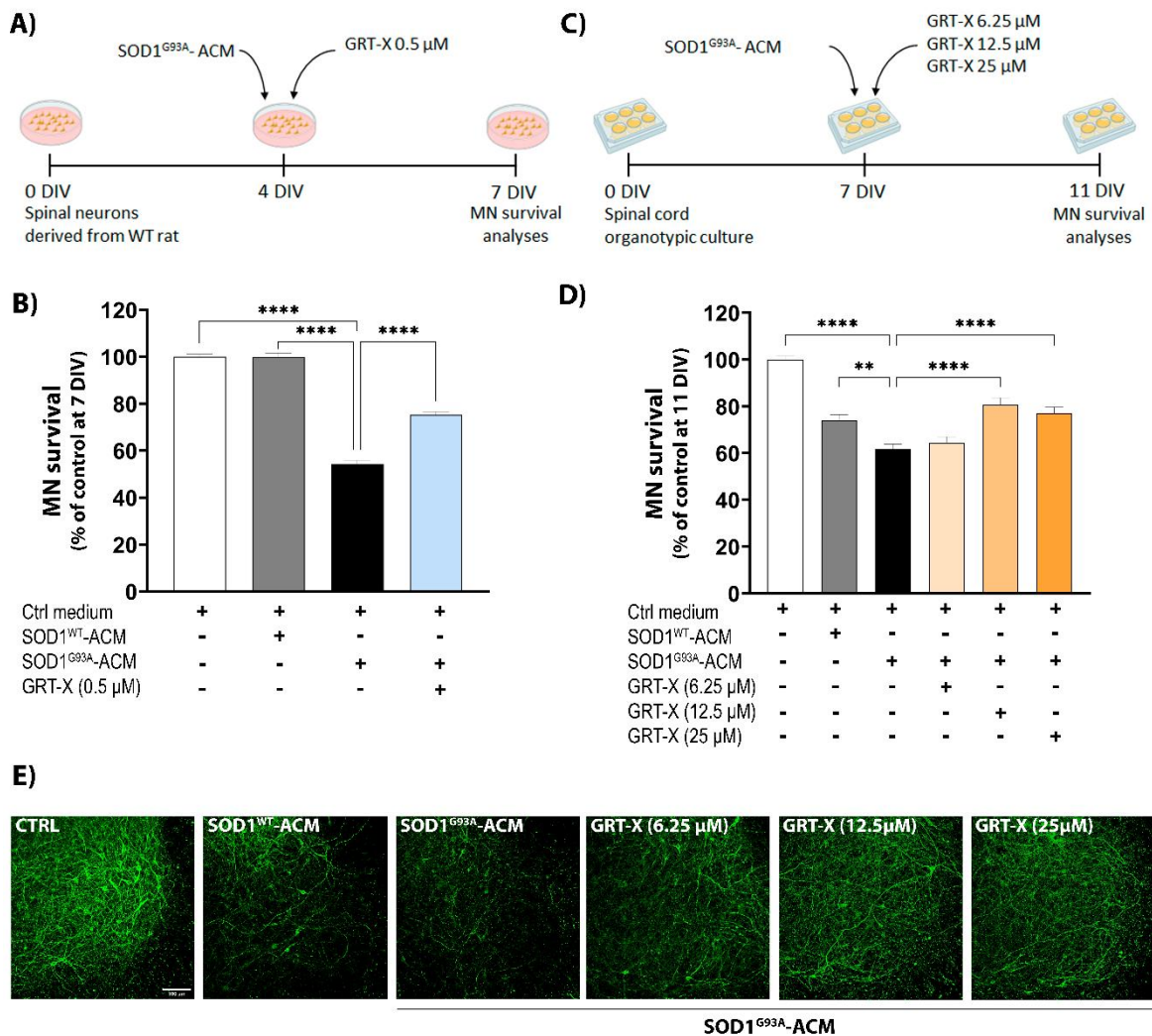


Figure 2. GRT-X treatment rescues MNs from cell death induced by mouse $SOD1^{G93A}$ -ACM. (A) Experimental design to test the effects of GRT-X treatment on VSCNs exposed to mouse $SOD1^{G93A}$ -ACM. (B) Bar graph showing that GRT-X (0.5 μ M) rescues MNs in VSCNs treated with $SOD1^{G93A}$ -ACM. (C) Experimental design to test the effects of GRT-X treatment on SCOCs exposed to $SOD1^{G93A}$ -ACM. (D) Bar graph showing that GRT-X at 12.5 and 25 μ M rescues MNs in SCOCs treated with $SOD1^{G93A}$ -ACM. (E) Representative images of SMI32⁺-MNs (green) in the ventral horn of spinal cords at 11 DIV under the tested conditions. Scale bar 100 μ m. Data are shown as mean \pm SEM. One-way ANOVA with Bonferroni's post hoc test: **** $p < 0.0001$ and ** $p < 0.01$ versus $SOD1^{G93A}$ -ACM condition.

Next, we explored the beneficial effects of GRT-X in ALS *in vitro* models with wild-type MNs and ALS-ACM harvested from primary astrocyte cultures that were generated from mice overexpressing the human $SOD1^{WT}$ and human $SOD1^{G93A}$ protein. These ACMs were added at 1:8 dilution to VSCNs at 4 DIV for 3 days (Fig. 2A). In agreement

with previous studies (Fritz et al., 2013; Rojas et al., 2014; Arredondo et al., 2022), exposure of the VSCNs to SODI^{G93A}-ACM, but not SODI^{WT}-ACM, induced 46% of MN death (54 ± 1 % MN preserved) (Fig. 2B). We found that the addition of 0.5 μ M GRT-X to these cultures partially prevented MN death, with MN survival rates of 75%.

In addition, we assessed the effects on MN survival in the ventral horn of wild-type rat SCOCs exposed to ALS-ACM in the absence and presence of GRT-X (Fig. 2C). In these SCOCs, exposure to SODI^{WT}-ACM led to a significant MN loss of around 25% (74 ± 2 % MN preserved) compared to the control condition. The toxic effect of SODI^{WT}-ACM might be related to previous studies in which aged human SODI^{WT} mice triggered astrocytic reactivity and MN loss in the mouse spinal cord (Jaarsma et al., 2000). Addition of SODI^{G93A}-ACM to SCOCs induced a more severe MN loss, around 40% (62 ± 2 % MN preserved), reaching significant difference between control and SODI^{WT}-ACM (Fig. 2D-E). When GRT-X was added simultaneously with the ACMs to the SCOCs, the 6.25 μ M dose was ineffective, while higher GRT-X doses of 12.5 μ M and 25 μ M significantly preserved MN viability (81 ± 3 ; 77 ± 3 % MN preserved, respectively) (Fig. 2D-E).

GRT-X treatment preserves MN survival in VSCNs exposed to human SODI^{D90A}-ACM

We also wanted to determine the beneficial effects of GRT-X using human ALS astrocyte-conditioned medium. For this, we generated mature astrocytes from ALS patient iPSCs carrying the D90A mutation in SODI (SODI^{D90A}) and from control subject iPSCs; we used similar protocols as recently described for the generation of TDP43 and control subject mature astrocytes (Arredondo et al., 2022). Immunofluorescence assays were performed to confirm that an efficient mature astrocyte phenotype (Cx43 and S100 β) was achieved for both control and ALS patient-derived iPSCs (Supplementary Fig. 1). Next, we collected conditioned medium from the human ALS astrocytes and assessed the toxicity of SODI^{D90A}-ACM (1:6 dilution) to MNs in VSCNs (Fig. 3A-B). Controls included SODI^{WT}-ACM and control medium. In agreement with previous studies studying human iPSC- or iNPC-derived astrocytes ACM carrying mutations in SODI (Meyer et al., 2014; Almad et al., 2022), we found that SODI^{D90A}-ACM, but not controls, led to a robust 40% MN death (59 ± 6 % MN preserved) (Fig. 3B). Next, two different concentrations of GRT-X compound, 1 and 2.5 μ M, were tested to evaluate its neuroprotective capacity against SODI^{D90A}-ACM. Results showed a dose-dependent rescue capacity of GRT-X, being statistically significant at both doses tested (89 ± 2 ; 104 ± 5 % MN preserved) (Fig. 3B).

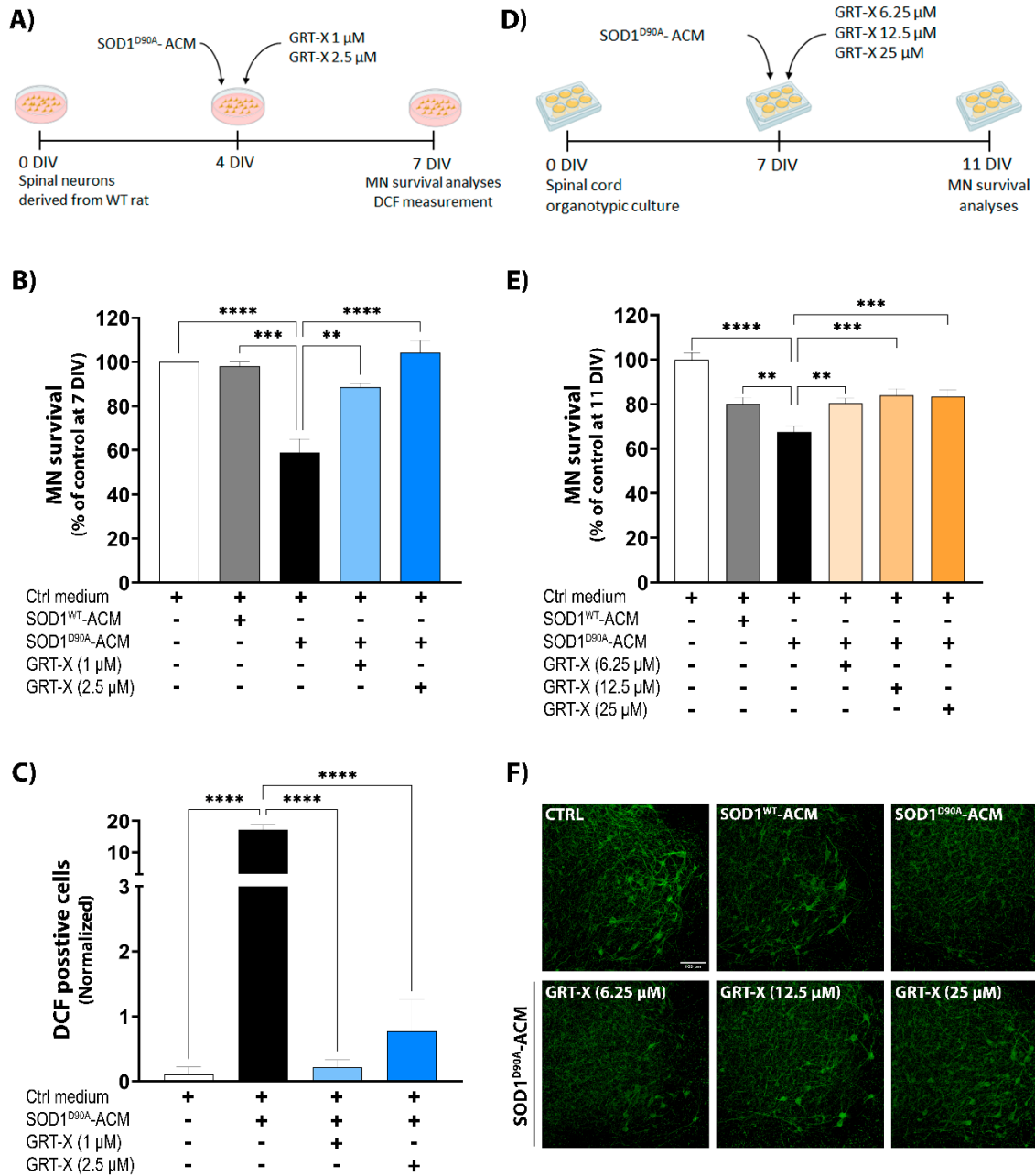


Figure 3. GRT-X treatment rescues MNs from cell death induced by human SOD1^{D90A}-ACM. (A) Experimental design to test the effects of GRT-X treatment on VSCNs exposed to human SOD1^{D90A}-ACM (diluted 1:6). (B) Bar graph showing that GRT-X rescues MNs in VSCNs treated with human SOD1^{D90A}-ACM. (C) Quantification of the intracellular ROS/RNS levels in VSCNs by measurement of DCF fluorescent neurons shows that GRT-X reduces ROS generation. (D) Experimental design to test beneficial effects of GRT-X treatment on SCOCs exposed to human SOD1^{D90A}-ACM. (E) Bar graph showing that GRT-X at all tested concentrations rescues MNs from cell death induced by human SOD1^{D90A}-ACM. (F) Representative images of SMI32⁺-MNs (green) in the ventral horn of spinal cord hemislices at 11 DIV under the tested conditions. Scale bar 100 μ m. Data are mean \pm SEM. One-way ANOVA with Bonferroni's post hoc test: **** p < 0.0001; *** p < 0.001; ** p < 0.01 versus human SOD1^{D90A}-ACM condition and Control medium.

Increased ROS/RNS levels in VSCNs exposed to human SOD1^{D90A}-ACM are reduced by GRT-X

Increased ROS/RNS levels are a shared feature of ALS patients and *in vitro* and *in vivo* ALS models. As previously demonstrated, mouse SOD1^{G93A}-ACM, SOD1^{G86R}-ACM and TDP43^{A315T}-ACM led to rapid increases in intracellular ROS/RNS levels in VSCNs, measured with DCF (Fritz et al., 2013; Rojas et al., 2014). CM-H2DCF-DA is a non-fluorescent dye that is hydrolyzed intracellularly and the oxidation of the DCFH group results in the formation of the fluorescent product DCF. Therefore, increases in fluorescent DCF intensities denote increased intracellular ROS/RNS levels. While under control conditions very few neurons exhibited detectable DCF levels, the application of SOD1^{D90A}-ACM strongly increased neuronal DCF levels (17 ± 2 DCF positive cells). Application of both doses of GRT-X, 1 and 2.5 μ M, markedly reduced DCF levels (0.2 ± 0.1 ; 0.8 ± 0.4 DCF positive cells, respectively) (Fig. 3C).

GRT-X treatment preserves the number of MNs in SCOCs exposed to human SOD1^{D90A}-ACM

In SCOCs, MN survival was assessed at 11 DIV after 4 days of chronic exposure to human SOD1^{D90A}-ACM, SOD1^{WT}-ACM or control ACM (Fig. 3D-F). The presence of human SOD1^{WT}-ACM in SCOCs caused a significant MN death of around 20% (80 ± 3 % MN preserved) compared to control slices, similarly to the effect observed after mouse SOD1^{WT}-ACM addition. The exposure to SOD1^{D90A}-ACM, however, induced a significantly stronger reduction of 32% (68 ± 3 % MN preserved) in the number of SMI-32 labeled MNs in the ventral horn. The three concentrations of GRT-X tested (6.25, 12.5 and 25 μ M) significantly rescued MN death induced by SOD1^{D90A}-ACM (80 ± 2 ; 84 ± 3 ; 83 ± 3 % MN preserved, respectively) (Fig. 3E-F).

GRT-X treatment preserves the number of MNs in VSCNs exposed to human TDP43^{A90V}-ACM

We also evaluated the toxicity of ACM collected from human iPSC-derived astrocytes generated from an ALS/FTD patient carrying an A90V mutation in *TARDBP* (TDP43^{A90V}) and a healthy family member (Zhang et al., 2013; Arredondo et al., 2022). In agreement with our previous study (Arredondo et al., 2022), chronic exposure of VSCNs for 4 days to TDP43^{A90V}-ACM, unlike TDP43^{WT}-ACM, induced around 50% of MN death (48

$\pm 5\%$ MN preserved). We found that both doses tested of GRT-X (1 and 2.5 mM) effectively reduced the TDP43^{A90V}-ACM induced MN death (Fig. 4A–B).

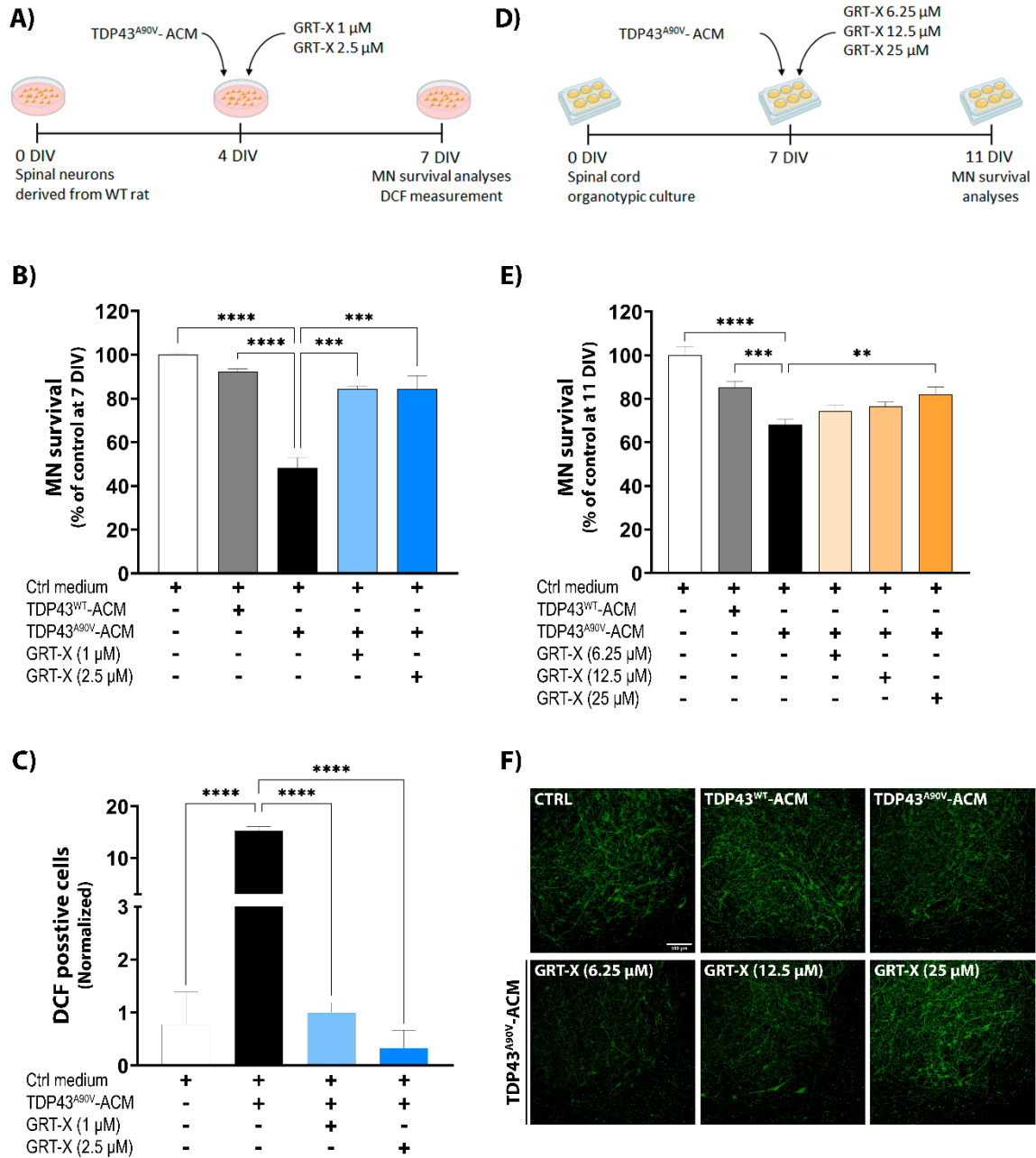


Figure 4. GRT-X treatment rescues MNs from cell death induced by human TDP43^{A90V}-ACM. (A) Experimental design to test the effects of GRT-X treatment on VSCNs exposed to human TDP43^{A90V}-ACM (diluted 1:6). (B) Bar graph showing that GRT-X preserves MN survival in VSCNs treated with human TDP43^{A90V}-ACM. (C) Quantification of the intracellular ROS/RNS levels in VSCNs by measurement of DCF fluorescent neurons, showing that GRT-X reduces ROS generation. (D) Experimental design to test the effects of GRT-X treatment on SCOCs exposed to human TDP43^{A90V}-ACM. (E) Bar graph showing that 25 mM GRT-X rescues MNs from cell death induced by TDP43^{A90V}-ACM in SCOCs. (F) Representative images of SMI32⁺ MNs (green) in the ventral horn of spinal cord hemislices at 11 DIV under the tested conditions. Scale bar 100 μ m. Data are mean \pm SEM. One-way ANOVA followed with Bonferroni's post hoc test: ****p < 0.0001, ***p < 0.001, **p < 0.01 versus TDP43^{A90V}-ACM condition.

Increased ROS/RNS levels in VSCNs exposed to TDP43^{A90V}-ACM are reduced after GRT-X treatment

Similar to SOD1^{D90A}-ACM, the application of human TDP43^{A90V}-ACM led to an increase in DCF levels (15.3 ± 0.7 DCF positive cells) compared to the control medium (0.8 ± 0.6 DCF positive cells). We found that the addition of GRT-X, at 1 μ M and especially at 2.5 μ M, strongly reduced DCF levels (0.9 ± 0.2 ; 0.3 ± 0.3 DCF positive cells, respectively), leading to DCF levels found in the control condition (Fig. 4C).

GRT-X treatment partially preserves the number of MNs from toxic human TDP43^{A90V}-ACM in SCOCs

SCOCs were exposed to TDP43^{A90V}-ACM or TDP43^{WT}-ACM at 7 DIV for 4 days (Fig. 4D). As for previous experiments with ACM in SCOCs, TDP43^{WT}-ACM induced a small but significant cell death (85 ± 3 % MN preserved) compared to control medium, an effect that might be explained by reported results in which ACM from TDP43^{WT} induces neuronal death (S. Lee et al., 2020b). Application of TDP43^{A90V}-ACM to SCOCs caused significantly more MN death (68 ± 2 % MN preserved) compared to TDP43^{WT}-ACM and control conditions (Fig. 4E–F) that was partially reverted by the treatment with GRT-X at 25 μ M (85 ± 3 % MN preserved). Lower doses of GRT-X did not cause significant MN preservation (74 ± 3 ; 76 ± 2 % MN preserved) compared to ACM-TDP43^{A90V} alone.

DISCUSSION

The results of the present study provide evidence of the neuroprotective effects exerted on ALS *in vitro* models by GRT-X, a drug that simultaneously activates the mitochondrial protein TSPO and the Kv7.2/3 potassium channel. GRT-X preserves MN survival in SCOCs exposed to an acute excitotoxic damage and rescues MNs from cell death in primary VSCNs and SCOCs exposed to ACM derived from astrocytes harvested from transgenic mice carrying ALS-causing mutation SOD1^{G93A} and from human astrocytes generated from patients iPSCs carrying pathogenic mutated SOD1^{D90A} or TDP43^{A90V}. Altogether, these data suggest that GRT-X is a good candidate to be explored for the treatment of ALS.

In order to evaluate the neuroprotective capacity of the GRT-X compound, we used *in vitro* models exposed to ACMs. In agreement with previous studies, we found that mouse SOD1-ACM (Nagai et al., 2007; Rojas et al., 2014; Arredondo et al., 2022), human SOD1-ACM (Meyer et al., 2014; Almad et al., 2022) and human TDP43-ACM (Arredondo et al., 2022) induce robust MN cell death in healthy MN spinal cord cultures. Interestingly, here we show for the first time that these human and mouse ALS/FTD-ACMs also cause the death of MNs in organotypic spinal cord cultures. SCOC is a more complex *in vitro* model to evaluate the neuroprotective effects on MNs since the anatomical organization of the neural circuitry and neuronal/non-neuronal cellular stoichiometry are preserved in the cultured spinal cord. These characteristics make SCOCs a good model to test the effects of new drugs that may be studied from an integrated perspective (Guzmán-Lenis et al., 2009; Herrando-Grabulosa et al., 2016). In the present study, we also found that human SOD1^{WT}-ACM and TDP43^{WT}-ACM led to a detrimental effect on MNs in SCOCs. We hypothesize that the astrocytes present in these slice cultures might be activated in the presence of ACM derived from unmutated cell cultures and produce a deleterious effect.

ALS is a multifactorial disease in which several molecular mechanisms are involved, including excitotoxicity, hyperexcitability, oxidative stress, mitochondrial dysfunction, impaired protein homeostasis and aberrant RNA metabolism (Hardiman et al., 2017; Mancuso & Navarro, 2015; van Zundert et al., 2012). Most of the used *in vitro* models focused only on one of the several altered mechanisms identified in ALS pathology, such as excitotoxicity. We report here that the GRT-X compound preserves MNs from excitotoxic damage, similarly to Riluzole, the first treatment approved for ALS, which is classified as an anti-excitotoxicity drug (Bellingham, 2011). While Riluzole has a wide range of effects, at

clinical relevant concentrations this pharmacological agent preserves MNs mainly by reducing repetitive firing (inhibiting Na⁺ currents and potentiating K⁺ channels) and glutamatergic neurotransmitter release (Bellingham, 2011; Doble, 1996). Even though GRT-X differs in targets from Riluzole, the activation of Kv7.2/3 generates a robust stabilization of the membrane resting potential that could counteract the disease hyperexcitability. GRT-X acts similarly to other Kv7.2/3 activators, such as retigabine (Ghezzi et al., 2018), but it has a higher affinity to Kv7.2/3 than retigabine (Bloms-Funke et al., 2022a).

We have shown that GRT-X reduces ROS/RNS levels in VSCNs when exposed to SOD1^{D90A}-ACM and TDP43^{A90V}-ACM. Previous studies using TSPO ligands have shown reduced ROS production in different cell types, such as isolated cardiomyocytes (de Tassigny et al., 2013) and endothelial cells (Biswas et al., 2018; Joo et al., 2015). While the exact mechanism has not been elucidated, it was demonstrated in endothelial cells treated with TSPO ligands decreased (or reverted increased) ROS production and increased catalase activity and glutathione levels (Biswas et al., 2018). Therefore, we hypothesize that GRT-X acts similarly to other TSPO ligands in reducing ROS/RNS levels in our experiments.

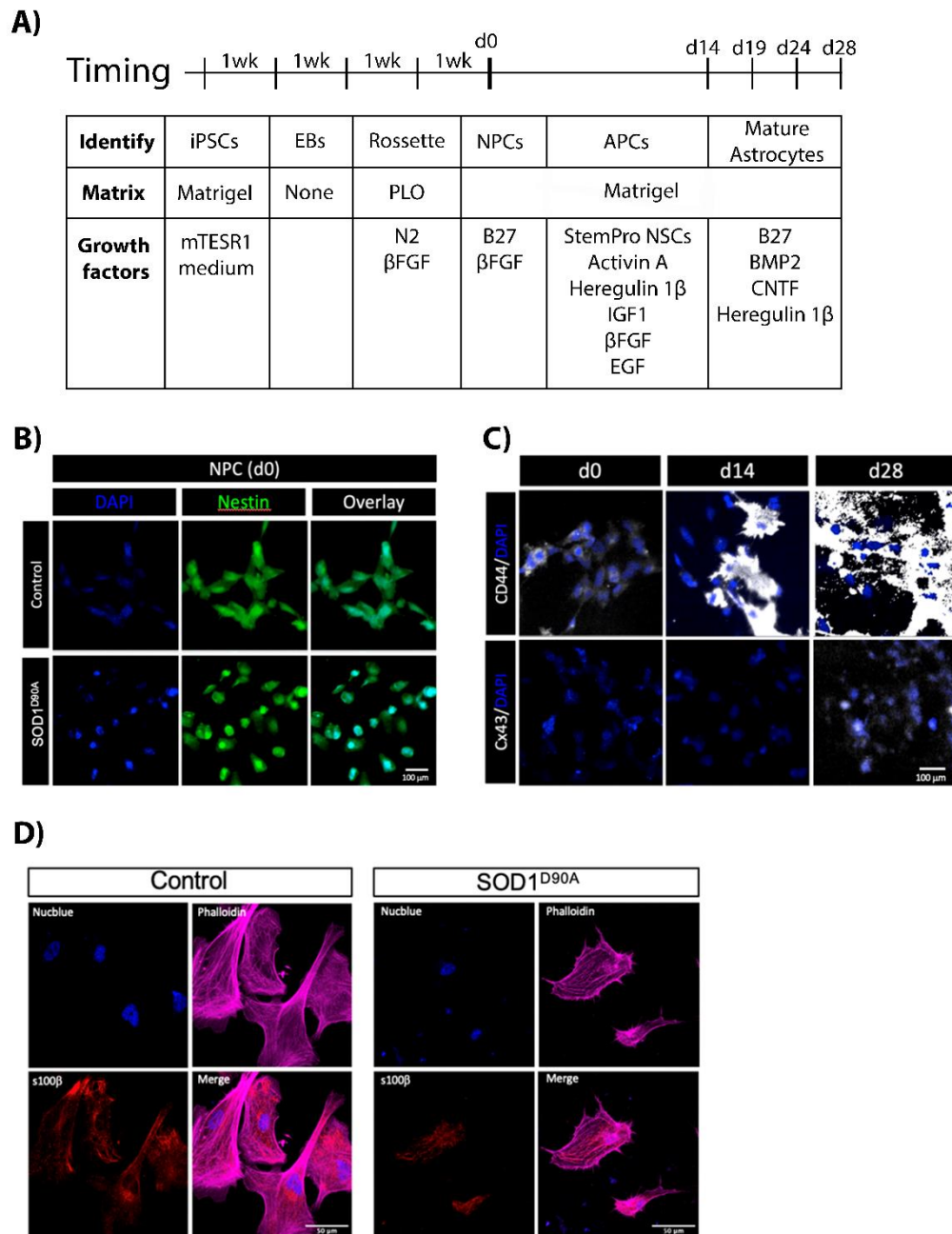
TSPO function has been also linked to mitochondrial energetic metabolism. The treatment with TSPO agonists Ro5-4864 and PK11195 had a stimulatory effect on basal respiration and ATP-related respiration in BV2 microglial cells (Bader et al., 2019). Besides, TSPO KO reduces mitochondrial membrane potential, impairment of mitochondrial function and inhibition of oxidative phosphorylation in BV2 microglial cells (Yao et al., 2020). Thus, activation of TSPO by GRT-X could contribute to maintaining mitochondrial energetic metabolism and, consequently, participate in MN preservation.

There is some controversy regarding the involvement of TSPO in steroidogenesis. Despite it was reported that the knock-out of TSPO did not induce changes in steroidogenesis (Banati et al., 2014; Morohaku et al., 2014; Tu et al., 2014), other studies showed that TSPO-KO mice have altered steroidogenic flux and reduced total steroidogenic output (Barron et al., 2018) and CRISPR/Cas9 TSPO deficiency reduced progesterone levels and steroid formation (Fan et al., 2015). A previous study using GRT-X in a model of cervical root injury demonstrated an increase of intramitochondrial cholesterol transport and stimulation of neurosteroidogenesis (Bloms-Funke et al., 2022a). Increased neurosteroid levels are beneficial due to their neuroprotective constitution by attenuating

excitotoxicity, neuroinflammation, oxidative stress or neuronal degeneration (Borowicz et al., 2011).

In summary, the significant neuroprotective effects of GRT-X on MNs exposed to glutamate to induce excitotoxicity or to human or mouse ALS/FTD-ACM are likely mediated by the dual-mode action of this drug, targeting TSPO and Kv7.2/3 channels. Our data suggest that the decrease in hyperexcitability, reduction of ROS/RNS levels, maintenance of mitochondrial energetic metabolism and homeostasis, and stimulation of neurosteroidogenesis contribute to this neuroprotective effect. Our data may open a new therapeutic window to protect MNs pharmacologically by using GRT-X in MN degenerative pathologies.

SUPPLEMENTARY FIGURES



Supplementary Figure 1. Differentiation and characterization of iPSC-derived astrocytes of a control subject and an ALS patient harboring mutant SOD1^{D90A}. (A) Schematic protocol showing the differentiation process from iPSCs to EBs, NPCs, APCs and finally mature astrocytes. (B) Representative fluorescence microscopy images for NPCs (day 0, d0) derived from a control subject and an ALS patient harboring mutant SOD1^{D90A}, both showing robust immunofluorescence staining with the NPC marker Nestin (green). (C) Immunofluorescence analysis performed from Control subject cells at d0 (NPCs), d14 (APCs) and d28 (mature astrocytes), showing staining with the APC marker CD44 from d0 and mature astrocyte marker Cx43 at d28. (D) Immunofluorescence analysis performed with phalloidin (violet) and mature astrocyte marker S100b (red). Note that a similar mature astrocytic phenotype is found in mature astrocytes derived from SOD1^{D90A} patients and control iPSCs. Cell nuclei were stained with Nucblue (blue).

Chapter III

The compound GRT-X promotes neuroprotection in the
SOD1^{G93A} mice

The compound GRT-X promotes neuroprotection in the SOD1^{G93A} mice

Vera M. Masegosa^{1,2}, Mireia Herrando-Grabulosa^{1,2}, Brigitte Van Zundert^{3,4}, Xavier Navarro^{1,2*}

¹Department of Cell Biology, Physiology and Immunology, Institute of Neuroscience, Universitat Autònoma de Barcelona, Bellaterra, Spain

²Centro de Investigación Biomédica en Red (CIBER), Instituto de Salud Carlos III, Madrid, Spain

³Institute of Biomedical Sciences (ICB), Faculty of Medicine & Faculty of Life Sciences, Universidad Andres Bello, Santiago, Chile

⁴Department of Neurology, University of Massachusetts Chan Medical School (UMMS), Worcester, MA, USA

*Corresponding author

Keywords: GRT-X compound, amyotrophic lateral sclerosis, SOD1^{G93A} transgenic mice, motoneuron degeneration.

ABSTRACT

Amyotrophic lateral sclerosis (ALS) is a fatal neurodegenerative disease characterized by the progressive degeneration of motoneurons (MNs) in the motor cortex and spinal cord. Currently, there is no effective therapy for ALS and patients die within 2-5 years after the disease onset. Given ALS is a multifactorial disease in which a wide variety of pathophysiological mechanisms have been reported to contribute to MN degeneration, targeting several of these altered mechanisms may be a better strategy for ALS treatment. In this study, we assessed the potential neuroprotective efficacy of the newly synthesized GRT-X compound, which produces simultaneous activation of the voltage-gated potassium channels Kv7.2/3 and the mitochondrial translocator protein (TSPO), in the SOD1^{G93A} ALS mice. GRT-X did not induce toxicity in the mice and readily crossed the blood-brain barrier. GRT-X was then administered daily by gavage from 8 to 16 weeks of age and disease progression was assessed using electrophysiology and locomotion tests. Our results showed that the GRT-X compound at 50 mg/kg, but not at lower doses, improves the decline of neuromuscular function and motor activity in SOD1^{G93A} mice. The beneficial effects were more marked in female than in male mice. Histological analysis proved that GRT-X promotes MN survival and neuromuscular junction innervation in treated SOD1^{G93A} mice. Altogether, these data highlight the effectiveness of the GRT-X compound for the treatment of ALS pathology.

INTRODUCTION

Amyotrophic lateral sclerosis (ALS) is a fatal neurodegenerative disorder characterized by progressive motor neuron (MN) degeneration in the motor cortex and spinal cord, leading to muscle weakness and atrophy. Most ALS cases are sporadic (sporadic ALS, sALS) and their cause remains unknown, while approximately 5-10%, are linked to several genetic mutations (familial ALS, fALS). The most common cause of fALS cases is the repeat expansion (G4C2) open reading frame 72 (C9orf72) region of the human chromosome 9 (DeJesus-Hernandez et al., 2011) followed by mutations in the SOD copper-zinc (SOD1) gene (Rosen et al., 1993) and, in less proportion, by mutations in genes encoding for 43kDa TAR DNA-binding protein (TDP-43) (Gitcho et al., 2008), among others. The SOD1^{G93A} mice which constitutively express high levels of the human SOD1 protein carrying the substitution of glycine for alanine at position 93 is the most explored model in ALS research. SOD1^{G93A} transgenic mice show a severe loss of MN in the ventral spinal cord that results in hindlimb weakness by the third month of age and progresses to muscle paralysis and finally death at 5-6 months recapitulating most of the clinical and histopathological features of ALS (Ripps et al., 1995).

Currently, there is no effective therapy for ALS. Treatments used for ALS are symptomatic, in addition to Riluzole or other drugs for specific patient populations, all of them have limited improvement on patient lifespan (Houzen et al., 2021; R. G. Miller et al., 2012). Hence, new therapies need to be assessed. Since ALS is a multifactorial disease in which a wide variety of pathophysiological mechanisms have been reported to contribute to MN degeneration, including excitotoxicity, mitochondrial dysfunction, oxidative stress, cytoplasmic protein aggregation, hyperexcitability, and others (Mancuso & Navarro, 2015; Van Damme et al., 2017), targeting several of these altered mechanisms at the same time could result in better outcome.

Therefore, based on this hypothesis and the encouraging results previously observed with single-action compounds, we propose a combinational therapy with the novel compound GRT-X in the SOD1^{G93A} mouse model of ALS. GRT-X has a unique pharmacological profile since it belongs to a novel class of small molecules able to activate both the mitochondrial translocator protein (TSPO) and the voltage-gated potassium channels 7.2/3 (Kv7.2/3) simultaneously. GRT-X was originally discovered as an analgesic, but due to its pharmacological profile, it was repurposed as a novel ALS therapy. GRT-X exhibits neuroprotective and neuroregenerative properties after cervical spinal nerve crush lesion in rats (Bloms-Funke et al., 2022a). Besides, we have

previously demonstrated that GRT-X exerts MN protection and restores increased oxidative levels when primary neuronal and spinal cord slice cultures are exposed to ALS-astrocyte conditioned medium (ACM) (see Chapter II).

The two molecular targets of GRT-X have been previously proposed for ALS therapy. TSPO is an 18 kDa integral protein localized in the outer mitochondrial membrane expressed in glial cells, neurons and endothelial and ependymal cells in the central nervous system. Although the role of TSPO in neurosteroidogenesis is well established (J. Fan et al., 2018; Mukhin et al., 1989; Papadopoulos et al., 1990), studies using TSPO knockout mice revealed that TSPO is also involved in other cellular processes, such as regulation of mitochondrial function, energy metabolism and oxidative stress (Banati et al., 2014; Gatliff et al., 2014; Tu et al., 2014). Interestingly, Olesoxime, an activator of TSPO, was found to promote MN survival and decrease oxidative stress (Bordet et al., 2007). In addition, Olesoxime decreased microglial and astroglial activation, prevented MN death, preserved NMJ integrity and increased the lifespan of SOD1^{G93A} mice (Bordet et al., 2007; Sunyach et al., 2012). However, a clinical trial demonstrated that Olesoxime did not provide significant beneficial effects for ALS patients (Lenglet et al., 2014).

The second target of GRT-X is the heteromeric form of Kv7.2 and Kv7.3, mainly localized in the nervous system and sensory organs. Kv7.2/3 plays a crucial role in maintaining the resting membrane potential by generating the M-current, which suppresses the tendency of neurons to burst repetitive action potentials in response to excitatory stimuli (Soldovieri et al., 2011). The activation of Kv7 channels is a promising target since they can be activated at subthreshold voltages and effectively regulate neuronal excitability. The activation of Kv7.2/3 by retigabine dose-dependently blocked hyperexcitability and enhanced survival of SOD1^{A4V/+} ALS MNs (Wainger et al., 2014). In addition, the activation of Kv7.2/3 decreased the mean firing rate of hPSC-derived and mouse MNs (Moakley et al., 2019). In two different clinical trials, it was demonstrated that the activation of Kv7.2/3 with retigabine reduced axonal excitability in ALS patients (Kovalchuk et al., 2018; Wainger et al., 2021). In the study in Chapter I, we also demonstrated that a more selective compound for Kv7.2/3, ICA-27243, dose-dependently prevented MN degeneration in spinal cord culture and in the transgenic SOD1^{G93A} mice.

Therefore, TSPO and Kv7.2/3 channels are potential combinatory targets for ALS therapy, since they act downstream on different cellular processes. Considering the

above evidence and the beneficial outcomes of GRT-X treatment *in vivo* and *in vitro* models of MN death, we aimed to assess its effectiveness in the ALS SOD1^{G93A} mice.

MATERIALS AND METHODS

Animals

Transgenic SOD1^{G93A} mice (B6SJL-Tg [SOD1-G93A] 1Gur) and non-transgenic wild-type (WT) littermates were used. Identification of transgenic offspring was carried out through PCR amplification of DNA extracted from the tail, using the following primer sequences: 1) hSOD1-forward CATCAG CCCTAATCCATCTGA, 2) hSOD1-reverse CGCGACTAACAA TCAAAGTGA, 3) mIL2-forward CTAGGCCACAGAATTGAA AGATCT and 4) mIL2-reverse GTAGGTGGAAATTCTAGC ATCATCC. All animals were kept under standard conditions and handled according to guidelines established by the European Union Council (Directive 2010/63/EU). The experimental procedures were approved by the Ethics Committee of the Universitat Autònoma de Barcelona.

This study included groups of WT mice, one group untreated or treated with GRT-X and groups of SOD1^{G93A} mice, treated with the vehicle solution or different doses of GRT-X. Specified in each procedure. All experiments were carried out with female and male mice.

Pharmacological treatment

GRT-X (N-[(3-fluorophenyl)-methyl]-1-(2-methoxyethyl)-4-methyl-2-oxo-(7-trifluoromethyl)-1H-quinoline-3-carboxylic acid amide) was synthesized by Grünenthal GmbH (Aachen, Germany). Mice were treated with 10, 30 or 50 mg/kg of GRT-X. The drug was administered daily by oral gavage in a volume of 10 ml/kg between 7 and 16 weeks of age (specified in each experiment). GRT-X compound was dissolved in HPMC (Cat. #H9262, Sigma) 1% with 0.5% Tween 80 (Cat. #1754, Sigma).

Toxicity study

Wild-type B6SJL female and male mice were treated daily by gavage with vehicle, 10 mg/kg and 30 mg/kg of GRT-X for 4 weeks, starting at week 13th of age. Body weight and locomotor test (rotarod and treadmill) were performed. Then, animals were euthanized with an overdose of pentobarbital sodium and perfused with 4% paraformaldehyde in PBS to perform a histopathological evaluation of different organs: brain, lung, liver, kidney, small and large bowel. The harvested samples were analyzed by

the accredited Service of Animal Research (SIAL) of the UAB. Briefly, samples were cut 5 mm thick and hematoxylin-eosin staining was performed. Histopathological examinations were performed in order to determine the toxicological profile of GRT-X. Lesions were graded from less severe to more severe considering if they could be attributed to the treatment, had pathological significance, and could affect the animal welfare or survival. The groups included in the toxicity study were: WT + vehicle (n=3), WT + GRT-X 10 mg/kg (n=6), WT + GRT-X 30 mg/kg (n=6).

BBB assay

Male and female SOD1^{G93A} mice at 16 weeks of age were treated with 30 mg/kg and 50 mg/kg GRT-X and after 4 hours post-administration brain samples were obtained. Samples were analyzed by the Service of Drug Analysis of the UAB, where the drug detection technique has been set up purposely. The analytical method is based on protein precipitation and subsequent separation and detection of GRT-X using HPLC-MS/MS. For the BBB assay, two groups of SOD1^{G93A} mice treated with GRT-X were used, one group with a dose of 30 mg/kg [n=4 (Female (F))/ 5 (Male (M))] and the other with 50 mg/kg [n=3 (F)/ 6 (M)].

Electrophysiological test

Motor nerve conduction tests were performed at 8, 12 and 16 weeks of age. Briefly, the sciatic nerve was stimulated with single pulses of 20 μ s and increasing intensity delivered at the sciatic notch. The compound muscle action potential (CMAP) was recorded from tibialis anterior (TA) and plantar interossei (PL) muscles with microneedle electrodes (Mancuso et al., 2011). Muscle evoked potentials (MEP) were recorded from the TA muscle to assess the central descending pathways by stimulating the motor cortex with needles placed over the skull (Mancuso et al., 2011).

The functional studies included the following SOD1^{G93A} mice: SOD1^{G93A} + vehicle [n=12 (F)/ 13 (M)], SOD1^{G93A} + GRT-X 30 mg/kg [n=10 (F)], SOD1^{G93A} + GRT-X 50 mg/kg [n=8 (F)/ 7 (M)], in addition to untreated WT littermates [n=7 (F) /9 (M)].

Locomotion tests

Rotarod test and treadmill test were performed to evaluate motor performance and locomotion. Rotarod test was performed weekly from 8 to 16 weeks of age by placing mice onto the rod at 14 rpm and recording the longest time of three trials without falling,

with a cut-off time at 180 s. Treadmill test was performed at 16 weeks of age. Mice were placed on a treadmill and the speed was increased from 6 rpm to 30 rpm. The maximum speed was recorded when animals could no longer keep up on the treadmill velocity.

Immunohistochemical analyses

Mice were euthanized at 16 weeks of age by an overdose of sodium pentobarbital and transcardially perfused with 4% paraformaldehyde in PBS. The lumbar segment of the spinal cord was post-fixed for 2 hours and cryopreserved in 30% sucrose solution in PBS while hindlimb muscles were directly cryopreserved. The spinal cord was cut serially in 20 µm thick transverse sections using a cryostat (Leica), collected sequentially on 10 slides. A solution of cresyl violet 3.1 mM was applied for 3h to slices corresponding to L4-L5 spinal segments. Then, the slides were washed, dehydrated and mounted with DPX. Identification of MNs relied on their location in the lateral ventral horn and strict morphological and size criteria: polygonal shape, prominent nucleoli and diameter larger than 20 µm.

To assess neuromuscular junctions (NMJ), TA muscle was serially cut into 50 µm thick longitudinal sections, collected in sequential series. Sections were blocked with blocking solution [10% normal donkey serum (Cat. #S30, Millipore) in PBS-Tx 0.3%] for 1 hour and incubated for 48 hours at 4°C with primary antibodies anti-neurofilament 200 (NF200) (1:1000; Cat. #AB5539, Millipore) and anti-synaptophysin (1:500; Cat. #AB32127, Abcam). After washes in PBS with 0.1% Tween-20, sections were incubated overnight at 4°C with Alexa Fluor 594-conjugated secondary antibody (1:200; Cat. #A11042 and #A21207, Invitrogen) and Alexa Fluor 488-conjugated alpha-bungarotoxin (1:200; Cat. #B13422, Life Technologies). Sections were mounted in Fluoromount-G medium (SouthernBiotech, USA). Z-stack fluorescence images were captured using a Zeiss LSM 510 Meta confocal microscope. The proportion of innervated NMJs was calculated by categorizing each endplate as occupied (innervated and partially innervated) or vacant (denervated). At least 60 endplates were analyzed per animal.

Groups for histological analysis at 16 weeks: SOD1^{G93A} + vehicle [n=8], SOD1^{G93A} + GRT-X 30 mg/kg [n=5], SOD1^{G93A} + GRT-X 50 mg/kg [n=8 (F)/ 7 (M)], in addition to untreated WT littermates [n=7 (F) /9 (M)].

Statistical Analysis

All data are expressed as mean \pm SEM. GraphPad Prism 9 software was used for data analyses. Electrophysiological and functional measurements were analyzed by repeated measurement two-way ANOVA. Histological and molecular data were analyzed using One-way ANOVA, followed by post-hoc Bonferroni's test for multiple comparisons. Differences were considered significant at $p \leq 0.05$.

RESULTS

GRT- X does not generate toxicity in mice

First, we evaluated the possible toxicity generated by GRT- X compound in wild- type B6SJL female and male mice. During the period of administration, body weight was maintained in the three groups analyzed, in female (Fig. 1A) as well as male mice (Fig. S1A). No changes were observed in locomotor performance on the rotarod (Fig. 1B and Fig. S1B) and treadmill tests (Fig. 1C and Fig. S1C).

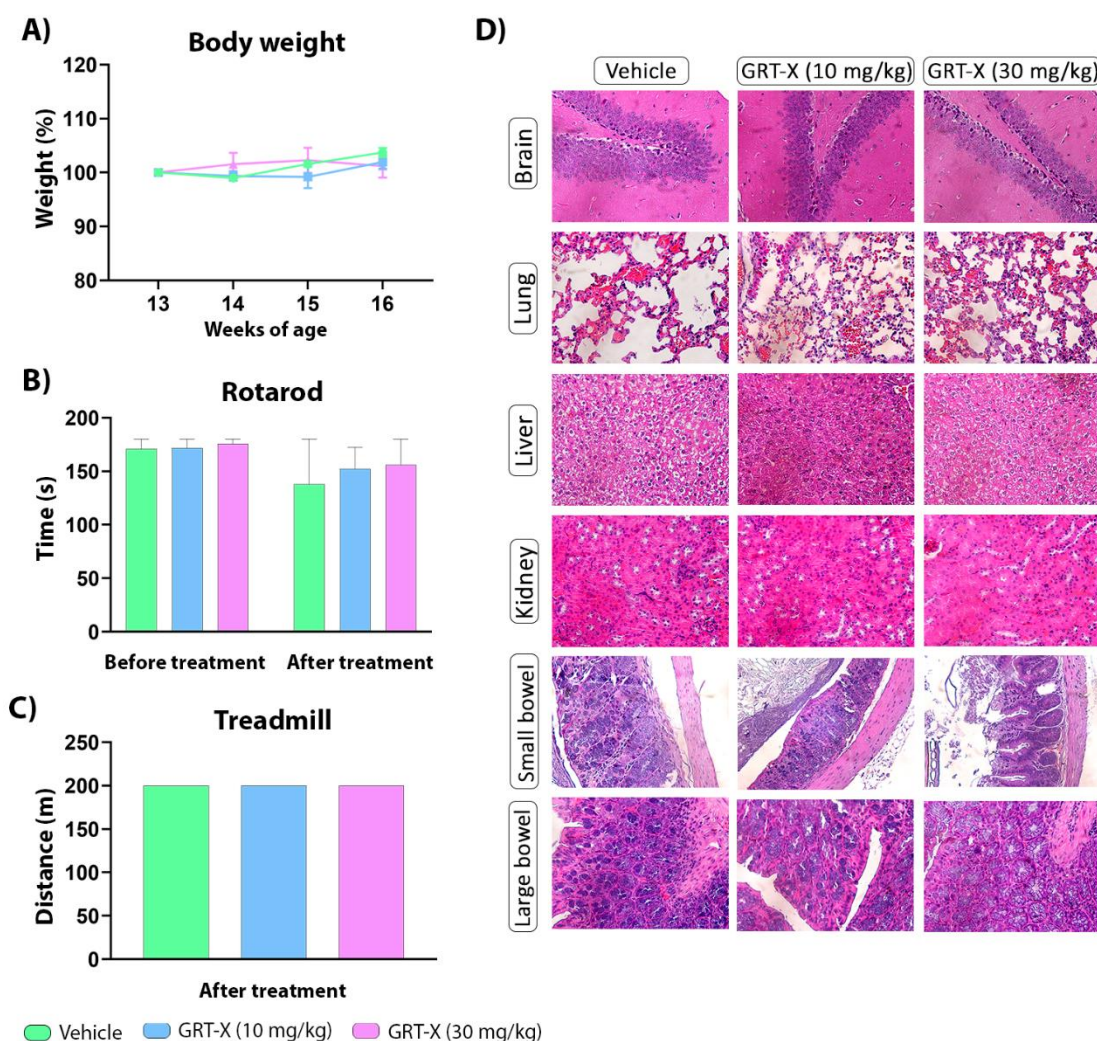


Figure 1 | Treatment with GRT- X does not generate toxicity in female WT mice (A) Body weight (in percentage) was monitored weekly throughout the experiment, from 13 to 16 weeks of age (B) Graph showing motor coordination outcome assessed by the rotarod test at the beginning and end of the study (C) Plot showing the effect of GRT- X on locomotion performance at the end of the study by distance ran in the treadmill (D) Representative images (40X) of brain, lung, liver, kidney and small and large bowel of all experimental conditions stained with eosin and hematoxylin. Data are mean \pm SEM, analyzed by One- way (B, C) and Two- way (A) ANOVA followed with Bonferroni's post hoc test.

Additionally, we performed necropsy and histopathological evaluation. No abnormalities were observed in the histopathological examinations in wild-type B6SJL females (Fig. 1D) and males (Fig. S1D). Therefore, we can conclude that GRT-X administration is safe and non-toxic.

GRT-X crosses the blood-brain barrier

GRT-X was administered as a single dose of 30 mg/kg and 50 mg/kg to female and male SOD1^{G93A} mice. Significant levels of GRT-X were found in the brain of the mice extracted 4 hours later, with higher levels in male than in female mice and at higher levels with the 50 than with the 30 mg/kg dose (Fig. 2A and S2A). Therefore, GRT-X has a good biodisposition and permeability through the BBB in ALS SOD1^{G93A} mice.

GRT-X preserved neuromuscular function in SOD1^{G93A} mice

Female and male SOD1^{G93A} mice treated with GRT-X at 30 mg/kg or 50 mg/kg maintained a gain of body weight as vehicle mice throughout the study, and did not show secondary effects, indicating that the compound does not cause toxicity even with the high dose of 50 mg/kg (Fig. 2B; Fig. S2B).

Regarding the nerve conduction tests GRT-X at 50 mg/kg, but not at 30 mg/kg, significantly preserved the CMAP amplitude of the TA muscle of female SOD1^{G93A} mice at 16 weeks (Fig. 2D), but not of the PL muscle (Fig. 2C). In male SOD1^{G93A} mice treated with 50 mg/kg of GRT-X, there were mild positive effects in the CMAP of the PL at 12 and 16 weeks of age (Fig. S2C), but no differences for the TA muscle (Fig. S2D). The MEP recorded on the TA muscle had significantly higher amplitude in female SOD1^{G93A} mice treated with 50 mg/kg GRT-X, but not 30 mg/kg (Fig. 1E-F), indicating preserved function of the upper MNs. In male SOD1^{G93A} mice treated with 50 mg/kg GRT-X, there is a tendency for higher MEP amplitude in the second component of the TA muscle (Fig. S2E-F).

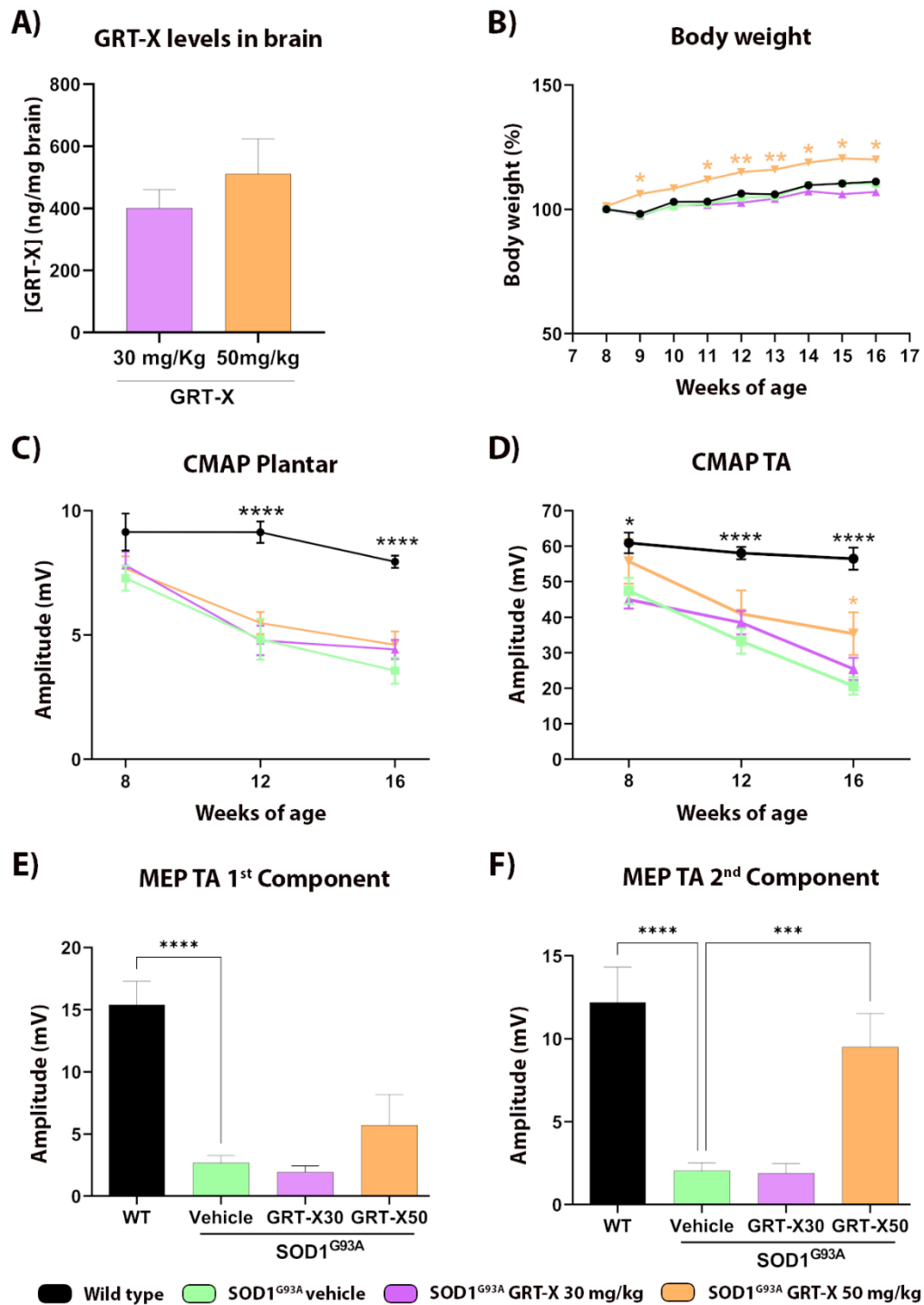


Figure 2 | Treatment with GRT-X enhances neuromuscular function in female SOD1^{G93A} mice (A) Plot showing the concentration of GRT-X compound in the brain of SOD1^{G93A} mice (B) Body weight (in percentage) was monitored weekly throughout the experiment, from 8 to 16 weeks of age (C-D) Values of the amplitude of compound muscle action potentials (CMAP) of tibialis anterior (TA) and plantar interosseus muscles (E-F) Plot of the amplitudes of first (E) and second (F) component of the motor evoked potentials (MEP) of TA muscle. Data are mean \pm SEM, analyzed by One-way (A, E, F) and Two-way (B, C, D) ANOVA followed with Bonferroni's post hoc test: **** $p < 0.0001$; *** $p < 0.001$; ** $p < 0.01$; * $p < 0.05$ vs SOD1^{G93A} - vehicle condition.

To analyze locomotor activity, rotarod and treadmill tests were performed. Rotarod test results showed that 50 mg/kg, but not 30 mg/kg, of GRT-X improved locomotor activity in female (Fig. 3A) and male (Fig. S3A) SOD1^{G93A} mice, with significant differences compared to vehicle mice from the 15th week of age. The disease onset, measured as the first time at which each mouse was not able to maintain 180 s on the rotarod, was delayed by 6 weeks (15 weeks of age) in female mice treated with 50 mg/kg GRT-X compound versus the vehicle group (9 weeks) (Fig. 3B), and by 3 weeks in male mice treated with 50 mg/kg GRT-X compound (15 weeks of age) compared to the vehicle group (12 weeks) (Fig. S3B). There were no significant differences between the vehicle group and the group treated with 30 mg/kg of GRT-X in either sex.

Treadmill test results showed that treatment with 50 mg/kg, but not with 30 mg/kg, of GRT-X significantly improved performance on the treadmill of female SOD1^{G93A} mice (Fig. 3C). In male SOD1^{G93A} mice, none of the doses tested improved the performance on the treadmill test (Fig. S3C).

The innervation of NMJ of the TA muscle was assessed at 16 weeks of age. Female SOD1^{G93A} mice treated with 50 mg/kg, but not 30 mg/kg, of GRT-X, had a significantly higher number of innervated endplates (Fig. 3D), supporting the preservation of CMAP and MEP amplitudes observed in the electrophysiology tests. In male SOD1^{G93A} mice, none of the tested doses enhanced NMJ preservation (Fig. S3D).

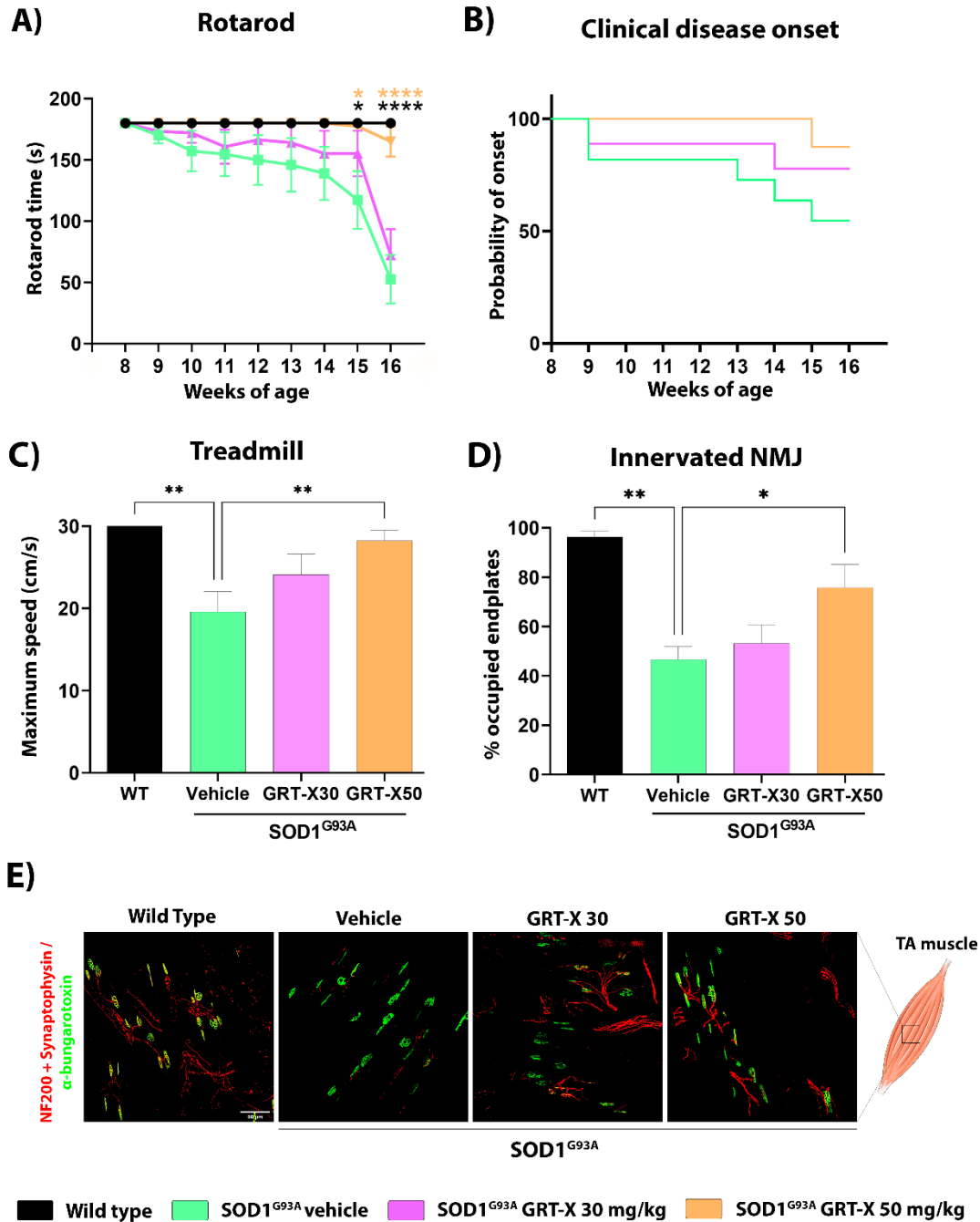


Figure 3 | Treatment with GRT-X improves coordination and motor activity in female SOD1^{G93A} mice (A) Graph showing the effect of different doses of GRT-X treatment on functional outcome assessed by the rotarod test. (B) The probability of clinical disease onset was evaluated based on the decline in performance observed in the rotarod test. (C) Graph showing the effect of different doses on maximum speed assessed by the treadmill test (D) Graph of the percentage of occupied NMJ in the different experimental groups. (E) Representative confocal images of the TA NMJs at 16 weeks of age of all experimental groups shown as maximum projection. Scale bar 100 μm. Data are mean ± SEM. One-way (C-D) and Two-way (A) ANOVA followed with Bonferroni's post hoc test: ****p < 0.0001; **p < 0.01 *p < 0.05 vs SOD1^{G93A}-vehicle condition.

GRT-X promotes MN survival in the lumbar spinal cord in SOD1^{G93A} mice

The counts of α -MNs in the ventral horn of the lumbar spinal cord showed that 50 mg/kg of GRT-X increased the number of surviving MNs in female SOD1^{G93A} mice ($60 \pm 5\%$ MN preserved), compared to vehicle-treated SOD1^{G93A} mice ($41 \pm 2\%$ MN preserved), whereas 30 mg/kg GRT-X had no noticeable effect ($41 \pm 3\%$ MN preserved) (Fig. 4A- B). This effect on MN preservation was not observed in male SOD1^{G93A} mice treated with 30 or 50 mg/kg of GRT-X (Fig. S4A- B).

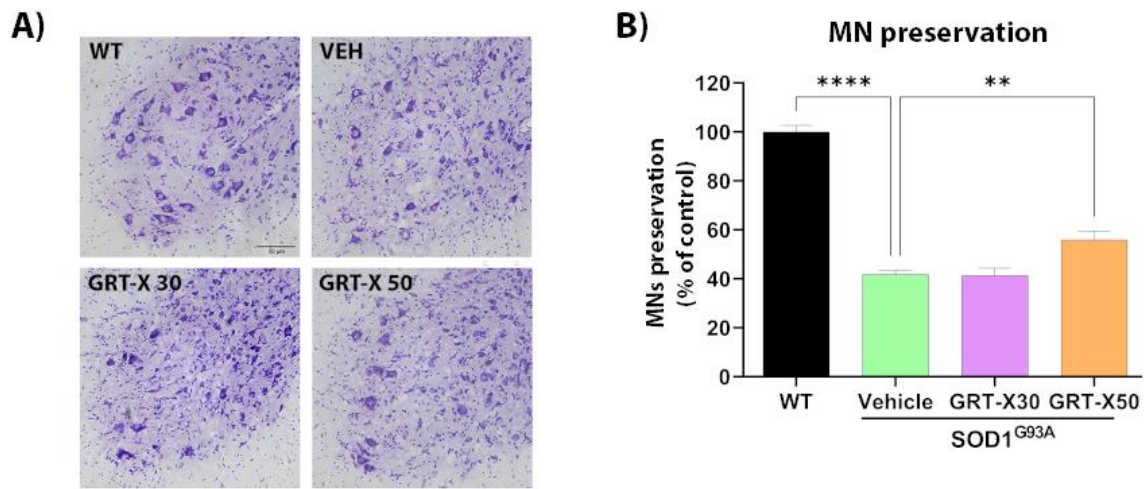


Figure 4 | GRT-X promotes MN survival in the lumbar spinal cord in female SOD1^{G93A} mice
 (A) Representative spinal cord images of MNs stained with cresyl violet. Scale bar 50 μ m. (B) Quantification of surviving MNs (expressed as % of surviving MN vs. WT mice). Data are mean \pm SEM. One-way ANOVA followed with Bonferroni's post hoc test: ****p < 0.0001; **p < 0.01 vs SOD1^{G93A} - vehicle condition.

DISCUSSION

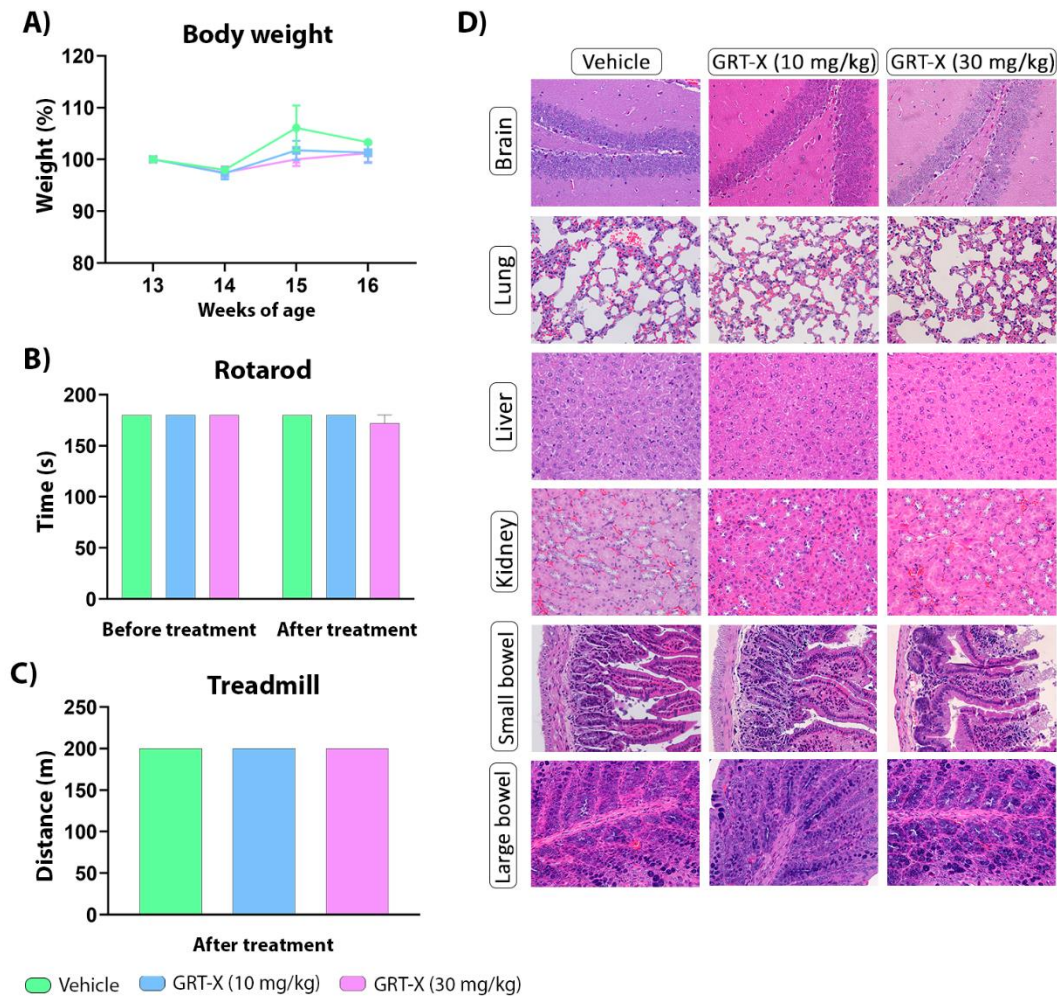
The results of this study demonstrated that the simultaneous activation of the mitochondrial protein TSPO and Kv7.2/3 potassium channel by the newly synthesized compound GRT-X exerts neuroprotection in the ALS SOD1^{G93A} mice. GRT-X has a safe toxicological profile and can cross the BBB reaching the CNS. The 50 mg/kg GRT-X compound dose improved electrophysiological and functional outcomes and delayed disease onset in the SOD1^{G93A} transgenic mice. Furthermore, this dose of GRT-X preserved the number of surviving MNs in the spinal cord and the innervation of NMJ in treated female SOD1^{G93A} mice, although it had only marginal benefit in male SOD1^{G93A} mice. The effects are, thus, sex and dose dependent, since we did not find positive outcomes with the lower dose of 30 mg/kg.

Further studies will be needed to assess the exact mechanisms underlying GRT-X MN neuroprotection. However, we can hypothesize several neuroprotective mechanisms for GRT-X. In previous studies performed in our lab, GRT-X reduced ROS/RNS levels in primary MN spinal cord cultures exposed to astrocyte-conditioned medium generated from ALS patient astrocytes derived from induced pluripotent stem cells carrying disease-causing mutations of SOD1 or TDP-43 (see Chapter II). In line with these results, other TSPO agonists have been shown to reduce oxidative stress (Biswas et al., 2018; Jayakumar et al., 2002). Therefore, GRT-X, as a TSPO agonist, could be acting similarly in SOD1^{G93A} mice, decreasing oxidative stress levels, and contributing to the survival of MNs. Additionally, TSPO was identified as an essential element in neurosteroidogenesis (Mukhin et al., 1989) where it is involved in the entrance of cholesterol in the mitochondria. Different TSPO agonists have also been found to increase neurosteroid production (Mukhin et al., 1989; Bader et al., 2019). In fact, a study using 10 mg/kg of GRT-X compound in a model of injury of the cervical spinal nerves demonstrated enhanced brain levels of pregnenolone, 3 α ,5 α -tetrahydroprogesterone, 3 α ,5 α -tetrahydrodeoxycorticosterone and their precursors 5 α -dihydroprogesterone and 5 α -deoxycorticosterone (Bloms-Funke et al., 2022a). Neurosteroids have a neuroprotective role for CNS and PNS injuries, ischemia, or neurodegenerative diseases (Borowicz et al., 2011). Therefore, stimulation of the neurosteroidogenesis pathway might be a mechanism contributing to MN survival. Additionally, dysregulations in hormone receptors, steroids and steroidogenic enzymes in the spinal cord of SOD1^{G93A} mice have already been demonstrated (McLeod et al., 2020), suggesting this cellular pathway as a novel approach to treat ALS.

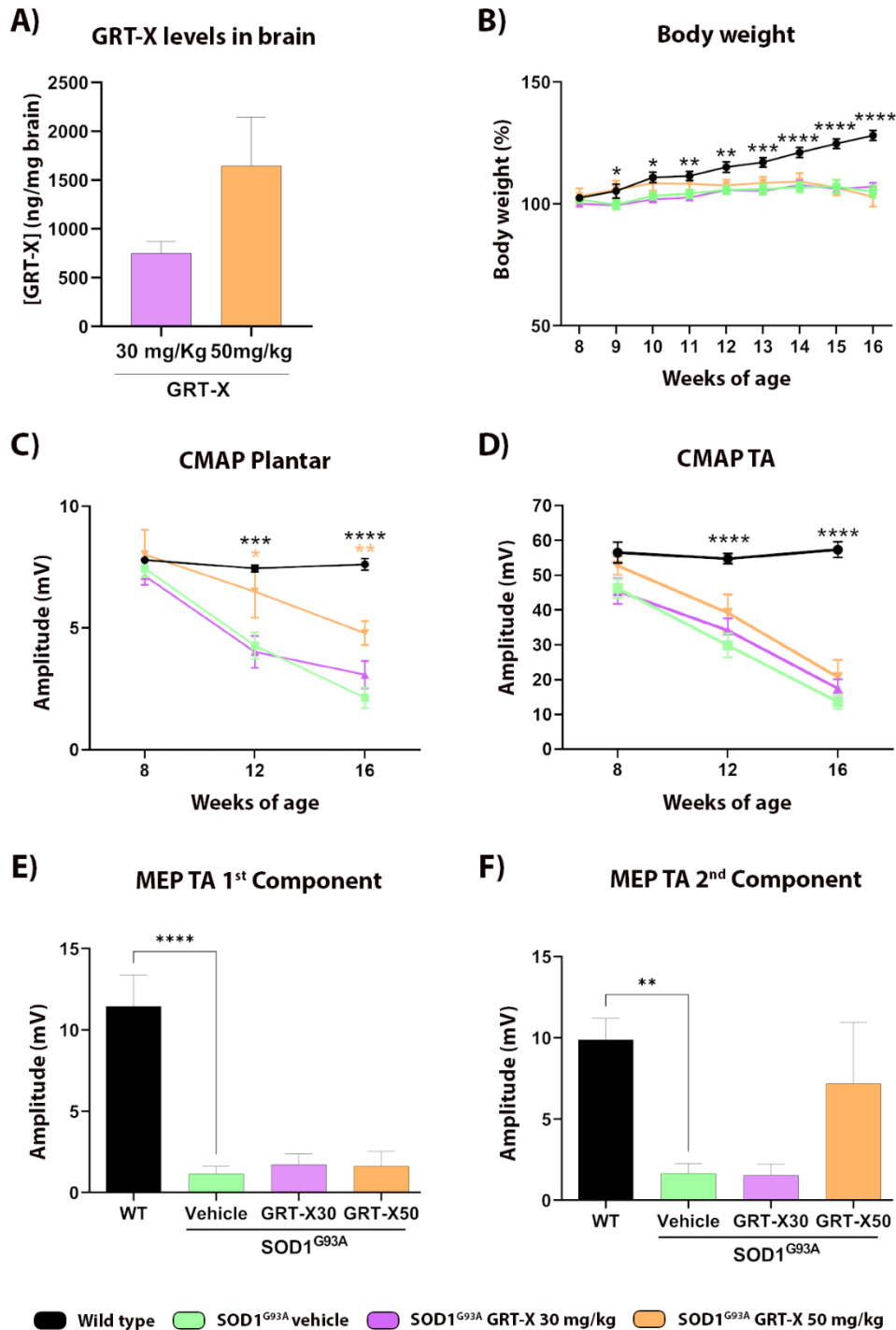
The activation of the Kv7.2/3 channel by GRT-X may also contribute to MN preservation, considering that it tends to hyperpolarize the resting membrane potential, regulating neuronal firing and reducing hyperexcitability. Previous studies have shown that the activation of Kv7.2/3 by Retigabine, decreases cortical and spinal neurons excitability (Wainger et al 2021). Thereby, we may expect that GRT-X works similarly diminishing excitability as a neuroprotective mechanism of GRT-X. Nevertheless, it was proved that GRT-X has a greater ability and effectiveness in activating neuronal Kv7.2/3 channels compared to Ezogabine (Bloms-Funke et al., 2022a), encouraging GRT-X as a possible treatment for ALS.

Therefore, the neuroprotective effects of GRT-X in SOD1^{G93A} ALS mice may be attributed to the combined activation of Kv7.2/3 potassium channels and the mitochondrial protein TSPO, which may lead to a reduction of hyperexcitability, oxidative stress and modulation of mitophagy. Thus, our study agrees with previous studies highlighting combinational therapies as promising treatments for ALS. These combination therapies use two different drugs for example Masinitib and Riluzole. Masinitib, a highly selective tyrosine kinase inhibition, was added to the Riluzole treatment in a phase II clinical trial, resulting in an elongation of survival of about two years compared to Riluzole plus placebo group (Mora et al., 2020); this treatment resulted in hyperexcitability reduction and microglia activation. Likewise, AMX0035 (or sodium phenylbutyrate (PB) and taurursodiol (TURSO). PB, a histone deacetylase and TURSO, a hydrophilic bile acid, slowed ALS progression and prolonged long-term survival by 6.5 months longer (Paganoni et al., 2021). Currently, both combinations are used in an international multicenter Phase III study (ClinicalTrials.gov; Masinitib: NCT03127267 and AMX0035: NCT05021536). Considering the current lack of knowledge regarding the exact mechanism underlying MN degeneration in ALS, combinatory therapies, such as represented by GRT-X administration, may represent a promising option for ALS therapy in the future.

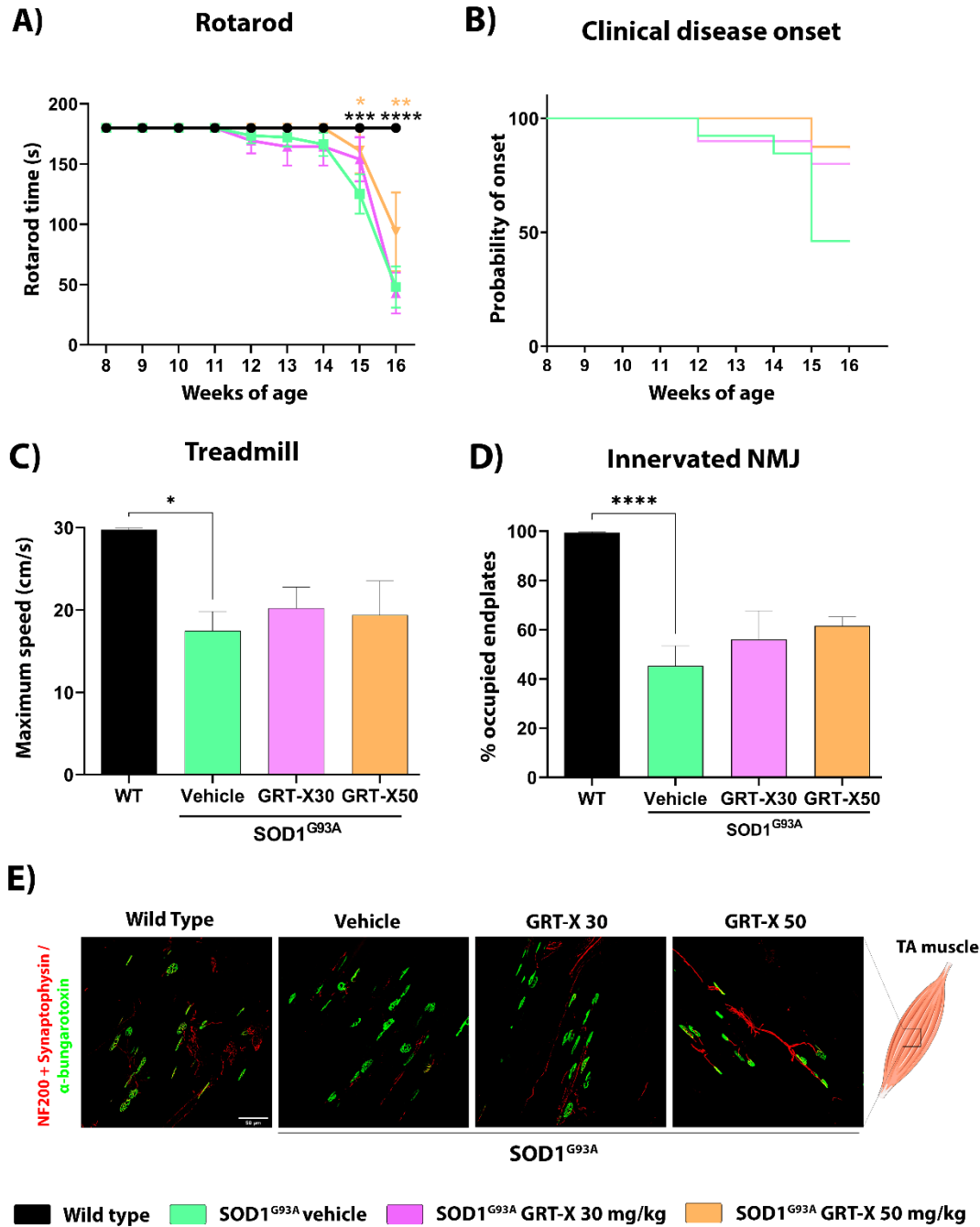
SUPPLEMENTARY FIGURES



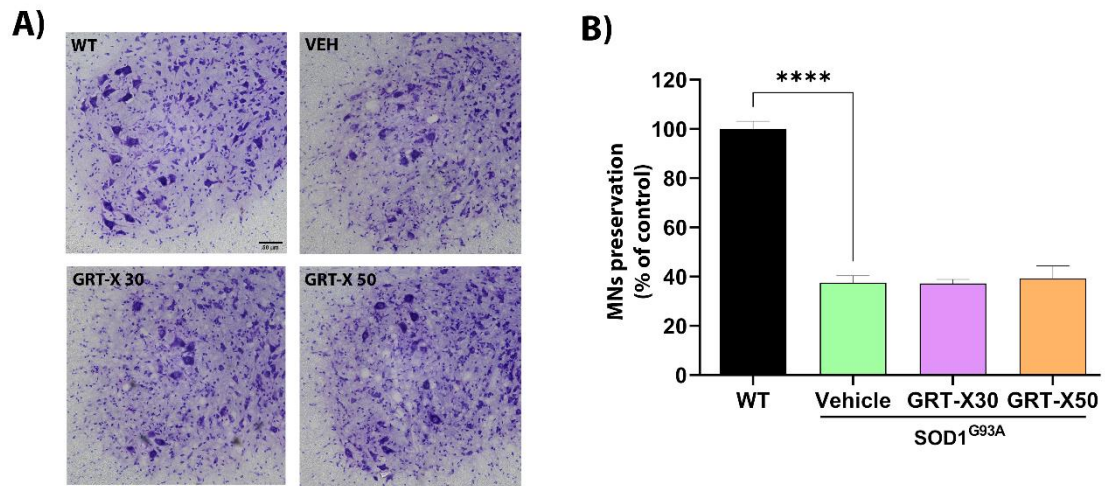
Supplementary Figure 1 | Treatment with GRT-X does not generate toxicity in male WT mice (A) Body weight (in percentage) was monitored weekly throughout the experiment, from 13 to 16 weeks of age (B) Graph showing motor coordination outcome assessed by the rotarod test at the beginning and end of the study (C) Plot showing the effect of GRT-X on locomotion performance at the end of the study by distance ran in the treadmill (D) Representative images (40X) of brain, lung, liver, kidney and small and large bowel of all experimental conditions stained with eosin and hematoxylin. Data are mean \pm SEM, analyzed by One-way (B, C) and Two-way (A) ANOVA followed with Bonferroni's post hoc test.



Supplementary Figure 2 | Treatment with GRT-X enhances neuromuscular function in male SOD1^{G93A} mice (A) Plot showing the concentration of GRT-X compound in the brain of SOD1^{G93A} mice (B) Body weight (in percentage) was monitored weekly throughout the experiment, from 8 to 16 weeks of age (C- D) Values of the amplitude of compound muscle action potentials (CMAP) of tibialis anterior (TA) and plantar interosseus muscles (E- F) Plot of the amplitudes of first (E) and second (F) component of the motor evoked potentials (MEP) of TA muscle. Data are mean \pm SEM, analyzed by One-way (A, E, F) and Two-way (B, C, D) ANOVA followed with Bonferroni's post hoc test: **** $p < 0.0001$; *** $p < 0.001$; ** $p < 0.01$; * $p < 0.05$ vs SOD1^{G93A} - vehicle condition.



Supplementary Figure 3 | Treatment with GRT-X improves coordination and motor activity in male SOD1^{G93A} mice (A) Graph showing the effect of different doses of GRT-X treatment on functional outcome assessed by the rotarod test. (B) The probability of clinical disease onset was evaluated based on the decline in performance observed in the rotarod test. (C) Graph showing the effect of different doses on maximum speed assessed by the treadmill test (D) Graph of the percentage of occupied NMJ in the different experimental groups. (E) Representative confocal images of the TA NMJs at 16 weeks of age of all experimental groups shown as maximum projection. Scale bar 100 μ m. Data are mean \pm SEM. One-way (B-C) and Two-way (A) ANOVA followed with Bonferroni's post hoc test: **** $p < 0.0001$; *** $p < 0.001$; ** $p < 0.01$; * $p < 0.05$ vs SOD1^{G93A}-vehicle condition.



Supplementary Figure 4 |GRT- X does not promote MN survival in the lumbar spinal cord in male SOD1^{G93A} mice (A) Representative spinal cord images of MNs stained with cresyl violet. Scale bar 50 μ m. (B) Quantification of surviving MNs (expressed as % of surviving MN vs. WT mice). Data are mean \pm SEM. One-way ANOVA followed with Bonferroni's post hoc test: **** $p < 0.0001$ vs SOD1^{G93A} - vehicle condition.

Chapter IV

Synergistic effect between the unimodal compounds

Olesoxime and ICA-27243

INTRODUCTION

In this thesis, our primary focus has been to assess the simultaneous activation of the neuronal Kv7.2/3 channel and the mitochondrial protein TSPO using the novel compound GRT-X as a promising therapy for ALS. We have demonstrated the interest of such simultaneous activation of these two targets, both in *in vitro* and *in vivo* models of MN degeneration. Previous evidence has highlighted the individual potential of these targets. It was proved that activating the Kv7.2/3 channel using Retigabine could be an effective therapy for ALS (Wainger et al., 2014, 2021). Similarly, we have shown that Kv7.2/3 channel activation via another drug, ICA-27243, also holds promise as a potential therapy, as it preserves neuromuscular function and mitigates MN loss. Additionally, TSPO activation through Olesoxime exhibited improved neuromuscular function and MN preservation in SOD1^{G93A} mice (Bordet et al., 2007; Sunyach et al., 2012), however, it failed to exhibit efficacy compared to the placebo group in clinical trials (Lenglet et al., 2014). Therefore, the hypothesis that activation of these two targets may be a good approach as an ALS therapy, since the two targets act through different, non-overlapping pathways appeared granted.

After establishing the efficacy of activating both targets, in this last section we have assessed whether they exhibit synergistic potential. Furthermore, this study determines whether the GRT-X compound represents a more effective therapeutic option compared to the combination of two unimodal agonists. For this objective, we employed a combination of Olesoxime and ICA-27243, which have been demonstrated to be effective as an ALS therapy when administered solely. This combination was evaluated both *in vitro*, using SCOCs exposed to acute glutamate, and *in vivo*, using the SOD1^{G93A} mice.

MATERIALS AND METHODS

The methodology employed in this work was the same as in the preceding chapters, for both *in vitro* and *in vivo* experimental models.

RESULTS

Combination of ICA-27243 and Olesoxime synergistically preserves MN survival in SCOCs under excitotoxicity

We first assessed the combined impact of Olesoxime and ICA-27243 on MN viability within glutamate-exposed SCOCs. Initially, we established the therapeutic window of Olesoxime since we already demonstrated the profile of ICA-27243 in the chapter 1. SCOCs, prepared as previously described, were subjected to excitotoxicity by exposing the slices to Locke's Solution containing L-glutamic acid at a concentration of 50 μ M for 30 minutes at 15 DIV. Following, Olesoxime was administered at doses of 2.5 μ M, 5 μ M, 10 μ M, and 20 μ M, all dissolved in dimethyl sulfoxide (DMSO). The cultures were maintained until the 20 DIV.

Cultures were fixed and MN viability was analyzed through immunostaining to neurofilament H non-phosphorylated (SMI-32; 1:250, Cat. #801701, Biolegend). The number of MNs preserved, evaluated as SMI-32+ cells within the ventral horn of L4-L5 slices, was significantly reduced by adding 50 μ M glutamate (60 ± 2 % MN preserved) compared to control slices (100 ± 2 % MN preserved). Olesoxime treatment at 5 μ M, 10 μ M, and 20 μ M showed a bell-shaped dose-response reduction in MN death (72 ± 5 ; 90 ± 5 ; 75 ± 5 % MN preserved, respectively). Dose of 2.5 was ineffective in preserving MN (53 ± 2 % MN preserved) (Fig. 1).

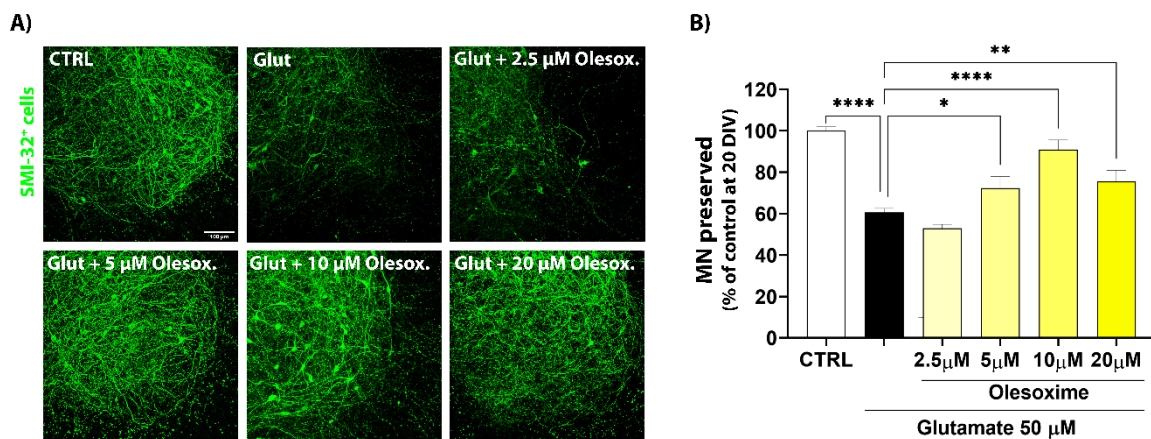


Figure 1 | Olesoxime prevents MN death in SCOCs exposed to glutamate. (A) Representative confocal images of the ventral horn of spinal cord hemislices immunostained with SMI-32 at 20 DIV of tested conditions. Scale bar 100 μ m. (B) Bar graph showing the neuroprotective effect of 5 μ M, 10 μ M and 20 μ M of Olesoxime in SCOCs exposed to glutamate. Data are shown as mean \pm SEM (n= 15- 35 hemisections per treatment). One-way ANOVA followed by Bonferroni's post hoc test: ****p<0.0001; **p<0.01; *p < 0.05 versus Glutamate condition.

Once the therapeutic windows of Olesoxime and the ICA- 27243 were established, we replicated the same protocol in the SCOCs, but in this case, the treatment consisted of the simultaneous administration of the same doses of both drugs: 2.5 μ M, 5 μ M, and 10 μ M each. Once again, the addition of glutamate significantly reduced the number of MNs by 38% ($62 \pm 2\%$ MN preserved) compared to control slices ($100 \pm 3\%$ MN preserved). Treatment with the combination of Olesoxime and ICA- 27243 significantly preserved MNs, with doses of 2.5 and 5 proving effective (98 ± 3 ; $92 \pm 3\%$ MN preserved). However, the 10 μ M dose was inefficient ($66 \pm 3\%$ MN preserved) (Fig. 2A- B). Interestingly, in the *in vitro* setting, a clear synergistic effect is observed with the 2.5 μ M and 5 μ M doses; however, the 10 μ M dose, which exhibited efficacy individually, did not yield the same results when both drugs were added (Fig. 2C, Fig. 3).

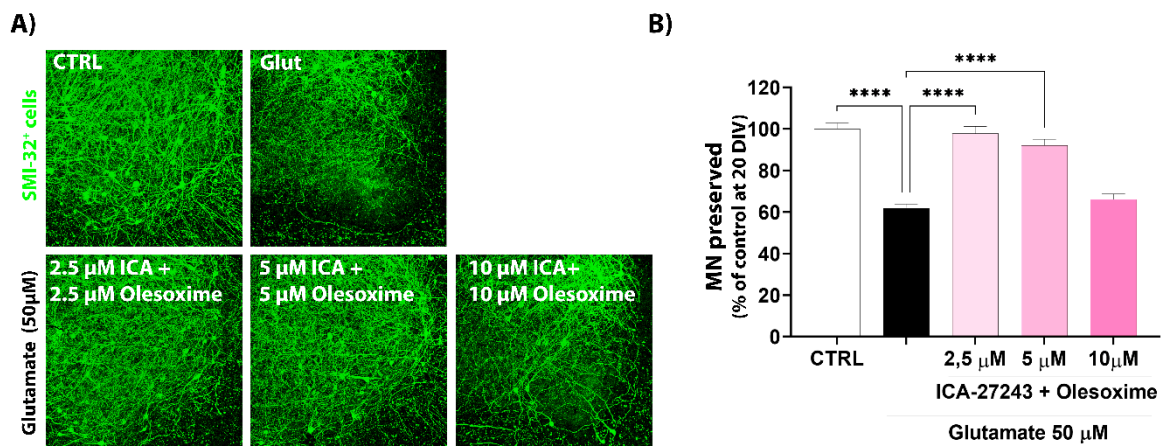


Figure 2 | The combination of ICA- 27243 and Olesoxime synergistically preserves MN survival in SCOCs exposed to glutamate. (A) Representative confocal images of the ventral horn of spinal cord hemislices immunostained with SMI- 32 at 20 DIV of tested conditions. Scale bar 100 μ m. **(B)** Bar graph showing the neuroprotective effect of 2.5 μ M and 5 μ M of each compound in SCOCs exposed to glutamate. Data are shown as mean \pm SEM (n= 20- 31 hemisections per treatment). One- way ANOVA followed by Bonferroni's post hoc test: ****p<0.0001 versus Glutamate condition.

As a summary of the results obtained in the SCOC model, Figure 3 shows the synergistic neuroprotection effect of the tested compounds used at all the conditions.

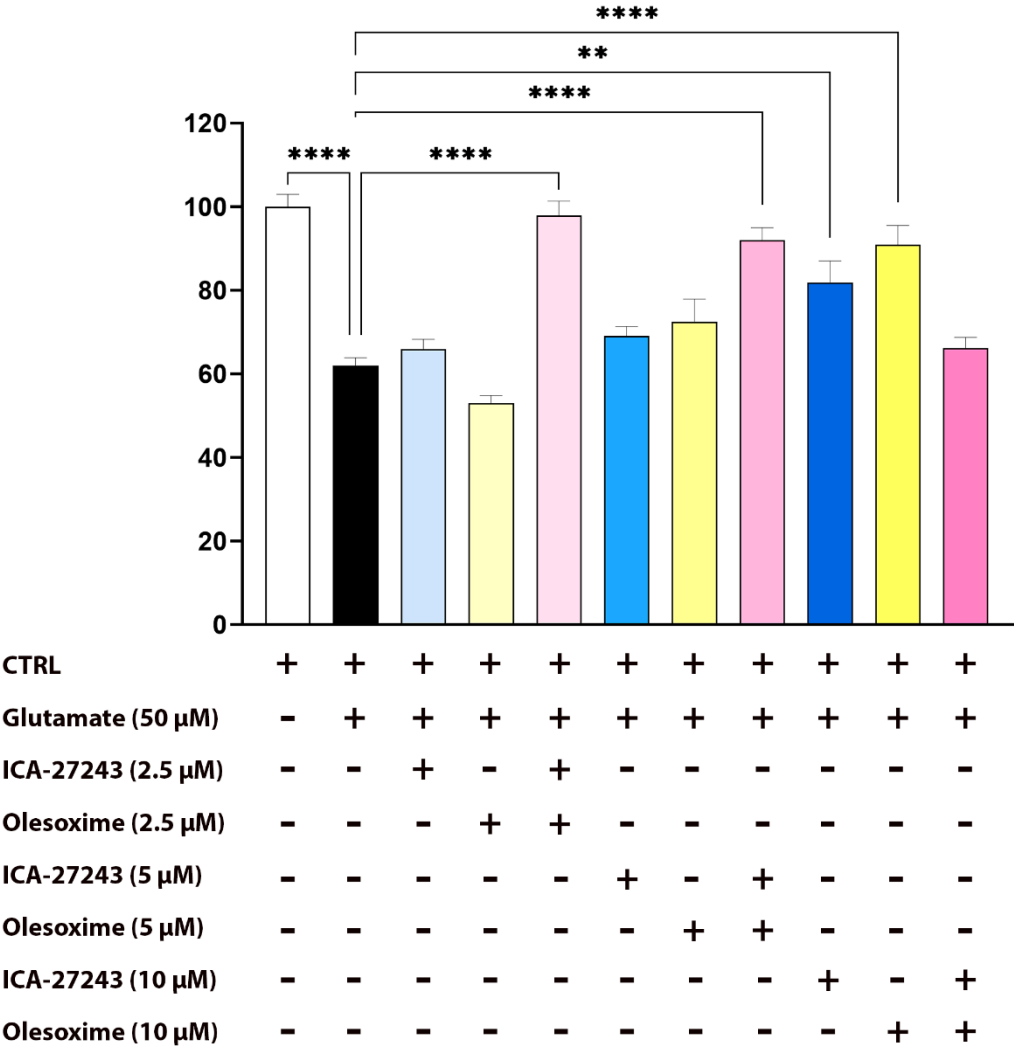


Figure 3 | The combination of ICA- 27243 and Olesoxime treatment synergistically enhances MN survival in glutamate-exposed SCOCs. (A) Bar graph showing the synergistic neuroprotection effect of 2.5 μ M and 5 μ M of each compound, compared to their individual effect in SCOCs exposed to glutamate.

Combination of ICA-27243 and Olesoxime treatment preserves neuromuscular function and slows disease progression in the SOD1^{G93A} mice

In this experiment, female SOD1^{G93A} mice were distributed in SOD1^{G93A} + vehicle (n=5) and SOD1^{G93A} + Olesoxime 3mg/kg and ICA- 27243 10 mg/kg, plus a group of WT untreated mice (n=7). The doses and the route of administration were chosen based on previous studies using Olesoxime in which this dose was proven to be neuroprotective in SOD1^{G93A} mice (Bordet et al., 2007). The effective dose and route of administration of ICA- 27243 were demonstrated in chapter I. Mice were treated daily intraperitoneally from

the 8th to the 16th week of age at 10 mg/kg/day. Olesoxime and ICA-27243 were dissolved in 5% dimethyl sulfoxide (DMSO) + 95% hydroxypropyl methylcellulose 0.5% (HPMC) (Cat. #H9262, Sigma), adding 2% Tween 80 (Cat. #1754, Sigma).

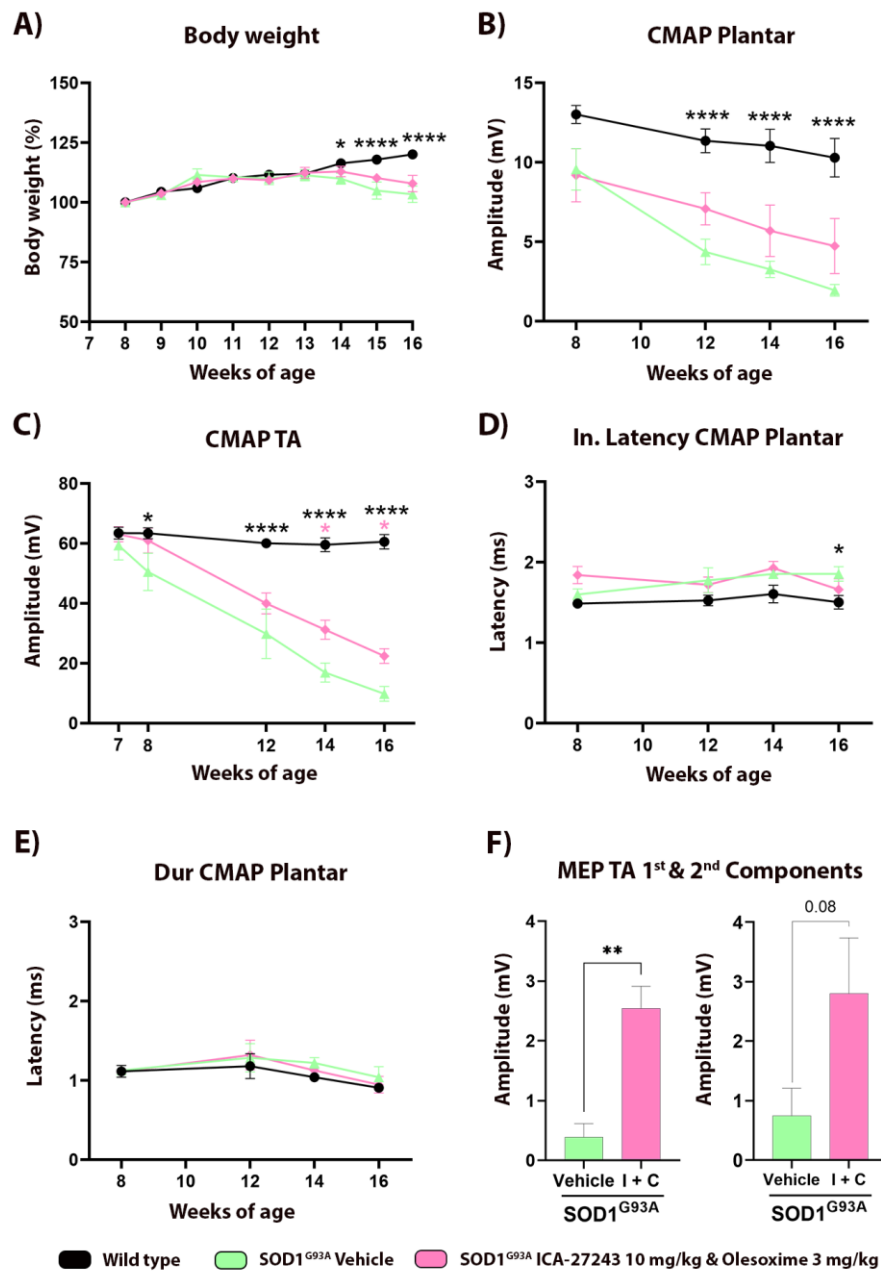


Figure 4 | ICA-27243 and Olesoxime treatment enhances neuromuscular function in SOD1^{G93A} mice. (A) Plot showing body weight (expressed as percentage of baseline) throughout the experiment. (B- C) Plots of the CMAP amplitude of plantar interossei (Plantar) and tibialis anterior (TA) muscles along follow-up. (D) Plot displaying the initial latency of the CMAP of the Plantar muscle during the follow-up period. (E) Plot of the duration of the Plantar CMAP during follow-up. (F) Plots showing the amplitude of both the first and second components of the MEP recorded in the TA muscle at 16 weeks. Data are mean \pm SEM, analyzed by One-way (F) and Two-way (A-E) ANOVA followed by Bonferroni's post hoc test. **** p < 0.0001; ** p < 0.01; * p < 0.05 vs SOD1^{G93A} vehicle group. Animals per group: WT, n =7; SOD1^{G93A} vehicle, n =5; SOD1^{G93A} + ICA-27243 + Olesoxime, n =6.

Weekly weight analyses revealed continuous weight gain for all three groups until week 14. Subsequently, WT mice exhibited ongoing weight gain, whereas both SODI^{G93A} mice groups, treated and untreated, remained stable without important weight variations (Fig. 4A).

Electrophysiological tests were conducted at weeks 8, 12, 14, and 16. The results demonstrated that the combination of Olesoxime and ICA- 27243 effectively maintained the amplitude of the CMAP in the TA muscle of treated SODI^{G93A} mice at 14 and 16 weeks of age (Fig. 4C). However, its impact on preserving the CMAP decline in the PL muscle was limited (Fig. 4B), compared to vehicle SODI^{G93A} mice. Differences were noted in the initial latency of the M wave of the PL muscle at the end of the study in the SODI^{G93A} mice compared to WT groups, being the first slightly delayed (Fig. 4D). However, no differences were observed between groups in the M wave duration (Fig. 4E). Regarding the MEPs of the TA muscles, treated SODI^{G93A} mice showed significantly higher amplitude in the first component and a tendency in the second component compared to vehicle SODI^{G93A} mice (Fig. 4F).

In the rotarod test, in which we measured the maximum time mice could maintain on the rotating rod at a consistent speed of 14 rpm, with a 180-second cut-off time, SODI^{G93A} group treated with Olesoxime and ICA- 27243 exhibited enhanced performance compared to the SODI^{G93A} vehicle group (Fig. 5A). This improvement translated into a one-week delay in motor impairment, as motor deficits were evident in the untreated SODI^{G93A} group from week 14 onward, whereas in the treated group, they manifested from week 15 (Fig. 5B). Furthermore, at week 16, the treadmill test was conducted. This trial revealed improved performance of mice treated with Olesoxime and ICA- 27243 in comparison to the vehicle-treated SODI group (Fig. 5C). The findings from both electrophysiology and motor tests were further supported by the analysis of neuromuscular junctions (NMJ) at 16 weeks. The treatment significantly increased the percentage of occupied endplates in the SODI^{G93A} mice compared to untreated SODI mice (Fig. 5D- E).

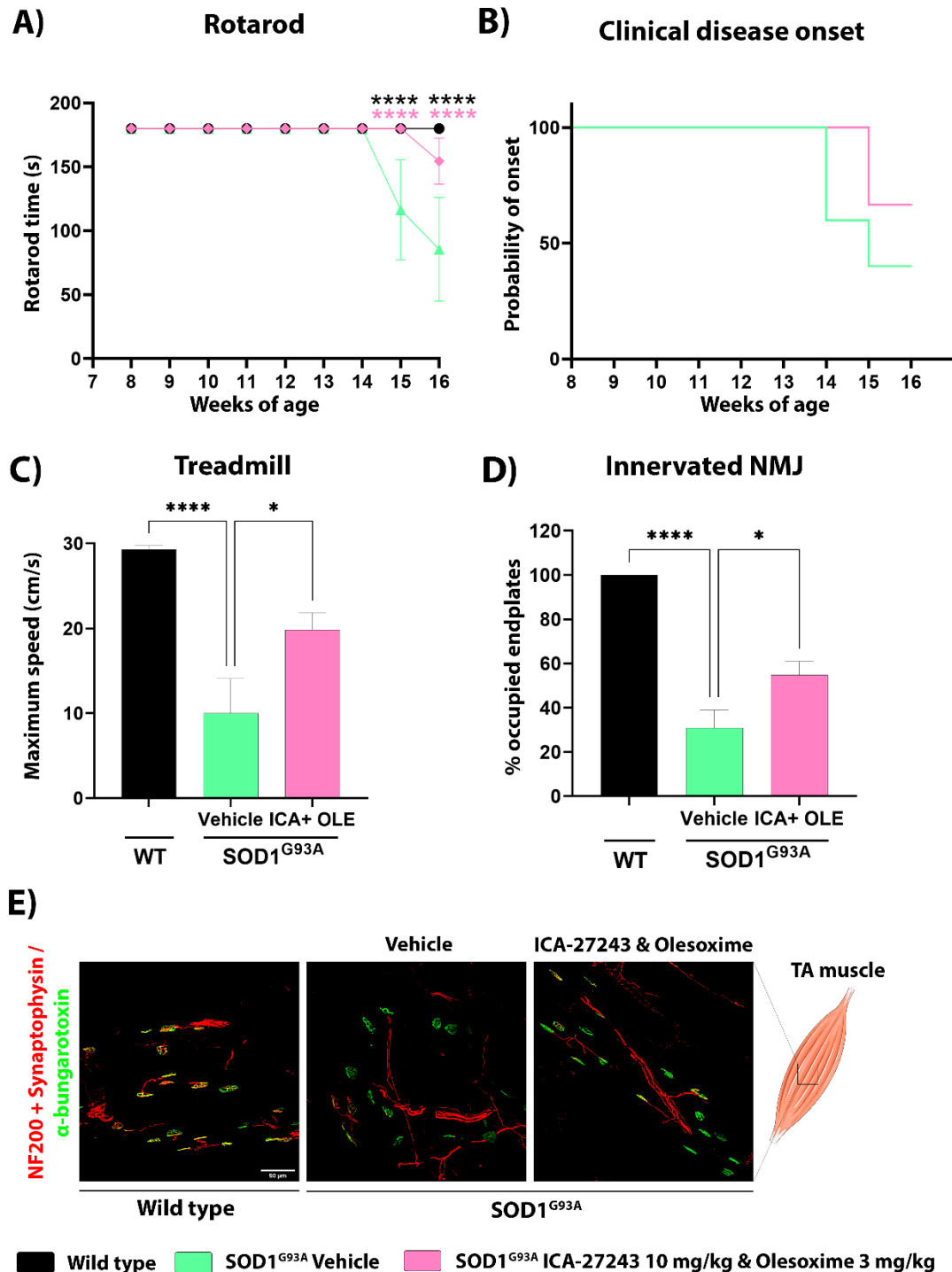


Figure 5 | The combination of ICA- 27243 and Olesoxime maintains motor activity in SOD1^{G93A} mice. (A) Graph showing the influence of ICA- 27243 and Olesoxime treatment on motor function, assessed by the rotarod test. (B) Clinical disease onset determined as the initial day when a decline in rotator test performance was observed. (C) Graph showing the effect of ICA- 27243 and Olesoxime on locomotion measured as the maximum speed achieved on the treadmill test. (D) Plot graph showing histological analyses of NMJ of the TA muscle represented as the proportion of occupied endplates at 16 weeks of age. (E) Representative confocal images of NMJ in the TA muscle of WT, SOD1^{G93A} mice with or without ICA- 27243 and Olesoxime treatment at 16 weeks of age. Scale bar: 50 μm. Data are mean ± SEM. One- way (C-D) and Two- way (A) ANOVA followed by Bonferroni's post hoc test: ****p < 0.0001; *p < 0.05 vs SOD1^{G93A} vehicle group.

Combination of ICA- 27243 and Olesoxime preserves MN survival and attenuates glial activation in the lumbar spinal cord of SOD1^{G93A} mice

At 16 weeks mice were euthanized and transcardially perfused with 4% PFA in PBS. The lumbar segment of the spinal cord was harvested and L4-L5 was serially and transversally cut into 20 μ m sections. The evaluation of MN survival in slices stained with Cresyl violet, showed that at 16 weeks of age, SOD1^{G93A} vehicle mice had a 67% decline in MN number (7 ± 1 MNs) compared to WT mice (22 ± 0.3 MNs). Notably, SOD1^{G93A} mice treated with ICA- 27243 and Olesoxime had significantly less spinal MN death (11 ± 1 MNs) compared to untreated SOD1^{G93A} mice (Fig. 6).

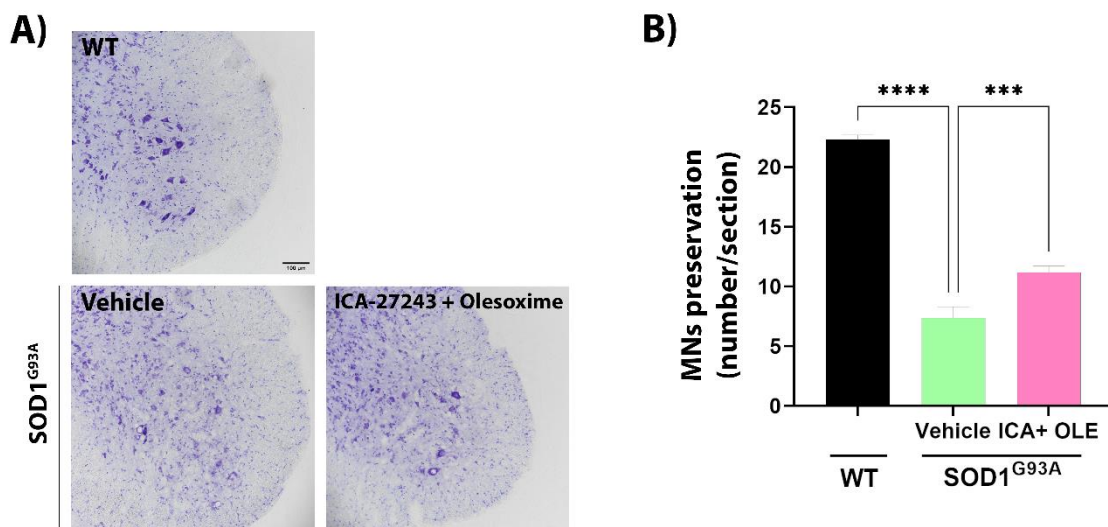


Figure 6 | Neuroprotective effects of ICA- 27243 and Olesoxime treatment on MNs in SOD1^{G93A} mice at 16 weeks. (A) Representative images of the ventral horn of L4-L5 spinal cord stained with Cresyl violet of WT, SOD1^{G93A} vehicle and SOD1^{G93A} with the ICA- 27243 and Olesoxime treatment at 16 weeks of age. Scale bar 100 μ m. (B) Bar graph showing a higher number of MNs preserved per section of the spinal cord in the SOD1^{G93A} mice treated with the combination of 10 mg/kg of ICA- 27243 plus 3 mg/kg of Olesoxime, in comparison to vehicle SOD1^{G93A} mice. Data are mean \pm SEM. One-way ANOVA followed by Bonferroni's post hoc test: ****p < 0.0001; ***p < 0.001 vs SOD1^{G93A} vehicle group.

To assess astroglial and microglial reactivity, lumbar sections were incubated with primary antibodies against GFAP and Iba-1. The treatment with Olesoxime and ICA- 27243 mitigated both microglial and astroglial reactivity, although without reaching statistical significance in comparison to SOD1^{G93A} mice (Fig. 7).

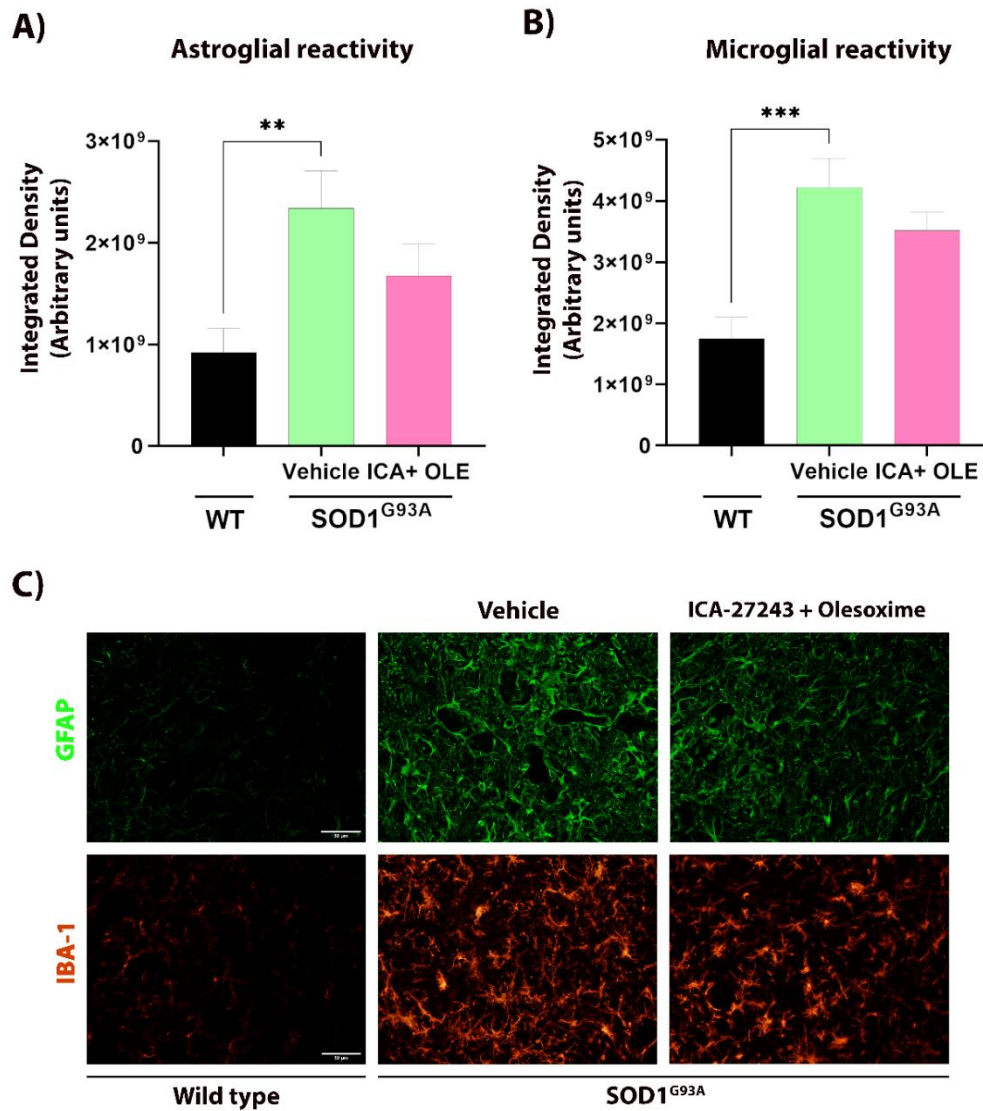


Figure 7 | Administration of ICA-27243 mitigates both astroglial and microglial reactivity in SOD1^{G93A} mice at 16 weeks. Bar graphs showing astroglial (A) and microglial (B) reactivity represented as integrated density within the ventral horn of the lumbar spinal cord. (C) Representative images of glia immunoreactivity assessed by GFAP and Iba-1 labeling in the ventral horn of L4-L5 spinal cord slices of WT, SOD1^{G93A} vehicle and SOD1^{G93A} with the combination of ICA-27243 and Olesoxime treatment at 16 weeks of age. Scale bar: 50 μ m. Data are mean \pm SEM. One-way (A-B) ANOVA followed by Bonferroni's post hoc test: *** $p < 0.001$ vs SOD1^{G93A} vehicle

DISCUSSION

The discussion of the data described in this chapter is integrated into the global discussion of the thesis.

VII. Discussion

Despite ALS being one of the most prevalent neurodegenerative diseases, its exact origin remains unknown and a cure has yet to be discovered. However, extensive research has revealed several underlying pathophysiological mechanisms contributing to MN degeneration throughout the progression of the disease. Currently, it is considered that this degenerative process results from a combination of multiple pathogenic mechanisms, which ultimately lead to a disruption of the broader neural network. Despite this understanding, most proved treatments primarily focus on targeting one of the involved pathways, resulting in low effectiveness in improving ALS. Therefore, novel and combinatorial therapeutic strategies are currently being pursued. Here, we have focused on studying the responses to complementary activation of the translocator protein TSPO and the voltage-gated potassium channel Kv7.2/3 as a promising approach to alleviate ALS symptoms. Both are potential targets for ALS based on their localization and function.

Potassium channel Kv7.2/3 is expressed exclusively in the nervous system (Jentsch, 2000), specifically this heteromeric form is located in the initial segment of the axon and the nodes of Ranvier (Devaux et al., 2004; Liu & Devaux, 2014), thereby offering the potential to control neuronal excitability through its regulation. Additionally, these channels underlie the M-current, which is a potent hyperpolarizing current. Therefore, their activation would allow for the control of neuronal hyperexcitability observed in ALS patients and experimental models (Bae et al., 2013). Retigabine, a Kv7.2/3 activator, reduces hyperexcitability and increases survival in a dose-dependent manner in iPSC-MNs (Wainger et al., 2014). In ALS patients, retigabine also decreased hyperexcitability (Wainger et al., 2021), although currently, no studies have been published regarding patient survival. Interestingly, there are no studies in MND models using ICA-27243, another activator of Kv7.2/3, which exhibits higher specificity for these channels and has a lower EC₅₀ of 0.38 μ M compared to 1.6 μ M for Retigabine.

Glial translocator protein TSPO has been widely associated with the stimulation of neurosteroidogenesis, leading to an increase in the production of neurosteroids that have been described as neuroprotectants (Borowicz et al., 2011). In fact, subcutaneous administration of progesterone was observed to provide neuroprotection in the Wobbler mice (Gonzalez-Deniselle et al., 2002) by reducing MN vacuolation, decreasing ROS levels, restoring mitochondrial respiratory chain activity, diminishing astrogliosis and microgliosis and increasing mouse survival. Furthermore, administration of allopregnanolone, metabolized from progesterone, decreased oxidative stress and glial reactivity (De Nicola et

al., 2022). Additionally, allopregnanolone is a positive modulator of GABA_A receptors that hyperpolarizes or prolongs the channel opening time, resulting in increased intracellular Cl⁻, which could contribute to the neuroprotective effect (Liang & Rasmusson, 2018). An anti-glutamatergic effect of allopregnanolone exerted upon NMDA receptors may also contribute to neuroprotection (De Nicola et al., 2022). TSPO has also been associated with other functions, such as neuroinflammation, where upregulation of its expression has been observed in pathological conditions like ALS (Chen et al., 2008). It plays a role in mitochondrial bioenergetics, where its activation is generally linked to increased mitochondrial activity (Yao et al., 2020; Banati et al., 2014). Furthermore, TSPO ligands contribute to ROS generation in neurons, astrocytes and microglia (Jayakumar et al., 2002). Therefore, modulating TSPO would affect a range of physiological mechanisms that have been identified as contributors to MN degeneration. PK11195 y Ro5-4864, an antagonist and an agonist of TSPO, respectively, are the most commonly used ligands for TSPO research. However, these have not been used to treat ALS models. Instead, Olesoxime, an agonist of TSPO, has been investigated and shown to have neuroprotective effects in iPSC-derived MN cultures (Yang et al., 2013) and in the SOD1^{G93A} mouse model (Bordet et al., 2007; Sunyach et al., 2012), although these results have not translated into successful treatments for ALS patients (Lenglet et al., 2014).

Therefore, in this thesis, we have assessed the activation of these two targets in combination, as a more efficient therapy for ALS. First, to screen the therapeutic potential of these compounds, we used the *in vitro* SCOCs. These cultures are suitable to study MN degeneration due to their ability to maintain the anatomical organization and cellular stoichiometry of the spinal cord. In our study, we employed the well-established model of acute excitotoxicity induced by glutamate exposure to investigate the effects of ICA-27243, Olesoxime, the combination of ICA-27243 and Olesoxime, and GRT-X on MN survival in SCOCs.

We consistently observed that glutamate exposure resulted in severe MN death in the SCOCs, as previously described by Guzmán-Lenis et al., 2009. Our results demonstrated that specific doses of all the tested compounds prevented MN death, thereby, highlighting their potential as therapeutics for ALS. Studies revealed a bell-shaped dose-response of ICA-27243 and Olesoxime, while this effect is not found in GRT-X nor in the combination of both ICA-27243 and Olesoxime. Furthermore, we observed a synergistic effect of TSPO and Kv7.2/3, as the simultaneous activation of both targets by their respective

unimodal agonists preserved the highest percentage of MNs. Surprisingly, the compound GRT-X, which acts on both targets simultaneously, did not preserve as many MNs as the combination of ICA-27243 and Olesoxime. Additionally, we must consider the difference in dosage between the two cases, as the dosage of GRT-X is five times higher than the combination of both compounds. A possible explanation for this difference could be the drug half-life or its affinity for different targets. However, it has been described that GRT-X exhibits a higher affinity for TSPO than Olesoxime and a higher affinity than ICA-27243 for Kv7.2/3 (Bloms-Funke et al., 2022a; Bloms-Funke et al., 2022b). Nonetheless, it is important to note that all tested compounds protected MNs against excitotoxicity, highlighting TSPO and Kv7.2/3 as potential targets for ALS.

By exposing the culture to glutamate, we are mimicking one of the pathological mechanisms associated with ALS, glutamate excitotoxicity. This leads to a massive influx of Ca^{2+} , resulting in oxidative stress, mitochondrial dysfunction and activation of apoptosis, among other effects. When considering the mechanisms that may protect MNs, it is crucial to focus on specific targets. In the case of Kv7.2/3, its activation, by compounds such as ICA-27243 or GRT-X, generates a robust outward K^+ current. Activation of this channel with ICA-27243 effectively prevents seizure activity in hippocampal slices, possibly due to ICA-27243 ability to shift the voltage-dependence of Kv7.2/3 activation to a hyperpolarized potential and generate the M-current (Wickenden et al., 2008). Translating these findings to our spinal cord model, we can hypothesize that administering ICA-27243 or GRT-X induces a change in the polarization state of Kv7.2/3 channels, leading to an outward flow of K^+ , regulating neuronal excitability and consequently reducing MN degeneration. This hypothesis is supported by observations that increasing Kv7 channel activity effectively decreases the excitability of spinal MNs in SCOCs derived from mouse pups (Lombardo et al., 2018). Furthermore, it has been described that Cl^- influx exacerbates the excitotoxic effect of glutamate, impacting neuronal viability (Van Damme et al., 2003). As a result, therapies blocking inward K^+ channels or compounds that promote K^+ efflux, such as ligands of the KCC2 transporter, have been suggested.

Regarding TSPO, it is more challenging to determine the mechanisms that could be protecting MNs. On one hand, it could involve a neuroprotective effect generated by the stimulation of neurosteroidogenesis. Other TSPO agonists, such as Ro5-4864, XBD173 and SSR180575, have been shown to increase pregnenolone levels (Hallé et al., 2017), which also have been shown to be neuroprotective in ALS models (De Nicola et al., 2022; Gonzalez

Deniselle et al., 2002). Although this effect has not been demonstrated with Olesoxime, it has been observed that GRT-X stimulates steroidogenesis (Bloms-Funke et al., 2022a). On the other hand, it could be related to the maintenance of mitochondrial homeostasis, since knocking out TSPO decreases mitochondrial membrane potential (Bader et al., 2019), and the agonist Ro5-4864 has been found to increase mitochondrial membrane potential (Rosenberg et al., 2018). Additionally, this hypothesis is supported by the fact that Olesoxime seems to affect the mitochondrial permeability transition pore (Martin, 2010).

Therefore, both GRT-X and the combination of ICA-27243 and Olesoxime were expected to protect MNs due to a summatory or synergistic effect of these neuroprotective actions.

ALS is a multifactorial pathology in which, among multiple mechanisms involved, non-neuronal cells seem to contribute to MN degeneration (Hardiman et al., 2017; Mancuso & Navarro et al., 2015). Here, we tested astrocyte-conditioned medium (ACM) derived from primary mouse ALS astrocytes expressing mutant human SOD1 (SOD1^{G93A}-ACM) or from ALS patient astrocytes generated from induced pluripotent stem cells carrying disease-causing mutations of SOD1 (SOD1^{D90A}-ACM) or TDP43 (TDP43^{A90V}-ACM) in order to generate an ALS-like environment. For this purpose, we have used two different primary cultures, VSCNs and SCOCs, both exposed to the three ACMs. This is a relatively novel approach that improves the relevance and translational application of *in vitro* MN degeneration models (Arredondo et al., 2022),

In the case of VSCNs, we observed that different mtACMs cause between 40% and 50% MN death, whereas in SCOCs it is around 30% to 40%. The difference in the percentages of neuronal death is due to variations in the cultures themselves, with SCOCs requiring a higher dose of ACM to generate the same percentage of neuronal death. Nonetheless, our results show similar outcomes to previous studies using ACMs (Arredondo et al., 2022). More importantly, we found that GRT-X preserves MNs in both VSCNs and SCOCs cultures exposed to SOD1^{G93A}-ACM, SOD1^{D90A}-ACM and TDP43^{A90V}-ACM. The main difference between the two types of cultures is that ACM^{WT} does not generate MN degeneration in VSCNs, whereas it has a detrimental effect in SCOCs. We hypothesize that the presence of glial cells in the SCOCs may be responsible for this effect. Thus, astrocytes present in the slice cultures may be activated by products in the ACM derived from unmutated cell cultures, leading to a deleterious effect. Moreover, this detrimental effect could also be attributed to microglia, since there is a crosstalk

between astrocytes and microglia polarization (Kim & Son, 2021). In fact, in a primary microglia culture, the addition of ACM leads to glial branching due to astrocyte-derived TGF- β (Zhang et al., 2020).

Moreover, in VSCNs, we demonstrated a significant increase in neuronal ROS levels upon application of SOD1^{G93A}-ACM, SOD1^{D90A}-ACM and TDP43^{A90V}-ACM, consistent with other studies (Rojas et al., 2014; Fritz et al., 2013; Arredondo et al., 2022). Application of GRT-X at different doses markedly reduced ROS levels induced by SOD1^{D90A}-ACM and TDP43^{A90V}-ACM. This is in line with previous research, where TSPO agonists Etifoxine and XBD-173 reduced ROS production and enhanced antioxidant capacity in endothelial cells (Biswas et al., 2018) and the application of the antagonist PK11195 increased ROS levels in rat cortical neuron cultures (Jayakumar et al., 2002). In contrast, in cardiomyocyte cultures, the application of both the agonist TRO40303 and the antagonist 4'-chlorodiazepam resulted in a significant reduction in ROS production (de Tassigny et al., 2013). Therefore, the effect of TSPO ligands on ROS production may vary depending on the cell type and culture conditions. Nonetheless, GRT-X effectively reduces oxidative stress in VSCNs, which is another mechanism contributing to the survival of MNs.

In the following *in vivo* studies, we analyzed the therapeutic potential of ICA-27243, GRT-X and the combination of ICA-27243 and Olesoxime in the animal model most used in ALS research, the SOD1^{G93A} mice. In the case of GRT-X, as it is a new-generation compound, we first conducted a toxicity study, including the major organs that could be affected, such as the liver and kidneys. After this study, we concluded that GRT-X did not induce toxicity in the B6SJL mice. Furthermore, it was essential to verify that the drug could cross the blood-brain barrier and reach the CNS in the WT as well as in the SOD1^{G93A} mice, which exhibit a breakdown of this barrier (Garbuzova-Davis & Sanberg, 2014). We observed that both tested doses, 30 mg/Kg and 50 mg/Kg, reached the brain. Additionally, we noticed that higher doses administered resulted in higher GRT-X concentrations in the brain. However, it is important to mention the difference in GRT-X concentration between males and females, with a significantly higher concentration in males. Several studies have reported sex-related differences in the pharmacokinetics of CNS drugs. The results regarding sex-related differences in drug concentrations are not consistent across all drugs; however, in some cases, concentrations are higher in one of the two sexes. It is hypothesized that the variation between males and females may be due to female hormonal status, such as the estrous cycle (Romanescu et al., 2022).

We tested the daily administration of ICA- 27243 (10 mg/Kg), GRT-X (30mg/Kg and 50 mg/Kg) and the combination of ICA- 27243 (10 mg/kg) and Olesoxime (3 mg/Kg) from 8 to 16 weeks of age in the female SODI^{G93A} mouse. In fact, we described for the first time that the daily administration of all these compounds had a neuroprotective effect in the female SODI^{G93A} mice, preserving the neuromuscular function of the hindlimbs assessed by electrophysiology and locomotion tests and preventing MN degeneration in the lumbar spinal cord.

Electrophysiology is a useful technique for assessing the MN function both cortical and spinal. We have analyzed the CMAP and MEP, to evaluate lower MN function and the motor central pathways in the CNS, respectively (Mancuso et al., 2011). Focusing on the CMAP of the TA muscle, animals treated with GRT-X (50 mg/kg) and ICA- 27243 maintained a 20% and 25% higher amplitude in this muscle compared to their respective SODI^{G93A} vehicles, respectively. However, neither GRT-X (30 mg/kg) nor the combination of ICA- 27243 with Olesoxime are significantly different from than SODI^{G93A} vehicle group, even though they showed a 10% and 19% improvement in motor function compared to their SODI^{G93A} vehicles. Both GRT-X (50 mg/kg) and ICA- 27243 treatments resulted in higher CMAP amplitude compared to vehicle-treated SODI^{G93A} mice, in contrast to Riluzole treatment, which showed no differences in CMAP amplitude compared to vehicle SODI^{G93A} mice (Li et al., 2013). Therefore, these treatments are effective in preserving the function of lower MNs in SODI^{G93A} mice. Regarding the effects of the treatments on MEPs, our findings revealed that both GRT-X (50 mg/kg) and ICA- 27243 treatments, but also the combination of ICA- 27243 and Olesoxime, exhibited significant improvement from their respective SODI^{G93A} vehicle groups. However, GRT-X (30 mg/kg) did not show any noticeable effects. Therefore, these treatments also improve the functional status of upper MNs in female SODI^{G93A} mice. The preservation of both upper and lower MNs due to the treatment may be related to a decrease in hyperexcitability, since in ALS patients the activation of Kv7.2/3 by Retigabine decreased both cortical and spinal MN excitability (Wainger et al., 2021).

Regarding the preservation of the motor function, the positive effects were also evident in the different locomotion tests performed, rotarod and treadmill tests. Similar to electrophysiology results, mice treated with the dose of 30 mg/Kg of GRT-X did not show significantly better outcomes in these tests performed in comparison to the vehicle group. Indeed, they exhibit a similar profile to the vehicle group, with an important decline at 15 weeks in the rotarod test. In contrast, mice treated with ICA- 27243, GRT-X (50 mg/Kg)

and the combination of ICA-27243 and Olesoxime show significantly better outcomes compared to vehicles, with ICA-27243 standing out in rotarod test and GRT-X in the treadmill test. Importantly, it was found that Riluzole does not improve motor function in the SODI^{G93A} mice analyzed by rotarod (Hogg et al., 2018).

Therefore, we can conclude that ICA-27243, GRT-X (50 mg/Kg) and the combination of ICA-27243 and Olesoxime are effective in preserving motor function in the ALS mice.

We have demonstrated that these three treatments also prevent MN degeneration in the lumbar spinal cord of female SODI^{G93A} mice, while the dose of 30 mg/kg of GRT-X was inefficient. In line with the observations in the *in vitro* cultures regarding MN preservation, both ICA-27243 and 50 mg/kg of GRT-X demonstrate a similar ability to promote MN survival and prove to be the most effective ones in these studies. Surprisingly, the *in vivo* results with the combination of ICA-27243 and Olesoxime were less potent than the *in vitro* results found in SCOCs. Despite the previously demonstrated neuroprotective effect of Olesoxime at 3 mg/kg in the SODI^{G93A} mice (Bordet et al., 2007; Sunyach et al., 2012), we lacked a SODI^{G93A} mice group treated with Olesoxime to further confirm its effects. One option is that the individual doses that show efficacy may not have the same effect when administered combined, similar to what we observed with the 10 μ m doses *in vitro*. Another explanation is that there might be a threshold of improvement in the SODI^{G93A} mice that we are unable to surpass. Notably, differences between the SODI^{G93A} and WT mice can be observed as early as 8 weeks (Mancuso et al., 2011), which is when we initiated the treatment. Due to the rapid neuronal degeneration of the model, it seems that as effective as the treatments may be, they might not be potent enough to fully halt the loss of MNs, initiated weeks earlier, which could potentially explain the observed threshold of improvement of around 50%-60%, as we found with our treatment and also observed in other studies in our laboratory (Mancuso et al., 2012a; Gaja-Capdevila et al., 2021).

Unfortunately, the results in male mice were not as promising as in female mice. Similar to females, the dose of 30 mg/kg of GRT-X did not preserve either motor function or the number of MNs in the spinal cord. In contrast, the dose of 50 mg/kg did slightly preserve motor function as demonstrated by both electrophysiology and locomotion tests. However, we did not observe a corresponding improvement at the histological level in the number of preserved MNs in the spinal cord. One possible explanation could be that, as the

disease progresses more rapidly in the male SOD1^{G93A} mice (Mancuso et al., 2012b), the treatment starting at 8 weeks may be less effective for males, and it is possible that a higher dose might be necessary.

Additionally, further evaluation of signaling pathways is necessary to determine the neuroprotective mechanisms of each drug. For example, the activation of Kv7.2/3 has been linked to a reduction in ROS production (Ghezzi et al., 2018) and downregulation of ER stress (Wainger et al., 2014). On the other hand, investigating the relationship between TSPO and neuroinflammation would be an intriguing avenue, especially considering its implication in ALS. Given TSPO's localization, we could explore several aspects related to mitochondria, such as potential changes in metabolism (Fu et al., 2020), alterations in oxygen consumption (Yao et al., 2020) or even the morphology of the mitochondria itself. TSPO was also linked to steroidogenesis; in fact, GRT-X treatment has been associated with an increase in neurosteroid production (Bloms-Funke et al., 2022a; Bloms-Funke et al., 2022b). Additionally, other TSPO agonists such as Ro5-4864 (Mukhin et al., 1989), DAA1097 and DAA1106 (Okuyama et al., 1999), as well as XBD173 (Bader et al., 2019) have also been demonstrated to stimulate mitochondrial neurosteroid synthesis. Therefore, at the molecular level, there remain further studies to be conducted that would shed light on how the different drugs tested in this thesis generate neuroprotection in the different models examined.

Further evaluation of the survival of SOD1^{G93A} mice treated with ICA-27243 and the combination of ICA-27243 and Olesoxime would be necessary. Survival of SOD1^{G93A} mice treated with GRT-X (50 mg/kg) was analyzed at our collaborators' laboratory at the University of Massachusetts (data not shown). Unfortunately, no differences were observed between the GRT-X and the vehicle treated SOD1^{G93A} mice. This is not surprising, since there are other drugs that delay disease onset but do not have an impact on mice survival (Wintz et al., 2023).

Overall, the results presented in this thesis provide evidence that TSPO and Kv7.2/3 are potentially valid targets for ALS. We have demonstrated that the activation of these targets, either individually or in combination, improved motor function and maintained the number of surviving MN in the SOD1^{G93A} mice at the symptomatic stage of the disease. These findings suggest that ICA-27243 and GRT-X hold potential as therapies for ALS.

VIII. Conclusions

Chapter I. ICA-27243 improves neuromuscular function and preserves motoneurons in the transgenic SODI^{G93A} mice

- ICA-27243 dose-dependently prevents MN degeneration in SCOCs under excitotoxic conditions.
- Administration of ICA-27243 (at 10 mg/kg) improves neuromuscular function decline in the SODI^{G93A} mice, preventing the decline in CMAP and MEP amplitude, and delaying the reduction of motor activity.
- ICA-27243 promotes MN survival in the lumbar spinal cord and mitigates glial activation in the SODI^{G93A} mice.

Chapter II. GRT-X prevents degeneration of MN exposed to mouse and human ALS astrocyte-conditioned medium

- GRT-X shows a dose-dependently effect preventing MN degeneration in SCOCs under excitotoxic conditions.
- ACM produced by primary astrocytes of mice expressing mutant human SODI (SODI^{G93A}-ACM) and by astrocytes generated from induced pluripotent stem cells of ALS patients carrying mutations of SODI (SODI^{D90A}-ACM) or TDP43 (TDP43^{A90V}-ACM) triggers MN degeneration in VSCNs and in SCOCs.
- GRT-X prevents MN death in both VSCNs and in SCOCs exposed to SODI^{G93A}-ACM, SODI^{D90A}-ACM and TDP43^{A90V}-ACM.

Chapter III. The compound GRT-X promotes neuroprotection in the SODI^{G93A} mice

- Administration of GRT-X is safe and non-toxic for both male and female B6SJL-Tg [SODI-G93A]-1Gur mice, as well as for B6SJL wild type mice.
- GRT-X crosses the blood-brain barrier, with higher GRT-X levels detected in male than in female mice.
- GRT-X at 50 mg/kg, but not at lower doses, preserves neuromuscular function of both female and male SODI^{G93A} mice, and mitigates the decline in motor activity in female but not in male SODI^{G93A} mice.
- GRT-X administration (50 mg/kg) enhances MN survival within the spinal cord of female SODI^{G93A} mice.

Chapter IV. Synergistic effect between TSPO and Kv7.2/3 activation

- Combination of ICA-27243 and Olesoxime treatment synergistically increased MN survival in SCOCs under excitotoxicity, achieving this outcome at doses lower than individually effective doses.
- Cotreatment with ICA-27243 (10 mg/kg) and Olesoxime (3 mg/kg) maintained neuromuscular function and motor activity in female SOD1^{G93A} mice.
- Combination of ICA-27243 and Olesoxime enhanced MN survival in the lumbar spinal cord and modulated glial activation in female SOD1^{G93A} mice.

IX. References

- Aguirre, N., Flint Beal, M., Matson, W. R., & Bogdanov, M. B. (2005). Increased oxidative damage to DNA in an animal model of amyotrophic lateral sclerosis. *Free Radical Research*, 39(4), 383–388. <https://doi.org/10.1080/10715760400027979>
- Al-Chalabi, A., Hardiman, O., Kiernan, M. C., Chiò, A., Rix-Brooks, B., & van den Berg, L. H. (2016). Amyotrophic lateral sclerosis: moving towards a new classification system. In *The Lancet Neurology* (Vol. 15, Issue 11, pp. 1182–1194). Lancet Publishing Group. [https://doi.org/10.1016/S1474-4422\(16\)30199-5](https://doi.org/10.1016/S1474-4422(16)30199-5)
- Alexianu, M. E., Ho, B.-K., Mohamed, A. H., La Bella, V., Smith, R. G., & Appel, S. H. (1994). The role of calcium-binding proteins in selective motoneuron vulnerability in amyotrophic lateral sclerosis. *Annals of Neurology*, 36(6), 846–858. <https://doi.org/10.1002/ana.410360608>
- Allodi, I., Montañana-Rosell, R., Selvan, R., Löw, P., & Kiehn, O. (2021). Locomotor deficits in a mouse model of ALS are paralleled by loss of V1-interneuron connections onto fast motor neurons. *Nature Communications*, 12(1), 3251. <https://doi.org/10.1038/s41467-021-23224-7>
- Almad, A. A., Taga, A., Joseph, J., Gross, S. K., Welsh, C., Patankar, A., Richard, J.-P., Rust, K., Pokharel, A., Plott, C., Lillo, M., Dastgheyb, R., Eggan, K., Haughey, N., Contreras, J. E., & Maragakis, N. J. (2022). Cx43 hemichannels contribute to astrocyte-mediated toxicity in sporadic and familial ALS. *Proceedings of the National Academy of Sciences*, 119(13). <https://doi.org/10.1073/pnas.2107391119>
- Alves, C. J., Maximino, J. R., & Chadi, G. (2015). Dysregulated expression of death, stress and mitochondrion related genes in the sciatic nerve of presymptomatic SOD1G93A mouse model of Amyotrophic Lateral Sclerosis. *Frontiers in Cellular Neuroscience*, 9(september). <https://doi.org/10.3389/fncel.2015.00332>
- Appaix, F., Girod, S., Boisseau, S., Römer, J., Vial, J.-C., Albrieux, M., Maurin, M., Depaulis, A., Guillemain, I., & van der Sanden, B. (2012). Specific In Vivo Staining of Astrocytes in the Whole Brain after Intravenous Injection of Sulforhodamine Dyes. *PLoS ONE*, 7(4), e35169. <https://doi.org/10.1371/journal.pone.0035169>
- Arredondo, C., Cefaliello, C., Dyrda, A., Jury, N., Martinez, P., Díaz, I., Amaro, A., Tran, H., Morales, D., Pertusa, M., Stoica, L., Fritz, E., Corvalán, D., Abarzúa, S., Méndez-Ruette, M., Fernández, P., Rojas, F., Kumar, M. S., Aguilar, R., ... van Zundert, B. (2022). Excessive release of inorganic polyphosphate by ALS/FTD astrocytes causes non-cell-autonomous toxicity to motoneurons. *Neuron*, 110(10), 1656-1670.e12. <https://doi.org/10.1016/j.neuron.2022.02.010>
- Atkin, J. D., Farg, M. A., Walker, A. K., McLean, C., Tomas, D., & Horne, M. K. (2008). Endoplasmic reticulum stress and induction of the unfolded protein response in human sporadic

References

- amyotrophic lateral sclerosis. In *Neurobiology of Disease* (Vol. 30, Issue 3, pp. 400–407). Academic Press Inc. <https://doi.org/10.1016/j.nbd.2008.02.009>
- Bader, S., Wolf, L., Milenkovic, V. M., Gruber, M., Nothdurfter, C., Rupprecht, R., & Wetzel, C. H. (2019). Differential effects of TSPO ligands on mitochondrial function in mouse microglia cells. *Psychoneuroendocrinology*, 106, 65–76. <https://doi.org/10.1016/j.psyneuen.2019.03.029>
- Bae, J. S., Simon, N. G., Menon, P., Vucic, S., & Kiernan, M. C. (2013). The Puzzling Case of Hyperexcitability in Amyotrophic Lateral Sclerosis. *Journal of Clinical Neurology*, 9(2), 65. <https://doi.org/10.3988/jcn.2013.9.2.65>
- Bae, K. R., Shim, H. J., Balu, D., Kim, S. R., & Yu, S. W. (2014). Translocator protein 18 kDa negatively regulates inflammation in microglia. *Journal of Neuroimmune Pharmacology*, 9(3), 424–437. <https://doi.org/10.1007/s11481-014-9540-6>
- Banati, R. B., Middleton, R. J., Chan, R., Hatty, C. R., Wai-Ying Kam, W., Quin, C., Graeber, M. B., Parmar, A., Zahra, D., Callaghan, P., Fok, S., Howell, N. R., Gregoire, M., Szabo, A., Pham, T., Davis, E., & Liu, G. J. (2014). Positron emission tomography and functional characterization of a complete PBR/TSPO knockout. *Nature Communications*, 5. <https://doi.org/10.1038/ncomms6452>
- Barres, B. A. (2008). The Mystery and Magic of Glia: A Perspective on Their Roles in Health and Disease. *Neuron*, 60(3), 430–440. <https://doi.org/10.1016/j.neuron.2008.10.013>
- Barrese, V., Stott, J. B., & Greenwood, I. A. (2018). KCNQ-Encoded Potassium Channels as Therapeutic Targets. *Annual Review of Pharmacology and Toxicology*, 58(1), 625–648. <https://doi.org/10.1146/annurev-pharmtox-010617-052912>
- Barron, A. M., Ji, B., Kito, S., Suhara, T., & Higuchi, M. (2018). Steroidogenic abnormalities in translocator protein knockout mice and significance in the aging male. *Biochemical Journal*, 475(1), 75–85. <https://doi.org/10.1042/BCJ20170645>
- Bartlett, R., Ly, D., Cashman, N. R., Sluyter, R., & Yerbury, J. J. (2022). P2X7 receptor activation mediates superoxide dismutase 1 (SOD1) release from murine NSC-34 motor neurons. *Purinergic Signalling*, 18(4), 451–467. <https://doi.org/10.1007/s11302-022-09863-5>
- Batra, R., & Lee, C. W. (2017). Mouse Models of C9orf72 Hexanucleotide Repeat Expansion in Amyotrophic Lateral Sclerosis/ Frontotemporal Dementia. *Frontiers in Cellular Neuroscience*, 11. <https://doi.org/10.3389/fncel.2017.00196>

- Beckers, J., Tharkeshwar, A. K., & Van Damme, P. (2021). C9orf72 ALS-FTD: recent evidence for dysregulation of the autophagy-lysosome pathway at multiple levels. In *Autophagy* (Vol. 17, Issue 11, pp. 3306–3322). Taylor and Francis Ltd. <https://doi.org/10.1080/15548627.2021.1872189>
- Beers, D. R., Ho, B.-K., Siklós, L., Alexianu, M. E., Mosier, D. R., Mohamed, A. H., Otsuka, Y., Kozovska, M. E., McAlhany, R. E., Smith, R. G., & Appel, S. H. (2008). Parvalbumin overexpression alters immune-mediated increases in intracellular calcium, and delays disease onset in a transgenic model of familial amyotrophic lateral sclerosis. *Journal of Neurochemistry*, 79(3), 499–509. <https://doi.org/10.1046/j.1471-4159.2001.00582.x>
- Beers, D. R., Zhao, W., Liao, B., Kano, O., Wang, J., Huang, A., Appel, S. H., & Henkel, J. S. (2011). Neuroinflammation modulates distinct regional and temporal clinical responses in ALS mice. *Brain, Behavior, and Immunity*, 25(5), 1025–1035. <https://doi.org/10.1016/j.bbi.2010.12.008>
- Bellingham, M. C. (2011). A Review of the Neural Mechanisms of Action and Clinical Efficiency of Riluzole in Treating Amyotrophic Lateral Sclerosis: What have we Learned in the Last Decade? *CNS Neuroscience & Therapeutics*, 17(1), 4–31. <https://doi.org/10.1111/j.1755-5949.2009.00116.x>
- Benatar, M., Wu, J., Andersen, P. M., Bucelli, R. C., Andrews, J. A., Otto, M., Farahany, N. A., Harrington, E. A., Chen, W., Mitchell, A. A., Ferguson, T., Chew, S., Gedney, L., Oakley, S., Heo, J., Chary, S., Fanning, L., Graham, D., Sun, P., ... Fradette, S. (2022). Design of a Randomized, Placebo-Controlled, Phase 3 Trial of Tofersen Initiated in Clinically Presymptomatic SOD1 Variant Carriers: the ATLAS Study. *Neurotherapeutics*, 19(4), 1248–1258. <https://doi.org/10.1007/s13311-022-01237-4>
- Bendotti, C., Marino, M., Cheroni, C., Fontana, E., Crippa, V., Poletti, A., & De Biasi, S. (2012). Dysfunction of constitutive and inducible ubiquitin-proteasome system in amyotrophic lateral sclerosis: Implication for protein aggregation and immune response. In *Progress in Neurobiology* (Vol. 97, Issue 2, pp. 101–126). <https://doi.org/10.1016/j.pneurobio.2011.10.001>
- Bilsland, L. G., Sahai, E., Kelly, G., Golding, M., Greensmith, L., & Schiavo, G. (2010). Deficits in axonal transport precede ALS symptoms in vivo. *Proceedings of the National Academy of Sciences*, 107(47), 20523–20528. <https://doi.org/10.1073/pnas.1006869107>
- Birger, A., Ben-Dor, I., Ottolenghi, M., Turetsky, T., Gil, Y., Sweetat, S., Perez, L., Belzer, V., Casden, N., Steiner, D., Izrael, M., Galun, E., Feldman, E., Behar, O., & Reubinoff, B. (2019). Human iPSC-derived astrocytes from ALS patients with mutated C9ORF72 show increased oxidative stress and neurotoxicity. *EBioMedicine*, 50, 274–289. <https://doi.org/10.1016/j.ebiom.2019.11.026>

References

- Biswas, L., Farhan, F., Reilly, J., Bartholomew, C., & Shu, X. (2018). TSPO ligands promote cholesterol efflux and suppress oxidative stress and inflammation in choroidal endothelial cells. *International Journal of Molecular Sciences*, 19(12). <https://doi.org/10.3390/ijms19123740>
- Blom, S. M., Schmitt, N., & Jensen, H. S. (2010). Differential effects of ICA-27243 on cloned KV7 channels. *Pharmacology*, 86(3), 174–181. <https://doi.org/10.1159/000317525>
- Bloms-Funke, P., Bankstahl, M., Bankstahl, J., Kneip, C., Schröder, W., & Löscher, W. (2022). The novel dual-mechanism Kv7 potassium channel/TSPO receptor activator GRT-X is more effective than the Kv7 channel opener retigabine in the 6-Hz refractory seizure mouse model. *Neuropharmacology*, 203, 108884. <https://doi.org/10.1016/j.neuropharm.2021.108884>
- Bloms-Funke, P., Schumacher, M., Liu, S., Su, D., Li, J., Liere, P., Rupprecht, R., Nothdurfter, C., Bahrenberg, G., Christoph, T., Habermann, C., Kneip, C., Schröder, W., Tzschentke, T. M., & Saunders, D. (2022). A novel dual mode-of-action anti-hyperalgesic compound in rats which is neuroprotective and promotes neuroregeneration. *European Journal of Pharmacology*, 923. <https://doi.org/10.1016/j.ejphar.2022.174935>
- Boërio, D., Kalmar, B., Greensmith, L., & Bostock, H. (2010). Excitability properties of mouse motor axons in the mutant SOD1^{G93A} model of amyotrophic lateral sclerosis. *Muscle & Nerve*, 41(6), 774–784. <https://doi.org/10.1002/mus.21579>
- Bogdanov, M. B., Andreassen, O. A., Dedeoglu, A., Ferrante, R. J., & Beal, M. F. (2002). Increased oxidative damage to DNA in a transgenic mouse model of Huntington's disease. *Journal of Neurochemistry*, 79(6), 1246–1249. <https://doi.org/10.1046/j.1471-4159.2001.00689.x>
- Boillée, S., Yamanaka, K., Lobsiger, C. S., Copeland, N. G., Jenkins, N. A., Kassiotis, G., Kollias, G., & Cleveland, D. W. (2006). Onset and Progression in Inherited ALS Determined by Motor Neurons and Microglia. *Science*, 312(5778), 1389–1392. <https://doi.org/10.1126/science.1123511>
- Bonfanti, E., Bonifacino, T., Raffaele, S., Milanese, M., Morgante, E., Bonanno, G., Abbracchio, M. P., & Fumagalli, M. (2020). Abnormal upregulation of gpr17 receptor contributes to oligodendrocyte dysfunction in SOD1G93A mice. *International Journal of Molecular Sciences*, 21(7). <https://doi.org/10.3390/ijms21072395>
- Bordet, T., Buisson, B., Michaud, M., Drouot, C., Galéa, P., Delaage, P., Akentieva, N. P., Evers, A. S., Covey, D. F., Ostuni, M. A., Lacapère, J. J., Massaad, C., Schumacher, M., Steidl, E. M., Maux, D., Delaage, M., Henderson, C. E., & Pruss, R. M. (2007). Identification and characterization of cholest-4-en-3-one, oxime (TRO19622), a novel drug candidate for amyotrophic lateral sclerosis. *Journal of Pharmacology and Experimental Therapeutics*, 322(2), 709–720. <https://doi.org/10.1124/jpet.107.123000>

- Borowicz, K. K., Piskorska, B., Banach, M., & Czuczwar, S. J. (2011). Neuroprotective actions of neurosteroids. In *Frontiers in Endocrinology* (Vol. 2, Issue OCT). <https://doi.org/10.3389/fendo.2011.00050>
- Boujrad, N., Vidic, B., & Papadopoulos, V. (1996). Acute action of choriogonadotropin on Leydig tumor cells: changes in the topography of the mitochondrial peripheral-type benzodiazepine receptor. *Endocrinology*, 137(12), 5727–5730. <https://doi.org/10.1210/endo.137.12.8940407>
- Brettschneider, J., Del Tredici, K., Toledo, J. B., Robinson, J. L., Irwin, D. J., Grossman, M., Suh, E., Van Deerlin, V. M., Wood, E. M., Baek, Y., Kwong, L., Lee, E. B., Elman, L., McCluskey, L., Fang, L., Feldengut, S., Ludolph, A. C., Lee, V. M.-Y., Braak, H., & Trojanowski, J. Q. (2013). Stages of pTDP-43 pathology in amyotrophic lateral sclerosis. *Annals of Neurology*, 74(1), 20–38. <https://doi.org/10.1002/ana.23937>
- Briese, M., Saal-Bauernschubert, L., Lüningschrör, P., Moradi, M., Dombert, B., Surrey, V., Appenzeller, S., Deng, C., Jablonka, S., & Sendtner, M. (2020). Loss of Tdp-43 disrupts the axonal transcriptome of motoneurons accompanied by impaired axonal translation and mitochondria function. *Acta Neuropathologica Communications*, 8(1). <https://doi.org/10.1186/s40478-020-00987-6>
- Brockington, A., Ning, K., Heath, P. R., Wood, E., Kirby, J., Fusi, N., Lawrence, N., Wharton, S. B., Ince, P. G., & Shaw, P. J. (2013). Unravelling the enigma of selective vulnerability in neurodegeneration: Motor neurons resistant to degeneration in ALS show distinct gene expression characteristics and decreased susceptibility to excitotoxicity. *Acta Neuropathologica*, 125(1), 95–109. <https://doi.org/10.1007/s00401-012-1058-5>
- Brown, A. L., Wilkins, O. G., Keuss, M. J., Hill, S. E., Zanovello, M., Lee, W. C., Bampton, A., Lee, F. C. Y., Masino, L., Qi, Y. A., Bryce-Smith, S., Gatt, A., Hallegger, M., Fagegaltier, D., Phatnani, H., Phatnani, H., Kwan, J., Sareen, D., Broach, J. R., ... Fratta, P. (2022). TDP-43 loss and ALS-risk SNPs drive mis-splicing and depletion of UNC13A. *Nature*, 603(7899), 131–137. <https://doi.org/10.1038/s41586-022-04436-3>
- Brown, D. A., & Passmore, G. M. (2009). Neural KCNQ (Kv7) channels. *British Journal of Pharmacology*, 156(8), 1185–1195. <https://doi.org/10.1111/j.1476-5381.2009.00111.x>
- Bruijn, L. I., Houseweart, M. K., Kato, S., Anderson, K. L., Anderson, S. D., Ohama, E., Reaume, A. G., Scott, R. W., & Cleveland, D. W. (1998). Aggregation and Motor Neuron Toxicity of an ALS-Linked SOD1 Mutant Independent from Wild-Type SOD1. *Science*, 281(5384), 1851–1854. <https://doi.org/10.1126/science.281.5384.1851>

References

- Bucchia, M., Merwin, S. J., Re, D. B., & Kariya, S. (2018). Limitations and challenges in modeling diseases involving spinal motor neuron degeneration in vitro. In *Frontiers in Cellular Neuroscience* (Vol. 12). Frontiers Media S.A. <https://doi.org/10.3389/fncel.2018.00061>
- Burk, K., & Pasterkamp, R. J. (2019). Disrupted neuronal trafficking in amyotrophic lateral sclerosis. *Acta Neuropathologica*, 137(6), 859–877. <https://doi.org/10.1007/s00401-019-01964-7>
- Caballero, B., Veenman, L., & Gavish, M. (2013). Role of Mitochondrial Translocator Protein (18 kDa) on Mitochondrial- Related Cell Death Processes. *Recent Patents on Endocrine, Metabolic & Immune Drug Discovery*, 7(2), 86–101. <https://doi.org/10.2174/1872214811307020002>
- Carrasco, D. I., Seburn, K. L., & Pinter, M. J. (2016). Altered terminal Schwann cell morphology precedes denervation in SOD1 mice. *Experimental Neurology*, 275, 172–181. <https://doi.org/10.1016/j.expneurol.2015.09.014>
- Cashman, N. R., Durham, H. D., Blusztajn, J. K., Oda, K., Tabira, T., Shaw, I. T., Dahrouge, S., & Antel, J. P. (1992). Neuroblastoma × spinal cord (NSC) hybrid cell lines resemble developing motor neurons. *Developmental Dynamics*, 194(3), 209–221. <https://doi.org/10.1002/aja.1001940306>
- Chang, Y., Kong, Q., Shan, X., Tian, G., Ilieva, H., Cleveland, D. W., Rothstein, J. D., Borchelt, D. R., Wong, P. C., & Lin, C. G. (2008). Messenger RNA Oxidation Occurs Early in Disease Pathogenesis and Promotes Motor Neuron Degeneration in ALS. *PLoS ONE*, 3(8), e2849. <https://doi.org/10.1371/journal.pone.0002849>
- Chen, H., Qian, K., Du, Z., Cao, J., Petersen, A., Liu, H., Blackburn, L. W., Huang, C.-L., Errigo, A., Yin, Y., Lu, J., Ayala, M., & Zhang, S.-C. (2014). Modeling ALS with iPSCs Reveals that Mutant SOD1 Misregulates Neurofilament Balance in Motor Neurons. *Cell Stem Cell*, 14(6), 796–809. <https://doi.org/10.1016/j.stem.2014.02.004>
- Chen, M. K., & Guilarte, T. R. (2008). Translocator protein 18 kDa (TSPO): Molecular sensor of brain injury and repair. In *Pharmacology and Therapeutics* (Vol. 118, Issue 1, pp. 1–17). <https://doi.org/10.1016/j.pharmthera.2007.12.004>
- Chew, J., Gendron, T. F., Prudencio, M., Sasaguri, H., Zhang, Y.-J., Castanedes-Casey, M., Lee, C. W., Jansen-West, K., Kurti, A., Murray, M. E., Bieniek, K. F., Bauer, P. O., Whitelaw, E. C., Rousseau, L., Stankowski, J. N., Stetler, C., Daugherty, L. M., Perkerson, E. A., Desaro, P., ... Petrucelli, L. (2015). C9ORF72 repeat expansions in mice cause TDP-43 pathology, neuronal loss, and behavioral deficits. *Science*, 348(6239), 1151–1154. <https://doi.org/10.1126/science.aaa9344>

- Chia, R., Chiò, A., & Traynor, B. J. (2018). Novel genes associated with amyotrophic lateral sclerosis: diagnostic and clinical implications. In *The Lancet Neurology* (Vol. 17, Issue 1, pp. 94–102). Lancet Publishing Group. [https://doi.org/10.1016/S1474-4422\(17\)30401-5](https://doi.org/10.1016/S1474-4422(17)30401-5)
- Chiot, A., Zaidi, S., Iltis, C., Ribon, M., Berriat, F., Schiaffino, L., Jolly, A., de la Grange, P., Mallat, M., Bohl, D., Millecamps, S., Seilhean, D., Lobsiger, C. S., & Boillée, S. (2020). Modifying macrophages at the periphery has the capacity to change microglial reactivity and to extend ALS survival. *Nature Neuroscience*, 23(11), 1339–1351. <https://doi.org/10.1038/s41593-020-00718-z>
- Clement, A. M., Nguyen, M. D., Roberts, E. A., Garcia, M. L., Boillée, S., Rule, M., McMahon, A. P., Doucette, W., Siwek, D., Ferrante, R. J., Brown, R. H., Julien, J.-P., Goldstein, L. S. B., & Cleveland, D. W. (2003). Wild-Type Nonneuronal Cells Extend Survival of SOD1 Mutant Motor Neurons in ALS Mice. *Science*, 302(5642), 113–117. <https://doi.org/10.1126/science.1086071>
- Colantoni, A., Capauto, D., Alfano, V., D'Ambra, E., D'Uva, S., Tartaglia, G. G., & Morlando, M. (2023). FUS Alters circRNA Metabolism in Human Motor Neurons Carrying the ALS-Linked P525L Mutation. *International Journal of Molecular Sciences*, 24(4). <https://doi.org/10.3390/ijms24043181>
- Collard, J.-F., Côté, F., & Julien, J.-P. (1995). Defective axonal transport in a transgenic mouse model of amyotrophic lateral sclerosis. *Nature*, 375(6526), 61–64. <https://doi.org/10.1038/375061a0>
- Comley, L., Allodi, I., Nichterwitz, S., Nizzardo, M., Simone, C., Corti, S., & Hedlund, E. (2015). Motor neurons with differential vulnerability to degeneration show distinct protein signatures in health and ALS. *Neuroscience*, 291, 216–229. <https://doi.org/10.1016/j.neuroscience.2015.02.013>
- Cunha-Oliveira, T., Montezinho, L., Mendes, C., Firuzi, O., Saso, L., Oliveira, P. J., & Silva, F. S. G. (2020). Oxidative Stress in Amyotrophic Lateral Sclerosis: Pathophysiology and Opportunities for Pharmacological Intervention. *Oxidative Medicine and Cellular Longevity*, 2020, 1–29. <https://doi.org/10.1155/2020/5021694>
- Dafinca, R., Scaber, J., Ababneh, N., Lalic, T., Weir, G., Christian, H., Vowles, J., Douglas, A. G. L., Fletcher-Jones, A., Browne, C., Nakanishi, M., Turner, M. R., Wade-Martins, R., Cowley, S. A., & Talbot, K. (2016). C9orf72 Hexanucleotide Expansions Are Associated with Altered Endoplasmic Reticulum Calcium Homeostasis and Stress Granule Formation in Induced Pluripotent Stem Cell-Derived Neurons from Patients with Amyotrophic Lateral Sclerosis and Frontotemporal Dementia. *Stem Cells*, 34(8), 2063–2078. <https://doi.org/10.1002/stem.2388>
- Damiano, M., Starkov, A. A., Petri, S., Kipiani, K., Kiaei, M., Mattiazzi, M., Flint Beal, M., & Manfredi, G. (2006). Neural mitochondrial Ca²⁺ capacity impairment precedes the onset of motor

References

- symptoms in G93A Cu/Zn-superoxide dismutase mutant mice. *Journal of Neurochemistry*, 96(5), 1349–1361. <https://doi.org/10.1111/j.1471-4159.2006.03619.x>
- De Luna, N., Turon-Sans, J., Cortes-Vicente, E., Carrasco-Rozas, A., Illán-Gala, I., Dols-Icardo, O., Clarimón, J., Lleó, A., Gallardo, E., Illa, I., & Rojas-García, R. (2020). Downregulation of miR-335-5P in Amyotrophic Lateral Sclerosis Can Contribute to Neuronal Mitochondrial Dysfunction and Apoptosis. *Scientific Reports*, 10(1). <https://doi.org/10.1038/s41598-020-61246-1>
- De Nicola, A. F., Meyer, M., Garay, L., Kruse, M. S., Schumacher, M., Guennoun, R., & Gonzalez Deniselle, M. C. (2022). Progesterone and Allopregnanolone Neuroprotective Effects in the Wobbler Mouse Model of Amyotrophic Lateral Sclerosis. *Cellular and Molecular Neurobiology*, 42(1), 23–40. <https://doi.org/10.1007/s10571-021-01118-y>
- de Tassigny, A. d. A., Assaly, R., Schaller, S., Pruss, R. M., Berdeaux, A., & Morin, D. (2013). Mitochondrial translocator protein (TSPO) ligands prevent doxorubicin-induced mechanical dysfunction and cell death in isolated cardiomyocytes. *Mitochondrion*, 13(6), 688–697. <https://doi.org/10.1016/j.mito.2013.10.001>
- Deardorff, A. S., Romer, S. H., & Fyffe, R. E. W. (2021). Location, location, location: the organization and roles of potassium channels in mammalian motoneurons. *The Journal of Physiology*, 599(5), 1391–1420. <https://doi.org/10.1113/JP278675>
- DeJesus-Hernandez, M., Mackenzie, I. R., Boeve, B. F., Boxer, A. L., Baker, M., Rutherford, N. J., Nicholson, A. M., Finch, N. A., Flynn, H., Adamson, J., Kouri, N., Wojtas, A., Sengdy, P., Hsiung, G.-Y. R., Karydas, A., Seeley, W. W., Josephs, K. A., Coppola, G., Geschwind, D. H., ... Rademakers, R. (2011). Expanded GGGGCC Hexanucleotide Repeat in Noncoding Region of C9ORF72 Causes Chromosome 9p-Linked FTD and ALS. *Neuron*, 72(2), 245–256. <https://doi.org/10.1016/j.neuron.2011.09.011>
- Devaux, J., Abidi, A., Roubertie, A., Molinari, F., Becq, H., Lacoste, C., Villard, L., Milh, M., & Aniksztejn, L. (2016). A Kv7.2 mutation associated with early onset epileptic encephalopathy with suppression-burst enhances Kv7/M channel activity. *Epilepsia*, 57(5), e87–e93. <https://doi.org/10.1111/epi.13366>
- Devaux, J. J., Kleopa, K. A., Cooper, E. C., & Scherer, S. S. (2004). KCNQ2 Is a Nodal K⁺ Channel. *The Journal of Neuroscience*, 24(5), 1236–1244. <https://doi.org/10.1523/JNEUROSCI.4512-03.2004>
- Devlin, A.-C., Burr, K., Borooah, S., Foster, J. D., Cleary, E. M., Geti, I., Vallier, L., Shaw, C. E., Chandran, S., & Miles, G. B. (2015). Human iPSC-derived motoneurons harbouring TARDBP or C9ORF72 ALS mutations are dysfunctional despite maintaining viability. *Nature Communications*, 6(1), 5999. <https://doi.org/10.1038/ncomms6999>

- Di Giorgio, F. P., Boulting, G. L., Bobrowicz, S., & Eggan, K. C. (2008). Human Embryonic Stem Cell-Derived Motor Neurons Are Sensitive to the Toxic Effect of Glial Cells Carrying an ALS-Causing Mutation. *Cell Stem Cell*, 3(6), 637–648. <https://doi.org/10.1016/j.stem.2008.09.017>
- Di Giorgio, F. P., Carrasco, M. A., Siao, M. C., Maniatis, T., & Eggan, K. (2007). Non-cell autonomous effect of glia on motor neurons in an embryonic stem cell-based ALS model. *Nature Neuroscience*, 10(5), 608–614. <https://doi.org/10.1038/nn1885>
- Doble, A. (1996). The pharmacology and mechanism of action of riluzole. In *Neurology* (Vol. 47, Issue 6 SUPPL. 4). Lippincott Williams and Wilkins. https://doi.org/10.1212/wnl.47.6_suppl_4.233s
- Do-Ha, D., Buskila, Y., & Ooi, L. (2018). Impairments in Motor Neurons, Interneurons and Astrocytes Contribute to Hyperexcitability in ALS: Underlying Mechanisms and Paths to Therapy. *Molecular Neurobiology*, 55(2), 1410–1418. <https://doi.org/10.1007/s12035-017-0392-y>
- Fan, J., Campioli, E., Midzak, A., Culty, M., & Papadopoulos, V. (2015). Conditional steroidogenic cell-targeted deletion of TSPO unveils a crucial role in viability and hormone-dependent steroid formation. *Proceedings of the National Academy of Sciences of the United States of America*, 112(23), 7261–7266. <https://doi.org/10.1073/pnas.1502670112>
- Fan, J., Rone, M. B., & Papadopoulos, V. (2009). Translocator protein 2 is involved in cholesterol redistribution during erythropoiesis. *Journal of Biological Chemistry*, 284(44), 30484–30497. <https://doi.org/10.1074/jbc.M109.029876>
- Fan, J., Wang, K., Zirkin, B., & Papadopoulos, V. (2018). CRISPR/Cas9-Mediated tspos gene mutations lead to reduced mitochondrial membrane potential and steroid formation in MA-10 mouse tumor leydig cells. *Endocrinology*, 159(2), 1130–1146. <https://doi.org/10.1210/en.2017-03065>
- Fan, Y.-Y., & Huo, J. (2021). A1/A2 astrocytes in central nervous system injuries and diseases: Angels or devils? *Neurochemistry International*, 148, 105080. <https://doi.org/10.1016/j.neuint.2021.105080>
- Farhan, F., Almarhoun, M., Wong, A., Findlay, A. S., Bartholomew, C., Williams, M. T. S., Hurd, T. W., & Shu, X. (2021). Deletion of tspos causes dysregulation of cholesterol metabolism in mouse retina. *Cells*, 10(11). <https://doi.org/10.3390/cells10113066>
- Fattorelli, N., Martinez-Muriana, A., Wolfs, L., Geric, I., De Strooper, B., & Mancuso, R. (2021). Stem-cell-derived human microglia transplanted into mouse brain to study human disease. *Nature Protocols*, 16(2), 1013–1033. <https://doi.org/10.1038/s41596-020-00447-4>
- Ferraiuolo, L., Meyer, K., Sherwood, T. W., Vick, J., Likhite, S., Frakes, A., Miranda, C. J., Braun, L., Heath, P. R., Pineda, R., Beattie, C. E., Shaw, P. J., Askwith, C. C., McTigue, D., & Kaspar, B. K. (2016). Oligodendrocytes contribute to motor neuron death in ALS via SOD1-dependent

References

- mechanism. *Proceedings of the National Academy of Sciences of the United States of America*, 113(42), E6496–E6505. <https://doi.org/10.1073/pnas.1607496113>
- Ferri, A., Cozzolino, M., Crosio, C., Nencini, M., Casciati, A., Gralla, E. B., Rotilio, G., Valentine, J. S., & Carri, M. T. (2006). Familial ALS-superoxide dismutases associate with mitochondria and shift their redox potentials. *Proceedings of the National Academy of Sciences*, 103(37), 13860–13865. <https://doi.org/10.1073/pnas.0605814103>
- Filipi, T., Hermanova, Z., Tureckova, J., Vanatko, O., & Anderova, M. (2020). Glial cells—The strategic targets in amyotrophic lateral sclerosis treatment. In *Journal of Clinical Medicine* (Vol. 9, Issue 1). MDPI. <https://doi.org/10.3390/jcm9010261>
- Fitzmaurice, P. S., Shaw, I. C., Kleiner, H. E., Miller, R. T., Monks, T. J., Lau, S. S., Mitchell, J. D., & Lynch, P. G. (1996). Evidence for DNA damage in amyotrophic lateral sclerosis. *Muscle & Nerve*, 19(6), 797–798.
- Fortuna, A., Gizzi, M., Bello, L., Martinelli, I., Bertolin, C., Pegoraro, E., Corbetta, M., & Sorarù, G. (2019). Safety and efficacy of edaravone compared to historical controls in patients with amyotrophic lateral sclerosis from North-Eastern Italy. *Journal of the Neurological Sciences*, 404, 47–51. <https://doi.org/10.1016/j.jns.2019.06.006>
- Fritz, E., Izaurieta, P., Weiss, A., Mir, F. R., Rojas, P., Gonzalez, D., Rojas, F., Brown, R. H., Madrid, R., & van Zundert, B. (2013). Mutant SOD1-expressing astrocytes release toxic factors that trigger motoneuron death by inducing hyperexcitability. *Journal of Neurophysiology*, 109(11), 2803–2814. <https://doi.org/10.1152/jn.00500.2012>
- Fu, Y., Wang, D., Wang, H., Cai, M., Li, C., Zhang, X., Chen, H., Hu, Y., Zhang, X., Ying, M., He, W., & Zhang, J. (2020). TSPO deficiency induces mitochondrial dysfunction, leading to hypoxia, angiogenesis, and a growth-promoting metabolic shift toward glycolysis in glioblastoma. *Neuro-Oncology*, 22(2), 240–252. <https://doi.org/10.1093/neuonc/noz183>
- Fujimori, K., Ishikawa, M., Otomo, A., Atsuta, N., Nakamura, R., Akiyama, T., Hadano, S., Aoki, M., Saya, H., Sobue, G., & Okano, H. (2018). Modeling sporadic ALS in iPSC-derived motor neurons identifies a potential therapeutic agent. *Nature Medicine*, 24(10), 1579–1589. <https://doi.org/10.1038/s41591-018-0140-5>
- Gaja-Capdevila, N., Hernández, N., Navarro, X., & Herrando-Grabulosa, M. (2021). Sigma-1 Receptor is a Pharmacological Target to Promote Neuroprotection in the SOD1G93A ALS Mice. *Frontiers in Pharmacology*, 12. <https://doi.org/10.3389/fphar.2021.780588>

- Garbuzova-Davis, S., & Sanberg, P. R. (2014). Blood-CNS barrier impairment in ALS patients versus an animal model. In *Frontiers in Cellular Neuroscience* (Vol. 8, Issue FEB). <https://doi.org/10.3389/fncel.2014.00021>
- Gatliff, J., East, D., Crosby, J., Abeti, R., Harvey, R., Craigen, W., Parker, P., & Campanella, M. (2014). TSPO interacts with VDAC1 and triggers a ROS-mediated inhibition of mitochondrial quality control. *Autophagy*, 10(12), 2279–2296. <https://doi.org/10.4161/15548627.2014.991665>
- Gautam, M., Jara, J. H., Sekerkova, G., Yasvoina, M. V., Martina, M., & Özdinler, P. H. (2015). Absence of alsin function leads to corticospinal motor neuron vulnerability via novel disease mechanisms. *Human Molecular Genetics*, 25(6), 1074–1087. <https://doi.org/10.1093/hmg/ddv631>
- Geloso, M. C., Corvino, V., Marchese, E., Serrano, A., Michetti, F., & D'Ambrosi, N. (2017). The Dual Role of Microglia in ALS: Mechanisms and Therapeutic Approaches. *Frontiers in Aging Neuroscience*, 9. <https://doi.org/10.3389/fnagi.2017.00242>
- Ghezzi, F., Monni, L., & Nistri, A. (2018). Functional up-regulation of the M-current by retigabine contrasts hyperexcitability and excitotoxicity on rat hypoglossal motoneurons. *Journal of Physiology*, 596(13), 2611–2629. <https://doi.org/10.1113/JP275906>
- Gitcho, M. A., Baloh, R. H., Chakraverty, S., Mayo, K., Norton, J. B., Levitch, D., Hatanpaa, K. J., White, C. L., Bigio, E. H., Caselli, R., Baker, M., Al-Lozi, M. T., Morris, J. C., Pestronk, A., Rademakers, R., Goate, A. M., & Cairns, N. J. (2008). TDP-43 A315T mutation in familial motor neuron disease. *Annals of Neurology*, 63(4), 535–538. <https://doi.org/10.1002/ana.21344>
- Gois, A. M., Mendonça, D. M. F., Freire, M. A. M., & Santos, J. R. (2020). IN VITRO AND IN VIVO MODELS OF AMYOTROPHIC LATERAL SCLEROSIS: AN UPDATED OVERVIEW. *Brain Research Bulletin*, 159, 32–43. <https://doi.org/10.1016/j.brainresbull.2020.03.012>
- Gomes, C., Escrevente, C., & Costa, J. (2010). Mutant superoxide dismutase 1 overexpression in NSC-34 cells: Effect of trehalose on aggregation, TDP-43 localization and levels of co-expressed glycoproteins. *Neuroscience Letters*, 475(3), 145–149. <https://doi.org/10.1016/j.neulet.2010.03.065>
- Gomes, C., Sequeira, C., Likhite, S., Dennys, C. N., Kolb, S. J., Shaw, P. J., Vaz, A. R., Kaspar, B. K., Meyer, K., & Brites, D. (2022). Neurotoxic Astrocytes Directly Converted from Sporadic and Familial ALS Patient Fibroblasts Reveal Signature Diversities and miR-146a Theragnostic Potential in Specific Subtypes. *Cells*, 11(7), 1186. <https://doi.org/10.3390/cells11071186>
- Gomez-Suaga, P., Mórotz, G. M., Markovinovic, A., Martín-Guerrero, S. M., Preza, E., Arias, N., Mayl, K., Aabdien, A., Gesheva, V., Nishimura, A., Annibali, A., Lee, Y., Mitchell, J. C., Wray, S.,

References

- Shaw, C., Noble, W., & Miller, C. C. J. (2022). Disruption of ER-mitochondria tethering and signalling in C9orf72 -associated amyotrophic lateral sclerosis and frontotemporal dementia. *Aging Cell*, 21(2). <https://doi.org/10.1111/ace.13549>
- Gong, Y. H., Parsadanian, A. S., Andreeva, A., Snider, W. D., & Elliott, J. L. (2000). Restricted Expression of G86R Cu/Zn Superoxide Dismutase in Astrocytes Results in Astrocytosis But Does Not Cause Motoneuron Degeneration. *The Journal of Neuroscience*, 20(2), 660–665. <https://doi.org/10.1523/JNEUROSCI.20-02-00660.2000>
- González, C., Baez-Nieto, D., Valencia, I., Oyarzún, I., Rojas, P., Naranjo, D., & Latorre, R. (2012). K⁺ channels: Function-structural overview. *Comprehensive Physiology*, 2(3), 2087–2149. <https://doi.org/10.1002/cphy.c110047>
- Gonzalez Deniselle, M. C., López-Costa, J. J., Saavedra, J. P., Pietranera, L., Gonzalez, S. L., Garay, L., Guennoun, R., Schumacher, M., & De Nicola, A. F. (2002). Progesterone neuroprotection in the Wobbler mouse, a genetic model of spinal cord motor neuron disease. *Neurobiology of Disease*, 11(3), 457–468. <https://doi.org/10.1006/nbdi.2002.0564>
- Goutman, S. A., Hardiman, O., Al-Chalabi, A., Chió, A., Savelieff, M. G., Kiernan, M. C., & Feldman, E. L. (2022). Recent advances in the diagnosis and prognosis of amyotrophic lateral sclerosis. In *The Lancet Neurology* (Vol. 21, Issue 5, pp. 480–493). Elsevier Ltd. [https://doi.org/10.1016/S1474-4422\(21\)00465-8](https://doi.org/10.1016/S1474-4422(21)00465-8)
- Gowing, G., Philips, T., Van Wijmeersch, B., Audet, J.-N., Dewil, M., Van Den Bosch, L., Billiau, A. D., Robberecht, W., & Julien, J.-P. (2008). Ablation of Proliferating Microglia Does Not Affect Motor Neuron Degeneration in Amyotrophic Lateral Sclerosis Caused by Mutant Superoxide Dismutase. *The Journal of Neuroscience*, 28(41), 10234–10244. <https://doi.org/10.1523/JNEUROSCI.3494-08.2008>
- Grad, L. I., Guest, W. C., Yanai, A., Pokrishevsky, E., O'Neill, M. A., Gibbs, E., Semchenko, V., Yousefi, M., Wishart, D. S., Plotkin, S. S., & Cashman, N. R. (2011). Intermolecular transmission of superoxide dismutase 1 misfolding in living cells. *Proceedings of the National Academy of Sciences of the United States of America*, 108(39), 16398–16403. <https://doi.org/10.1073/pnas.1102645108>
- Groen, E. J. N., van Es, M. A., van Vught, P. W. J., Spliet, W. G. M., van Engelen-Lee, J., de Visser, M., Wokke, J. H. J., Schelhaas, H. J., Ophoff, R. A., Fumoto, K., Pasterkamp, R. J., Dooijes, D., Cuppen, E., Veldink, J. H., & van den Berg, L. H. (2010). FUS Mutations in Familial Amyotrophic Lateral Sclerosis in the Netherlands. *Archives of Neurology*, 67(2). <https://doi.org/10.1001/archneurol.2009.329>

- Guilarte, T. R., Rodichkin, A. N., McGlothan, J. L., Acanda De La Rocha, A. M., & Azzam, D. J. (2022). Imaging neuroinflammation with TSPO: A new perspective on the cellular sources and subcellular localization. In *Pharmacology and Therapeutics* (Vol. 234). Elsevier Inc. <https://doi.org/10.1016/j.pharmthera.2021.108048>
- Gurney, M. E., Pu, H., Chiu, A. Y., Dal Canto, M. C., Polchow, C. Y., Alexander, D. D., Caliendo, J., Hentati, A., Kwon, Y. W., Deng, H.-X., Chen, W., Zhai, P., Sufit, R. L., & Siddique, T. (1994). Motor Neuron Degeneration in Mice that Express a Human Cu,Zn Superoxide Dismutase Mutation. *Science*, 264(5166), 1772–1775. <https://doi.org/10.1126/science.8209258>
- Guttenplan, K. A., Weigel, M. K., Adler, D. I., Couthouis, J., Liddelow, S. A., Gitler, A. D., & Barres, B. A. (2020). Knockout of reactive astrocyte activating factors slows disease progression in an ALS mouse model. *Nature Communications*, 11(1). <https://doi.org/10.1038/s41467-020-17514-9>
- Guzmán-Lenis, M. S., Navarro, X., & Casas, C. (2009). Selective sigma receptor agonist 2-(4-morpholinethyl)-1-phenylcyclohexanecarboxylate (PRE084) promotes neuroprotection and neurite elongation through protein kinase C (PKC) signaling on motoneurons. *Neuroscience*, 162(1), 31–38. <https://doi.org/10.1016/j.neuroscience.2009.03.067>
- Hafezparast, M., Klocke, R., Ruhrberg, C., Marquardt, A., Ahmad-Annuar, A., Bowen, S., Lalli, G., Witherden, A. S., Hummerich, H., Nicholson, S., Jeffrey Morgan, P., Oozageer, R., Priestley, J. V., Averill, S., King, V. R., Ball, S., Peters, J., Toda, T., Yamamoto, A., ... C Fisher, E. M. (1994). Mutations in Dynein Link Motor Neuron Degeneration to Defects in Retrograde Transport. In *Annu. Rev. Biochem* (Vol. 8). www.sciencemag.org/cgi/content/full/300/5620/805/
- Hallé, F., Lejri, I., Abarghaz, M., Grimm, A., Klein, C., Maitre, M., Schmitt, M., Bourguignon, J. J., Mensah-Nyagan, A. G., Eckert, A., & Bihel, F. (2017). Discovery of Imidazoquinazolinone Derivatives as TSPO Ligands Modulating Neurosteroidogenesis and Cellular Bioenergetics in Neuroblastoma Cells Expressing Amyloid Precursor Protein. *ChemistrySelect*, 2(22), 6452–6457. <https://doi.org/10.1002/slct.201701565>
- Hannaford, A., Pavey, N., van den Bos, M., Geevasinga, N., Menon, P., Shefner, J. M., Kiernan, M. C., & Vucic, S. (2021). Diagnostic Utility of Gold Coast Criteria in Amyotrophic Lateral Sclerosis. *Annals of Neurology*, 89(5), 979–986. <https://doi.org/10.1002/ana.26045>
- Hardiman, O., Al-Chalabi, A., Chio, A., Corr, E. M., Logroscino, G., Robberecht, W., Shaw, P. J., Simmons, Z., & Van Den Berg, L. H. (2017). Amyotrophic lateral sclerosis. In *Nature Reviews Disease Primers* (Vol. 3). Nature Publishing Group. <https://doi.org/10.1038/nrdp.2017.71>
- Hasegawa, T., Zhao, L., Caron, K. M., Majdic, G., Suzuki, T., Shizawa, S., Sasano, H., & Parker, K. L. (2000). Developmental Roles of the Steroidogenic Acute Regulatory Protein (StAR) as

References

- Revealed by StAR Knockout Mice. In *Molecular Endocrinology* (Vol. 14). <https://academic.oup.com/mend/article/14/9/1462/2751100>
- Hasselmann, J., Coburn, M. A., England, W., Figueroa Velez, D. X., Kiani Shabestari, S., Tu, C. H., McQuade, A., Kolahdouzan, M., Echeverria, K., Claes, C., Nakayama, T., Azevedo, R., Coufal, N. G., Han, C. Z., Cummings, B. J., Davtyan, H., Glass, C. K., Healy, L. M., Gandhi, S. P., ... Blurton-Jones, M. (2019). Development of a Chimeric Model to Study and Manipulate Human Microglia In Vivo. *Neuron*, 103(6), 1016-1033.e10. <https://doi.org/10.1016/j.neuron.2019.07.002>
- Hayashi, H., Iwata, M., Tsuchimori, N., & Matsumoto, T. (2014). Activation of peripheral KCNQ channels attenuates inflammatory pain. *Molecular Pain*, 10(1). <https://doi.org/10.1186/1744-8069-10-15>
- Hegedus, J., Putman, C. T., & Gordon, T. (2007). Time course of preferential motor unit loss in the SOD1G93A mouse model of amyotrophic lateral sclerosis. *Neurobiology of Disease*, 28(2), 154-164. <https://doi.org/10.1016/j.nbd.2007.07.003>
- Hegedus, J., Putman, C. T., Tyreman, N., & Gordon, T. (2008). Preferential motor unit loss in the SOD1^{G93A} transgenic mouse model of amyotrophic lateral sclerosis. *The Journal of Physiology*, 586(14), 3337-3351. <https://doi.org/10.1113/jphysiol.2007.149286>
- Herrando-Grabulosa, M., Casas, C., Talbot, K., & Aguilera, J. (2020). Neurotrophic Properties of C-Terminal Domain of the Heavy Chain of Tetanus Toxin on Motor Neuron Disease. *Toxins*, 12(10), 666. <https://doi.org/10.3390/toxins12100666>
- Herrando-Grabulosa, M., Mulet, R., Pujol, A., Mas, J. M., Navarro, X., Aloy, P., Coma, M., & Casas, C. (2016). Novel neuroprotective multicomponent therapy for amyotrophic lateral sclerosis designed by networked systems. *PLoS ONE*, 11(1). <https://doi.org/10.1371/journal.pone.0147626>
- Hewitt, C., Kirby, J., Highley, J. R., Hartley, J. A., Hibberd, R., Hollinger, H. C., Williams, T. L., Ince, P. G., McDermott, C. J., & Shaw, P. J. (2010). Novel FUS/TLS Mutations and Pathology in Familial and Sporadic Amyotrophic Lateral Sclerosis. *Archives of Neurology*, 67(4). <https://doi.org/10.1001/archneurol.2010.52>
- Hirano, A., Donnenfeld, H., Sasaki, S., & Nakano, I. (1984). Fine Structural Observations of Neurofilamentous Changes in Amyotrophic Lateral Sclerosis. *Journal of Neuropathology and Experimental Neurology*, 43(5), 461-470. <https://doi.org/10.1097/00005072-198409000-00001>
- Hirsch, T., Decaudin, D., Susin, S. A., Marchetti, P., Larochette, N., Resche-Rigon, M., & Kroemer, G. (1998). PK11195, a Ligand of the Mitochondrial Benzodiazepine Receptor, Facilitates the

- Induction of Apoptosis and Reverses Bcl-2-Mediated Cytoprotection. *Experimental Cell Research*, 241(2), 426–434. <https://doi.org/10.1006/excr.1998.4084>
- Hoell, J. I., Larsson, E., Runge, S., Nusbaum, J. D., Duggimpudi, S., Farazi, T. A., Hafner, M., Borkhardt, A., Sander, C., & Tuschl, T. (2011). RNA targets of wild-type and mutant FET family proteins. *Nature Structural and Molecular Biology*, 18(12), 1428–1431. <https://doi.org/10.1038/nsmb.2163>
- Hogg, M. C., Halang, L., Woods, I., Coughlan, K. S., & Prehn, J. H. M. (2018). Riluzole does not improve lifespan or motor function in three ALS mouse models. *Amyotrophic Lateral Sclerosis and Frontotemporal Degeneration*, 19(5–6), 438–445. <https://doi.org/10.1080/21678421.2017.1407796>
- Hounoum, B. M., Vourc'h, P., Felix, R., Corcia, P., Patin, F., Guéguinou, M., Potier-Cartereau, M., Vandier, C., Raoul, C., Andres, C. R., Mavel, S., & Blasco, H. (2016). NSC-34 motor neuron-like cells are unsuitable as experimental model for glutamate-mediated excitotoxicity. *Frontiers in Cellular Neuroscience*, 10(MAY). <https://doi.org/10.3389/fncel.2016.00118>
- Houzen, H., Kano, T., Horiuchi, K., Wakita, M., Nagai, A., & Yabe, I. (2021). Improved long-term survival with edaravone therapy in patients with amyotrophic lateral sclerosis: A retrospective single-center study in Japan. *Pharmaceuticals*, 14(8). <https://doi.org/10.3390/ph14080705>
- Huang, S. L., Wu, L. S., Lee, M., Chang, C. W., Cheng, W. C., Fang, Y. S., Chen, Y. R., Cheng, P. L., & Shen, C. K. J. (2020). A robust TDP-43 knock-in mouse model of ALS. *Acta Neuropathologica Communications*, 8(1). <https://doi.org/10.1186/s40478-020-0881-5>
- Hunter, M., Spiller, K. J., Dominique, M. A., Xu, H., Hunter, F. W., Fang, T. C., Canter, R. G., Roberts, C. J., Ransohoff, R. M., Trojanowski, J. Q., & Lee, V. M. Y. (2021). Microglial transcriptome analysis in the rNLS8 mouse model of TDP-43 proteinopathy reveals discrete expression profiles associated with neurodegenerative progression and recovery. *Acta Neuropathologica Communications*, 9(1). <https://doi.org/10.1186/s40478-021-01239-x>
- Ince, P., Stout, N., Shaw, P., Slade, J., Hunziker, W., Heizmann, C. W., & Baimbridge, K. G. (1993). Parvalbumin and calbindin D-28k in the human motor system and in motor neuron disease. *Neuropathology and Applied Neurobiology*, 19(4), 291–299. <https://doi.org/10.1111/j.1365-2990.1993.tb00443.x>
- Israelson, A., Arbel, N., Da Cruz, S., Ilieva, H., Yamanaka, K., Shoshan-Barmatz, V., & Cleveland, D. W. (2010). Misfolded mutant SOD1 directly inhibits VDAC1 conductance in a mouse model of inherited ALS. *Neuron*, 67(4), 575–587. <https://doi.org/10.1016/j.neuron.2010.07.019>

References

- Iwai, Y., Shibuya, K., Misawa, S., Sekiguchi, Y., Watanabe, K., Amino, H., & Kuwabara, S. (2016). Axonal Dysfunction Precedes Motor Neuronal Death in Amyotrophic Lateral Sclerosis. *PLOS ONE*, 11(7), e0158596. <https://doi.org/10.1371/journal.pone.0158596>
- Izrael, M., Slutsky, S. G., & Revel, M. (2020). Rising Stars: Astrocytes as a Therapeutic Target for ALS Disease. *Frontiers in Neuroscience*, 14. <https://doi.org/10.3389/fnins.2020.00824>
- Jaarsma, D., Haasdijk, E. D., Grashorn, J. A. C., Hawkins, R., van Duijn, W., Verspaget, H. W., London, J., & Holstege, J. C. (2000). Human Cu/Zn Superoxide Dismutase (SOD1) Overexpression in Mice Causes Mitochondrial Vacuolization, Axonal Degeneration, and Premature Motoneuron Death and Accelerates Motoneuron Disease in Mice Expressing a Familial Amyotrophic Lateral Sclerosis Mutant SOD1. *Neurobiology of Disease*, 7(6), 623–643. <https://doi.org/10.1006/nbdi.2000.0299>
- Jayakumar, A. R., Panickar, K. S., & Norenberg, M. D. (2002). Effects on free radical generation by ligands of the peripheral benzodiazepine receptor in cultured neural cells. *Journal of Neurochemistry*, 83(5), 1226–1234. <https://doi.org/10.1046/j.1471-4159.2002.01261.x>
- Jentsch, T. J. (2000). Neuronal KCNQ potassium channels: physiology and role in disease. *Nature Reviews Neuroscience*, 1(1), 21–30. <https://doi.org/10.1038/35036198>
- Jeyachandran, A., Mertens, B., McKissick, E. A., & Mitchell, C. S. (2015). Type I vs. Type II cytokine levels as a function of SOD1 G93A mouse amyotrophic lateral sclerosis disease progression. *Frontiers in Cellular Neuroscience*, 9(DEC), 1–11. <https://doi.org/10.3389/fncel.2015.00462>
- Jiang, J., Zhu, Q., Gendron, T. F., Saberi, S., McAlonis-Downes, M., Seelman, A., Stauffer, J. E., Jafarnejad, P., Drenner, K., Schulte, D., Chun, S., Sun, S., Ling, S.-C., Myers, B., Engelhardt, J., Katz, M., Baughn, M., Platoshyn, O., Marsala, M., ... Lagier-Tourenne, C. (2016). Gain of Toxicity from ALS/FTD-Linked Repeat Expansions in C9ORF72 Is Alleviated by Antisense Oligonucleotides Targeting GGGGCC-Containing RNAs. *Neuron*, 90(3), 535–550. <https://doi.org/10.1016/j.neuron.2016.04.006>
- Jiménez-Villegas, J., Kirby, J., Mata, A., Cadenas, S., Turner, M. R., Malaspina, A., Shaw, P. J., Cuadrado, A., & Rojo, A. I. (2022). Dipeptide Repeat Pathology in C9orf72-ALS Is Associated with Redox, Mitochondrial and NRF2 Pathway Imbalance. *Antioxidants*, 11(10). <https://doi.org/10.3390/antiox11101897>
- Joo, H. K., Lee, Y. R., Kang, G., Choi, S., Kim, C. S., Ryoo, S., Park, J. B., & Jeon, B. H. (2015). The 18-kDa translocator protein inhibits vascular cell adhesion molecule-1 expression via inhibition of mitochondrial reactive oxygen species. *Molecules and Cells*, 38(12), 1064–1070. <https://doi.org/10.14348/molcells.2015.0165>

- Joseph-Liauzun, E., Delmas, P., Shire, D., & Ferrara, P. (1998). Topological analysis of the peripheral benzodiazepine receptor in yeast mitochondrial membranes supports a five-transmembrane structure. *Journal of Biological Chemistry*, 273(4), 2146–2152. <https://doi.org/10.1074/jbc.273.4.2146>
- Julien, J. P., & Mushynski, W. E. (1998). Neurofilaments in health and disease. *Progress in Nucleic Acid Research and Molecular Biology*, 61, 1–23. [https://doi.org/10.1016/s0079-6603\(08\)60823-5](https://doi.org/10.1016/s0079-6603(08)60823-5)
- Kabashi, E., Lin, L., Tradewell, M. L., Dion, P. A., Bercier, V., Bourgouin, P., Rochefort, D., Bel Hadj, S., Durham, H. D., Velde, C. Vande, Rouleau, G. A., & Drapeau, P. (2009). Gain and loss of function of ALS-related mutations of TARDBP (TDP-43) cause motor deficits in vivo. *Human Molecular Genetics*, 19(4), 671–683. <https://doi.org/10.1093/hmg/ddp534>
- Kamelgarn, M., Chen, J., Kuang, L., Jin, H., Kasarskis, E. J., & Zhu, H. (2018). ALS mutations of FUS suppress protein translation and disrupt the regulation of nonsense-mediated decay. *Proceedings of the National Academy of Sciences of the United States of America*, 115(51), E11904–E11913. <https://doi.org/10.1073/pnas.1810413115>
- Kanai, K., Kuwabara, S., Misawa, S., Tamura, N., Ogawara, K., Nakata, M., Sawai, S., Hattori, T., & Bostock, H. (2006). Altered axonal excitability properties in amyotrophic lateral sclerosis: impaired potassium channel function related to disease stage. *Brain: A Journal of Neurology*, 129(Pt 4), 953–962. <https://doi.org/10.1093/brain/awl024>
- Kang, S. H., Li, Y., Fukaya, M., Lorenzini, I., Cleveland, D. W., Ostrow, L. W., Rothstein, J. D., & Bergles, D. E. (2013). Degeneration and impaired regeneration of gray matter oligodendrocytes in amyotrophic lateral sclerosis. *Nature Neuroscience*, 16(5), 571–579. <https://doi.org/10.1038/nn.3357>
- Kapell, H., Fazio, L., Dyckow, J., Schwarz, S., Cruz-Herranz, A., Mayer, C., Campos, J., D'Este, E., Möbius, W., Cordano, C., Probstel, A.-K., Gharagozloo, M., Zulji, A., Narayanan Naik, V., Delank, A., Cerina, M., Muntefering, T., Lerma-Martin, C., Sonner, J. K., ... Schirmer, L. (2023). Neuron-oligodendrocyte potassium shuttling at nodes of Ranvier protects against inflammatory demyelination. *Journal of Clinical Investigation*, 133(7). <https://doi.org/10.1172/JCI164223>
- Kaplan, A., Spiller, K. J., Towne, C., Kanning, K. C., Choe, G. T., Geber, A., Akay, T., Aebischer, P., & Henderson, C. E. (2014). Neuronal matrix Metalloproteinase-9 is a determinant of selective Neurodegeneration. *Neuron*, 81(2), 333–348. <https://doi.org/10.1016/j.neuron.2013.12.009>
- Kawamata, T., Akiyama, H., Yamada, T., & McGeer, P. L. (1992). Immunologic Reactions in Amyotrophic Lateral Sclerosis Brain and Spinal Cord Tissue. In *American Journal of Pathology* (Vol. 140, Issue 3).

References

- Keating, S. S., Bademosi, A. T., San Gil, R., & Walker, A. K. (2023). Aggregation-prone TDP-43 sequesters and drives pathological transitions of free nuclear TDP-43. *Cellular and Molecular Life Sciences*, 80(4). <https://doi.org/10.1007/s00018-023-04739-2>
- Kiatpakdee, B., Sato, K., Otsuka, Y., Arashiki, N., Chen, Y., Tsumita, T., Otsu, W., Yamamoto, A., Kawata, R., Yamazaki, J., Sugimoto, Y., Takada, K., Mohandas, N., & Inaba, M. (2020). Cholesterol-binding protein TSPO2 coordinates maturation and proliferation of terminally differentiating erythroblasts. *Journal of Biological Chemistry*, 295(23), 8048–8063. <https://doi.org/10.1074/JBC.RA119.011679>
- Kikuchi, H., Almer, G., Yamashita, S., Guégan, C., Nagai, M., Xu, Z., Sosunov, A. A., McKhann, G. M., & Przedborski, S. (2006). Spinal cord endoplasmic reticulum stress associated with a microsomal accumulation of mutant superoxide dismutase-1 in an ALS model. *Proceedings of the National Academy of Sciences*, 103(15), 6025–6030. <https://doi.org/10.1073/pnas.0509227103>
- Kim, S., & Son, Y. (2021). Astrocytes Stimulate Microglial Proliferation and M2 Polarization In Vitro through Crosstalk between Astrocytes and Microglia. *International Journal of Molecular Sciences Article*. <https://doi.org/10.3390/ijms>
- Klim, J. R., Williams, L. A., Limone, F., Guerra San Juan, I., Davis-Dusenbery, B. N., Mordes, D. A., Burberry, A., Steinbaugh, M. J., Gamage, K. K., Kirchner, R., Moccia, R., Cassel, S. H., Chen, K., Wainger, B. J., Woolf, C. J., & Eggan, K. (2019). ALS-implicated protein TDP-43 sustains levels of STMN2, a mediator of motor neuron growth and repair. *Nature Neuroscience*, 22(2), 167–179. <https://doi.org/10.1038/s41593-018-0300-4>
- Komiya, H., Takeuchi, H., Ogawa, Y., Suzuki, K., Ogasawara, A., Takahashi, K., Azuma, Y. T., Doi, H., & Tanaka, F. (2021). Ablation of interleukin-19 improves motor function in a mouse model of amyotrophic lateral sclerosis. *Molecular Brain*, 14(1). <https://doi.org/10.1186/s13041-021-00785-8>
- Kondo, T., Funayama, M., Tsukita, K., Hotta, A., Yasuda, A., Nori, S., Kaneko, S., Nakamura, M., Takahashi, R., Okano, H., Yamanaka, S., & Inoue, H. (2014). Focal Transplantation of Human iPSC-Derived Glial-Rich Neural Progenitors Improves Lifespan of ALS Mice. *Stem Cell Reports*, 3(2), 242–249. <https://doi.org/10.1016/j.stemcr.2014.05.017>
- Kovalchuk, M. O., Heuberger, J. A. A. C., Sleutjes, B. T. H. M., Ziagkos, D., van den Berg, L. H., Ferguson, T. A., Franssen, H., & Groeneveld, G. J. (2018). Acute Effects of Riluzole and Retigabine on Axonal Excitability in Patients With Amyotrophic Lateral Sclerosis: A Randomized, Double-Blind, Placebo-Controlled, Crossover Trial. *Clinical Pharmacology & Therapeutics*, 104(6), 1136–1145. <https://doi.org/10.1002/cpt.1096>

- Kuang, Q., Purhonen, P., & Hebert, H. (2015). Structure of potassium channels. In *Cellular and Molecular Life Sciences* (Vol. 72, Issue 19, pp. 3677–3693). Birkhauser Verlag AG. <https://doi.org/10.1007/s00018-015-1948-5>
- Kuhle, J., Lindberg, R. L. P., Regeniter, A., Mehling, M., Steck, A. J., Kappos, L., & Czaplinski, A. (2009). Increased levels of inflammatory chemokines in amyotrophic lateral sclerosis. *European Journal of Neurology*, 16(6), 771–774. <https://doi.org/10.1111/j.1468-1331.2009.02560.x>
- Kumar, V., Hasan, G. M., & Hassan, M. I. (2017). Unraveling the role of RNA mediated toxicity of C9orf72 repeats in C9-FTD/ALS. In *Frontiers in Neuroscience* (Vol. 11, Issue DEC). Frontiers Media S.A. <https://doi.org/10.3389/fnins.2017.00711>
- Kuo, J. J., Siddique, T., Fu, R., & Heckman, C. J. (2005). Increased persistent Na⁺ current and its effect on excitability in motoneurons cultured from mutant SOD1 mice. *The Journal of Physiology*, 563(3), 843–854. <https://doi.org/10.1113/jphysiol.2004.074138>
- Kwak, S., & Kawahara, Y. (2005). Deficient RNA editing of GluR2 and neuronal death in amyotrophic lateral sclerosis. *Journal of Molecular Medicine*, 83(2), 110–120. <https://doi.org/10.1007/s00109-004-0599-z>
- Lee, I. C., Yang, J. J., Wong, S. H., Liou, Y. M., & Li, S. Y. (2020a). Heteromeric Kv7.2 current changes caused by loss-of-function of KCNQ2 mutations are correlated with long-term neurodevelopmental outcomes. *Scientific Reports*, 10(1). <https://doi.org/10.1038/s41598-020-70212-w>
- Lee, S., Kim, S., Kang, H.-Y., Lim, H. R., Kwon, Y., Jo, M., Jeon, Y.-M., Kim, S. R., Kim, K., Ha, C. M., Lee, S., & Kim, H.-J. (2020b). The overexpression of TDP-43 in astrocytes causes neurodegeneration via a PTP1B-mediated inflammatory response. *Journal of Neuroinflammation*, 17(1), 299. <https://doi.org/10.1186/s12974-020-01963-6>
- Lee, Y., Park, Y., Nam, H., Lee, J.-W., & Yu, S.-W. (2020c). Translocator protein (TSPO): the new story of the old protein in neuroinflammation. *BMB Reports*, 53(1), 20–27. <https://doi.org/10.5483/BMBRep.2020.53.1.273>
- Lee, Y.-B., Baskaran, P., Gomez-Deza, J., Chen, H.-J., Nishimura, A. L., Smith, B. N., Troakes, C., Adachi, Y., Stepto, A., Petrucelli, L., Gallo, J.-M., Hirth, F., Rogelj, B., Guthrie, S., & Shaw, C. E. (2017). C9orf72 poly GA RAN-translated protein plays a key role in amyotrophic lateral sclerosis via aggregation and toxicity. *Human Molecular Genetics*, 30(3–4), 318–320. <https://doi.org/10.1093/hmg/ddaa181>

References

- Lenglet, T., Lacomblez, L., Abitbol, J. L., Ludolph, A., Mora, J. S., Robberecht, W., Shaw, P. J., Pruss, R. M., Cuvier, V., & Meininger, V. (2014). A phase II-III trial of olesoxime in subjects with amyotrophic lateral sclerosis. *European Journal of Neurology*, 21(3), 529–536. <https://doi.org/10.1111/ene.12344>
- Levine, J. B., Kong, J., Nadler, M., & Xu, Z. (1999). Astrocytes interact intimately with degenerating motor neurons in mouse amyotrophic lateral sclerosis (ALS). *Glia*, 28(3), 215–224.
- Lewinski, F. von, & Keller, B. U. (2005). Ca²⁺, mitochondria and selective motoneuron vulnerability: implications for ALS. *Trends in Neurosciences*, 28(9), 494–500. <https://doi.org/10.1016/j.tins.2005.07.001>
- Lewis, K. E., Rasmussen, A. L., Bennett, W., King, A., West, A. K., Chung, R. S., & Chuah, M. I. (2014). Microglia and motor neurons during disease progression in the SOD1G93A mouse model of amyotrophic lateral sclerosis: Changes in arginase1 and inducible nitric oxide synthase. *Journal of Neuroinflammation*, 11. <https://doi.org/10.1186/1742-2094-11-55>
- Li, H., & Papadopoulos, V. (1998). Peripheral-Type Benzodiazepine Receptor Function in Cholesterol Transport. Identification of a Putative Cholesterol Recognition/Interaction Amino Acid Sequence and Consensus Pattern¹. *Endocrinology*, 139(12), 4991–4997. <https://doi.org/10.1210/endo.139.12.6390>
- Li, J., Sung, M., & Rutkove, S. B. (2013). Electrophysiologic Biomarkers for Assessing Disease Progression and the Effect of Riluzole in SOD1 G93A ALS Mice. *PLoS ONE*, 8(6), e65976. <https://doi.org/10.1371/journal.pone.0065976>
- Liang, J. J., & Rasmusson, A. M. (2018). Overview of the Molecular Steps in Steroidogenesis of the GABAergic Neurosteroids Allopregnanolone and Pregnanolone. In *Chronic Stress* (Vol. 2). SAGE Publications Inc. <https://doi.org/10.1177/2470547018818555>
- Liao, B., Zhao, W., Beers, D. R., Henkel, J. S., & Appel, S. H. (2012). Transformation from a neuroprotective to a neurotoxic microglial phenotype in a mouse model of ALS. *Experimental Neurology*, 237(1), 147–152. <https://doi.org/10.1016/j.expneurol.2012.06.011>
- Lino, M. M., Schneider, C., & Caroni, P. (2002). Accumulation of SOD1 Mutants in Postnatal Motoneurons Does Not Cause Motoneuron Pathology or Motoneuron Disease. *The Journal of Neuroscience*, 22(12), 4825–4832. <https://doi.org/10.1523/JNEUROSCI.22-12-04825.2002>
- Liu, G.-J., Middleton, R. J., Kam, W. W.-Y., Chin, D. Y., Hatty, C. R., Chan, R. H. Y., & Banati, R. B. (2017). Functional gains in energy and cell metabolism after TSPO gene insertion. *Cell Cycle*, 16(5), 436–447. <https://doi.org/10.1080/15384101.2017.1281477>

- Liu, W., & Devaux, J. J. (2014). Calmodulin orchestrates the heteromeric assembly and the trafficking of KCNQ2/3 (Kv7.2/3) channels in neurons. *Molecular and Cellular Neuroscience*, 58, 40–52. <https://doi.org/10.1016/j.mcn.2013.12.005>
- Liu, Y., Pattamatta, A., Zu, T., Reid, T., Bardhi, O., Borchelt, D. R., Yachnis, A. T., & Ranum, L. P. W. (2016). C9orf72 BAC Mouse Model with Motor Deficits and Neurodegenerative Features of ALS/FTD. *Neuron*, 90(3), 521–534. <https://doi.org/10.1016/j.neuron.2016.04.005>
- Lobsiger, C. S., Boillee, S., McAlonis-Downes, M., Khan, A. M., Feltri, M. L., Yamanaka, K., & Cleveland, D. W. (2009). Schwann cells expressing dismutase active mutant SOD1 unexpectedly slow disease progression in ALS mice. *Proceedings of the National Academy of Sciences*, 106(11), 4465–4470. <https://doi.org/10.1073/pnas.0813339106>
- Logroscino, G., Traynor, B. J., Hardiman, O., Chió, A., Mitchell, D., Swingler, R. J., Millul, A., Benn, E., & Beghi, E. (2010). Incidence of amyotrophic lateral sclerosis in Europe. *Journal of Neurology, Neurosurgery and Psychiatry*, 81(4), 385–390. <https://doi.org/10.1136/jnnp.2009.183525>
- Lombardo, J., Sun, J., & Harrington, M. A. (2018). Rapid activity-dependent modulation of the intrinsic excitability through up-regulation of KCNQ/Kv7 channel function in neonatal spinal motoneurons. *PLOS ONE*, 13(3), e0193948. <https://doi.org/10.1371/journal.pone.0193948>
- Longinetti, E., & Fang, F. (2019). Epidemiology of amyotrophic lateral sclerosis: an update of recent literature. *Current Opinion in Neurology*, 32(5), 771–776. <https://doi.org/10.1097/WCO.0000000000000730>
- Lopez-Gonzalez, R., Lu, Y., Gendron, T. F., Karydas, A., Tran, H., Yang, D., Petrucelli, L., Miller, B. L., Almeida, S., & Gao, F. B. (2016). Poly(GR) in C9ORF72-Related ALS/FTD Compromises Mitochondrial Function and Increases Oxidative Stress and DNA Damage in iPSC-Derived Motor Neurons. *Neuron*, 92(2), 383–391. <https://doi.org/10.1016/j.neuron.2016.09.015>
- Loth, M. K., Guariglia, S. R., Re, D. B., Perez, J., de Paiva, V. N., Dziedzic, J. L., Chambers, J. W., Azzam, D. J., & Guilarte, T. R. (2020). A Novel Interaction of Translocator Protein 18 kDa (TSPO) with NADPH Oxidase in Microglia. *Molecular Neurobiology*, 57(11), 4467–4487. <https://doi.org/10.1007/s12035-020-02042-w>
- Ma, X. R., Prudencio, M., Koike, Y., Vatsavayai, S. C., Kim, G., Harbinski, F., Briner, A., Rodriguez, C. M., Guo, C., Akiyama, T., Schmidt, H. B., Cummings, B. B., Wyatt, D. W., Kurylo, K., Miller, G., Mekhoubad, S., Sallee, N., Mekonnen, G., Ganser, L., ... Gitler, A. D. (2022). TDP-43 represses cryptic exon inclusion in the FTD-ALS gene UNC13A. *Nature*, 603(7899), 124–130. <https://doi.org/10.1038/s41586-022-04424-7>

References

- Mackenzie, I. R., Rademakers, R., & Neumann, M. (2010). TDP-43 and FUS in amyotrophic lateral sclerosis and frontotemporal dementia. *The Lancet Neurology*, 9(10), 995–1007. [https://doi.org/10.1016/S1474-4422\(10\)70195-2](https://doi.org/10.1016/S1474-4422(10)70195-2)
- Maghera, J., Li, J., Lamothe, S. M., Braun, M., Appendino, J. P., Au, P. Y. B., & Kurata, H. T. (2020). Familial neonatal seizures caused by the Kv7.3 selectivity filter mutation T313I. *Epilepsia Open*, 5(4), 562–573. <https://doi.org/10.1002/epi4.12438>
- Magrané, J., Cortez, C., Gan, W.-B., & Manfredi, G. (2014). Abnormal mitochondrial transport and morphology are common pathological denominators in SOD1 and TDP43 ALS mouse models. *Human Molecular Genetics*, 23(6), 1413–1424. <https://doi.org/10.1093/hmg/ddt528>
- Mancuso, R., & Navarro, X. (2015). Amyotrophic lateral sclerosis: Current perspectives from basic research to the clinic. In *Progress in Neurobiology* (Vol. 133, pp. 1–26). Elsevier Ltd. <https://doi.org/10.1016/j.pneurobio.2015.07.004>
- Mancuso, R., Oliván, S., Mancera, P., Pastén-Zamorano, A., Manzano, R., Casas, C., Osta, R., & Navarro, X. (2012b). Effect of genetic background on onset and disease progression in the SOD1-G93A model of amyotrophic lateral sclerosis. *Amyotrophic Lateral Sclerosis*, 13(3), 302–310. <https://doi.org/10.3109/17482968.2012.662688>
- Mancuso, R., Oliván, S., Rando, A., Casas, C., Osta, R., & Navarro, X. (2012a). Sigma-1R Agonist Improves Motor Function and Motoneuron Survival in ALS Mice. *Neurotherapeutics*, 9(4), 814–826. <https://doi.org/10.1007/s13311-012-0140-y>
- Mancuso, R., Santos-Nogueira, E., Osta, R., & Navarro, X. (2011). Electrophysiological analysis of a murine model of motoneuron disease. *Clinical Neurophysiology*, 122(8), 1660–1670. <https://doi.org/10.1016/j.clinph.2011.01.045>
- Marrone, L., Drexler, H. C. A., Wang, J., Tripathi, P., Distler, T., Heisterkamp, P., Anderson, E. N., Kour, S., Moraiti, A., Maharana, S., Bhatnagar, R., Belgard, T. G., Tripathy, V., Kalmbach, N., Hosseinzadeh, Z., Crippa, V., Abo-Rady, M., Wegner, F., Poletti, A., ... Sternecker, J. (2019). FUS pathology in ALS is linked to alterations in multiple ALS-associated proteins and rescued by drugs stimulating autophagy. *Acta Neuropathologica*, 138(1), 67–84. <https://doi.org/10.1007/s00401-019-01998-x>
- Martin, L. J. (2010). Olesoxime, a cholesterol-like neuroprotectant for the potential treatment of amyotrophic lateral sclerosis. *IDrugs : The Investigational Drugs Journal*, 13(8), 568–580.
- Martínez-Silva, M. de L., Imhoff-Manuel, R. D., Sharma, A., Heckman, C., Shneider, N. A., Roselli, F., Zytnicki, D., & Manuel, M. (2018). Hypoexcitability precedes denervation in the large fast-

- contracting motor units in two unrelated mouse models of ALS. *ELife*, 7. <https://doi.org/10.7554/eLife.30955>
- Masrori, P., & Van Damme, P. (2020). Amyotrophic lateral sclerosis: a clinical review. In *European Journal of Neurology* (Vol. 27, Issue 10, pp. 1918–1929). Blackwell Publishing Ltd. <https://doi.org/10.1111/ene.14393>
- Mattiazzi, M., D'Aurelio, M., Gajewski, C. D., Martushova, K., Kiaei, M., Flint Beal, M., & Manfredi, G. (2002). Mutated human SOD1 causes dysfunction of oxidative phosphorylation in mitochondria of transgenic mice. *Journal of Biological Chemistry*, 277(33), 29626–29633. <https://doi.org/10.1074/jbc.M203065200>
- Mcenery, M. W., Snowman, A. M., Trifiletti, R. R., & Snyder, S. H. (1992). Isolation of the mitochondrial benzodiazepine receptor: Association with the voltage-dependent anion channel and the adenine nucleotide carrier. In *Biochemistry* (Vol. 89).
- McLeod, V. M., Chiam, M. D. F., Lau, C. L., Rupasinghe, T. W., Boon, W. C., & Turner, B. J. (2020). Dysregulation of Steroid Hormone Receptors in Motor Neurons and Glia Associates with Disease Progression in ALS Mice. *Endocrinology*, 161(9). <https://doi.org/10.1210/endocr/bqaa113>
- Medinas, D. B., Rozas, P., Traub, F. M., Woehlbier, U., Brown, R. H., Bosco, D. A., & Hetz, C. (2018). Endoplasmic reticulum stress leads to accumulation of wild-type SOD1 aggregates associated with sporadic amyotrophic lateral sclerosis. *Proceedings of the National Academy of Sciences of the United States of America*, 115(32), 8209–8214. <https://doi.org/10.1073/pnas.1801109115>
- Medinas, D. B., Valenzuela, V., & Hetz, C. (2017). Proteostasis disturbance in amyotrophic lateral sclerosis. *Human Molecular Genetics*, 26(R2), R91–R104. <https://doi.org/10.1093/hmg/ddx274>
- Mejzini, R., Flynn, L. L., Pitout, I. L., Fletcher, S., Wilton, S. D., & Akkari, P. A. (2019). ALS Genetics, Mechanisms, and Therapeutics: Where Are We Now? In *Frontiers in Neuroscience* (Vol. 13). Frontiers Media S.A. <https://doi.org/10.3389/fnins.2019.01310>
- Meyer, K., Ferraiuolo, L., Miranda, C. J., Likhite, S., McElroy, S., Rensch, S., Ditsworth, D., Lagier-Tourenne, C., Smith, R. A., Ravits, J., Burghes, A. H., Shaw, P. J., Cleveland, D. W., Kolb, S. J., & Kaspar, B. K. (2014). Direct conversion of patient fibroblasts demonstrates non-cell autonomous toxicity of astrocytes to motor neurons in familial and sporadic ALS. *Proceedings of the National Academy of Sciences of the United States of America*, 111(2), 829–832. <https://doi.org/10.1073/pnas.1314085111>

References

- Miller, R. G., Mitchell, J. D., & Moore, D. H. (2012). Riluzole for amyotrophic lateral sclerosis (ALS)/motor neuron disease (MND). *Cochrane Database of Systematic Reviews*. <https://doi.org/10.1002/14651858.cd001447.pub3>
- Miller, T. M., Cudkowicz, M. E., Genge, A., Shaw, P. J., Sobue, G., Bucelli, R. C., Chiò, A., Van Damme, P., Ludolph, A. C., Glass, J. D., Andrews, J. A., Babu, S., Benatar, M., McDermott, C. J., Cochrane, T., Chary, S., Chew, S., Zhu, H., Wu, F., ... Fradette, S. (2022). Trial of Antisense Oligonucleotide Tofersen for SOD1 ALS. *New England Journal of Medicine*, 387(12), 1099–1110. <https://doi.org/10.1056/NEJMoa2204705>
- Miller, W. L., & Auchus, R. J. (2011). The Molecular Biology, Biochemistry, and Physiology of Human Steroidogenesis and Its Disorders. *Endocrine Reviews*, 32(1), 81–151. <https://doi.org/10.1210/er.2010-0013>
- Mishra, V., Re, D. B., Le Verche, V., Alvarez, M. J., Vasciaveo, A., Jacquier, A., Doulias, P. T., Greco, T. M., Nizzardo, M., Papadimitriou, D., Nagata, T., Rinchetti, P., Perez-Torres, E. J., Politi, K. A., Ikiz, B., Clare, K., Than, M. E., Corti, S., Ischiropoulos, H., ... Przedborski, S. (2020). Systematic elucidation of neuron-astrocyte interaction in models of amyotrophic lateral sclerosis using multi-modal integrated bioinformatics workflow. *Nature Communications*, 11(1). <https://doi.org/10.1038/s41467-020-19177-y>
- Moakley, D., Koh, J., Pereira, J. D., DuBreuil, D. M., Devlin, A. C., Berezovski, E., Zhu, K., & Wainger, B. J. (2019). Pharmacological Profiling of Purified Human Stem Cell-Derived and Primary Mouse Motor Neurons. *Scientific Reports*, 9(1). <https://doi.org/10.1038/s41598-019-47203-7>
- Mòdol-Caballero, G., Santos, D., Navarro, X., & Herrando-Grabulosa, M. (2018). Neuregulin 1 reduces motoneuron cell death and promotes neurite growth in an in vitro model of motoneuron degeneration. *Frontiers in Cellular Neuroscience*, 11. <https://doi.org/10.3389/fncel.2017.00431>
- Moldovan, M., Alvarez, S., Pinchenko, V., Marklund, S., Graffmo, K. S., & Krarup, C. (2012). Nerve excitability changes related to axonal degeneration in amyotrophic lateral sclerosis: Insights from the transgenic SOD1G127X mouse model. *Experimental Neurology*, 233(1), 408–420. <https://doi.org/10.1016/j.expneurol.2011.11.008>
- Mora, J. S., Bradley, W. G., Chaverri, D., Hernández-Barral, M., Mascias, J., Gamez, J., Gargiulo-Monachelli, G. M., Moussy, A., Mansfield, C. D., Hermine, O., & Ludolph, A. C. (2021). Long-term survival analysis of masitinib in amyotrophic lateral sclerosis. *Therapeutic Advances in Neurological Disorders*, 14, 175628642110303. <https://doi.org/10.1177/17562864211030365>

- Mora, J. S., Genge, A., Chio, A., Estol, C. J., Chaverri, D., Hernández, M., Marín, S., Mascias, J., Rodriguez, G. E., Povedano, M., Paipa, A., Dominguez, R., Gamez, J., Salvado, M., Lunetta, C., Ballario, C., Riva, N., Mandrioli, J., Moussy, A., ... Hermine, O. (2020). Masitinib as an add-on therapy to riluzole in patients with amyotrophic lateral sclerosis: a randomized clinical trial. *Amyotrophic Lateral Sclerosis and Frontotemporal Degeneration*, 21(1–2), 5–14. <https://doi.org/10.1080/21678421.2019.1632346>
- Morohaku, K., Pelton, S. H., Daugherty, D. J., Butler, W. R., Deng, W., & Selvaraj, V. (2014). Translocator Protein/Peripheral Benzodiazepine Receptor Is Not Required for Steroid Hormone Biosynthesis. *Endocrinology*, 155(1), 89–97. <https://doi.org/10.1210/en.2013-1556>
- Moser, J. M., Bigini, P., & Schmitt-John, T. (2013). The wobbler mouse, an ALS animal model. *Molecular Genetics and Genomics*, 288(5–6), 207–229. <https://doi.org/10.1007/s00438-013-0741-0>
- Moujalled, D., Grubman, A., Acevedo, K., Yang, S., Ke, Y. D., Moujalled, D. M., Duncan, C., Caragounis, A., Perera, N. D., Turner, B. J., Prudencio, M., Petrucelli, L., Blair, I., Ittner, L. M., Crouch, P. J., Liddell, J. R., & White, A. R. (2017). TDP-43 mutations causing amyotrophic lateral sclerosis are associated with altered expression of RNA-binding protein hnRNP K and affect the Nrf2 antioxidant pathway. *Human Molecular Genetics*, 26(9), 1732–1746. <https://doi.org/10.1093/hmg/ddx093>
- Mukhin, A. G., Papadopoulos, V., Costa, E., & Krueger, K. E. (1989). Mitochondrial benzodiazepine receptors regulate steroid biosynthesis. *Proceedings of the National Academy of Sciences*, 86(24), 9813–9816. <https://doi.org/10.1073/pnas.86.24.9813>
- Münch, C., O'Brien, J., Bertolotti, A., & Henderson, R. (2011). Prion-like propagation of mutant superoxide dismutase-1 misfolding in neuronal cells. *Proceedings of the National Academy of Sciences of the United States of America*, 108, 3548–3553. <https://doi.org/10.1073/pnas.1017275108/-/DCSupplemental>
- Munch, C., Sedlmeier, R., Meyer, T., Homberg, V., Sperfeld, A. D., Kurt, A., Prudlo, J., Peraus, G., Hanemann, C. O., Stumm, G., & Ludolph, A. C. (2004). Point mutations of the p150 subunit of dynactin (DCTN1) gene in ALS. *Neurology*, 63(4), 724–726. <https://doi.org/10.1212/01.WNL.0000134608.83927.B1>
- Nagai, M., Re, D. B., Nagata, T., Chalazonitis, A., Jessell, T. M., Wichterle, H., & Przedborski, S. (2007). Astrocytes expressing ALS-linked mutated SOD1 release factors selectively toxic to motor neurons. *Nature Neuroscience*, 10(5), 615–622. <https://doi.org/10.1038/nn1876>
- Naujock, M., Stanslowsky, N., Bufler, S., Naumann, M., Reinhardt, P., Sternecker, J., Kefalakes, E., Kassebaum, C., Bursch, F., Lojewski, X., Storch, A., Frickenhaus, M., Boeckers, T. M., Putz, S.,

References

- Demestre, M., Liebau, S., Klingenstein, M., Ludolph, A. C., Dengler, R., ... Petri, S. (2016). 4-Aminopyridine Induced Activity Rescues Hypoexcitable Motor Neurons from Amyotrophic Lateral Sclerosis Patient-Derived Induced Pluripotent Stem Cells. *Stem Cells*, 34(6), 1563–1575. <https://doi.org/10.1002/stem.2354>
- Neumann, M., Sampathu, D. M., Kwong, L. K., Truax, A. C., Micsenyi, M. C., Chou, T. T., Bruce, J., Schuck, T., Grossman, M., Clark, C. M., McCluskey, L. F., Miller, B. L., Masliah, E., Mackenzie, I. R., Feldman, H., Feiden, W., Kretzschmar, H. A., Trojanowski, J. Q., & Lee, V. M.-Y. (2006). Ubiquitinated TDP-43 in Frontotemporal Lobar Degeneration and Amyotrophic Lateral Sclerosis. *Science*, 314(5796), 130–133. <https://doi.org/10.1126/science.1134108>
- Ng, W., & Ng, S.-Y. (2022). Remodeling of astrocyte secretome in amyotrophic lateral sclerosis: uncovering novel targets to combat astrocyte-mediated toxicity. *Translational Neurodegeneration*, 11(1), 54. <https://doi.org/10.1186/s40035-022-00332-y>
- Nicolas, A., Kenna, K., Renton, A. E., Ticozzi, N., Faghri, F., Chia, R., Dominov, J. A., Kenna, B. J., Nalls, M. A., Keagle, P., Rivera, A. M., van Rheenen, W., Murphy, N. A., van Vugt, J. J. F. A., Geiger, J. T., van der Spek, R., Pliner, H. A., Shankaracharya, Smith, B. N., ... Traynor, B. J. (2018). Genome-wide Analyses Identify KIF5A as a Novel ALS Gene. *Neuron*, 97(6), 1268-1283.e6. <https://doi.org/10.1016/j.neuron.2018.02.027>
- Nonaka, T., Masuda-Suzukake, M., Arai, T., Hasegawa, Y., Akatsu, H., Obi, T., Yoshida, M., Murayama, S., Mann, D. M. A., Akiyama, H., & Hasegawa, M. (2013). Prion-like Properties of Pathological TDP-43 Aggregates from Diseased Brains. *Cell Reports*, 4(1), 124–134. <https://doi.org/10.1016/j.celrep.2013.06.007>
- Ohgomori, T., Yamada, J., Takeuchi, H., Kadomatsu, K., & Jinno, S. (2016). Comparative morphometric analysis of microglia in the spinal cord of SOD1^{G93A} transgenic mouse model of amyotrophic lateral sclerosis. *European Journal of Neuroscience*, 43(10), 1340–1351. <https://doi.org/10.1111/ejn.13227>
- Okada, M., Yamashita, S., Ueyama, H., Ishizaki, M., Maeda, Y., & Ando, Y. (2018). Long-term effects of edaravone on survival of patients with amyotrophic lateral sclerosis. *ENeurologicalSci*, 11, 11–14. <https://doi.org/10.1016/j.ensci.2018.05.001>
- Okuyama, S., Chaki, S., Yoshikawa, R., Ogawa, S., Suzuki, Y., Okubo, T., Nakazato, A., Nagamine, M., & Tomisawa, K. (1999). Neuropharmacological profile of peripheral benzodiazepine receptor agonists, DAA1097 and DAA1106. *Life Sciences*, 64(16), 1455–1464. [https://doi.org/10.1016/S0024-3205\(99\)00079-X](https://doi.org/10.1016/S0024-3205(99)00079-X)

- O'Rourke, J. G., Bogdanik, L., Muhammad, A. K. M. G., Gendron, T. F., Kim, K. J., Austin, A., Cady, J., Liu, E. Y., Zarrow, J., Grant, S., Ho, R., Bell, S., Carmona, S., Simpkinson, M., Lall, D., Wu, K., Daugherty, L., Dickson, D. W., Harms, M. B., ... Baloh, R. H. (2015). C9orf72 BAC Transgenic Mice Display Typical Pathologic Features of ALS/FTD. *Neuron*, 88(5), 892–901. <https://doi.org/10.1016/j.neuron.2015.10.027>
- O'Rourke, J. G., Bogdanik, L., Yáñez, A., Lall, D., Wolf, A. J., Muhammad, A. K. M. G., Ho, R., Carmona, S., Vit, J. P., Zarrow, J., Kim, K. J., Bell, S., Harms, M. B., Miller, T. M., Dangler, C. A., Underhill, D. M., Goodridge, H. S., Lutz, C. M., & Baloh, R. H. (2016). C9orf72 is required for proper macrophage and microglial function in mice. *Science*, 351(6279), 1324–1329. <https://doi.org/10.1126/science.aaf1064>
- Padilla, K., Wickenden, A. D., Gerlach, A. C., & McCormack, K. (2009). The KCNQ2/3 selective channel opener ICA-27243 binds to a novel voltage-sensor domain site. *Neuroscience Letters*, 465(2), 138–142. <https://doi.org/10.1016/j.neulet.2009.08.071>
- Paganoni, S., Hendrix, S., Dickson, S. P., Knowlton, N., Macklin, E. A., Berry, J. D., Elliott, M. A., Maisei, S., Karam, C., Caress, J. B., Owegi, M. A., Quick, A., Wymer, J., Goutman, S. A., Heitzman, D., Heiman-Patterson, T. D., Jackson, C. E., Quinn, C., Rothstein, J. D., ... Cudkowicz, M. E. (2021). Long-term survival of participants in the CENTAUR trial of sodium phenylbutyrate-taurursodiol in amyotrophic lateral sclerosis. *Muscle and Nerve*, 63(1), 31–39. <https://doi.org/10.1002/mus.27091>
- Paganoni, S., Macklin, E. A., Hendrix, S., Berry, J. D., Elliott, M. A., Maisei, S., Karam, C., Caress, J. B., Owegi, M. A., Quick, A., Wymer, J., Goutman, S. A., Heitzman, D., Heiman-Patterson, T., Jackson, C. E., Quinn, C., Rothstein, J. D., Kasarskis, E. J., Katz, J., ... Cudkowicz, M. E. (2020). Trial of Sodium Phenylbutyrate–Taurursodiol for Amyotrophic Lateral Sclerosis. *New England Journal of Medicine*, 383(10), 919–930. <https://doi.org/10.1056/NEJMoal916945>
- Papadeas, S. T., Kraig, S. E., O'Banion, C., Lepore, A. C., & Maragakis, N. J. (2011). Astrocytes carrying the superoxide dismutase 1 (SOD1 G93A) mutation induce wild-type motor neuron degeneration in vivo. *Proceedings of the National Academy of Sciences of the United States of America*, 108(43), 17803–17808. <https://doi.org/10.1073/pnas.1103141108>
- Papadopoulos, V., Amri, H., Boujrad, N., Cascio, C., Culty, M., Garnier, M., Hardwick, M., Li, H., Vidic, B., Brown, A. S., Reversa, J. L., Bernassau, J. M., & Drieu, K. (1997). Peripheral benzodiazepine receptor in cholesterol transport and steroidogenesis. *Steroids*, 62(1), 21–28. [https://doi.org/10.1016/S0039-128X\(96\)00154-7](https://doi.org/10.1016/S0039-128X(96)00154-7)

References

- Papadopoulos, V., Baraldi, M., Guilarte, T. R., Knudsen, T. B., Lacapère, J.-J., Lindemann, P., Norenberg, M. D., Nutt, D., Weizman, A., Zhang, M.-R., & Gavish, M. (2006). Translocator protein (18kDa): new nomenclature for the peripheral-type benzodiazepine receptor based on its structure and molecular function. *Trends in Pharmacological Sciences*, 27(8), 402–409. <https://doi.org/10.1016/j.tips.2006.06.005>
- Papadopoulos, V., Mukhin, A. G., Costa, E., & Krueger, K. E. (1990). The peripheral-type benzodiazepine receptor is functionally linked to Leydig cell steroidogenesis. *Journal of Biological Chemistry*, 265(7), 3772–3779. [https://doi.org/10.1016/s0021-9258\(19\)39661-9](https://doi.org/10.1016/s0021-9258(19)39661-9)
- Park, J. M., Park, D., Kim, H. J., & Park, J. S. (2022). Long-term outcomes of edaravone in amyotrophic lateral sclerosis in South Korea: 72-week observational study. *BMC Neurology*, 22(1). <https://doi.org/10.1186/s12883-022-02788-x>
- Peters, O. M., Cabrera, G. T., Tran, H., Gendron, T. F., McKeon, J. E., Metterville, J., Weiss, A., Wightman, N., Salameh, J., Kim, J., Sun, H., Boylan, K. B., Dickson, D., Kennedy, Z., Lin, Z., Zhang, Y.-J., Daugherty, L., Jung, C., Gao, F.-B., ... Brown, R. H. (2015). Human C9ORF72 Hexanucleotide Expansion Reproduces RNA Foci and Dipeptide Repeat Proteins but Not Neurodegeneration in BAC Transgenic Mice. *Neuron*, 88(5), 902–909. <https://doi.org/10.1016/j.neuron.2015.11.018>
- Phatnani, H. P., Guarnieri, P., Friedman, B. A., Carrasco, M. A., Muratet, M., O'Keeffe, S., Nwakeze, C., Pauli-Behn, F., Newberry, K. M., Meadows, S. K., Tapia, J. C., Myers, R. M., & Maniatis, T. (2013). Intricate interplay between astrocytes and motor neurons in ALS. *Proceedings of the National Academy of Sciences of the United States of America*, 110(8). <https://doi.org/10.1073/pnas.1222361110>
- Philips, T., Bento-Abreu, A., Nonneman, A., Haeck, W., Staats, K., Geelen, V., Hersmus, N., Küsters, B., Van Den Bosch, L., Van Damme, P., Richardson, W. D., & Robberecht, W. (2013). Oligodendrocyte dysfunction in the pathogenesis of amyotrophic lateral sclerosis. *Brain*, 136(2), 471–482. <https://doi.org/10.1093/brain/aws339>
- Phukan, J., Elamin, M., Bede, P., Jordan, N., Gallagher, L., Byrne, S., Lynch, C., Pender, N., & Hardiman, O. (2012). The syndrome of cognitive impairment in amyotrophic lateral sclerosis: A population-based study. *Journal of Neurology, Neurosurgery and Psychiatry*, 83(1), 102–108. <https://doi.org/10.1136/jnnp-2011-300188>
- Pieri, M., Carunchio, I., Curcio, L., Mercuri, N. B., & Zona, C. (2009). Increased persistent sodium current determines cortical hyperexcitability in a genetic model of amyotrophic lateral

- sclerosis. *Experimental Neurology*, 215(2), 368–379. <https://doi.org/10.1016/j.expneurol.2008.11.002>
- Polymenidou, M., Lagier-Tourenne, C., Hutt, K. R., Huelga, S. C., Moran, J., Liang, T. Y., Ling, S.-C., Sun, E., Wancewicz, E., Mazur, C., Kordasiewicz, H., Sedaghat, Y., Donohue, J. P., Shiue, L., Bennett, C. F., Yeo, G. W., & Cleveland, D. W. (2011). Long pre-mRNA depletion and RNA missplicing contribute to neuronal vulnerability from loss of TDP-43. *Nature Neuroscience*, 14(4), 459–468. <https://doi.org/10.1038/nn.2779>
- Porter, R. J., Partiot, A., Sachdeo, R., Nohria, V., & Alves, W. M. (2007). Randomized, multicenter, dose-ranging trial of retigabine for partial-onset seizures. *Neurology*, 68(15), 1197–1204. <https://doi.org/10.1212/01.wnl.0000259034.45049.00>
- Pramatarova, A., Laganière, J., Roussel, J., Brisebois, K., & Rouleau, G. A. (2001). Neuron-Specific Expression of Mutant Superoxide Dismutase 1 in Transgenic Mice Does Not Lead to Motor Impairment. *The Journal of Neuroscience*, 21(10), 3369–3374. <https://doi.org/10.1523/JNEUROSCI.21-10-03369.2001>
- Prudencio, M., Belzil, V. V., Batra, R., Ross, C. A., Gendron, T. F., Pregent, L. J., Murray, M. E., Overstreet, K. K., Piazza-Johnston, A. E., Desaro, P., Bieniek, K. F., DeTure, M., Lee, W. C., Biendarra, S. M., Davis, M. D., Baker, M. C., Perkerson, R. B., Van Blitterswijk, M., Stetler, C. T., ... Petrucelli, L. (2015). Distinct brain transcriptome profiles in C9orf72-associated and sporadic ALS. *Nature Neuroscience*, 18(8), 1175–1182. <https://doi.org/10.1038/nn.4065>
- Pu, M., Tai, Y., Yuan, L., Zhang, Y., Guo, H., Hao, Z., Chen, J., Qi, X., Wang, G., Tao, Z., & Ren, J. (2022). The contribution of proteasomal impairment to autophagy activation by C9orf72 poly-GA aggregates. *Cellular and Molecular Life Sciences*, 79(9), 501. <https://doi.org/10.1007/s00018-022-04518-5>
- Raffaele, S., Boccazzi, M., & Fumagalli, M. (2021). Oligodendrocyte dysfunction in amyotrophic lateral sclerosis: Mechanisms and therapeutic perspectives. In *Cells* (Vol. 10, Issue 3, pp. 1–32). MDPI. <https://doi.org/10.3390/cells10030565>
- Ragagnin, A. M. G., Shadfar, S., Vidal, M., Jamali, M. S., & Atkin, J. D. (2019). Motor Neuron Susceptibility in ALS/FTD. *Frontiers in Neuroscience*, 13. <https://doi.org/10.3389/fnins.2019.00532>
- Ramírez-Jarquín, U. N., Rojas, F., van Zundert, B., & Tapia, R. (2017). Chronic infusion of SOD1G93A astrocyte-secreted factors induces spinal motoneuron degeneration and neuromuscular dysfunction in healthy rats. *Journal of Cellular Physiology*, 232(10), 2610–2615. <https://doi.org/10.1002/jcp.25827>

References

- Re, D. B., Le Verche, V., Yu, C., Amoroso, M. W., Politi, K. A., Phani, S., Ikiz, B., Hoffmann, L., Koolen, M., Nagata, T., Papadimitriou, D., Nagy, P., Mitsumoto, H., Kariya, S., Wichterle, H., Henderson, C. E., & Przedborski, S. (2014). Necroptosis Drives Motor Neuron Death in Models of Both Sporadic and Familial ALS. *Neuron*, 81(5), 1001–1008. <https://doi.org/10.1016/j.neuron.2014.01.011>
- Reaume, Andrew. G., Elliott, J. L., Hoffman, E. K., Kowall, N. W., Ferrante, R. J., Siwek, D. R., Wilcox, H. M., Flood, D. G., Beal, M. F., Brown, R. H., Scott, R. W., & Snider, W. D. (1996). Motor neurons in Cu/Zn superoxide dismutase-deficient mice develop normally but exhibit enhanced cell death after axonal injury. *Nature Genetics*, 13(1), 43–47. <https://doi.org/10.1038/ng0596-43>
- Rezvykh, A. P., Ustyugov, A. A., Chaprov, K. D., Teterina, E. V., Nebogatikov, V. O., Spasskaya, D. S., Evgen'ev, M. B., Morozov, A. V., & Funikov, S. Y. (2023). Cytoplasmic aggregation of mutant FUS causes multistep RNA splicing perturbations in the course of motor neuron pathology. *Nucleic Acids Research*, 51(11), 5810–5830. <https://doi.org/10.1093/nar/gkad319>
- Richard, J. P., & Maragakis, N. J. (2015). Induced pluripotent stem cells from ALS patients for disease modeling. In *Brain Research* (Vol. 1607, pp. 15–25). Elsevier B.V. <https://doi.org/10.1016/j.brainres.2014.09.017>
- Richards, D., Morren, J. A., & Pioro, E. P. (2020). Time to diagnosis and factors affecting diagnostic delay in amyotrophic lateral sclerosis. *Journal of the Neurological Sciences*, 417, 117054. <https://doi.org/10.1016/j.jns.2020.117054>
- Ripps, M. E., Huntley, G. W., Hoft, P. R., Morrisontt, J. H., & Gordont, J. W. (1995). Transgenic mice expressing an altered murine superoxide dismutase gene provide an animal model of amyotrophic lateral sclerosis. In *Genetics* (Vol. 92).
- Riva, N., Gentile, F., Cerri, F., Gallia, F., Podini, P., Dina, G., Falzone, Y. M., Fazio, R., Lunetta, C., Calvo, A., Logroscino, G., Lauria, G., Corbo, M., Iannaccone, S., Chiò, A., Lazzerini, A., Nobile-Orazio, E., Filippi, M., & Quattrini, A. (2022). Phosphorylated TDP-43 aggregates in peripheral motor nerves of patients with amyotrophic lateral sclerosis. *Brain*, 145(1), 276–284. <https://doi.org/10.1093/brain/awab285>
- Rochat, C., Bernard-Marissal, N., & Schneider, B. L. (2016). Selective Vulnerability of Neuronal Subtypes in ALS: A Fertile Ground for the Identification of Therapeutic Targets. In *Update on Amyotrophic Lateral Sclerosis*. InTech. <https://doi.org/10.5772/63703>
- Roeloffs, R., Wickenden, A. D., Crean, C., Werness, S., McNaughton-Smith, G., Stables, J., McNamara, J. O., Ghodadra, N., & Rigdon, G. C. (2008). In vivo profile of ICA-27243 [N-(6-

- chloro-pyridin-3-yl)-3,4-difluoro- benzamide], a potent and selective KCNQ2/Q3 (Kv7.2/Kv7.3) activator in rodent anticonvulsant models. *Journal of Pharmacology and Experimental Therapeutics*, 326(3), 818–828. <https://doi.org/10.1124/jpet.108.137794>
- Rojas, F., Cortes, N., Abarzua, S., Dyrda, A., & van Zundert, B. (2014). Astrocytes expressing mutant SOD1 and TDP43 trigger motoneuron death that is mediated via sodium channels and nitroxidative stress. *Frontiers in Cellular Neuroscience*, 8(FEB). <https://doi.org/10.3389/fncel.2014.00024>
- Rojas, F., Gonzalez, D., Cortes, N., Ampuero, E., HernÁndez, D. E., Fritz, E., Abarzua, S., Martinez, A., Elorza, A. A., Alvarez, A., Court, F., & van Zundert, B. (2015). Reactive oxygen species trigger motoneuron death in non-cell-autonomous models of ALS through activation of c-Abl signaling. *Frontiers in Cellular Neuroscience*, 09. <https://doi.org/10.3389/fncel.2015.00203>
- Romanescu, M., Buda, V., Lombrea, A., Andor, M., Ledeti, I., Suci, M., Danciu, C., Dehelean, C. A., & Dehelean, L. (2022). Sex-Related Differences in Pharmacological Response to CNS Drugs: A Narrative Review. *Journal of Personalized Medicine*, 12(6). <https://doi.org/10.3390/jpm12060907>
- Rosen, D. R., Siddique, T., Patterson, D., Figlewicz, D. A., Sapp, P., Hentati, A., Donaldson, D., Goto, J., O'Regan, J. P., Deng, H.-X., Rahmani, Z., Krizus, A., McKenna-Yasek, D., Cayabyab, A., Gaston, S. M., Berger, R., Tanzi, R. E., Halperin, J. J., Herzfeldt, B., ... Brown, R. H. (1993). Mutations in Cu/Zn superoxide dismutase gene are associated with familial amyotrophic lateral sclerosis. *Nature*, 362(6415), 59–62. <https://doi.org/10.1038/362059a0>
- Rosenberg, N., Rosenberg, O., Weizman, A., Veenman, L., & Gavish, M. (2018). In vitro Effects of the Specific Mitochondrial TSPO Ligand Ro5 4864 in Cultured Human Osteoblasts. *Experimental and Clinical Endocrinology & Diabetes*, 126(02), 77–84. <https://doi.org/10.1055/s-0043-103282>
- Rothstein, J. D., Jin, L., Dykes-Hoberg, M., & Kuncl, R. W. (1993). Chronic inhibition of glutamate uptake produces a model of slow neurotoxicity. In *Proc. Natl. Acad. Sci. USA* (Vol. 90).
- Rothstein, J. D., Tsai, G., Kuncl, R. W., Clawson, L., Cornblath, D. R., Drachman, D. B., Pestronk, A., Stauch, B. L., & Coyle, J. T. (1990). Abnormal excitatory amino acid metabolism in amyotrophic lateral sclerosis. *Annals of Neurology*, 28(1), 18–25. <https://doi.org/10.1002/ana.410280106>
- Rothstein, J. D., Van Kammen, M., Levey, A. I., Martin, L. J., & Kuncl, R. W. (1995). Selective loss of glial glutamate transporter GLT-1 in amyotrophic lateral sclerosis. *Annals of Neurology*, 38(1), 73–84. <https://doi.org/10.1002/ana.410380114>

References

- Ruegsegger, C., & Saxena, S. (2016). Proteostasis impairment in ALS. *Brain Research*, 1648, 571–579. <https://doi.org/10.1016/j.brainres.2016.03.032>
- Rupprecht, R., Papadopoulos, V., Rammes, G., Baghai, T. C., Fan, J., Akula, N., Groyer, G., Adams, D., & Schumacher, M. (2010). Translocator protein (18 kDa) (TSPO) as a therapeutic target for neurological and psychiatric disorders. In *Nature Reviews Drug Discovery* (Vol. 9, Issue 12, pp. 971–988). <https://doi.org/10.1038/nrd3295>
- Salvany, S., Casanovas, A., Piedrafita, L., Gras, S., Calderó, J., & Esquerda, J. E. (2022). Accumulation of misfolded SOD1 outlines distinct patterns of motor neuron pathology and death during disease progression in a SOD1G93A mouse model of amyotrophic lateral sclerosis. *Brain Pathology*, 32(6). <https://doi.org/10.1111/bpa.13078>
- Sander, S. E., Lemm, C., Lange, N., Hamann, M., & Richter, A. (2012). Retigabine, a KV7 (KCNQ) potassium channel opener, attenuates L-DOPA-induced dyskinesias in 6-OHDA-lesioned rats. *Neuropharmacology*, 62(2), 1052–1061. <https://doi.org/10.1016/j.neuropharm.2011.10.016>
- Sasaki, S., & Iwata, M. (2007). Mitochondrial Alterations in the Spinal Cord of Patients With Sporadic Amyotrophic Lateral Sclerosis. *Journal of Neuropathology and Experimental Neurology*, 66(1), 10–16. <https://doi.org/10.1097/nen.0b013e31802c396b>
- Sbodio, J. I., Snyder, S. H., & Paul, B. D. (2019). Redox Mechanisms in Neurodegeneration: From Disease Outcomes to Therapeutic Opportunities. *Antioxidants & Redox Signaling*, 30(11), 1450–1499. <https://doi.org/10.1089/ars.2017.7321>
- Scarf, A. M., Ittner, L. M., & Kassiou, M. (2009). The Translocator Protein (18 kDa): Central Nervous System Disease and Drug Design. *Journal of Medicinal Chemistry*, 52(3), 581–592. <https://doi.org/10.1021/jm8011678>
- Schiffer, D., Cordera, S., Cavalla, P., & Migheli, A. (1996). Reactive astrogliosis of the spinal cord in amyotrophic lateral sclerosis. In *Journal of the Neurological Sciences* (Vol. 139).
- Shah, N. H., & Aizenman, E. (2014). Voltage-Gated Potassium Channels at the Crossroads of Neuronal Function, Ischemic Tolerance, and Neurodegeneration. *Translational Stroke Research*, 5(1), 38–58. <https://doi.org/10.1007/s12975-013-0297-7>
- Sharma, A., Lyashchenko, A. K., Lu, L., Nasrabad, S. E., Elmaleh, M., Mendelsohn, M., Nemes, A., Tapia, J. C., Mentis, G. Z., & Shneider, N. A. (2016). ALS-associated mutant FUS induces selective motor neuron degeneration through toxic gain of function. *Nature Communications*, 7. <https://doi.org/10.1038/ncomms10465>

- Shaw, P. J., Ince, P. G., Falkous, G., & Mantle, D. (1995). Oxidative damage to protein in sporadic motor neuron disease spinal cord. *Annals of Neurology*, 38(4), 691–695. <https://doi.org/10.1002/ana.410380424>
- Shefner, J. M., Reaume, A. G., Flood, D. G., Scott, R. W., Kowall, N. W., Ferrante, R. J., Siwek, D. F., Upton-Rice, M., & Brown, R. H. (1999). Mice lacking cytosolic copper/zinc superoxide dismutase display a distinctive motor axonopathy. *Neurology*, 53(6), 1239–1239. <https://doi.org/10.1212/WNL.53.6.1239>
- Shibata, N., Hirano, A., Kobayashi, M., Sasaki, S., Takeo, K., Matsumoto, S., Shiozawa, Z., Komori, T., Ikemoto, A., Umahara, T., & Asayama, K. (1994). superoxide dismutase-like immunoreactivity in Lewy body-like inclusions of sporadic amyotrophic lateral sclerosis. *Neuroscience Letters*, 179(1–2), 149–152. [https://doi.org/10.1016/0304-3940\(94\)90956-3](https://doi.org/10.1016/0304-3940(94)90956-3)
- Simpson, E. P., Henry, Y. K., Henkel, J. S., Smith, R. G., & Appel, S. H. (2004). Increased lipid peroxidation in sera of ALS patients: A potential biomarker of disease burden. *Neurology*, 62(10), 1758–1765. <https://doi.org/10.1212/WNL.62.10.1758>
- Smith, E. F., Shaw, P. J., & De Vos, K. J. (2019). The role of mitochondria in amyotrophic lateral sclerosis. *Neuroscience Letters*, 710, 132933. <https://doi.org/10.1016/j.neulet.2017.06.052>
- Soldovieri, M. V., Miceli, F., & Taglialatela, M. (2011). Driving with no brakes: Molecular pathophysiology of Kv7 potassium channels. In *Physiology* (Vol. 26, Issue 5, pp. 365–376). <https://doi.org/10.1152/physiol.00009.2011>
- Spiller, K. J., Khan, T., Dominique, M. A., Restrepo, C. R., Cotton-Samuel, D., Levitan, M., Jafar-Nejad, P., Zhang, B., Soriano, A., Rigo, F., Trojanowski, J. Q., & Lee, V. M. Y. (2019). Reduction of matrix metalloproteinase 9 (MMP-9) protects motor neurons from TDP-43-triggered death in rNLS8 mice. *Neurobiology of Disease*, 124, 133–140. <https://doi.org/10.1016/j.nbd.2018.11.013>
- Spiller, K. J., Restrepo, C. R., Khan, T., Dominique, M. A., Fang, T. C., Canter, R. G., Roberts, C. J., Miller, K. R., Ransohoff, R. M., Trojanowski, J. Q., & Lee, V. M. Y. (2018). Microglia-mediated recovery from ALS-relevant motor neuron degeneration in a mouse model of TDP-43 proteinopathy. *Nature Neuroscience*, 21(3), 329–340. <https://doi.org/10.1038/s41593-018-0083-7>
- Starr, A., & Sattler, R. (2018). Synaptic dysfunction and altered excitability in C9ORF72 ALS/FTD. *Brain Research*, 1693, 98–108. <https://doi.org/10.1016/j.brainres.2018.02.011>
- Statland, J. M., Barohn, R. J., McVey, A. L., Katz, J. S., & Dimachkie, M. M. (2015). Patterns of Weakness, Classification of Motor Neuron Disease, and Clinical Diagnosis of Sporadic

References

- Amyotrophic Lateral Sclerosis. In *Neurologic Clinics* (Vol. 33, Issue 4, pp. 735–748). W.B. Saunders. <https://doi.org/10.1016/j.ncl.2015.07.006>
- Stoica, R., De Vos, K. J., Paillusson, S., Mueller, S., Sancho, R. M., Lau, K.-F., Vizcay-Barrena, G., Lin, W.-L., Xu, Y.-F., Lewis, J., Dickson, D. W., Petrucelli, L., Mitchell, J. C., Shaw, C. E., & Miller, C. C. J. (2014). ER-mitochondria associations are regulated by the VAPB-PTPIP51 interaction and are disrupted by ALS/FTD-associated TDP-43. *Nature Communications*, 5(1), 3996. <https://doi.org/10.1038/ncomms4996>
- Stoklund Dittlau, K., Terrie, L., Baatsen, P., Kerstens, A., De Swert, L., Janky, R., Corthout, N., Masrori, P., Van Damme, P., Hyttel, P., Meyer, M., Thorrez, L., Freude, K., & Van Den Bosch, L. (2023). FUS-ALS hiPSC-derived astrocytes impair human motor units through both gain-of-toxicity and loss-of-support mechanisms. *Molecular Neurodegeneration*, 18(1), 5. <https://doi.org/10.1186/s13024-022-00591-3>
- Sunyach, C., Michaud, M., Arnoux, T., Bernard-Marissal, N., Aebischer, J., Latyszenok, V., Gouarné, C., Raoul, C., Pruss, R. M., Bordet, T., & Pettmann, B. (2012). Olesoxime delays muscle denervation, astrogliosis, microglial activation and motoneuron death in an ALS mouse model. *Neuropharmacology*, 62(7), 2346–2353. <https://doi.org/10.1016/j.neuropharm.2012.02.013>
- Taha, D. M., Clarke, B. E., Hall, C. E., Tyzack, G. E., Ziff, O. J., Greensmith, L., Kalmar, B., Ahmed, M., Alam, A., Thelin, E. P., Garcia, N. M., Helmy, A., Sibley, C. R., & Patani, R. (2022). Astrocytes display cell autonomous and diverse early reactive states in familial amyotrophic lateral sclerosis. *Brain*, 145(2), 481–489. <https://doi.org/10.1093/brain/awab328>
- Tak, Y. J., Park, J. H., Rhim, H., & Kang, S. (2020). ALS-related mutant SOD1 aggregates interfere with mitophagy by sequestering the autophagy receptor optineurin. *International Journal of Molecular Sciences*, 21(20), 1–17. <https://doi.org/10.3390/ijms21207525>
- Takanashi, K., & Yamaguchi, A. (2014). Aggregation of ALS-linked FUS mutant sequesters RNA binding proteins and impairs RNA granules formation. *Biochemical and Biophysical Research Communications*, 452(3), 600–607. <https://doi.org/10.1016/j.bbrc.2014.08.115>
- Tian, Y. P., Che, F. Y., Su, Q. P., Lu, Y. C., You, C. P., Huang, L. M., Wang, S. G., Wang, L., & Yu, J. X. (2017). Effects of mutant TDP-43 on the Nrf2/ARE pathway and protein expression of MafK and JDP2 in NSC-34 cells. *Genetics and Molecular Research*, 16(2). <https://doi.org/10.4238/gmr16029638>
- Tiryaki, E., & Horak, H. A. (2014). ALS and Other Motor Neuron Diseases. *CONTINUUM: Lifelong Learning in Neurology*, 20, 1185–1207. <https://doi.org/10.1212/01.CON.0000455886.14298.a4>

- Tong, J., Huang, C., Bi, F., Wu, Q., Huang, B., Liu, X., Li, F., Zhou, H., & Xia, X.-G. (2013). Expression of ALS-linked TDP-43 mutant in astrocytes causes non-cell-autonomous motor neuron death in rats. *The EMBO Journal*, 32(13), 1917–1926. <https://doi.org/10.1038/emboj.2013.122>
- Trias, E., Ibarburu, S., Barreto-Núñez, R., Babdor, J., Maciel, T. T., Guillo, M., Gros, L., Dubreuil, P., Díaz-Amarilla, P., Cassina, P., Martínez-Palma, L., Moura, I. C., Beckman, J. S., Hermine, O., & Barbeito, L. (2016). Post-paralysis tyrosine kinase inhibition with masitinib abrogates neuroinflammation and slows disease progression in inherited amyotrophic lateral sclerosis. *Journal of Neuroinflammation*, 13(1). <https://doi.org/10.1186/s12974-016-0620-9>
- Trias, E., Kovacs, M., King, P. H., Si, Y., Kwon, Y., Varela, V., Ibarburu, S., Moura, I. C., Hermine, O., Beckman, J. S., & Barbeito, L. (2020). Schwann cells orchestrate peripheral nerve inflammation through the expression of CSF1, IL-34, and SCF in amyotrophic lateral sclerosis. *GLIA*, 68(6), 1165–1181. <https://doi.org/10.1002/glia.23768>
- Tu, L. N., Morohaku, K., Manna, P. R., Pelton, S. H., Butler, W. R., Stocco, D. M., & Selvaraj, V. (2014). Peripheral benzodiazepine receptor/translocator protein global knock-out mice are viable with no effects on steroid hormone biosynthesis. *Journal of Biological Chemistry*, 289(40), 27444–27454. <https://doi.org/10.1074/jbc.M114.578286>
- Turner, B. J., Ackerley, S., Davies, K. E., & Talbot, K. (2010). Dismutase-competent SOD1 mutant accumulation in myelinating Schwann cells is not detrimental to normal or transgenic ALS model mice. *Human Molecular Genetics*, 19(5), 815–824. <https://doi.org/10.1093/hmg/ddp550>
- Urrutia, J., Aguado, A., Gomis-Perez, C., Muguruza-Montero, A., Ballesteros, O. R., Zhang, J., Nuñez, E., Malo, C., Chung, H. J., Leonardo, A., Bergara, A., & Villarroel, A. (2021). An epilepsy-causing mutation leads to co-translational misfolding of the Kv7.2 channel. *BMC Biology*, 19(1). <https://doi.org/10.1186/s12915-021-01040-1>
- Van Damme, P., Callewaert, G., Eggermont, J., Robberecht, W., & Van Den Bosch, L. (2003). Chloride Influx Aggravates Ca^{2+} -Dependent AMPA Receptor-Mediated Motoneuron Death. *The Journal of Neuroscience*, 23(12), 4942–4950. <https://doi.org/10.1523/JNEUROSCI.23-12-04942.2003>
- Van Damme, P., Callewaert, G., Robberecht, W., Van, L., & Bosch, D. (2005). GluR2 Deficiency Accelerates Motor Neuron Degeneration in a Mouse Model of Amyotrophic Lateral Sclerosis. In *J Neuropathol Exp Neurol* (Vol. 64, Issue 7). <http://jnen.oxfordjournals.org/>
- Van Damme, P., Robberecht, W., & Van Den Bosch, L. (2017). Modelling amyotrophic lateral sclerosis: Progress and possibilities. In *DMM Disease Models and Mechanisms* (Vol. 10, Issue 5, pp. 537–549). Company of Biologists Ltd. <https://doi.org/10.1242/dmm.029058>

References

- Van Den Bosch, L., Schwaller, B., Vleminckx, V., Meijers, B., Stork, S., Ruehlicke, T., Van Houtte, E., Klaassen, H., Celio, M. R., Missiaen, L., Robberecht, W., & Berchtold, M. W. (2002). Protective Effect of Parvalbumin on Excitotoxic Motor Neuron Death. *Experimental Neurology*, 174(2), 150–161. <https://doi.org/10.1006/exnr.2001.7858>
- Van Den Bosch, L., Van Damme, P., Bogaert, E., & Robberecht, W. (2006). The role of excitotoxicity in the pathogenesis of amyotrophic lateral sclerosis. *Biochimica et Biophysica Acta (BBA) - Molecular Basis of Disease*, 1762(11–12), 1068–1082. <https://doi.org/10.1016/j.bbadis.2006.05.002>
- Van Den Bosch, L., Vandenberghe, W., Klaassen, H., Van Houtte, E., & Robberecht, W. (2000). Ca²⁺-permeable AMPA receptors and selective vulnerability of motor neurons. *Journal of the Neurological Sciences*, 180(1–2), 29–34. [https://doi.org/10.1016/S0022-510X\(00\)00414-7](https://doi.org/10.1016/S0022-510X(00)00414-7)
- Van Harten, A. C. M., Phatnani, H., & Przedborski, S. (2021). Non-cell-autonomous pathogenic mechanisms in amyotrophic lateral sclerosis. In *Trends in Neurosciences* (Vol. 44, Issue 8, pp. 658–668). Elsevier Ltd. <https://doi.org/10.1016/j.tins.2021.04.008>
- van Zundert, B., Izaurieta, P., Fritz, E., & Alvarez, F. J. (2012). Early pathogenesis in the adult-onset neurodegenerative disease amyotrophic lateral sclerosis. *Journal of Cellular Biochemistry*, 113(11), 3301–3312. <https://doi.org/10.1002/jcb.24234>
- van Zundert, B., Peuscher, M. H., Hynynen, M., Chen, A., Neve, R. L., Brown, R. H., Constantine-Paton, M., & Bellingham, M. C. (2008). Neonatal Neuronal Circuitry Shows Hyperexcitable Disturbance in a Mouse Model of the Adult-Onset Neurodegenerative Disease Amyotrophic Lateral Sclerosis. *The Journal of Neuroscience*, 28(43), 10864–10874. <https://doi.org/10.1523/JNEUROSCI.1340-08.2008>
- Vande Velde, C., McDonald, K. K., Boukhedimi, Y., McAlonis-Downes, M., Lobsiger, C. S., Bel Hadj, S., Zandona, A., Julien, J.-P., Shah, S. B., & Cleveland, D. W. (2011). Misfolded SOD1 Associated with Motor Neuron Mitochondria Alters Mitochondrial Shape and Distribution Prior to Clinical Onset. *PLoS ONE*, 6(7), e22031. <https://doi.org/10.1371/journal.pone.0022031>
- Varcianna, A., Myszczyńska, M. A., Castelli, L. M., O'Neill, B., Kim, Y., Talbot, J., Nyberg, S., Nyamali, I., Heath, P. R., Stopford, M. J., Hautbergue, G. M., & Ferraiuolo, L. (2019). Micro-RNAs secreted through astrocyte-derived extracellular vesicles cause neuronal network degeneration in C9orf72 ALS. *EBioMedicine*, 40, 626–635. <https://doi.org/10.1016/j.ebiom.2018.11.067>
- Veenman, L., Shandalov, Y., & Gavish, M. (2008). VDAC activation by the 18 kDa translocator protein (TSPO), implications for apoptosis. *Journal of Bioenergetics and Biomembranes*, 40(3), 199–205. <https://doi.org/10.1007/s10863-008-9142-1>

- Verber, N., & Shaw, P. J. (2020). Biomarkers in amyotrophic lateral sclerosis: A review of new developments. In *Current Opinion in Neurology* (Vol. 33, Issue 5, pp. 662–668). Lippincott Williams and Wilkins. <https://doi.org/10.1097/WCO.0000000000000854>
- Vilhardt, F., Haslund-Vinding, J., Jaquet, V., & McBean, G. (2017). Microglia antioxidant systems and redox signalling. *British Journal of Pharmacology*, 174(12), 1719–1732. <https://doi.org/10.1111/bph.13426>
- Vukosavic, S., Dubois-Dauphin, M., Romero, N., & Przedborski, S. (2002). Bax and Bcl-2 Interaction in a Transgenic Mouse Model of Familial Amyotrophic Lateral Sclerosis. *Journal of Neurochemistry*, 73(6), 2460–2468. <https://doi.org/10.1046/j.1471-4159.1999.0732460.x>
- Wainger, B. J., Kiskinis, E., Mellin, C., Wiskow, O., Han, S. S. W., Sandoe, J., Perez, N. P., Williams, L. A., Lee, S., Boulting, G., Berry, J. D., Brown, R. H., Cudkowicz, M. E., Bean, B. P., Eggan, K., & Woolf, C. J. (2014). Intrinsic membrane hyperexcitability of amyotrophic lateral sclerosis patient-derived motor neurons. *Cell Reports*, 7(1), 1–11. <https://doi.org/10.1016/j.celrep.2014.03.019>
- Wainger, B. J., Macklin, E. A., Vucic, S., McIllduff, C. E., Paganoni, S., Maragakis, N. J., Bedlack, R., Goyal, N. A., Rutkove, S. B., Lange, D. J., Rivner, M. H., Goutman, S. A., Ladha, S. S., Mauricio, E. A., Baloh, R. H., Simmons, Z., Pothier, L., Kassis, S. B., La, T., ... Cudkowicz, M. E. (2021). Effect of Ezogabine on Cortical and Spinal Motor Neuron Excitability in Amyotrophic Lateral Sclerosis: A Randomized Clinical Trial. *JAMA Neurology*, 78(2), 186–196. <https://doi.org/10.1001/jamaneurol.2020.4300>
- Wang, L., Gutmann, D. H., & Roos, R. P. (2011). Astrocyte loss of mutant SOD1 delays ALS disease onset and progression in G85R transgenic mice. *Human Molecular Genetics*, 20(2), 286–293. <https://doi.org/10.1093/hmg/ddq463>
- Wang, L., Pytel, P., Feltri, M. L., Wrabetz, L., & Roos, R. P. (2012). Selective knockdown of mutant SOD1 in Schwann cells ameliorates disease in G85R mutant SOD1 transgenic mice. *Neurobiology of Disease*, 48(1), 52–57. <https://doi.org/10.1016/j.nbd.2012.05.014>
- Wang, W., Li, L., Lin, W.-L., Dickson, D. W., Petrucelli, L., Zhang, T., & Wang, X. (2013). The ALS disease-associated mutant TDP-43 impairs mitochondrial dynamics and function in motor neurons. *Human Molecular Genetics*, 22(23), 4706–4719. <https://doi.org/10.1093/hmg/ddt319>
- Wang, W., Wang, L., Lu, J., Siedlak, S. L., Fujioka, H., Liang, J., Jiang, S., Ma, X., Jiang, Z., da Rocha, E. L., Sheng, M., Choi, H., Lerou, P. H., Li, H., & Wang, X. (2016). The inhibition of TDP-43 mitochondrial localization blocks its neuronal toxicity. *Nature Medicine*, 22(8), 869–878. <https://doi.org/10.1038/nm.4130>

References

- Watanabe, S., Ilieva, H., Tamada, H., Nomura, H., Komine, O., Endo, F., Jin, S., Mancias, P., Kiyama, H., & Yamanaka, K. (2016). Mitochondria-associated membrane collapse is a common pathomechanism in *SIGMAR1* and *SOD1*-linked *ALS*. *EMBO Molecular Medicine*, 8(12), 1421–1437. <https://doi.org/10.15252/emmm.201606403>
- Wegorzewska, I., Bell, S., Cairns, N. J., Miller, T. M., & Baloh, R. H. (2009). TDP-43 mutant transgenic mice develop features of ALS and frontotemporal lobar degeneration. *Proceedings of the National Academy of Sciences*, 106(44), 18809–18814. <https://doi.org/10.1073/pnas.0908767106>
- White, M. A., Kim, E., Duffy, A., Adalbert, R., Phillips, B. U., Peters, O. M., Stephenson, J., Yang, S., Massenzio, F., Lin, Z., Andrews, S., Segonds-Pichon, A., Metterville, J., Saksida, L. M., Mead, R., Ribchester, R. R., Barhomi, Y., Serre, T., Coleman, M. P., ... Sreedharan, J. (2018). TDP-43 gains function due to perturbed autoregulation in a Tardbp knock-in mouse model of ALS-FTD. *Nature Neuroscience*, 21(4), 552–563. <https://doi.org/10.1038/s41593-018-0113-5>
- Wickenden, A. D., Krajewski, J. L., London, B., Wagoner, P. K., Wilson, W. A., Clark, S., Roeloffs, R., McNaughton-Smith, G., & Rigdon, G. C. (2008). N-(6-chloro-pyridin-3-yl)-3,4-difluorobenzamide (ICA-27243): A novel, selective KCNQ2/Q3 potassium channel activator. *Molecular Pharmacology*, 73(3), 977–986. <https://doi.org/10.1124/mol.107.043216>
- Wiedemann, F. R., Manfredi, G., Mawrin, C., Beal, M. F., & Schon, E. A. (2002). Mitochondrial DNA and respiratory chain function in spinal cords of ALS patients. *Journal of Neurochemistry*, 80(4), 616–625. <https://doi.org/10.1046/j.0022-3042.2001.00731.x>
- Wils, H., Kleinberger, G., Janssens, J., Pereson, S., Joris, G., Cuijt, I., Smits, V., Ceuterick-De Groote, C., Van Broeckhoven, C., & Kumar-Singh, S. (2010). TDP-43 transgenic mice develop spastic paralysis and neuronal inclusions characteristic of ALS and frontotemporal lobar degeneration. *Proceedings of the National Academy of Sciences of the United States of America*, 107(8), 3858–3863. <https://doi.org/10.1073/pnas.0912417107>
- Wintz, K., Post, J., Langen, K. J., Willbold, D., Willuweit, A., & Kutzsche, J. (2023). Oral Treatment with d-RD2RD2 Impedes Early Disease Mechanisms in SOD1*G93A Transgenic Mice but Does Not Prolong Survival. *Biomedicines*, 11(4). <https://doi.org/10.3390/biomedicines11040995>
- Witzel, S., Maier, A., Steinbach, R., Grosskreutz, J., Koch, J. C., Sarikidi, A., Petri, S., Günther, R., Wolf, J., Hermann, A., Prudlo, J., Cordts, I., Lingor, P., Löscher, W. N., Kohl, Z., Hagenacker, T., Ruckes, C., Koch, B., Spittel, S., ... Ludolph, A. C. (2022). Safety and Effectiveness of Long-term Intravenous Administration of Edaravone for Treatment of Patients With Amyotrophic Lateral Sclerosis. *JAMA Neurology*, 79(2), 121. <https://doi.org/10.1001/jamaneurol.2021.4893>

- Xia, C. H., Roberts, E. A., Her, L. S., Liu, X., Williams, D. S., Cleveland, D. W., & Goldstein, L. S. B. (2003). Abnormal neurofilament transport caused by targeted disruption of neuronal kinesin heavy chain KIF5A. *Journal of Cell Biology*, 161(1), 55–66. <https://doi.org/10.1083/jcb.200301026>
- Yang, C., Wang, H., Qiao, T., Yang, B., Aliaga, L., Qiu, L., Tan, W., Salameh, J., McKenna-Yasek, D. M., Smith, T., Peng, L., Moore, M. J., Brown, R. H., Cai, H., & Xu, Z. (2014). Partial loss of TDP-43 function causes phenotypes of amyotrophic lateral sclerosis. *Proceedings of the National Academy of Sciences of the United States of America*, 111(12). <https://doi.org/10.1073/pnas.1322641111>
- Yang, Y. M., Gupta, S. K., Kim, K. J., Powers, B. E., Cerqueira, A., Wainger, B. J., Ngo, H. D., Rosowski, K. A., Schein, P. A., Ackeifi, C. A., Arvanites, A. C., Davidow, L. S., Woolf, C. J., & Rubin, L. L. (2013). A small molecule screen in stem-cell-derived motor neurons identifies a kinase inhibitor as a candidate therapeutic for ALS. *Cell Stem Cell*, 12(6), 713–726. <https://doi.org/10.1016/j.stem.2013.04.003>
- Yao, R., Pan, R., Shang, C., Li, X., Cheng, J., Xu, J., & Li, Y. (2020). Translocator Protein 18 kDa (TSPO) Deficiency Inhibits Microglial Activation and Impairs Mitochondrial Function. *Frontiers in Pharmacology*, 11. <https://doi.org/10.3389/fphar.2020.00986>
- Yoshino, H. (2019). Edaravone for the treatment of amyotrophic lateral sclerosis. *Expert Review of Neurotherapeutics*, 19(3), 185–193. <https://doi.org/10.1080/14737175.2019.1581610>
- Yuan, J.-H., Estacion, M., Mis, M. A., Tanaka, B. S., Schulman, B. R., Chen, L., Liu, S., Dib-Hajj, F. B., Dib-Hajj, S. D., & Waxman, S. G. (2021). KCNQ variants and pain modulation: a missense variant in Kv7.3 contributes to pain resilience. *Brain Communications*, 3(3). <https://doi.org/10.1093/braincomms/fcab212>
- Zhang, F., Ström, A.-L., Fukada, K., Lee, S., Hayward, L. J., & Zhu, H. (2007). Interaction between Familial Amyotrophic Lateral Sclerosis (ALS)-linked SOD1 Mutants and the Dynein Complex. *Journal of Biological Chemistry*, 282(22), 16691–16699. <https://doi.org/10.1074/jbc.M609743200>
- Zhang, J., Zhang, L., Yi, S., Jiang, X., Qiao, Y., Zhang, Y., Xiao, C., & Zhou, T. (2020). Mouse Astrocytes Promote Microglial Ramification by Releasing TGF- β and Forming Glial Fibers. *Frontiers in Cellular Neuroscience*, 14. <https://doi.org/10.3389/fncel.2020.00195>
- Zhang, Y.-J., Gendron, T. F., Grima, J. C., Sasaguri, H., Jansen-West, K., Xu, Y.-F., Katzman, R. B., Gass, J., Murray, M. E., Shinohara, M., Lin, W.-L., Garrett, A., Stankowski, J. N., Daugherty, L., Tong, J., Perkerson, E. A., Yue, M., Chew, J., Castaneda-Casey, M., ... Petrucelli, L. (2016). C9ORF72 poly(GA) aggregates sequester and impair HR23 and nucleocytoplasmic transport proteins. *Nature Neuroscience*, 19(5), 668–677. <https://doi.org/10.1038/nn.4272>

References

- Zhang, Y.-J., Jansen-West, K., Xu, Y.-F., Gendron, T. F., Bieniek, K. F., Lin, W.-L., Sasaguri, H., Caulfield, T., Hubbard, J., Daugherty, L., Chew, J., Belzil, V. V., Prudencio, M., Stankowski, J. N., Castanedes-Casey, M., Whitelaw, E., Ash, P. E. A., DeTure, M., Rademakers, R., ... Petrucelli, L. (2014). Aggregation-prone c9FTD/ALS poly(GA) RAN-translated proteins cause neurotoxicity by inducing ER stress. *Acta Neuropathologica*, 128(4), 505–524. <https://doi.org/10.1007/s00401-014-1336-5>
- Zhang, Z., Almeida, S., Lu, Y., Nishimura, A. L., Peng, L., Sun, D., Wu, B., Karydas, A. M., Tartaglia, M. C., Fong, J. C., Miller, B. L., Farese, R. V., Moore, M. J., Shaw, C. E., & Gao, F.-B. (2013). Downregulation of MicroRNA-9 in iPSC-Derived Neurons of FTD/ALS Patients with TDP-43 Mutations. *PLoS ONE*, 8(10), e76055. <https://doi.org/10.1371/journal.pone.0076055>
- Zhou, Y., Liu, S., Öztürk, A., & Hicks, G. G. (2014). FUS-regulated RNA metabolism and DNA damage repair. *Rare Diseases*, 2(1), e29515. <https://doi.org/10.4161/rdis.29515>
- Zürcher, N. R., Loggia, M. L., Lawson, R., Chonde, D. B., Izquierdo-Garcia, D., Yasek, J. E., Akeju, O., Catana, C., Rosen, B. R., Cudkowicz, M. E., Hooker, J. M., & Atassi, N. (2015). Increased in vivo glial activation in patients with amyotrophic lateral sclerosis: Assessed with [11C]-PBR28. *NeuroImage: Clinical*, 7, 409–414. <https://doi.org/10.1016/j.nicl.2015.01.009>

X. Acknowledgements

Quisiera dar las gracias a todas las personas que han formado parte de esta tesis.

En primer lugar, quiero agradecer a mis directores Mireia y Xavi por abrirme las puertas del laboratorio y darme la oportunidad de realizar la tesis con ellos. Gracias por toda la dedicación, la motivación y los conocimientos que habéis compartido conmigo.

En segundo lugar, gracias a todos mis compañeros sin los que estos 4 años no hubieran sido igual.

I also want to express my gratitude to The Amyotrophic Lateral Sclerosis Association and Fight MND for their funding, which made this thesis possible. Additionally, I appreciate the financial support from CIBERNED and TERAV RICORS.

I extend my thanks to all the international collaborators on this project, including Dr. van Zundert, Dr. Fritz, Dr. Brown, and Dr. Belligham.

Y, por último, dar gracias a mi familia que me ha apoyado en todo momento y que sin ellos no hubiera llegado hasta aquí.